



Boletín del Instituto de Fisiografía y Geología

Volumenes 79-81 (2011)



Boletín del Instituto de Fisiografía y Geología

ISSN 1666-115X

Edición del Instituto de Fisiografía y Geología
"Dr. Alfredo Castellanos"
Facultad de Ciencias Exactas, Ingeniería y Agrimensura
Universidad Nacional de Rosario
Pellegrini 250, 2000 Rosario, Argentina

E-mail: ifg@fceia.unr.edu.ar

URL: <http://www.fceia.unr.edu.ar/fisiografia>

Características y alcance

El Boletín IFG es una revista internacional de publicación periódica de artículos científicos originales sobre temas de las denominadas Ciencias de la Tierra (Geología, Estratigrafía, Paleontología, y disciplinas afines), cuyos tópicos estén o no incluidos en los campos de investigación del Instituto de Fisiografía y Geología. Sólo son aceptados manuscritos de trabajos inéditos consistentes en contribuciones científicas significativas a criterio de los Editores y los árbitros. Todos los manuscritos son sometidos a arbitraje internacional de por, al menos, dos reconocidos especialistas en la materia. La decisión final de aceptación de un manuscrito para su publicación es de los editores y el comité editorial.

Ediciones anteriores

El Boletín IFG es la serie única que reemplaza y sucede a todas las ediciones anteriores del Instituto de Fisiografía y Geología que se publicaron con los nombres "Publicaciones" [ISSN 0041-8684], "Notas A" [ISSN 0325-4100] y "Notas B" [ISSN 0326-470X]. La numeración de la nueva y única serie comienza en el Volumen 70, correlativo con el último número de la antigua serie principal "Publicaciones", finalizada en 1996 con el número 69. Se publicará un volumen anual, dividido en un número variable de fascículos que dependerá de la extensión y número de contribuciones que se incluyan.

Suscripción e intercambio

El Boletín IFG puede obtenerse por intercambio institucional, suscripción individual o suscripción institucional, dirigiéndose a la dirección indicada arriba. La nómina de los números anteriores disponibles puede obtenerse del sitio de internet indicado arriba, así como todos los números anteriores disponibles en formato pdf.

Aim and scope

The Boletín IFG is an international periodical journal containing original scientific articles on the so called Earth Sciences (Geology, Stratigraphy, Paleontology, and related matters), related or not with the fields or research of the Instituto de Fisiografía y Geología. Only are accepted manuscripts of unpublished results consisting of significant scientific contributions. Every manuscript is subject to international peer review by at least two reviewers or referees, well known specialists on the matter. Final decision of publication is of the editors and the editorial board.

Past editions

The Boletín IFG is the unique series of publications which replace and follows any former and past editions of the Instituto de Fisiografía y Geología which were published under the following names: "Publicaciones" [ISSN 0041-8684], "Notas A" [ISSN 0325-4100] y "Notas B" [ISSN 0326-470X]. The first volume of the series is the volume 70 correlative with the last of the former series "Publicaciones", ended in 1996 with the number 69. It will be published a single volume per year, subdivided in a number of fascicules depending on the number and size of contributions included.

Suscription and exchange

The Boletín IFG can be obtained by institutional exchange, individual suscription or institutional suscription contacting to the addresses given above. All current and past publications are free available on-line from the website cited above, in pdf format.

Editores

Horacio Parent (Universidad Nacional de Rosario, Rosario)
Eduardo P. Peralta (Universidad Nacional de Rosario, Rosario)

Comité editorial

Antonio Introcaso (Universidad Nacional de Rosario, Rosario)
Andrés F. Greco (Universidad Nacional de Rosario, Rosario)
Günter Schweigert (Staatliches Museum für Naturkunde, Stuttgart)
Alberto C. Garrido (Museo Provincial Ciencias Naturales "Prof. Olsacher", Dir. Prov. Minería de Neuquén)

Fotografía de portada: Vista hacia el Este de la Fm. Tordillo aflorante en la desembocadura del Arroyo Cieneguita sobre el Río Salado, Mendoza, Argentina (véase figura en p. 23 de este volumen).



Contenido / Contents

Platform to basin correlations in Cretaceous times. Abstracts <i>D. Grosheny, B. Granier & N. Sander (editors)</i>	1
The Tithonian-Berriasian ammonite fauna and stratigraphy of Arroyo Cieneguita, Neuquén-Mendoza Basin, Argentina <i>H. Parent, A. Scherzinger & G. Schweigert</i>	21
Study of the Claromecó Basin from gravity, magnetic and geoid undulation charts <i>F. Ruiz & A. Introcaso</i>	95
Copper in Deccan basalts (India): review of the abundance and patterns of distribution <i>P.O. Alexander & H. Thomas</i>	107

PLATFORM TO BASIN CORRELATIONS IN CRETACEOUS TIMES - ABSTRACTS -

Danièle GROSHENY (editor), Bruno GRANIER (editor),
Nestor SANDER (associate editor)



Boletín
del Instituto de
Fisiografía y Geología

Danièle Grosheny, Bruno Granier & Nestor Sander (editors), 2011. Platform to basin correlations in Cretaceous times. Abstracts. *Boletín del Instituto de Fisiografía y Geología* 79-81: 1-19. Rosario, 01-07-2011. ISSN 1666-115X.

Foreword

The "5th Thematic Meeting" of the "French Working Group on the Cretaceous" (GFC), organized by Danièle Grosheny and Bruno Granier, was held in Paris from November 30 to December 1st, 2009, on the broad topic "platform to basin correlations". It was attended by 34 people from France, Switzerland, Belgium and Morocco. Twelve communications were presented on subtopics ranging from biostratigraphy to sequence stratigraphy. Invited speaker Philippe Razin from the University of Bordeaux 3 made an outstanding synthesis on the stratigraphic architecture of Lower Cretaceous carbonate platforms of the Sultanate of Oman.

Danièle Grosheny [grosheny@unistra.fr]: *Université de Strasbourg, Institut de Physique du Globe, UMR 7516, 1 rue Blessig, 67084 Strasbourg cedex (France)*; Bruno Granier [bruno.granier@univ-brest.fr]: *Université Européenne de Bretagne, Brest (France); Université de Brest; CNRS; IUEM; Domaines Océaniques UMR 6538, 6 Avenue Le Gorgeu, CS 93837, F-29238 Brest Cedex 3 (France); adresse postale: Département des Sciences de la Terre et de l'Univers, UFR des Sciences et Techniques, Université de Bretagne Occidentale (UBO), 6 avenue Le Gorgeu - CS 93837, F-29238 Brest Cedex 3 (France)*; Nestor Sander: *1916 Temescal Drive, Modesto CA 95355-9171 (USA)*

Abstracts

- Stratigraphic, sedimentological and palaeoenvironmental constraints on the rise of the Urganian platform in the western Swiss Jura, correlation with the Helvetic Zone of the Alps and the Northern Subalpine Chains (Chartreuse, Vercors). *T. Adatte, A. Godet, K.B. Föllmi, S. Bodin, E. De Kaenel, A. Arnaud-Vanneau & H. Arnaud*. 2
- Urganian carbonate platform to Vocontian Basin correlation (France SE) by means of biostratigraphy. *H. Arnaud, A. Arnaud-Vanneau, F. Bastide, G. Massonnat, J. Vermeulen & A. Virgone*. 3
- Expression of the oceanic Anoxic Event 2 in carbonate platform and in hemipelagic basin, example from Mexico and Tibet. *B. Bomou, T. Adatte, K.B. Föllmi, A. Arnaud-Vanneau, M. Caron, A. Tantawy, D. Fleitmann, V. Matera & Y. Huang*. 4
- Impact of meteoric diagenesis on microporous carbonates of the Middle-East. Example from the Mishrif Fm. (Cenomanian - Lower Turonian) of Qatar. *M. D. De Périère, C. Durllet, E. Vennin, B. Caline, L. Lambert, R. Bourillot, C. Maza, E. Poli & C. Pabian-Goyheneche*. 5
- The fluvial-marine transition in genetic sequences of the uppermost Albian ("Vraconnian") of the Moroccan Atlantic Margin (Agadir area). *B. Essafraoui, D. Groshény, N. Icame, S. Ferry, M. Masrour, M. Aoutem, L. Bulot & C. Lecuyer*. 6
- Sequential organization of a fluvial to marine sedimentary wedge (Upper Hauterivian of the Moroccan Atlantic margin). *S. Ferry, M. Masrour & O. Parize*. 7
- Facies partitioning in the prograding genetic sequences of the Subalpine Urganian carbonate platform. Their relationship to the significance given the Urganian Rudistid facies. *S. Ferry, D. Quesne & M. Khaska*. 8
- Stratigraphic ranges of some Tithonian-Berriasian benthic foraminifers and dasycladales. Re-evaluation of their use in identifying this stage boundary in carbonate platform settings. *B. Granier & I.I. Bucur*. 9
- New data on the Hawar, Shu'aiba, Bab, and Sabsab regional stages of the Lower Cretaceous in the United Arab Emirates and in Oman. *B. Granier, R. Busnardo & B. Pittet*. 11
- The Cenomanian-Turonian transition on a W-E transect of the Moroccan Atlantic margin (Agadir). Isotope geochemistry and sequence stratigraphy. *M. Jati, D. Grosheny, S. Ferry & D. Desmares*. 14
- The RGF program (Geologic Reference Map of France): A geodynamic geologic map. *E. Lasseur, L. Beccaletto, Y. Callec, R. Couëffé, F. Paquet, J.-P. Platel, O. Serrano & I. Thinon*. 15
- OAE1a: late Early or early Late Bedoulian event? *M. Moullade, W. Kuhnt, G. Tronchetti, P. Ropolo & B. Granier*. 16
- The Cretaceous carbonate series of the Oman mountains. *P. Razin & C. Grélaud*. 18

STRATIGRAPHIC, SEDIMENTOLOGICAL AND PALAEOENVIRONMENTAL CONSTRAINTS ON THE RISE OF THE URGONIAN PLATFORM IN THE WESTERN SWISS JURA, CORRELATION WITH THE HELVETIC ZONE OF THE ALPS AND THE NORTHERN SUBALPINE CHAINS (CHARTREUSE, VERCORS)

Thierry ADATTE, Alexis GODET, Karl B. FÖLLMI, Stéphane BODIN,
Eric De KAENEL, Annie ARNAUD-VANNEAU & Hubert ARNAUD

Urgonian-type carbonates are a characteristic feature of many late Early Cretaceous shallow-marine, tropical and subtropical environments. The presence of typical photozoan carbonate-producing communities including corals and rudists indicates the prevalence of warm, transparent and presumably oligotrophic conditions in a period otherwise characterised by the high density of globally occurring anoxic episodes. Of particular interest, therefore, is the exploration of relationships between Urgonian platform growth and palaeoceanographic change. In the French and Swiss Jura Mountains, the onset and evolution of the Urgonian platform have been controversially dated, and a correlation with other, better dated successions is correspondingly difficult. It is for this reason that a series of recently exposed sections were sampled (Éclépens, Vaumarcus, Neuchâtel), in addition to the Gorges de l'Areuse section. The stratigraphy and sedimentology of these sections were analysed. Calcareous nannofossil biostratigraphy, the evolution of phosphorus contents of bulk rock, a sequence-stratigraphic interpretation, and a correlation of drowning unconformities with better dated sections in the Helvetic Alps were used to constrain the age of the Urgonian platform. The sum of the data and field observations suggests the following evolution. During the Hauterivian, important outward and upward growth of a bioclastic and oolitic carbonate platform is documented in two sequences, separated by a phase of platform drowning during the late Early Hauterivian. Following these two phases of platform

growth, a second drowning phase occurred during the latest Hauterivian and Early Barremian, which was accompanied by important platform erosion and sediment reworking. The Late Barremian witnessed the renewed installation of a carbonate platform, which initiated with a phase of oolite production, which progressively evolved into an Urgonian-type carbonate production under the inclusion of corals and rudists. This phase terminated at the latest in the middle Early Aptian, due to a further drowning event. The evolution of this particular platform segment is compatible with that of more distal and well-dated segments of the same northern Tethyan platform preserved in the Helvetic zone of the Alps and in the northern subalpine chains (Chartreuse, Vercors).

Key words: Barremian, Early Cretaceous, nannofossil biostratigraphy, phosphorus, sequence stratigraphy, Urgonian, Western Swiss Jura.

Thierry Adatte [thierry.adatte@unil.ch]: *Institut de Géologie et Paléontologie, Université de Lausanne, Anthropôle, 1015 Lausanne (Switzerland)*. Alexis Godet: *Neftex Petroleum Consultants Ltd, 79 Milton Park, Abingdon, Oxfordshire, OX14 4RY (United Kingdom)*. Karl B. Föllmi: *Institut de Géologie et Paléontologie, Université de Lausanne, Anthropôle, 1015 Lausanne (Switzerland)*. Stéphane Bodin: *North Africa Research Group, School of Earth, Atmospheric and Environmental Science, University of Manchester, Williamson Building, Oxford Road, Manchester, M13 9PL (United Kingdom)*. Eric De Kaenel: *DeKaenel Paleo-Research, 2000 Neuchâtel (Switzerland)*. Annie Arnaud-Vanneau: *Université Joseph Fourier, Institut Dolomieu, 15, rue Maurice Gignoux, 38031 Grenoble (France)*. Hubert Arnaud: *Université Joseph Fourier, Institut Dolomieu, 15, rue Maurice Gignoux, 38031 Grenoble (France)*.

URGONIAN CARBONATE PLATFORM TO VOCONTIAN BASIN CORRELATION (FRANCE SE) BY MEANS OF BIOSTRATIGRAPHY

Hubert ARNAUD, Annie ARNAUD-VANNEAU, Fanny BASTIDE, Gérard MASSONNAT,
Jean VERMEULEN & Aurélien VIRGONE

The Vercors is the only one of the northern subalpine massifs of which the outcrop is good enough to have permitted the establishment over a period of more than thirty years of excellent correlations between the Urgonian platform and the Vocontian basin. The hemipelagic facies of the northern border of the Vocontian basin has been dated by ammonites, particularly near surfaces of maximum flooding (mfs). Some of these levels are intercalated in the carbonate facies at the edge of the Urgonian platform. This very favorable juxtaposition permits the unambiguous recognition of the stratigraphic location of certain organisms, in particular that of the benthic foraminifers that inhabited the shallow waters of this platform during the Barremian and Early Aptian.

South of the Vercors a major transgression of which the marls of Font Froide (mfs) are located in the *Gerhardtia sartousiana* zone in the middle portion of the Upper Barremian allows the carbonates of the subalpine carbonates of the Urgonian platform to be divided into two lithologic entities: below the Calcaires de Glandasse Formation (Glandasse Limestones) and above the Formation des Calcaires urgoniens (Urgonian Limestones Formation) where sedimentation under oligotrophic conditions provided fewer nutrients than those obtaining during the Early Barremian. So the lower unit is essentially of Early Barremian age, while the upper one has been dated or attributed to Late Barremian-Early Aptian.

Farther north, detailed analysis of the sections and the Urgonian cliff that can be followed almost continuously for more than a hundred kilometers has permitted, although ammonites are not present, dating the Urgonian Limestones

Formation as Late Barremian - earliest Aptian in the northern Vercors and in the subalpine massifs even farther north. Until recently, this dating could have been questioned because it is based in part on interpretation of sequences and in part on the distribution of orbitolinids that had been established in the southern Vercors and Diois in series dated by ammonites. Recently its validity has been confirmed by the study of the Urgonian limestones of the Gard region.

In the Gard the Urgonian Limestones Formation begins abruptly. It rests on marls (Seynes marls) of which the uppermost levels have been dated by ammonites as being at the top of the Early Barremian (*Coronites darsi* Zone of Vermeulen). Above them, the succession of orbitolinids in the Urgonian limestones of the Gard has been found to be identical to that known for a long time in the northern subalpine massifs.

In addition to the clarification of sequence, from another point of view the correlations established make possible in certain instances the recognition of parasequences allowing a better understanding of the geometric relationships of the deposits that in turn allow a better approach to the paleogeography and evolution of the platform. Furthermore, the platform-basin correlations proposed for the Barremian-Lower Aptian interval, and current geochemical studies will improve our knowledge of climate changes at that time.

Key words: Urgonian platform, Vercors, Gard, Barremian, Early Aptian.

Hubert Arnaud: Association Dolomieu, 18 boulevard Maréchal Leclerc, F-38000 Grenoble (France) ; Annie Arnaud-Vanneau [annie.arnaud@orange.fr]: Association Dolomieu, 18 boulevard Maréchal Leclerc, F-38000 Grenoble (France); Fanny Bastide: TOTAL SA, CSTJF, avenue Larribau, 64018 Pau cedex (France); Gérard Massonnat: TOTAL SA, CSTJF, avenue Larribau, 64018 Pau cedex (France), Jean Vermeulen: Grand'rue, 04330 Barrême (France); Aurélien Virgone: TOTAL SA, CSTJF, avenue Larribau, 64018 Pau cedex (France)

EXPRESSION OF THE OCEANIC ANOXIC EVENT 2 IN CARBONATE PLATFORM AND IN HEMIPELAGIC BASIN, EXAMPLE FROM MEXICO AND TIBET

Brahimsamba BOMOU, Thierry ADATTE, Karl B. FÖLLMI, Annie ARNAUD-VANNEAU, Michèle CARON, Abdel TANTAWY, Dominik FLEITMANN, Virginie MATERA & Yongjian HUANG

The majority of the published sections that span the Cenomanian-Turonian oceanic anoxic event when production of black shale was at a maximum concern the Atlantic, western Tethys and Western Interior (Kerr, 1998). The deposition of these black-shales is the result of an interruption of normal pelagic sedimentation by several discrete episodes of widespread oceanic anoxia (Schlanger & Jenkyns 1976, Jenkyns 1980, Arthur et al. 1990) that coincide with a positive excursion of the ^{13}C isotope. Several studies show that the onset of this anoxia called the OAE2 event was triggered by a short-lived but significant increase in the burial of phosphorus (Mort et al. 2007). This increase caused bottom waters to become anoxic as the sea floor became a source of P rather than a recipient for it, with its continuity maintained by a positive feedback loop. On a larger scale, away from the main depocenters of black shale, the behaviour of Total Phosphorus (P_{tot}) and trace metals in different paleogeographies and paleodepths is still poorly known. Here we discuss the expression of this OAE2 event in the outer shelf/slope environment of northern Tibet and in the shallow carbonate platform of central Mexico.

The Gongzha section (Tibet, China) is at the north margin of the Indian plate (SE Tethys). It consists of a succession of monotonous hemipelagic marly limestones. ^{13}C data exhibit the classical C-T positive shift. Significant peaks in P_{tot} occur at the onset of the shift, followed by a depletion at the end of *R. cushmani* zone that persists up to the end of the *W. archaeocretacea* zone. A similar P maximum and decrease is observed in the western Tethys and central Atlantic sections, so it appears to be global, coinciding in part with increased detrital inputs. At Gongzha, trace-metals contents are less than the background level of sections in which anoxic conditions are strong. Redox sensitive elements such as Va, Ni, Co, U, generally indicative of anoxic conditions, do not increase during the ^{13}C shift, suggesting that dysoxic rather than anoxic conditions prevailed in the Tibet area during OAE2. The Axaxacualco and Barranca El Cañon sections are on the Guerrero-Morelos carbonate platform in southern Mexico. Their ^{13}C curves can be correlated. In the distal part of the carbonate platform at Axaxacualco, the

maximum ^{13}C positive excursion coincides with oligotrophic carbonate platform environments, characterized by an abundant and diversified benthic microfauna and rudists, and low concentrations of P_{tot}. The impact of OAE appears to be more significant in the proximal part of the carbonate platform at Barranca, where it is associated with the deposition of thick laminated microbialites indicative of mesotrophic conditions. Oligotrophic to mesotrophic conditions persisted on the Morelos Carbonate platform and throughout the entire OAE2 in Central Mexico despite the proximity of the Caribbean plateau. Definitive drowning, marked by the deposition of black shale and turbidite, occurs only in the lower Turonian (*P. flexuosum* zone), well above the end of the $\delta^{13}\text{C}$ shift.

Key words: Carbonate platform, hemipelagic basin, OAE 2, geochemistry, Cenomanian-Turonian, Mexico, Tibet.

REFERENCES

- Arthur M.A., Jenkyns H.C., Brumsack H.J. & Schlanger S.O., 1990. Stratigraphy, geochemistry and paleoceanography of organic carbon-rich Cretaceous sequences. *In: Ginsburg R.N. & Beaudoin B. (eds.): Cretaceous resources, events and rhythms. NATO ASI Series C304: 75-119.*
- Jenkyns H.C., 1980. Cretaceous anoxic events: from continents to oceans. *Journal of the Geological Society* **137**: 171-188.
- Kerr A.C., 1998. Oceanic plateau formation: a cause of mass extinction and black shale deposition around the Cenomanian-Turonian boundary? *Journal of the Geological Society* **155**: 619-626.
- Mort H., Adatte T., Föllmi K., Keller G., Steinmann P., Matera V., Berner Z. & Stüben D., 2007. Phosphorus and the roles of productivity and nutrient recycling during Oceanic Anoxic Event 2. *Geology* **35**: 483-486.
- Schlanger S.O. & Jenkyns H.C., 1976. Cretaceous anoxic events: causes and consequences. *Geologie en Mijnbouw* **55**: 179-184.

Brahimsamba Bomou [brahimsamba.bomou@unil.ch]: Institute of Geology and Paleontology, University of Lausanne, Unil-Dorigny, Anthropole, CH-1015 Lausanne, (Switzerland); Thierry Adatte: Institute of Geology and Paleontology, University of Lausanne, Unil-Dorigny, Anthropole, CH-1015 Lausanne, (Switzerland); Karl B. Föllmi: Institute of Geology and Paleontology, University of Lausanne, Unil-Dorigny, Anthropole, CH-1015 Lausanne, (Switzerland); Annie Arnaud-Vanneau [annie.arnaud@ujf-grenoble.fr]: Institut Dolomieu, 15 rue M. Grignoux, 38031 Grenoble, (France); Michèle Caron: Geosciences departement, University of Fribourg, Chemin du Musée 6, CH-1700 Fribourg (Switzerland); Abdel Tantawy: Geology department, Aswan Faculty of Science, South Valley University, 81528 Aswan (Egypt); Dominik Fleitmann: Institute of Geological Sciences, University of Bern, Baltzerstrasse 1-3, CH-3012 Bern (Switzerland); Virginie Matera: Institut of Hydrogeology, University of Neuchâtel, rue Emile Argand 11, CH-2000 Neuchâtel (Switzerland); Yongjian Huang: Institute of Sedimentology, Chengdu University of Technology, Erxianqiao, Chengdu 610059, Sichuan (China).

IMPACT OF METEORIC DIAGENESIS ON MICROPOROUS CARBONATES OF THE MIDDLE-EAST. EXAMPLE FROM THE MISHRIF FM. (CENOMANIAN - LOWER TURONIAN) OF QATAR

Matthieu Deville DE PÉRIÈRE, Christophe DURLET, Emmanuelle VENNIN, Bruno CALINE, Laurent LAMBERT, Raphaël BOURILLOT, Carine MAZA, Emmanuelle POLI & Cécile PABIAN-GOYHENECHÉ

The marine carbonates of the Mishrif Formation (Middle Cenomanian - Lower Turonian) were deposited in shallow, low energy ramp environments, before the fall of the eustatic level during the Middle Turonian. Depositional environments change laterally from an internal ramp facies to the more open facies of a median ramp. These facies are associated locally with very shallow, higher energy rudistid biostromes. In the predominating micritic facies (mudstones and floatstones) the vertical and lateral heterogeneity of petrophysical properties (porosity, permeability, the distribution of pore sizes) seem to be linked closely to variations in the microtexture of the micritic matrix. Microporosity is relatively uniform, high (up to 35% porosity) and may represent up to 98% of the total porosity measured in plugs. Permeability is low (less than 1 mD) to moderate (up to 100 mD).

Use of cathodoluminescence (CL) and a scanning electron microscope (SEM) on 240 samples, as well as spaced isotopic analyses permitted identification of the sedimentologic and diagenetic factors that controlled variations in the microtexture of micritic matrices as well as the associated reservoir properties associated with them.

Our results show two poles of micronitic organization (each with its own crystalometry, luminescence and petrological properties) that can be discriminated:

(A) The micritic facies with the best permeabilities (up to 100 mD) as well as the largest mean-size pore throats (more than 0.5 μm) are generally coarse micrites (crystal size more than 2 mm) that are poorly sorted and but slightly luminescent under CL. These micrites are associated both spatially and chronologically with a early diagenesis indicating the development of a zone of high energy (up to 30 m thick in the axial region of the field) sited below the mid-Turonian discontinuity. These diagenetic phases are (1) endoklastic cavities, (2) low magnesian calcites (LMC), weakly luminescent and with minor of ^{18}O and ^{13}C , (3) intervals of corrosion between the different phases of calcite. In the Vadose zone the development of coarse

micrites with low luminescence is explained by the early dissolution of fine aragonite and magnesian calcite (HMC) with the concomitant development of overgrowths on the LMC particles (phenomena of Ostwald ripening).

(B) Under the zone of high energy most of the micritic facies have low permeabilities and very small pore throats (respectively less than 10 mD and 0.5 μm). The particles of micrite are fine (less than 2 μm) fairly well sorted and luminescent under CL. This micritic group is spatially and chronologically associated with a later development of luminescent calcite crystals (probably precipitated under a moderate depth of cover and locally with a high concentration of pyrite, pseudomorphs of sulfates and positive ^{13}C values. The micrite particles are generally polyhedral and only rarely show important traces of dissolution. This grouping of micrites may then be explained by a slower mineralogic stabilization with the neomorphism of metastable particles (aragonite and HMC). This phenomenon may have taken place in waters low in oxygen content, probably after the deposition of the Laffan shales (uppermost Turonian - Lower Coniacian) which seals the Mishrif reservoir.

The initial distribution of certain sediments influenced the dichotomous distribution of these two micritic groups. The sediments initially the finest and most argillaceous (deposited in the calmest environments) hindered the renewal of meteoric waters and caused a confinement capable of delaying the mineralogic stabilization of fine particles in HMC and in aragonite. Consequently, these micrites were more affected by pressure-dissolution during burial, thus altering their reservoir properties. On the other hand the coarsest bioclastic sediments favored the drainage of meteoric waters and so favored the genesis of permeable micrites toward the coarser pole.

Key words: diagenesis, microporosity, micrite, Upper Cretaceous, Middle-East.

THE FLUVIAL-MARINE TRANSITION IN GENETIC SEQUENCES OF THE UPPERMOST ALBIAN ("VRACONNIAN") OF THE MOROCCAN ATLANTIC MARGIN (AGADIR AREA)

Badre ESSAFRAOUI, Danièle GROSHÉNY, Nourrisaid ICAME, Serge FERRY, Moussa MASROUR, Mohamed AOUTEM, Luc BULOT & Christophe LECUYER

Four sections correlated in detail and together covering about 100 km extend inland from the present-day coast at Taghazoute north of the Agadir City to the lower slopes of the High Atlas Mountains (Tamaloukt/Afansou north of the Taroudant Town). They examine the so-called "Vraconnian bar" (uppermost Albian) of authors in order to clarify the relationships between marine and fluvial facies in the 6 to 8 short-term depositional sequences (genetic sequences) that comprise the sedimentary wedge at the Albian - Cenomanian (A - C) transition. In all these sequences fluvial aggradation is concurrent with the seaward shift of the beach facies in a regime of stepped forced regression. The fluvial facies is thus the upper regressive half-cycle of the transgressive-regressive (T/R) sequence. Work in progress shows that this relationship holds for the overlying Cenomanian sequences, and in the same area for the upper Hauterivian Talmest Fm. (see Ferry et al., this

volume). One major findings of this study is that despite the absence of biostratigraphic markers, it offers the possibility of making very precise stratigraphic correlations between beach facies in the distal area, and red fluvial facies upslope.

The "Vraconno" - Cenomanian successions discussed herein include several intercalations of gypsum between the regressive beach facies and the red continental shales. These lagoonal evaporites do not occur in the Hauterivian successions seen along the same transect so it is possible that the climate became more humid as the Cretaceous period approached its end.

Work done as part of the "Volubilis" cooperative programme between France and Morocco HC MA/09/208).

Key words: Morocco, Cretaceous, Albian, sequence stratigraphy, fluvial-marine transition.

Badre Essafroui [badre.essafroui@gmail.com]: Université Ibn Zohr, Faculté des Sciences, Laboratoire de Géologie Appliquée et Geo Environnement (LAGAGE), BP 8106, Agadir (Morocco); Danièle Groshény [grosheny@unistra.fr]: Université de Strasbourg, Institut de Physique du Globe, UMR 7516, 1 rue Blessig, 67084 Strasbourg cedex (France); Nourrisaid Icame [ns_icame@yahoo.fr]: Université Ibn Zohr, Faculté des Sciences, Laboratoire de Géologie Appliquée et Geo Environnement (LAGAGE), BP 8106, Agadir (Morocco); Serge Ferry [serge.ferry@univ-lyon1.fr]: Université de Lyon, Faculté des Sciences et Technologies, UMR 5125, 43 Bd du 11 Novembre, 69622 Villeurbanne cedex (France); Moussa Masrour [moussamasrour@yahoo.fr]: Université Ibn Zohr, Faculté des Sciences, Laboratoire de Géologie Appliquée et Geo Environnement (LAGAGE), BP 8106, Agadir (Morocco); Mohamed Aoutem [aoutem@yahoo.fr]: Université Ibn Zohr, Faculté des Sciences, Laboratoire de Géologie Appliquée et Geo Environnement (LAGAGE), BP 8106, Agadir (Morocco); Luc Bulot [LucGBulot@aol.com]: Université de Provence Aix-Marseille 1, Géologie des Systèmes Carbonatés, EA 4234, Centre de Sédimentologie- Paléontologie, 13331 Marseille Cedex (France); Christophe Lecuyer [christophe.lecuyer@univ-lyon1.fr]: Université de Lyon, Faculté des Sciences et Technologies, UMR 5125, 43 Bd du 11 Novembre, 69622 Villeurbanne cedex (France).

SEQUENTIAL ORGANIZATION OF A FLUVIAL TO MARINE SEDIMENTARY WEDGE (UPPER HAUTERIVIAN OF THE MOROCCAN ATLANTIC MARGIN)

Serge FERRY, Moussa MASROUR & Olivier PARIZE

An Upper Hauterivian sedimentary wedge, the Talmest Formation, has been mapped by eighteen correlated sections from its marine expression in the west on the coast up to its fully continental facies in the central High Atlas in the east, a distance of about 200 km. The section of the Insouane-Amizmiz transect reveals in detail how fluvial aggradation in the Tamest Fm. follows the forced strong regression of beach deposits at the upper limit of the Loryi Zone. The red beds then retreat in four major steps during the upper Hauterivian before Barremian - Aptian flooding. Each step comprises a set of aggrading genetic T/R sequences. In all of them fluvial aggradation as a meandering fluvial cycle occurs during the regressive phase and results in the progradation of distal red clays on

the sands and calcareous deposits of the beach facies. This sequence demonstrates that the "Exxon" model of sequence stratigraphy is completely valid at the parasequence level (fluvial aggradation is caused by the seaward displacement of the "bayline"). This concept is not new for it was formulated by Élie de Beaumont during the mid-19th century. Consequently, we must disagree with the "transgressive" concept of fluvial aggradation used in some applications of genetic stratigraphy (Cross, Homewood, Guillocheau).

Key words: Morocco, Cretaceous, sequence stratigraphy, fluvial-marine transition.

Serge Ferry [serge.ferry@univ-lyon1.fr]: Université de Lyon, Faculté des Sciences et Technologies, UMR 5125), 43 Bd du 11 Novembre, 69622 Villeurbanne cedex (France); Moussa Masrouir [moussamasrouir@yahoo.fr]: Université Ibn Zohr, Faculté des Sciences, Laboratoire de Géologie Appliquée et Geo Environnement (LAGAGE), BP 8106, Agadir (Morocco); Olivier Parize [olivier.parize@areva.com]: AREVA-NC, Exploration Dpt., Geosciences Technologies, Tour Areva, 92084 Paris-La Défense (France)

FACIES PARTITIONING IN THE PROGRADING GENETIC SEQUENCES OF THE SUBALPINE URGONIAN CARBONATE PLATFORM. THEIR RELATIONSHIP TO THE SIGNIFICANCE GIVEN THE URGONIAN RUDISTID FACIES

Serge FERRY, Didier QUESNE & Mahmoud KHASKA

The succession of facies and the geometric relationships of the genetic units that constitute the limestone cliffs of the Archiane area (southern Vercors) again brings into question the validity of the classical concept of an 'Urgonian sequence' in which calcarenitic, coral-reef and rudistid facies are taken to be contemporaneous (Quesne & Ferry 1995, Quesne 1998, Quesne et al. 2006). On the contrary, the calcarenites are formed during a lowstand when the width of transgression is minimal and are overlain by a platform facies during the subsequent highstand when coral and rudistid facies occupy a broader area, either the entire platform or a large part of it. This coral-rudistid facies is interpreted as having been deposited at moderate depths (?20-30 m), by an open advancing sea and not as an inner platform facies protected by outer calcarenitic shoals, as the current interpretation would have it.

In our view, the "outer" calcarenites represent a seaward border of swell-dominated deposits which precede the true Urgonian facies that we take to be open-marine deposits. Because of the lowstand, the rudistid limestones are exposed, so a true boundary thus exists in any genetic sequence. This boundary is at the base of the calcarenites at the edge of the platform, and at the upper limit of the exposed rudistid facies on the platform. The fact that the open-marine flooding facies is terminated by a surface demonstrating emergence is explained by the extremely low gradient of the platform profile which does not accommodate a prograding "highstand wedge" that is commonly emplaced during the first stages of a lowering of sea level. The classical "Urgonian sequence" is thus based on a mistaken application of Walther's law because all the facies involved do not coexist at any one period of time.

The high frequency sequences in the Archiane area are also found in the low-angled progradational

clinoforms studied along the eastern cliff-face of the Vercors plateau between Grenoble and Archiane (Khaska 2008). The "outer" "peri-Urgonian" calcarenites of some authors do not represent shoals that protected an inner platform rudistid facies. They are lowstand wedges laid down at the time when the open-marine rudistid platform was exposed.

Key words: SE France, Cretaceous, Barremian, Urgonian, sequence stratigraphy.

REFERENCES

- Khaska M., 2008. Analyse de la progradation de la plateforme urgonienne du Vercors (Sud-Est de la France). *Mémoire Mastère 2, Université Claude Bernard - Lyon I* (unpublished).
- Quesne D. & Ferry S., 1995. Detailed relationships between platform and pelagic carbonates (Barremian, SE France). *In: House M.R. & Gale A.S. (eds.): Orbital forcing timescales and cyclostratigraphy. Geological Society of London special publication* **85**: 165-176.
- Quesne D., 1998. Propositions pour une nouvelle interprétation séquentielle du Vercors méridional. *Bulletin de la Société géologique de France* **169(4)**: 537-546.
- Quesne D. & Benard D., 2006. Interprétations nouvelles sur les relations entre calcarénites et calcaires à rudistes du Barrémien inférieur dans le Vercors méridional (sud-est de la France). *Geodiversitas* **28(3)**: 421-432.

Serge Ferry [serge.ferry@univ-lyon1.fr]: Université de Lyon, Faculté des Sciences et Technologies, UMR 5125), 43 Bd du 11 Novembre, 69622 Villeurbanne cedex (France); Didier Quesne [Didier.Quesne@u-bourgogne.fr]: Université de Bourgogne, UFR Sciences de la Terre et Environnement, UMR 5561, 6, Bd Gabriel, 21100 Dijon (France); Mahmoud Khaska [MahmoudKhaska@unimes.fr]: Université de Nîmes, Laboratoire de Géochimie Isotopique Environnementale CEREGE - UMR 6635, 150 rue Georges Besse, 30035 Nîmes Cedex 1 (France).

STRATIGRAPHIC RANGES OF SOME TITHONIAN-BERRIASIAN BENTHIC FORAMINIFERS AND DASYCLADALES. RE-EVALUATION OF THEIR USE IN IDENTIFYING THIS STAGE BOUNDARY IN CARBONATE PLATFORM SETTINGS

Bruno GRANIER & Ioan I. BUCUR

INTRODUCTION

This review is dedicated to our late colleagues É. Fourcade (specialist of large benthic foraminifers) and M. Jaffrezo (expert on dasycladalean algae), who in 1973 (*in Benest et al. 1973*) published a first attempt to make use of these forms for boundary resolution at this level. It deals only with species of which the FAD (First Appearance Datum) or LAD (Last Appearance Datum) are near the Tithonian-Berriasian boundary or has been reported as being so.

BENTHIC FORAMINIFERS

Anchispirocyclina lusitanica (Egger) was formerly considered the best marker of the Tithonian for its range was thought to be restricted to this Jurassic stage. However its find by Galbrun et al. (1990) in the M18 and M18n of the Bias do Norte section (Portugal) documented its occurrence in strata of earliest Berriasian age.

Stratigraphic ranges of the foraminifers cited below either span the boundary {*Mohlerina basiliensis* (Mohler) [formerly *Conicospirillina basiliensis* Mohler], *Pseudocyclammina lituus* (Yokohama), *Feurtillia frequens* Maync} or their LAD is well below the upper limit of the Tithonian {*Kurnubia palastiniensis* Henson, *Everticyclammina virguliana* (Koechlin)}, or their FAD is far above the lower limit of the Berriasian {*Pseudotextulariella courtionensis* Brönnimann, *Pfenderina neocomiensis* (Pfender)}. Although not considered by Fourcade (*in Benest et al. 1973*) *Protepenneroplis striata* Weynschenk is a long-ranging species (it appears in the Aalenian) that in the current state of knowledge terminates in the Late Tithonian and hence should not be overlooked. A second representative of *Protepenneroplis*, *P. trochangulata* Septfontaine [Remark: according to one of us (I.I.B.), this species is a junior synonym of *Hoeglundina* (?) *ultragranulata* Gorbatchik] is another long-ranging species (extinct in the Barremian according to Bucur 1993) that should merit our attention. Its first appearance seems to be Early Berriasian although Heinz & Isenschmid (1988) tentatively correlated the strata containing this microfossil with basinal Tithonian strata. On the basis of this indirect dating, some authors presume *P. trochangulata* has appeared in the Late Tithonian. However, we retain the Berriasian FAD as a working hypothesis. If it is correct the find of an assemblage with both *P. trochangulata* and *Anchispirocyclina lusitanica* in Crimea, Ukraine (Granier et al. 2009), would necessitate the assignement of an Early Berriasian age to these strata. The poorly known *Dobrogelina ovidi* Neagu that spans the Berriasian and Valanginian stages (Krajewski & Olszewska, 2007) is another species with some biostratigraphical potential for it too is in the Crimean assemblage. There are some limitations on the use of the

benthic foraminifers, among which is endemism (for instance *Pavlovecina* [formerly *Keramosphaera*] *allobrogensis* (Steinhauser et al.)) and paleoenvironmental constraints (*Protepenneroplis trochangulata* is found in high-energy, commonly transgressive, environments).

As Benest et al. (1973) did earlier we conclude that: ... “il ne paraît pas possible de fixer la limite entre ces deux étages en utilisant ce groupe d'organismes” [*translation*: it does not appear possible to set the boundary between these two stages using this group of organisms].

DASYCLADALES

Jaffrezo (*in Benest et al. 1973*) deals only with 6 key species:

(1) *Campbelliella* [formerly *Vaginella*] *striata* (Carozzi) spans both the Kimmeridgian and the Tithonian; it becomes extinct before the Tithonian ends.

(2) The well known *Clypeina sulcata* (Alth), formerly called *C. jurassica* Favre (a “misleading” name), appears in the Kimmeridgian and dies out in the Berriasian well before the stage ends.

(3) *Salpingoporella annulata* Carozzi is a long ranging species known from both the Tithonian and below and from the Berriasian and above.

(4) *Selliporella* [formerly *Triploporella*?] *neocomiensis* (Radoi i), a rare species, was thought to be restricted to the Berriasian until its find in Tithonian strata in association with *Campbelliella striata*.

(5) Similarly *Zergabriella* [formerly *Macroporella*] *embergeri* (Bouroullec & Deloffre), a species characteristic of innermost platform settings, was thought to be restricted to Berriasian and Lower Valanginian strata until its find in Tithonian strata in association with *Anchispirocyclina lusitanica*.

(6) The Rajkaella group with the species “*Goniolina minima* Jaffrezo” and “*Kopetdagaria iailaensis* Maslov” was considered Middle-Late Berriasian and Early Valanginian in age. The find of *Rajkaella iailaensis* in its type area in association with the foraminifers: *Dobrogelina ovidi*, *Protepenneroplis trochangulata* and *Anchispirocyclina lusitanica*, documents its occurrence in lowermost Berriasian strata (Granier et al. 2009).

With respect to the three later forms, Benest et al. (1973) conclude that: ... “il semble nécessaire d'indiquer que ces Algues sont pour la plupart de description récente et que leur répartition, tant stratigraphique que géographique, est peut-être encore mal connue” [*translation*: it appears necessary to indicate that most of these Algae were described recently and that both their stratigraphic and geographic distributions are perhaps still poorly known]. If this is so, we can extend this conclusion to species not considered by Jaffrezo (*in Benest et al. 1973*). For instance: *Salpingoporella* (*Hensonella*) *dinarica* Radoi i was known

only from the Hauterivian-Aptian interval until its find in Lower Berriasian strata (Granier 2002, 2008). *Otternstella* [formerly *Heteroporella*] *lemmensis* (Bernier) was first thought to be restricted to Kimmeridgian and Tithonian strata, but there are several records of it in Berriasian strata. In addition, the understanding of the structure of most of them has been significantly revised: the revised genus *Heteroporella* Pratulon -to which *H. lemmensis* Bernier was originally ascribed- now has only one representative, its type-species *H. lepina* (Pratulon).

The list of species erected by Jaffrezo (*in* Benest et al. 1973) should be supplemented. A new list would include *Macroporella ? pratuloni* Dragastan, a form characteristic of high energy environments and apparently restricted to Berriasian and Lower Valanginian strata.

CONCLUSION

The definition of biozones using benthic foraminifers and dasycladales together demands further investigation. There are few paleontological "tools" available to define the Tithonian-Berriasian boundary in carbonate platform/ramp settings. Very few species end at, or appear first near the boundary, and many species span it. This conclusion does not dispute our understanding of this stage boundary but questions the current view of the criteria used to define the Jurassic-Cretaceous systems boundary in non-basinal settings.

ERRATUM

Some time after the Thematic Meeting of the GFC took place the first author (B.G.) received a reprint of a newly published paper by Gawlick & Schlagintweit (2009) in which the authors report the co-occurrence of "*Protopenneroplis ultragranulata* (Gorbachik, 1971)" and a calpionellid assemblage which characterizes zone A: *Calpionella alpina* Lorenz and *Crassicollaria intermedia* (Durand-Delga). Consequently the transition from the ancestral *Protopenneroplis striata* Weynschenk to its descendant *P. trochangulata* Septfontaine [? = *Protopenneroplis ultragranulata* (Gorbachik)] seems to have occurred in latest Tithonian times, not in the earliest Berriasian as postulated previously.

REFERENCES

Benest M.-C., Coiffait P., Fourcade É. & Jaffrezo M., 1973. Essai de détermination de la limite Jurassique-Crétacé par l'étude des microfaciès dans les séries de plate-forme du domaine méditerranéen occidental. *In*: Colloque sur la

limite Jurassique-Crétacé (Lyon, Neuchâtel, septembre 1973). *Mémoires du B.R.G.M.* **86**: 169-181.

Bassoullet J.-P. & Fourcade É., 1979. Essai de synthèse de répartition de foraminifères benthiques du Jurassique carbonaté mésogéen. *C.R. sommaire de la Société géologique de France* **2**: 69-71.

Bucur I.I., 1993. Les représentants du genre *Protopenneroplis* Weynschenk dans les dépôts du Crétacé inférieur de la zone de Resita-Moldova Noua (Carpathes méridionales, Roumanie). *Revue de Micropaléontologie* **36**(3): 213-223.

Galbrun B., Berthou P.-Y., Moussin C. & Azéma J., 1990. Magnétostratigraphie de la limite Jurassique-Crétacé en faciès de plate-forme carbonatée: la coupe de Bias do Norte (Algarve, Portugal). *Bulletin de la Société géologique de France* (8e série) **4**(1): 133-143.

Gawlick H.J. & Schlagintweit F., 2009. Revision des Tressensteinkalkes: Neuinterpretation der späten Ober-Jura- bis ?Unter-Kreide-Entwicklung des Plattform-Becken-Überganges der Plassen-Karbonatplattform (Österreich, Nördliche Kalkalpen). *Journal of Alpine Geology* **51**: 1-30.

Granier B., 2002. Algues dasycladales, nouvelles ou peu connues, du Jurassique supérieur et du Crétacé inférieur du Moyen-Orient. *In*: Bucur I.I. & Filipescu S. (eds.): Research advances in calcareous algae and microbial carbonates. *Proceedings of the 4th IFAA Regional Meeting, Cluj-Napoca*, August 29 - September 5, 2001: 103-113.

Granier B., 2008. Holostratigraphy of the Kahmah regional Series in Oman, Qatar, and the United Arab Emirates. *Carnets de Géologie - Notebooks on Geology*, **CG2008_A07**: 1-33.

Granier B., Bucur I.I., Krajewski M. & Schlagintweit F., 2009. Calcareous algae from the Yaila Series near Bilohirsk (Crimea, Ukraine). *In*: 6th Regional Symposium of the International "Fossil Algae" Association, Milan (July 1st-5th). *Museologia Scientifica e Naturalistica Volume Speciale* **2009**: 30.

Heinz R.A. & Isenschmid C.H., 1988. Microfazielle undstratigraphische Untersuchungen im Massivkalk (Malm) der Préalpes médians. *Eclogae geologicae Helveticae* **81**(1):1-62.

Krajewski M. & Olszewska B., 2007. Foraminifera from the Late Jurassic and Early Cretaceous carbonate platform facies of the southern part of the Crimea Mountains; Southern Ukraine. *Annales Societatis Geologorum Poloniae* **77**: 291-311.

Key words: Tithonian, Berriasian, foraminifers, algae.

NEW DATA ON THE HAWAR, SHU'AIBA, BAB, AND SABSAB REGIONAL STAGES OF THE LOWER CRETACEOUS IN THE UNITED ARAB EMIRATES AND IN OMAN

Bruno GRANIER, Robert BUSNARDO & Bernard PITTET

INTRODUCTION

The boundaries of most regional stages of the Kahmah and Wasia regional series have been recently revised (Granier 2000, 2008, Granier et al. 2003). However some authors (most of them employees of the oil industry or service companies) persist in duplicating either wrong or obsolete information and unsupported interpretations derived therefrom.

HAWAR*

To comply with nomenclatural rules regarding stages, Hawar should be supplemented by an 'ian' ending, i.e. Hawarian. But since the designation Hawar was agreed on more than two decades ago, this rule has been ignored by the petroleum industry operating in the Middle East. This non-compliance applies to most oil-industry-named stages there. Here an asterisk following the name of each stage indicates the omission of an 'ian' termination.

In the ADMA offshore field 'A', the base of the Hawar, the oldest of the four units discussed here, is a karstified surface: vugs found in the uppermost level of the underlying Kharaiab are due to the subaerial dissolution of formerly aragonitic rudist shells and are partially filled with sediment (Granier 2000, 2008, Granier et al. 2003, P. Skelton, pers. comm. 2009). In the ADMA reference well (see Granier 2008: fig. 9), the Hawar sequence is 7.6 m thick: most of it is the TST while the uppermost 0.8 m, a shaly interval, represents the HST. Keystone vugs (see Granier 2008: pl. 3: E) at the base of the TST are indicative of a beach deposit; the remainder of the systems tract consists predominantly of offshore carbonate-sand deposits with abundant *Palorbitolina* (including *P. cf. ultima*, see Schroeder et al. 2007). *Choffatella decipiens*, a foraminifer that after Early Barremian times became a marker of deeper-water environments, is found in the upper half of the systems tract. Consequently both facies and fossil assemblages record a deepening of the succession. The maximum flooding surface is thought to be just above a glauconitic packstone bed (see Granier 2008: pl. 3: F). As stated by Granier (2008): "The upper limit of the Hawar Formation is coincident with an abrupt change in sedimentation from the uppermost shale (characteristic of open-marine environments and deposited below storm-wave base) to very shallow-water carbonates (with a rich photophylic algal association characteristic of shallow protected environments). As does the lower boundary, the upper one records a forced regression: the fall in sea level can be estimated to have been 40 meters or more". To date most authors (Azer & Toland 1993, Boichard et al. 1994, Sharland et al. 2001, van Buchem et al. 2002) have not recognized the existence of this major sequence boundary. In Oman, at Wadi Bani Kharus (van Buchem et al. 2002, Pittet et al. 2002), the Hawar interval is 25 m thick (i.e., it is

more than triple that of the equivalent section in the ADMA well). With respect to paleogeographical settings this Omani locality was considered to have been sited in a sea shallower than that over the Emirati oil field (which is in the earlier "Kharaiab 2" and the later "Bab" basins). While revising a set of thin sections from Wadi Bani Kharus, one of us (B.G.) found *Choffatella decipiens* in the lowermost 5 m of the unit. Consequently this level records the deeper-water facies of an interval spanning not only the Hawar but also the next term in the succession, the Shu'aiba. This find confutes the sequential interpretations of authors who consider the Hawar comprising the entire TST or being the lower part of the TST of a higher scale sequence that extends into the Shu'aiba (Sharland et al. 2001, van Buchem et al. 2002, Strohmenger et al. 2004, 2006; see Granier et al. 2003: fig. 2, Granier 2008: fig. 10). We suggest that in the Omani outcrop the maximum flooding surface of the Hawar sequence is at about the 5 m level in a marly layer with the highest shaliness (Fig. 1).

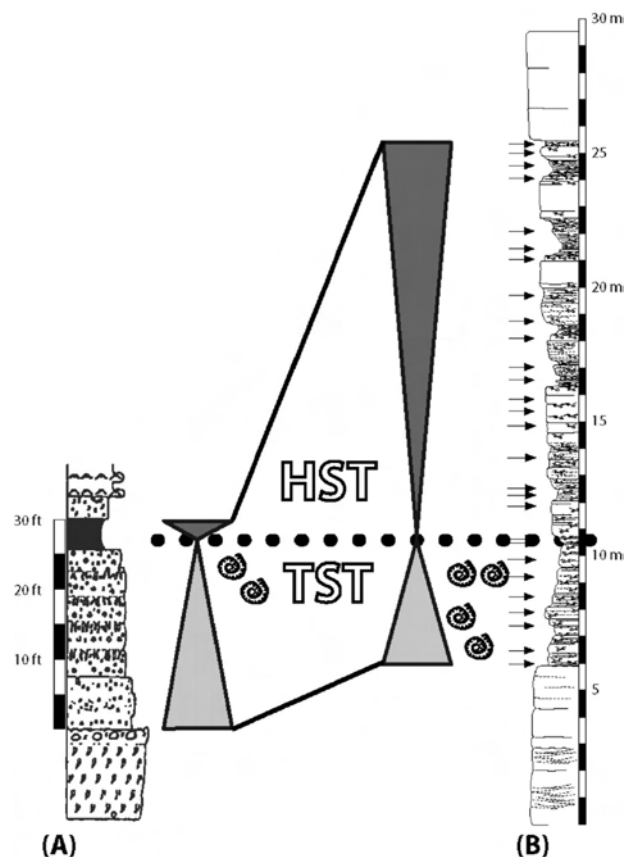


Figure 1: Correlation of the Hawar sequence from the Abu Dhabi offshore (field "A", left column), with that of the Oman Mountains (Wadi Bani Kharus, right column). Paleogeographically, the section of field "A" was sited in an area deeper bathymetrically than that of the Wadi Bani Kharus succession.

SHU'AIBA* (SHUAIBAIAN)

In field 'A', offshore Abu Dhabi, the Shua'iba succession begins with a facies characteristic of protected shallow-water (Granier et al. 2003) with aragonitic 'calcareous algae', such as *Clypeina ummshaiensis* (Granier 2002: pl. I: 2, 2008: pl. 3: B), *Gyroporella lukicae* and *Cylindroporella lyrata* among others and foraminifers, such as *Voloshinoides murgensi*. It is succeeded by a set of facies that contain *Choffatella decipiens*, *Epistominids* (Granier 2008: pl. 4: B) and planktonic foraminifers, all confirming the overall deepening-upward trend of the remainder of the section, a 18.3 m thick interval representing the TST of the Shu'aiba sequence. Two ammonite-rich subnodular beds that represent the highly condensed HST (less than 0.9 m thick) end the sequence. Ammonites (Busnardo & Granier work in progress) of the genera *Chelonicerias*, *Gargasicerias* and *Pseudohaploceras* indicate a Gargasian (middle Aptian) age for this HST. In Oman, in wells Dhulaima-5 and Yibal-201, the record by Witt & Gökgag (1994: pl. 10.1: 8 and 10) of *Orbitolina* (*Mesorbitolina*) *parva* from correlative shallow-water facies provide additional evidence for disregarding the assignment of a Bedoulian (Early Aptian) age to these strata.

BAB* (BABIAN)

Still in field 'A' the Bab interval begins and ends with dark-colored organic-rich chinks (respectively ~7.6 m and ~6.1 m thick). The lower interval rests on the condensed section of the Shu'aiba, the upper interval predates the transgressive shaly facies of the Sabsab / Nahr Umr. Both episodes of anoxic sedimentation were probably caused by eustatic isolation of the "Bab" intrashelf basin. Depending on their location, surrounding contemporaneous carbonate platforms record either one or two falls in relative sea-level (Granier 2000: fig. 3, 2008: fig. 18, Granier et al. 2003: fig. 21). Between these LST episodes a rise in sea-level (TST + HST) led to a temporary interruption of anoxia and to the sedimentation of beige chalk facies (the main constituent of these chinks is nannoconids). The lower LST facies yields *Colombicerias* although the remainder of the Bab includes representatives of the genera *Chelonicerias*, *Epicheloniceras* and *Pseudohaploceras* (Busnardo & Granier, work in progress).

SABSAB* (SABSABIAN)

The Sabsab records a main transgressive event at the base of the Nahr Umr shales. This unit caps both the Shu'aiba and the Bab carbonate platforms and is a major seal for lower "mid-Cretaceous" oil reservoirs in the area. The record of *Orbitolina* (*Mesorbitolina*) *texana* (Roemer) by Witt & Gökgag (1994: pl. 10.1: 7, 9) from shallow-water facies in wells Lekhwair-87 and 69, should be taken cum grano salis for they were found not more than 2 m below the top of their so-called Shu'aiba. This interval could have been deposited above the subaerial surface of the exposed Shu'aiba and represent sedimentation that took place after a significant hiatus and including a period of time equivalent to the Sabsab.

CONCLUSIONS

With respect to stratonomy, both the Hawar and the

Shu'aiba sequences in field 'A' are highly asymmetrical: thick TST and thin HST; at Wadi Bani Kharus, the Hawar is asymmetrical but the pattern is the reverse: a thin TST and a thick HST.

With respect to the calibration of these regional stages in the international stratigraphic chart, the model of correlation presented here provides the best available to date: the Hawar is Bedoulian in age, the Bab is Gargasian in age. The transition from Bedoulian to Gargasian probably takes place during the TST of the Shu'aiba sequence. The beginning of the Nahr Umr transgression (its first TST corresponding to the Sabsab) is Gargasian (middle Aptian sensu gallico = early Late Aptian sensu anglico) in age, not Clansayesian (late Aptian sensu gallico = late Late Aptian sensu anglico), nor is it Albian.

REFERENCES

- Azer S.R. & Toland C., 1993. Sea level changes in the Aptian and Barremian (Upper Thamama) of offshore Abu Dhabi, UAE. *Proceedings 8th Middle East Oil Show and Conference 2*: 141-154.
- Boichard R.A., Al Suwaidi A.S. & Karakhanian H., 1994. Cycle boundary types and related porosity evolutions: examples of the Upper Thamama Group in Field "A" (Offshore Abu Dhabi, UAE). *6th Abu Dhabi International Petroleum Exhibition and Conference [ADSPE#76: 417-428]*. *The Middle East Petroleum Geosciences 1*: 191-201.
- Buchem F.S.P. van, Pittet B., Hillgärtner H., Grötsch J., Al Mansouri A.I., Billing I.M., Droste H.H.J., Oterdom W.H. & Steenwinkel M. van, 2002. High-resolution sequence stratigraphic architecture of Barremian/Aptian carbonate systems in northern Oman and the United Arab Emirates (Kharab and Shu'aiba formations). *GeoArabia 7* (3): 461-500.
- Granier B., 2000. Lower Cretaceous stratigraphy of Abu Dhabi and the United Arab Emirates - A reappraisal. *Proceedings 9th Abu Dhabi International Petroleum Exhibition & Conference*: 526-535.
- Granier B., 2002. Algues Dasycladales, nouvelles ou peu connues, du Jurassique supérieur et du Crétacé inférieur du Moyen-Orient - New or little known Dasyclad algae from Upper Jurassic and Lower Cretaceous series of the Middle East. In: Bucur I.I. & Filipescu S. (eds.): Research advances in calcareous algae and microbial carbonates. Proceedings 4th IFAA Regional Meeting (Cluj-Napoca, August 29 - September 5, 2001). *Presa Universitara Clujeana*: 103-113.
- Granier B., 2008. Holostratigraphy of the Kahmah regional Series in Oman, Qatar, and the United Arab Emirates. *Carnets de Géologie. Notebooks on Geology CG2008_A07*: 33 p.
- Granier B., Al Suwaidi A.S., Busnardo R., Aziz S.K. & Schroeder R., 2003. New insight on the stratigraphy of the "Upper Thamama" in offshore Abu Dhabi (U.A.E.). *Carnets de Géologie. Notebooks on Geology*: 1-17.
- Pittet B., Buchem F.S.P. van., Hillgärtner H., Razin P., Grötsch J. & Droste H., 2002. Ecological succession, palaeoenvironmental change, and depositional sequences of Barremian-Aptian shallow-water carbonates in northern Oman. *Sedimentology 49*: 555-581.
- Schroeder R., Buchem F.S.P. van, Immenhauser A., Granier B., Cherchi A. & Vincent B., 2007. Orbitolinid

- biostratigraphic zonation of Barremian-Aptian carbonate platforms of the southern Arabian plate. *In: Regional depositional history, stratigraphy and palaeogeography of the Shu'aiba - First Arabian plate geology workshop [abstracts], 12-15 January 2008, Muscat (Oman). GeoArabia* **12** (4): 148-149.
- Sharland P.R., Archer R., Casey D.M., Davies R.B., Hall S.H., Heward A.P., Horbury A.D. & Simmons M.D., 2001. Arabian plate sequence stratigraphy. *GeoArabia Special Publication* **2**: 1-371.
- Strohmenger C.J., Weber L.J., Ghani A., Rebelle M., Al-Mehsin K., Al-Jeelani O., Al-Mansoori A. & Suwaina O., 2004. High-resolution sequence stratigraphy of the Kharab Formation (Lower Cretaceous, UAE). *11th Abu Dhabi International Petroleum Exhibition and Conference*: 1-10.
- Strohmenger C.J., Ghani A., Al-Jeelani O., Al-Mansoori A., Al-Dayyani T., Weber L.J., Al-Mehsin K., Vaughan L., Khan S.A. & Mitchell J.C., 2006. High-resolution sequence stratigraphy and reservoir characterization of Upper Thamama (Lower Cretaceous) reservoirs of a giant Abu Dhabi oil field, United Arab Emirates. *In: Harris P.M. & Weber L.J. (eds.): Giant hydrocarbon reservoirs of the world: From rocks to reservoir characterization and modeling. American Association of Petroleum Geologists, Memoir* **88**: 139-171.
- Witt W. & Gökdag H., 1995. Orbitolinid Biostratigraphy of the Shuaiba Formation (Aptian), Oman - implications for reservoir development. *In: Simmons M.D. (ed.), Micropaleontology and hydrocarbon exploration in the Middle East. Chapman and Hall, Cambridge*: 221-241.
- Key words:** Bab, Hawar, Shu'aiba, Sabsab, Nahr Umr, Gargasian, Bedoulian, ammonites.

Bruno Granier [bruno.granier@univ-brest.fr]: Université Européenne de Bretagne, Brest (France); Université de Brest; CNRS; IUEM; Domaines Océaniques UMR 6538, 6 Avenue Le Gorgeu, CS 93837, F-29238 Brest Cedex 3 (France); adresse postale: Département des Sciences de la Terre et de l'Univers, UFR des Sciences et Techniques, Université de Bretagne Occidentale (UBO), 6 avenue Le Gorgeu - CS 93837, F-29238 Brest Cedex 3 (France); Robert Busnardo [robert.busnardo@wanadoo.fr]: 13 ch. du Méruzin, 69370 Saint Didier au Mont d'or (France); Bernard Pittet: Université de Lyon 1, Département des Sciences de la Terre; UMR 5125 PaléoEnvironnements et PaléobioSphère, CNRS; Campus de la Doua, 21-43 Avenue du 11 Novembre 1918, F-69622 Villeurbanne Cedex (France).

THE CENOMANIAN-TURONIAN TRANSITION ON A W-E TRANSECT OF THE MOROCCAN ATLANTIC MARGIN (AGADIR). ISOTOPE GEOCHEMISTRY AND SEQUENCE STRATIGRAPHY

Mohamed JATI, Daniele GROSHENY, Serge FERRY & Delphine DESMARES

The Cenomanian-Turonian transition associated with the global oceanic anoxic event OAE2 is coincident with a triple anomaly: (1) a lithologic anomaly consisting of organic-rich deposits (black shales) wherever conditions favored the preservation of such deposits, (2) a geochemical anomaly (a positive ^{13}C found in both carbonates and in organic material), and (3) a biological crisis, particularly among planktonic foraminifers.

For explaining the causes of the anoxic event, most authors propose the major transgression associated with the passage from Cenomanian to Turonian. This explanation is often based on interpretations of the sedimentary successions in deep basins where changes in water depth are difficult to demonstrate. The only valid approach to the elucidation of changes in sea level is through the study of platform-basin transitions. In the Agadir basin deposits of Cenomanian age are generally very thick (500 to 800 m) made up of a large number of repeated small sequences. The series exposed on the western and eastern flanks of the Haut Atlas too are repetitive, made up mainly of lagoonal successions deposited by a transgressive phase following an emergence. In the intervening area between the Atlas and the existing Atlantic coast the sections are coastal progradations in which the deepest facies are marls and nodular, bioturbated limestones that are more or less bioclastic and with a variable content of oysters. The shallowest facies are calcarenitic and/or fine grained sandstones beach deposits that represent a low sea level coincident with emergence in the Atlas sequences.

As regards the interval in which to place the Cenomanian-Turonian boundary, several sections have been measured ranging from the current shore (the most distal portion of the Taghazoute-Plage section) to the foothills of the Atlas (the most proximal portions of the Tamaloukt and Afansou sections) with the Askoutti section between them. The lithology, paleontology and geochemistry of these sections have been studied in detail. Proximal-distal correlations have been proposed and validated by data from stable isotopes and foraminifers.

The results obtained show that the Cenomanian-Turonian transition occurred in a shallow sedimentary succession, characterized by oyster shell mounds and

interbedded marl and limestone, not in the black shale facies where it has been sited classically in the literature. The base of the deposits of black shale is coincident with that of the total range of *Helvetoglobotruncan helvetica*. So these beds are of Turonian age, both later in time and in a transgressive facies. In addition the ^{13}C anomaly which develops in the partial range of *Whiteinella archaeocretacea* occurs before black shale deposition begins. It is marked by the three peaks as commonly seen in other basins. On either side of the anomaly are two remarkable surfaces. The first is a karstified surface, the second is a conglomerate. If the first is interpreted as an indication of emergence (karst of which the cavities are filled by debris from the transgressive oyster shell beds); the second would then represent a transgression after emergence (wave erosion). The East-West correlations of the Agadir transect, validated by isotopic and micropaleontologic data, integrate the two surfaces that indicate emergence. The results show that the Cenomanian-Turonian transition occurred during a succession of forced regressions. The transgression proposed as the only explanation of the anoxic event should be put in question. The regressive nature of the Cenomanian-Turonian transition on the Atlantic coast of Morocco demonstrates that the establishment of an anoxic regime cannot be explained as being caused by a single event (a transgression). Local events influence strongly the development of anoxic conditions (local tectonics, subsidence). Considering the displacement between the sites of occurrence of black shales and those of the geochemical anomaly and the biologic crisis, it is possible to ask which of the three is truly related to the global anoxic event. The geochemical anomaly (disturbance of the Carbon cycle) in the deep basins indicates precisely the beginning and end of anoxic conditions. Therefore the global synchronous existence of the ^{13}C anomaly may be a criterion better than the black shales. Their deposition is dependent on local and biologic conditions, extinctions being caused by the anoxic environment.

Key words: Morocco, Upper Cretaceous, Cenomanian-Turonian boundary, isotope geochemistry, sequence stratigraphy.

THE RGF PROGRAM (GEOLOGIC REFERENCE MAP OF FRANCE): A GEODYNAMIC GEOLOGIC MAP

Eric LASSEUR, Laurent BECCALETTO, Yannick CALLEC, Renaud COUËFFÉ, Fabien PAQUET, Jean-Pierre PLATEL, Olivier SERRANO & Isabelle THINON.

The BRGM (Bureau des Recherches Géologiques et Minières = French Geological Survey) is now undertaking scientific programs which in the near future will replace the Geologic Map program. As a continuation of previous work, the main purpose of these programs is to improve understanding of the subsurface and to gain an increasingly precise representation of it that in the end will provide a three-dimensional homogeneous and continuous coverage of the geology of the whole of metropolitan territory. This will permit the completion of diverse academic and industrial projects (specialized geologic maps, three-dimensional models, 4D representations of the evolution of the French substratum).

The construction of these maps on a nationwide scale requires that the evolution over time of geologic entities of the metropolitan territory (sedimentary basins and orogenic areas s.l.) be adjusted to a common scale. This adjustment can be accomplished only by a thorough comprehension of the dynamic and sequential aspects of the geologic phenomena that formed the substratum of France, and so requires a deep comprehension of its geodynamic evolution. This can be gained by understanding the influence of events taking place at plate boundaries (rifting, orogenesis, subduction) as they affect sedimentary sequences in several basins, and the precise determination of the phases of basinal evolution that have molded the geology of France.

Based on the available bibliography, the method used consists of the construction of a chart that plots the Mesozoic-Cenozoic evolution of each of the sedimentary basins (Paris Basin, Aquitaine Basin, Southeastern Basin, Eocene-Oligocene sunken troughs, continental plateau). These charts include a second order sequential breakdown of the basins development along with any potential indicators of deformation (discordances, changes in the paleogeography, changes in the distribution of thickness, major influxes of terrigenous detritus, tectonic deformations). In the case that during a given period, areas in any one basin are found to be in discrete geodynamic provinces (for example the Aquitaine and Southeastern

basins) a chart is constructed for each of these discrete subdomains.

Comparison of these charts will permit categorization of the deformations recorded according to their geographic extent (from local deformations up to deformations that included all the basins of France) and according to their duration in time. In addition, they will allow the evaluation of their synchronicity (or diachronicity) and the ways in which the sediments respond to the major phases of deformation of the substratum. The several events so recorded are then correlated with the the known developments at the edge of the plate.

Here we present the results of the first work carried out on the Mesozoic, comparing the effects on sedimentation in the several basins of the major phases of deformation identified over large areas ranging in age from the Triassic to the end of the Cretaceous (Cimmerian, Austrian, Subhercynian, Laramide).

One of the main aims of this project is to bring to light elements for understanding the response of the European plate to the different constraints affecting its boundaries. The Cretaceous Period is of particular interest because the transition between the end of the opening of the great oceanic domains and the beginning of the compression caused by the convergence of Europe and Africa.

To constrain more precisely the timing of the beginning of that compression and its effects on the deformation of the European plate we must consider a synthesis of Upper Cretaceous geometry and paleogeography, as well as data provided by metamorphism in the mountain chains and information concerning alteration and thermochronology from areas now without sediments. This is the kind of work under way, and we hope to invite the participation of all of the community working on the Cretaceous.

Key words: Basin analysis, deformations, geodynamic, French sedimentary basins.

OAE1a: LATE EARLY OR EARLY LATE BEDOULIAN EVENT?

Michel MOULLADE, Wolfgang KUHNT, Guy TRONCHETTI, Pierre ROPOLO & Bruno GRANIER

Oceanic anoxic events are usually thought to be global and thus isochronous. Through several examples (see Fig. 1) selected in both basin and platform or transitional facies, an attempt is made to clarify the temporal correlation of the "Selli" - "Goguel" (i.e. OAE1a) Early Aptian event.

These examples show that either Lower Aptian micropaleontological and ammonite datums are insufficiently calibrated, or the isotopic signatures are not always properly elucidated. By using orbitochronologic methods it is now possible to obtain relatively accurate estimations of the duration of the various steps of OAE1a, but the position of this worldwide event in the Early Aptian (Bedoulian) substage is still uncertain.

The Lower Aptian series in the Cassis-La Bédoule historical stratotype is expanded and rich in ammonites, benthic and planktonic foraminifers and calcareous nannofossils, which allow good biostratigraphic control. Preliminary investigations based on a too loosely spaced sampling in the now poorly cropping out upper Bedoulian provided a somewhat atypical ^{13}C record. Thus the lower Gargasian to lower Bedoulian interval has recently been drilled and cored in La Bédoule, with a complete recovery. Detailed investigations based on various methods of the integrated stratigraphy, which will lead to a more precise calibration and better positioning of the OAE1a, are being currently processed in the framework of the Aptian

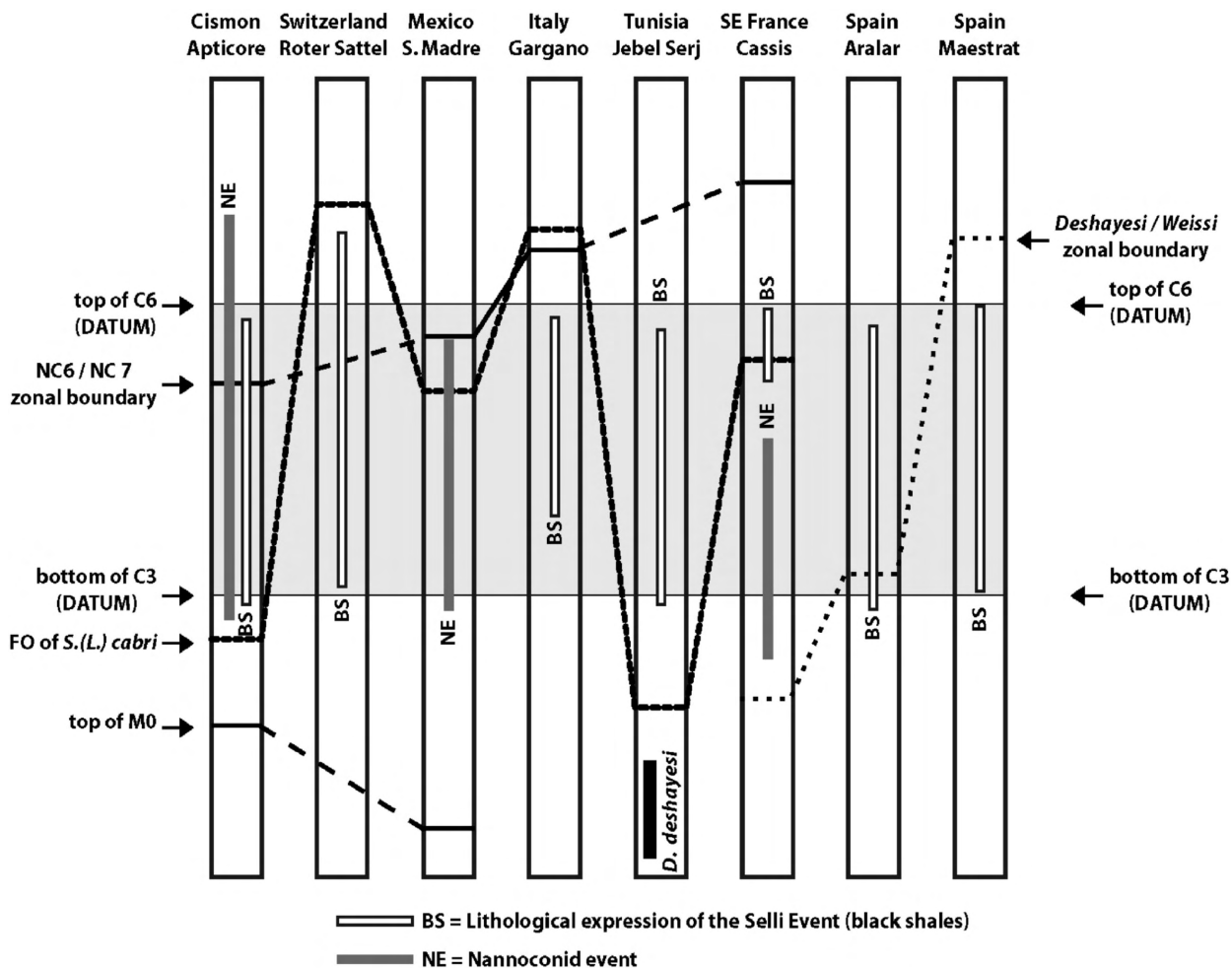


Figure 1: Correlation of sections from Italy (Cismon Apticore, Gargano Promontory), Switzerland (Roter Sattel), SE France (Cassis-La Bédoule), Spain (Maestrat, Aralar Mts.), Tunisia (Jebel Serj) and Mexico (Sierra Madre). C3 at the bottom and C6 at the top are datums assumed to be isochronous and used here for flattening.

Working Group.

REFERENCES

- Erba E., 2004. Calcareous nannofossils and Mesozoic oceanic anoxic events. *Marine Micropaleontology* **52**(1-4): 85-106.
- García-Mondéjar J., Owen H.G., Raisossadat N., Millán M.I. & Fernández-Mendiola P.A., 2009. The Early Aptian of Aralar (northern Spain): stratigraphy, sedimentology, ammonite biozonation, and OAE1. *Cretaceous Research* **30**(2): 434-464.
- Heldt M., Bachmann M. & Lehmann J., 2008. Microfacies, biostratigraphy, and geochemistry of the hemipelagic Barremian-Aptian in north-central Tunisia: Influence of the OAE1a on the southern Tethys margin. *Palaeogeography, Palaeoclimatology, Palaeoecology* **261**(3-4): 246-260.
- Herrle J.O. & Mutterlöse J., 2003. Calcareous nannofossils from the Aptian-Lower Albian of southeast France: palaeoecological and biostratigraphic implications. *Cretaceous Research* **24**(1): 1-22.
- Kuhnt W., Moullade M., Masse J.-P. & Erlenkeuser H., 1998. Carbon isotope stratigraphy of the lower Aptian historical stratotype at Cassis-La Bédoule (SE France). *Géologie Méditerranéenne* **25**(3-4): 63-79.
- Lehmann J., Heldt M., Bachmann M. & Negra M.E.H., 2009. Aptian (Lower cretaceous) biostratigraphy and cephalopods from north central Tunisia. *Cretaceous Research* **30**(4): 895-910.
- Li Y., Bralower T., Montañez I.P., Osleger D.A., Arthur M.A., Bice D.M., Herbert T.D., Erba E. & Premoli Silva I., 2008. Toward an orbital chronology for the early Aptian Oceanic Anoxic Event (OAE1a, ~120 Ma). *Earth and Planetary Science Letters* **271**(1-4): 88-100.
- Luciani V., Cobianchi M. & Lupi C., 2006. Regional record of a global oceanic anoxic event: OAE1a on the Apulia Platform margin, Gargano Promontory, southern Italy. *Cretaceous Research* **27**(6): 754-772.
- Menegatti A.P., Weissert H., Brown R.S., Tyson R.V., Farrimoud P., Strasser A. & Caron M., 1998. High-resolution ¹³C stratigraphy through the early Aptian "Livello Selli" of the Alpine Tethys. *Paleoceanography* **13**(5): 530-545.
- Millán M.I., Weissert H.J., Fernández-Mendiola P.A. & García-Mondéjar J., 2009. Impact of Early Aptian carbon cycle perturbations on evolution of a marine shelf system in the Basque-Cantabrian Basin (Aralar, N Spain). *Earth and Planetary Science Letters* **287**(3-4): 392-401.
- Moreno-Bedmar J.A., Company M., Bover-Arnal T., Salas R., Delanoy G., Martínez R. & Grauges A., 2009. Biostratigraphic characterization by means of ammonoids of the lower Aptian Oceanic Anoxic Event (OAE1a) in the eastern Iberian Chain. *Cretaceous Research* **30**(4): 864-872.
- Moullade M., Tronchetti G. & Masse J.-P. (eds.), 1998. Le stratotype historique de l'Aptien inférieur (Bédoulien) dans la région de Cassis - La Bédoule (S.E. France). *Géologie Méditerranéenne* **25**(3-4): 1-298.
- Renard M. & Rafélis M. de, 1998. Géochimie des éléments traces de la phase carbonatée des calcaires de la coupe du stratotype historique de l'Aptien inférieur dans la région de Cassis-La Bédoule (S.E. France). *Géologie Méditerranéenne* **25**(3-4): 43-54.

Key words: OAE1a, Bedoulian, Aptian, Early Cretaceous.

Michel Moullade [Michel.Moullade@unice.fr]: Centre de Recherches Micropaléontologiques, Museum d'Histoire Naturelle, 60 Bd Rissou, 06000 Nice (France); EA 4234 Laboratoire de Géologie des Systèmes et des Réservoirs Carbonatés, Université de Provence (Aix-Marseille I), Campus St Charles, Case 67, 3 Pl. Victor Hugo, 13331 Marseille Cedex 03 (France); Wolfgang Kuhnt [wk@gpi.uni-kiel.de]: Institute of Geosciences, Christian-Albrechts-University Kiel, Olshausenstr. 40, 24118 Kiel (Germany); Guy Tronchetti: EA 4234 Laboratoire de Géologie des Systèmes et des Réservoirs Carbonatés, Université de Provence (Aix-Marseille I), Campus St Charles, Case 67, 3 Pl. Victor Hugo, 13331 Marseille Cedex 03 (France); Pierre Ropolo [ropolo.geol@wanadoo.fr]: Centre d'Études Méditerranéennes, Barrême (France); 83 Bd du Redon, Bât. E-9 La Rouvière 13009 Marseille (France); Bruno Granier [bruno.granier@univ-brest.fr]: Université Européenne de Bretagne, Brest (France); Université de Brest; CNRS; IUEM; Domaines Océaniques UMR 6538, 6 Avenue Le Gorgeu, CS 93837, F-29238 Brest Cedex 3 (France); adresse postale: Département des Sciences de la Terre et de l'Univers, UFR des Sciences et Techniques, Université de Bretagne Occidentale (UBO), 6 avenue Le Gorgeu - CS 93837, F-29238 Brest Cedex 3 (France).

THE CRETACEOUS CARBONATE SERIES OF THE OMAN MOUNTAINS

Philippe RAZIN & Carine GRÉLAUD

A succession of carbonates of Cretaceous age more than 1300 m thick crops out in the autochthonous units of the Oman Mountains and extends southward in the subsurface where it includes several petroliferous sequences that are being produced (Fig. 1). This series accumulated on the Arabian platform under passive margin conditions. The base of this succession is a local discordant relationship between Tithonian-Berriasian strata on an eroded Jurassic, but is made more apparent because of the subsidence and an important drowning of this edge of the Arabian platform shown by hemipelagic deposits of the basal Cretaceous. The uppermost unit of the succession is dated lower Turonian. It was subjected to synsedimentary deformation and the development of the flexured Muti basin because of the initiation of the processes of obduction.

The Tithonian-Turonian stratigraphic succession is divided into two groups: the Khama Group and the Wasia Group. They are separated by a major unconformity that includes the absence almost everywhere of upper Aptian and lower Albian strata linked to an uplift and emergence of the platform. Both groups include some ten formations of which the limits are either time-planes (sequence limits, maximum flooding surfaces) or facies limits, or both. The formations are conformed of facies associations including the several domains of the carbonate systems: open pelagic basins (Raydah Fm.), the foot of clinoforms with gravitational and hemipelagic sedimentation (Salih Fm.), intra-shelf basins (Bab Fm., Natih Fm. p.p.), oolitic or bioclastic platform edge ("Habshan" Fm., Al Hassanat Fm., Shu'aiba Fm. p.p., Natih Fm. p.p.), inner platform carbonates (Lekhwaib Fm., Kharaib Fm., Shu'aiba Fm. p.p., Natih Fm. p.p.), mixed inner domain (Nahr Umr Fm.).

This series is made up of a succession of third order sequences, their length ranging between 2 and 5 Ma. These sequences record aperiodic cycles resulting from

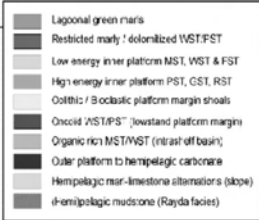
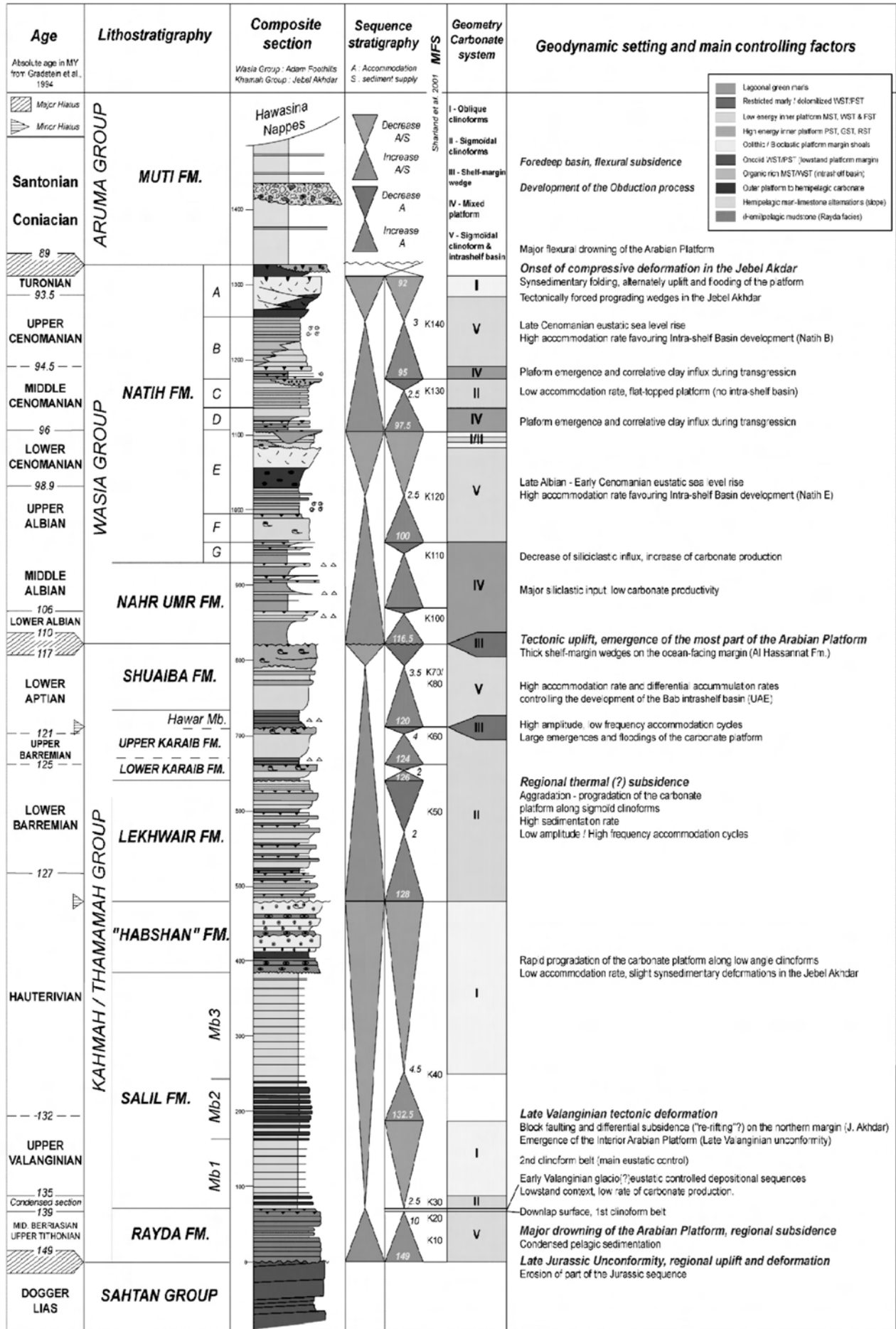
changing relationships between accommodation and production of carbonates, and are bounded by more or less pronounced emergent surfaces. These carbonate systems formed as a succession of prisms of prograding and/or aggrading deposits which fill more than 300 km² of the Rayda basin caused by a marked subsidence of the eastern edge of the platform during the Jurassic-Cretaceous transition. At the outer edge of the platform progradational clinoforms are 200 to 300 m thick. In the platform interior, intra-shelf basins 50 to 80 m deep developed through differential aggradation that also caused the formation of clinoforms.

Generally speaking, the type and geometry of the deposits expresses the way the different kinds of sedimentary systems behave under relatively stable tectonic conditions. Thus, this series offers the opportunity of analysing in detail the architecture and dynamics of carbonate systems on the margin of a platform (Berriasian-Albian) and in the interior (Hauterivian-Turonian) and to attempt to understand the respective roles of the factors that control them. An integrated approach is under way for this study, based on the analysis of studies on the field over a large area (Mountains of Oman and Iran) and subsurface information (Interior of Oman). This approach will lead to the quantification of certain parameters such as the angle and geometry of clinoforms, the rapidity of progradation, the orientation and geometry of the platform incisions, and the changes in rates of sedimentation among others. It will also allow the characterization of platform-basin relationships whether on the outer border of the system on the oceanic side, or in the intra-shelf basins.

Key words: Arabian platform, carbonate depositional sequences, prograding systems, platform to basin correlations.

Philippe Razin [razin@egid.u-bordeaux 3.fr]: Institut EGID Université de Bordeaux 3, 33607 Pessac (France); Carine Grélaud: Institut EGID Université de Bordeaux 3, 33607 Pessac (France).

Figure 1. Stratigraphy, sedimentary systems and geodynamic context of the Cretaceous series of the Oman mountains.



THE TITHONIAN-BERRIASIAN AMMONITE FAUNA AND STRATIGRAPHY OF ARROYO CIENEGUITA, NEUQUÉN-MENDOZA BASIN, ARGENTINA

Horacio PARENT, Armin SCHERZINGER & Günter SCHWEIGERT



Boletín
del Instituto de
Fisiografía y Geología

Parent H., Scherzinger A. & Schweigert G., 2011. The Tithonian-Berriasian ammonite fauna and stratigraphy of Arroyo Cieneguita, Neuquén-Mendoza Basin, Argentina. *Boletín del Instituto de Fisiografía y Geología* 79-81: 21-94. Rosario, 01-07-2011. ISSN 1666-115X.

Abstract.- In this paper we present the results of the revision of the ammonite fauna and the stratigraphy of the Tithonian-Berriasian succession of Arroyo Cieneguita (Mendoza, Argentina), based on new material recently collected and the collections studied by Steuer, Gerth and Krantz. The studied succession belongs to the Vaca Muerta Formation which overlies the Tordillo Formation in concordance. The lower part of the succession consists of marls and shales, being rich in ammonites, bivalves and gastropods; the middle (shales) and upper (limestones and marls) parts contain almost exclusively ammonites. The majority of the species described by Steuer and a part of those studied by Gerth and Krantz have been revised and several type specimens designated and refigured.

Ammonites of the Haploceratoidea have been only recorded in the interval Picunleufuense - lower Internispinosum zones including the genera *Pseudolissoceras*, *Cieneguiticeras*, *Pasottia*, *?Parastreblites*, *?Uhligites* and *?Semiformiceras*. The *Catutosphinctes* and *Choicensisphinctes* genera are recorded from the Picunleufuense Zone (lowermost Tithonian) up to the Koeneni Zone (uppermost Tithonian). Two new genera of the Lithacoceratinae (family Ataxioceratae) are introduced: *Krantziceras* n. gen. and *Platydiscus* n. gen. Remaining Ataxioceratid genera recorded are: *Lithacoceras*, *Mazatepites* and probably *Malagasites* (a doubtful specimen). The Berriasellinae are represented by *Parodontoceras*, *Substeueroceras*, *Blanfordiceras* and *Chigaroceras* (a single specimen), and the Spiticeratinae by *Spiticeras* and *Groebericeras*. The Himalayitidae include species of *Steueria* n. gen., *Micracanthoceras*, *Windhauseniceras*, *Corongoceras* and *Himalayites* (a single specimen). The Aspidoceratinae are well represented by *Aspidoceras*, *Toulisphinctes*, *Pseudhimalayites* and *Physodoceras*, although as typical in the basin, the material is scarce.

The chronostratigraphic classification and time-correlation of the studied succession are based, as usual, on the biostratigraphy of its ammonites. In some levels occur associations which enable the definition of ammonite (bio-)horizons, useful biostratigraphic units consisting of beds with a characteristic fauna. Eight new ammonite horizons are introduced, from below: cf. *erinoides* hz. (Zitteli Z.), *falculatum* hz. (Proximus Z.), *vetustum* hz., *bardense* hz. (Alternans Z.), *striolatus* hz. (Koeneni Z.), *compressum* hz., *noduliferum* hz. (Noduliferum Z.) and *transgrediens* hz. (Damesi Z.). The succession of these horizons and other ones already defined in previous papers, are associated to the Andean chronostratigraphic scale which is then used for fine time-correlation between sections of several localities of the Neuquén-Mendoza Basin where a number of them could be recognized by means of their characteristic ammonite assemblages.

The *vetustum* hz., Alternans Zone, upper Tithonian is recognized in Madagascar and probably in parts of Antarctica.

Key-words: Tithonian-Berriasian; Arroyo Cieneguita; Neuquén-Mendoza Basin; Argentina; Ammonite-horizon; Time-correlation.

Resúmen.- Fauna de amonites y estratigrafía del Tithoniano-Berriasiano de Arroyo Cieneguita, Cuenca Neuquén-Mendoza, Argentina. En este informe se presentan los resultados de la revisión de la fauna de amonites y la estratigrafía de la sucesión del intervalo Tithoniano-Berriasiano de Arroyo Cieneguita (Mendoza, Argentina), basado en material nuevo colectado recientemente y el material estudiado originalmente por Steuer, Gerth y Krantz. La sucesión estudiada corresponde a la Formación Vaca Muerta que suprayace en concordancia a la Formación Tordillo. La parte baja de la sucesión consiste en margas y lutitas, con abundantes amonites, bivalvos y gastrópodos; las partes media (lutitas) y superior (calizas y margas) contienen casi exclusivamente amonites. La mayor parte de las especies descriptas por Steuer y una parte de aquellas descriptas por Gerth y Krantz han sido revisadas y algunos especímenes tipo designados y refigurados.

Amonites de la superfamilia Haploceratoidea fueron registrados únicamente en los niveles del intervalo de las Zonas Picunleufuense (Tithoniano inferior basal) - Internispinosum inferior incluyendo representantes de los géneros *Pseudolissoceras*, *Cieneguiticeras*, *Pasottia*, *?Parastreblites*, *?Uhligites* y *?Semiformiceras*. Los linajes que representan los géneros *Catutosphinctes* y *Choicensisphinctes* han sido registrados, mas o menos saltuariamente, en todo el Tithoniano, desde la base (Zona Picunleufuense) hasta su parte más alta (Zona Koeneni). Se proponen dos nuevos géneros incluidos en la subfamilia Lithacoceratinae (familia Ataxioceratae): *Krantziceras* n. gen. y *Platydiscus* n. gen. Los restantes Ataxioceratae registrados son: *Lithacoceras*, *Mazatepites* y probablemente *Malagasites* (un único espécimen dudoso). Los Berriasellinae están representados por *Parodontoceras*, *Substeueroceras*, *Blanfordiceras* y *Chigaroceras* (un único espécimen). Los Spiticeratinae están representados por *Spiticeras* y *Groebericeras*. Los Himalayitidae incluyen especies asignadas al nuevo género *Steueria* n. gen., así como a *Micracanthoceras*, *Windhauseniceras*, *Corongoceras* e *Himalayites* (un único espécimen). Los Aspidoceratinae se encuentran bien representados por los géneros *Aspidoceras*, *Toulisphinctes*, *Pseudhimalayites* y *Physodoceras* aunque, como es común en la cuenca, el material es relativamente escaso.

La clasificación cronoestratigráfica y la correlación temporal de los niveles de la sección estudiada se han desarrollado, como es habitual, a partir de la bioestratigrafía de los amonites descriptos. En algunos niveles, de la sección estudiada y de otras de la cuenca, ocurren asociaciones que permiten la definición de bio-horizontes de amonites, que constituyen útiles unidades bioestratigráficas consistentes en estratos con una fauna característica diferenciable de las inmediatamente subyacentes y suprayacentes. Ocho nuevos de estos horizontes de amonites son introducidos para el intervalo Tithoniano-Berriasiano de la cuenca. De abajo hacia arriba ellos son: hz. cf. *erinoides* (Z. Zitteli), hz. *falculatum* (Z. Proximus), hz. *vetustum*, hz. *bardense* (Z. Alternans), hz. *striolatus* (Z. Koeneni), hz. *compressum*, hz. *noduliferum* (Z. Noduliferum) y hz. *transgrediens* (Z. Damesi). La sucesión de estos horizontes y otros ya definidos previamente, en trabajos anteriores son asociados a la escala cronoestratigráfica andina que es entonces utilizada para correlación temporal de detalle entre secciones de numerosas localidades de la Cuenca Neuquén-Mendoza donde ellos son reconocidos por medio de los conjuntos de sus

amonites característicos.

El *hz. vetustum* de la Zona Alternans, Tithoniano superior, puede reconocerse en Madagascar y muy probablemente en partes de Antártida.

Palabras clave: Tithoniano-Berriasiano; Arroyo Cieneguita; Cuenca Neuquén-Mendoza; Argentina; Horizonte de amonites; Correlación temporal.

Addresses of the authors:

H. Parent [parent@fceia.unr.edu.ar]: *Laboratorio de Paleontología, IFG, Facultad de Ingeniería,*

Universidad Nacional de Rosario, Pellegrini 250, 2000 Rosario, Argentina.

A. Scherzinger [armin.scherzinger@hotmail.de]: *Lämmerhalde 3, 71735 Eberdingen, Germany.*

G. Schweigert [guenter.schweigert@smns-bw.de]: *Staatliches Museum für Naturkunde, Rosenstein 1, 70191*

Stuttgart, Germany.

Received: 06/12/2010; accepted: 07/03/2011.

Editors: E. P. Peralta and A.F. Greco.

CONTENTS

INTRODUCTION	23	BIOSTRATIGRAHY	82
STRATIGRAPHY	24	Biostratigraphy of the studied section	82
Geological setting	24	Regional biostratigraphic time-correlation	84
Description of the section	24	Time-correlation with the Primary Standard	84
Taphonomic and biostratigraphic features	24	Acknowledgements	86
SYSTEMATIC PALAEONTOLOGY	26	REFERENCES	86
Conventions	26		
Delimitation of species	26	Appendix 1. Measurements of type and selected specimens ...	90
Composition of the fauna.....	26	Appendix 2. Additional photographic refiguration of specimens figured or	
Perisphinctoidea Steinmann, 1890	26	described by Steuer (1897, transl. 1921) and Weaver (1931) ...	91
Ataxioceratidae Buckman, 1921	26		
Lithacoceratinae Zeiss, 1968	26		
<i>Lithacoceras</i> Hyatt, 1900	26		
<i>Choicensisphinctes</i> Leanza, 1980	28		
<i>Krantziceras</i> n. gen.	40		
<i>Platydiscus</i> n. gen.	42		
Virgatosphinctinae Spath, 1923.....	43		
<i>Malagasites</i> Enay, 2009	43		
Torquatisphinctinae Tavera, 1985	43		
<i>Catutosphinctes</i> Leanza & Zeiss, 1992	43		
<i>Mazatepites</i> Cantú, 1967	50		
Neocomitidae Salfeld, 1921	54		
Berriasellinae Spath, 1922	54		
<i>Parodontoceras</i> Spath, 1923	54		
<i>Blanfordiceras</i> Cossmann, 1907	55		
<i>Chigaroceras</i> Howarth, 1992	62		
Olcostephanidae Haug, 1910	62		
Spiticeratinae Spath, 1924	62		
<i>Spiticeras</i> Uhlig, 1903	63		
<i>Groebericeras</i> Leanza, 1945	64		
Himalayitidae Spath, 1925	65		
<i>Windhauseniceras</i> Leanza, 1945	65		
<i>Steueria</i> n. gen.	65		
<i>Corongoceras</i> Spath, 1925	69		
<i>Micracanthoceras</i> Spath, 1925	75		
<i>Himalayites</i> Uhlig in Boehm, 1904	75		
Aspidoceratidae Zittel, 1895	76		
Aspidoceratinae Zittel, 1895	76		
<i>Aspidoceras</i> Zittel, 1868	76		
<i>Physdoceras</i> Hyatt, 1900	77		
<i>Toulisphinctes</i> Sapunov, 1979	77		
<i>Pseudhimalayites</i> Spath, 1925	78		
Haploceratoidea Zittel, 1884	79		
Haploceratidae Zittel, 1884	79		
<i>Pseudolissoceras</i> Spath, 1925	79		
Oppeliidae H. Douvillé, 1890	79		
Taramelliceratinae Spath, 1928	79		
<i>Cieneguiticeras</i> Parent et al., 2010	79		
<i>Pasottia</i> Parent et al., 2008	80		
<i>Parastreblites</i> Donze & Enay, 1961	81		
Streblitinae Spath, 1925	81		
<i>Uhligites</i> Kilian, 1907	81		
<i>Semiformiceras</i> Spath, 1925	81		

INTRODUCTION

The outcrop of Kimmeridgian-Berriasian rocks at the locality named Arroyo Cieneguita, on the left margin of the Cieneguita Creek (Fig. 1), was the first section described yielding Tithonian ammonites in Argentina (Leanza & Hugo 1977: 261). It was Bodenbender who made in 1887-1888 and 1891 the first collections of ammonites from that locality. These collections were studied partially by Behrendsen (1891, 1921 Spanish translation) who established their Tithonian age, but the main contribution is the master monograph by Steuer (1897, 1921 Spanish translation). However, since those times there have been published only short accounts in the form of lists of ammonite occurrences from this locality (Leanza & Hugo 1977, Leanza in Gulisano & Gutiérrez 1995). A detailed analysis of facies, local sedimentology, ichnology and paleogeography of the studied area has been published by Doyle et al. (2005).

Steuer (1897) described 53 new species distributed in 10 genera and illustrated by fine hand-drawings. Most of his new species have been deeply entrenched in literature but

only recently partial revisions of the type material have been published (Parent 2003a, Parent et al. 2007, Parent et al. 2010, and 2011). Following with this revision the present paper presents the description of new material from the outcrops from where the material described by Steuer comes, based on recent collections made by the authors and on the original material.

The ammonite fauna of Arroyo Cieneguita is abundant and moderately well-preserved at several horizons, ranging, our sampling, from the lowermost to the uppermost Tithonian and with extensions into the lower Berriasian. The rocks of this interval belong to the Vaca Muerta Fm. which overlies the continental Kimmeridgian Tordillo Fm. in concordance, passing from sandstones and mudstones to sandy limestones and shales, marls and shales with concretions and black limestones in the upper part.

This report is part of a research program of the authors consisting of the study of the Tithonian ammonite fauna and stratigraphy of the Neuquén-Mendoza Basin based on the description of the faunas of key localities. We present herein the description of the samples obtained in the same outcrop

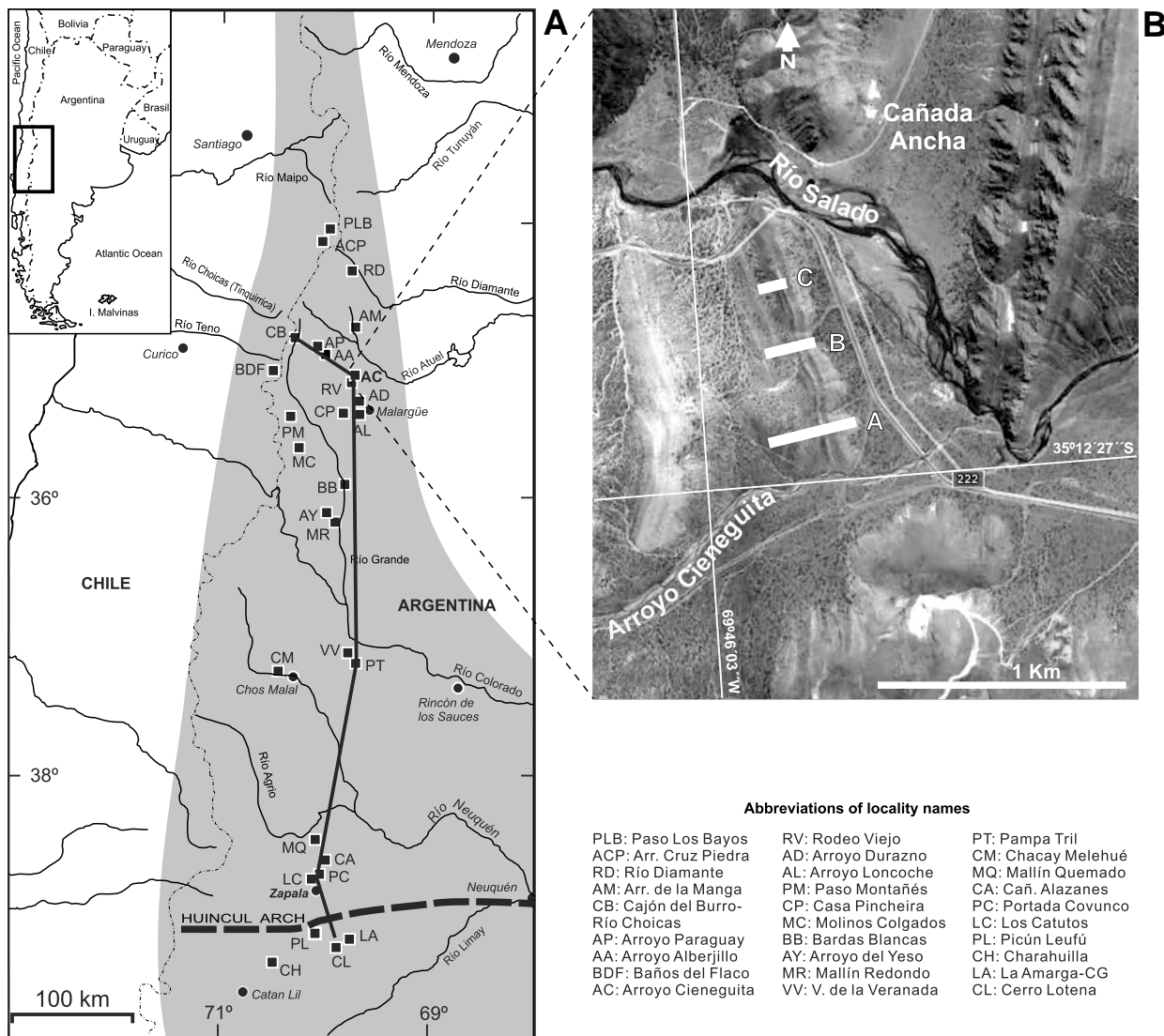


Figure 1. A: Map of West-Central Argentina and Central Chile showing the location of the fossiliferous localities (black squares) cited in text and approximate limits of the Neuquén-Mendoza Basin (gray area). The black line indicates the transect used in Fig. 40 for regional time-correlation by faunal horizons; the broken line indicates the Huincul Arch. **B:** Aerial view of the studied region with indication of the three sections sampled.

from where the fauna studied by Steuer (1897) was collected. Type specimens of some of the species described by the latter author are refigured photographically as the basis of the present revision.

The biostratigraphic approach followed in this paper is based on the bed-by-bed samples available, which in some cases, analyzed in the biostratigraphic chapter, allow to define ammonite (bio-)horizons. In the comparison of published ammonite successions for correlation purposes we distinguish (1) *ensemble*: a set of ammonites not horizoned or listed altogether with no specification of association, from (2) *assemblage* or *association*: a set of ammonites from a single stratigraphic horizon or single bed.

The regional subdivision of the Tithonian adopted is the tripartite, with a middle part differentiated. All the localities cited along the text are positioned in Fig. 1A. For short the following references are abbreviated: Parent, Garrido, Schweigert & Scherzinger 2011 (PGSS 2011); Parent, Myczinski, Schweigert & Scherzinger 2010 (PMSS 2010); Parent, Schweigert, Scherzinger & Enay 2008 (PSSE 2008). Other abbreviations: AC (Arroyo Cieneguita, locality or section), NMB (Neuquén-Mendoza Basin), Biozone (Bz.), Chronostratigraphic Zone (Zone, Z.).

STRATIGRAPHY

Geological setting

The NMB was situated along West-Central Argentina and East-Central Chile at about 32°-39°S (Fig. 1A). It was limited to the West by the Andean magmatic arc with connections to the Palaeopacific Ocean, and the Sierra Pintada and North Patagonian massifs to the East. Two main depositional areas can be recognized: the Neuquén Embayment (Bracaccini 1970), in the South, and the narrow Mendoza Shelf in the North. The studied section is located on the northern part of the Mendoza Shelf, between the Cieneguita Creek and the Salado River (Fig. 1B).

The studied area shows part of the regional outcrops of the Vaca Muerta Fm. (Mendoza Group), which overlies the Tordillo Fm. and underlies the Chachao Fm. The geological features of this area have been recently reviewed by Gulisano & Gutiérrez (1995), and the local stratigraphy has been studied by Leanza (in Gulisano & Gutiérrez 1995). The Vaca Muerta Fm. ranges from the lowermost Tithonian up to the lower Valanginian.

Description of the section

Three close sections were sampled (A-C in Fig. 1B). The most complete of these exposures (section A) is taken as reference for the other two, which are used as complementary, show no differences in lithology and thickness of the stratigraphic levels in which was subdivided the column for sampling. The whole succession is assigned to the Vaca Muerta Fm.

The rock succession is presented below (see Fig. 2). Occurrence of fossils is abbreviated: Am (ammonites), Ap (aptychi), Be (belemnites), Bi (bivalves), Gr (gastropods); the abundance is noted 0: absent, 1: single specimen, 2: few specimens to abundant.

Bed AC-1: 3 m of dark gray to black, nodular fine calcareous sandstone (reddish to brownish weathered).

- Am[2], Ap[0], Be[0], Bi[2], Gr[0].
- Bed AC-2:** 3 to 5 m of dark gray muddy sandstone with sandy calcareous concretions with ammonites (bluish weathered). Am[2], Ap[0], Be[0], Bi[2], Gr[0].
- Bed AC-3:** 4 m of black shale with calcareous concretions. Am[2], Ap[0], Be[0], Bi[0], Gr[0].
- Bed AC-4:** 7 m of black shale, fetid and locally calcareous. Am[2], Ap[0], Be[0], Bi[2], Gr[0].
- Bed AC-5:** 3 m of black shale, fetid, with large calcareous concretions with ammonites. Am[2], Ap[0], Be[0], Bi[2], Gr[0].
- Bed AC-6:** 7 m of gray shaly marl. Two rows of calcareous concretions with ammonites. Am[2], Ap[0], Be[0], Bi[2], Gr[0].
- Bed AC-7:** 8 to 10 m of dark gray to black shaly marl, locally finely laminated. Abundant hard, sandy calcareous concretions, sometimes enclosing bitumen and containing ammonites, aptychi, bivalves, and gastropods. Am[2], Ap[2], Be[0], Bi[2], Gr[2].
- Bed AC-8:** 10 m of dark gray to black shaly marl. Am[2], Ap[0], Be[1], Bi[2], Gr[2].
- Bed AC-9:** 3 m of dark gray to black shaly marl with calcareous concretions with ammonites. Am[2], Ap[0], Be[0], Bi[0], Gr[0].
- Bed AC-10:** 7 m of dark gray to black shaly marl with calcareous concretions with ammonites. Am[2], Ap[0], Be[0], Bi[0], Gr[0].
- Bed AC-11:** 13 m of dark gray to black shaly marl. Am[2], Ap[0], Be[0], Bi[0], Gr[0].
- Bed AC-12:** 5 m of dark gray to black shaly marl with calcareous concretions with ammonites. Am[2], Ap[0], Be[0], Bi[0], Gr[0].
- Bed AC-13:** 14 m of dark gray to black shaly marl without macrofossils. Am[0], Ap[0], Be[0], Bi[0], Gr[0].
- Bed AC-14:** 6 m black shales with calcareous concretions with ammonites. Am[2], Ap[0], Be[0], Bi[0], Gr[0].
- Bed AC-15:** 5 m with calcareous concretions with ammonites. Am[2], Ap[0], Be[0], Bi[0], Gr[0].
- Bed AC-16:** 10 to 11 m with calcareous concretions with ammonites. Am[2], Ap[0], Be[0], Bi[0], Gr[0].
- Bed AC-17:** mostly covered, 1 m of black marl visible. Am[2], Ap[0], Be[0], Bi[0], Gr[0].
- Bed AC-18:** covered, estimated 6 to 10 m. A single ammonite loose in the field.
- Bed AC-19:** partially covered and hardly distinguishable form overlying bed, 6 to 8 m of black marl. Am[2], Ap[0], Be[0], Bi[2], Gr[0].
- Bed AC-20:** more than 20 m of black limestone, not completely observed. Am[2], Ap[0], Be[0], Bi[0], Gr[0].

Taphonomic and biostratigraphic features

In the lower part of the section, beds AC-1 to AC-6, the mollusc fauna is composed of ammonites and bivalves. The bivalves are the most commonly encrusted on ammonites. The ammonites are generally fragmentary, medium- to large-sized, commonly poorly preserved, and most of them occur in concretions. In the top of bed AC-1 the ammonites in horizontal position and eroded equatorially, thus indicating an erosive episode or non-sequence between bed AC-1 (*picunleufuense* α hz.) and bed AC-2. This non-

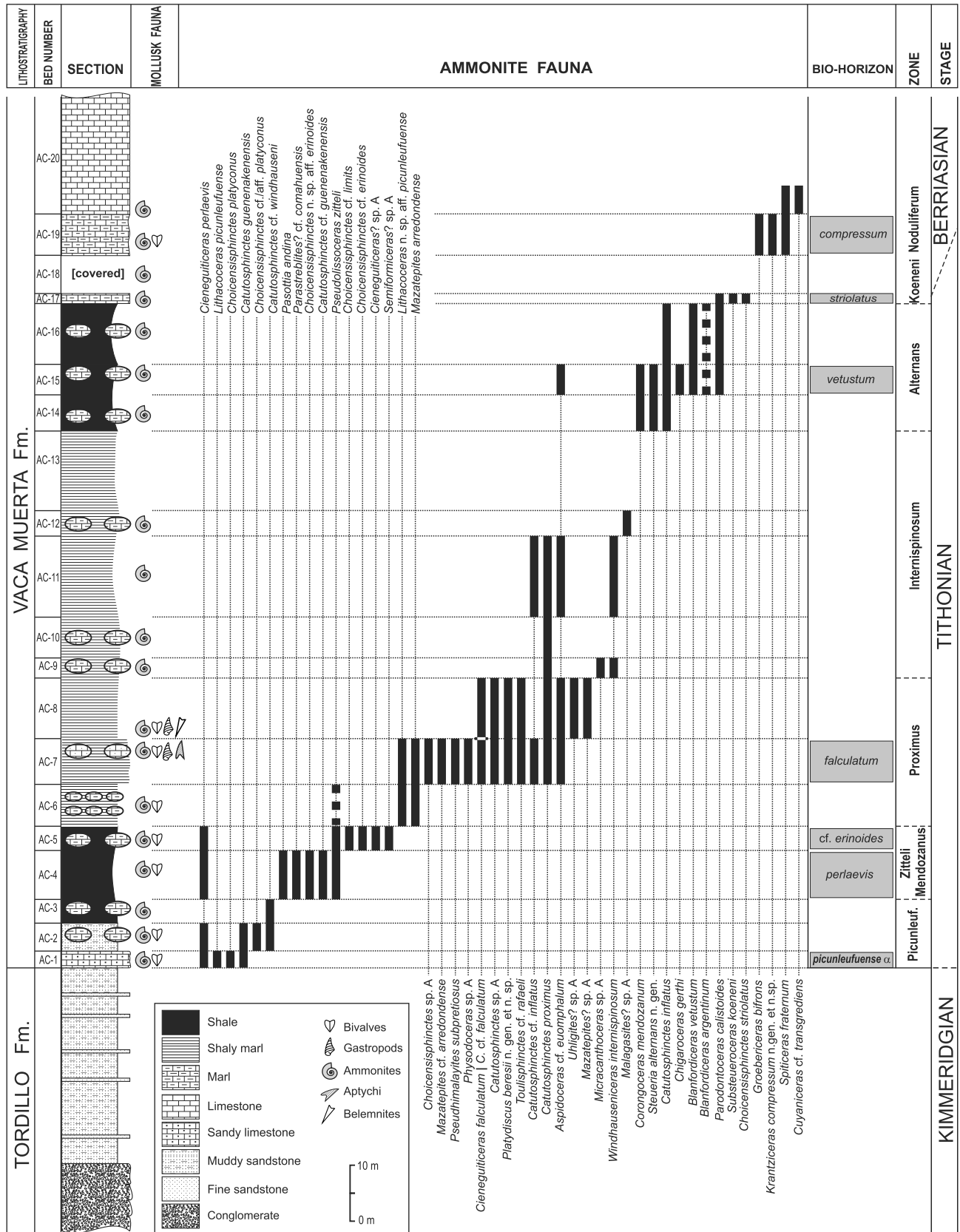


Figure 2. Stratigraphic chart of the studied outcrops at Arroyo Cieneguita showing the litho-, bio- and chronostratigraphic features of the composite log-section. The biostratigraphical chronostratigraphic classification based on the ammonite occurrences indicated by black vertical bars (dashed for uncertain occurrence of loose specimens from the range of beds indicated). The Andean chronostratigraphic ammonite zonation based on Leanza (1981a), Parent et al. (2007 and 2011) and explained in text. The bio-horizons after Parent et al. (2011) and introduced in the present paper (cf. *erinoides*, *falculatum*, *vetustum*, *bardense*, *striolatus*, *compressum* horizons). Boundaries between zones are time planes, indicated by solid lines for standard zones and by dashed lines for non-standard boundaries or tentative correlation. Abbreviation: Picunleuf. (Picunleufuense).

sequence spans at least the *picunleufuense* β hz. which was defined in Picún Leufú and recognized in other localities (PGSS 2011).

In the interval AC-7–AC-8 the molluscan fauna is much more variable, including ammonites (and aptychi), bivalves, gastropods, and belemnites. The bivalves are mainly small oysters encrusting the ammonites. Ammonites are mainly excellently preserved, in several cases even with their peristomes and the microconchs with their lappets. Their size ranges from very small (nuclei but not juveniles) to large (aspidoceratids). The larger specimens are very hard to extract from the rock. Gastropods (Aporrhaidae) are small- to medium-sized, well-preserved, sometimes with delicate ornamental structures in their peristomes.

The interval AC-9–AC-17 is a rather monotonous succession of shales and marls with concretions yielding only ammonites. The dominant lithology suggests a rather deep sedimentary environment, poorly oxygenated and relatively quiet. However, the assumption of continuous sedimentation as the fine grain suggests can not definitely assumed. It could well have been episodic as shown by Paul et al. (2008).

From bed AC-19 upwards the lithology changes to black marls and limestones with rare concretions. In these beds ammonites and medium-sized bivalves occur. In the lower part of bed AC-20 only fragmentary ammonites were collected.

SYSTEMATIC PALAEOLOGY

Conventions.- The described material is housed in the collections of the Museo A. Moyano, Mendoza (MCNAM-PI), the Laboratorio de Paleontología y Biocronología, Universidad Nacional de Rosario (LPB), and the Museo Prof. Olsacher, Zapala (MOZ-PI). Casts, photographs, and information about types and other specimens described by Steuer (1987), Krantz (1926), Opper (1865) and Weaver (1931) were kindly provided by H. Jahnke and M. Reich (Institut für Geowissenschaften der Universität Göttingen; GZG); Gerhard Schairer and Alexander Nützel (Bayerische Staatssammlung für Paläontologie und Geologie, München; BSPG); and E.A. Nesbitt and R.C. Eng (Burke Museum, University of Washington, Seattle; BM). Bodychamber is abbreviated with Bc and phragmocone with Ph; macroconch (female): [M], microconch (male): [m]. Measurements are indicated as follows: diameter (D), diameter at the last adult septum (D_s), final adult diameter at peristome (D_p), umbilical width (U), whorl width (W), whorl height (H_1), and whorl ventral (or apertural) height (H_2), all given in millimeters [mm]; approximated or estimated values marked with (e); length of body chamber (L_{bc}) in degrees [°]. Number of primary (P) and ventral (V) ribs per half whorl. This form of counting ribs per half whorl is more sensitive for reflecting changes in ribbing density, and less exigent in quality of material for obtaining the sets of measurements for ontogenetic trajectories.

Report of biometric features of shell shape is given in App. 1 and text in the form of dimensionless numbers or "indexes", mainly relative to the size (D). This form of reporting has the advantage of giving a direct reference to the relative morphology which, moreover, allows comparisons in a range of comparable sizes, unaffected by the exponential allometric growth variations. The metric linear dimensions can be easily obtained using D which is reported besides.

Nomenclature adopted for description of ribbing follows PGSS (2011). Measurements of type and other selected specimens are given in Appendix 1. Other abbreviations are: HT: holotype, LT: lectotype, PT: paratype, TL: type locality, TH: type horizon, MT: monotypy, TS: type species, OD: original designation, SD: subsequent designation. Codification of indicative marks on synonymy lists: figuration of type specimen (*), doubtful synonym (?), partially (p), not belonging to the species (n). Innermost whorls are very important to be described since they are especially considered for classification at the genus level. When possible this part of the ammonite is figured in double size.

Delimitation of species.- Taking advantage that all the samples studied were collected bed-by-bed, the taxonomic approach followed herein is based on the assumption that the slowly evolving lineages are seen in the stratigraphic record as incomplete successions of more or less variable transients. This approach of horizontal classification is useful for the identification of species from the morphotypes available. Lineages are, if convenient and possible, subdivided into successive segments (groups of transients) in order to reflect their relative ages and morphological differences (see e.g. Dietze et al. 2005 for further details).

It is widely accepted that ammonites were widely variable intraspecifically in morphology (e.g. Sturani 1971, Callomon 1985, Landman et al. 2010) and frequently in adult size (Parent 1998). However, the sequence of sculptural stages (sculpture ontogeny) is rather stable. Variation in shell shape and sculpture arises mainly because of variations in the size (or individual age) at which the ontogenetic changes occur, in sequences which are otherwise very constant through the spectrum of variation (cf. Hantzpergue 1989: 80).

This variation in timing seems to be originated in developmental heterochronies, the processes modelling the phenotypic plasticity through a range of more or less paedo- or peramorphic variants (see Meister 1989). It should be, at least in part, a response to different variable environmental conditions (Parent 1998, Wilmsen & Mosavinia 2010), thus a source for evolutionary change. These changes in the timing of expression of the successive morpho-ornamental stages, originate the gradual variation and the more or less discrete polyphenism usually described in ammonites (commonly called polymorphism which actually means discrete genetic variation, undetectable in fossils).

Composition of the fauna.- The complete list of ammonite species identified in the material collected by the authors and described in this paper is given in Fig. 2. There have been identified 48 species assigned to 27 genera of 7 families. The complete list of ammonites cited and/or described by Steuer (1921) from Arroyo Cieneguita is given in Tab. 1.

Superfamily Perisphinctoidea Steinmann, 1890

Family Ataxioceratidae Buckman, 1921

Subfamily Lithacoceratinae Zeiss, 1968

Genus *Lithacoceras* Hyatt, 1900

Type species.- Ammonites ulmensis Opper, 1858; by OD.

Lithacoceras picunleufuense Parent, Garrido, Schweigert & Scherzinger, 2011

Fig. 3A-C

Table 1. List of the species of ammonites described or cited by Steuer (1897, transl. 1921: table in pp. 43-45) considering material from Arroyo Cieneguita with indication of (1) type locality and horizon of Andean species (AC: A. Cieneguita, LM: Arroyo La Manga, LO: Arroyo Loncoche, RV: Rodeo Viejo; see Fig. 1), (2) range of occurrence in AC cited in, and based on levels Cieneguita I-V defined by Steuer (1921: 41-47), (3) classification proposed in the present paper (discussion in text).

Classification by Steuer (1897, 1921)	TL-TH	Range AC	Taxonomy adopted in this paper
<i>Reineckeia grandis</i> Steuer	AC-V	V	<i>Argentincerias? grandis</i> (Steuer)
<i>R. cf. stephanooides</i> (Oppel)	-	I	<i>Catutosphinctes windhauseni</i> (Weaver)
<i>R. eudichtoma</i> (Zittel) [not figured]	-	II	-
<i>R. transitoria</i> (Oppel)	-	III	<i>Krantzicerias cf. compressum</i> n. gen. et n. sp.
<i>R. proxima</i> Steuer	AC-II	II	<i>Catutosphinctes proximus</i> (Steuer)
<i>R. striolata</i> Steuer	LM	II	<i>Choicensisphinctes striolatus</i> (Steuer)
<i>R. striolatissima</i> Steuer	LM	II	<i>Choicensisphinctes striolatus</i> (Steuer)
<i>Odontoceras calistoides</i> (Behrendsen)	RV	III - IV	<i>Parodontoceras calistoides</i> (Behrendsen)
<i>O. beneckeii</i> Steuer	AC-IV	III - IV	<i>Parodontoceras calistoides</i> (Behrendsen)
<i>O. laxicosta</i> Steuer	AC-IV	IV	<i>Blanfordicerias laxicosta</i> (Steuer)
<i>O. koeneni</i> Steuer	AC-IV	IV	<i>Substeuerocherias koeneni</i> (Steuer)
<i>O. intercostatum</i> Steuer	AC-IV	IV	<i>Choicensisphinctes? intercostatum</i> (Steuer)
<i>O. fasciatum</i> Steuer	LO-II	IV	? <i>Choicensisphinctes striolatus</i> (Steuer)
<i>O. subfasciatum</i> Steuer	LO-II	IV	<i>Parodontoceras? subfasciatum</i> (Steuer, 1897)
<i>O. theodorii</i> (Oppel)	-	V	<i>Krantzicerias cf. compressum</i> n. gen. et n. sp.
<i>O. ellipsostomum</i> Steuer	AC-V	V	<i>Krantzicerias ellipsostomum</i> (Steuer)
<i>O. nodulosum</i> Steuer	AC-II	II	<i>Parodontoceras calistoides</i> (Behrendsen)
<i>O. cf. perornatum</i> Retowski [not figured]	-	II - III	-
<i>Hoplites vetustus</i> Steuer	AC-II	II - III	<i>Blanfordicerias vetustum</i> (Steuer)
<i>H. subvetustus</i> Steuer	AC-III	II - III	<i>Blanfordicerias vetustum</i> (Steuer)
<i>H. wallichi</i> (Gray) = <i>Blanf. steueri</i> Uhlig	RV-III	III	<i>Blanfordicerias vetustum</i> (Steuer)
<i>H. mendozanus</i> (Behr.) [not figured]	RV	II	<i>Corongoceras mendozanum</i> (Behrendsen)
<i>Perisphinctes colubrinus</i> (Reinecke)	-	I	<i>Catutosphinctes proximus</i> (Steuer)
<i>P. densistriatus</i> Steuer	AC-I	I	<i>Choicensisphinctes densistriatus</i> (Steuer)
<i>P. roubyanus</i> Fontannes [not figured]	-	I	-
<i>Aspidoceras cyclotum</i> (Oppel)	-	I	<i>Physodoceras neoburgense</i> (Oppel)
<i>Aspidoceras cieneguitense</i> Steuer	AC-II	II	<i>Aspidoceras cieneguitense</i> Steuer
<i>A. euomphalum</i> Steuer	AC-III	III	<i>Aspidoceras euomphalum</i> Steuer
<i>A. aff. haynaldi</i> (Herbich)	-	II	<i>Physodoceras</i> sp.
<i>Oppelia perlaevis</i> Steuer	AC-I	I - II	<i>Cieneguiticerias perlaevis</i> (Steuer) [M]
<i>O. nimbata</i> (Oppel)	-	II	<i>Cieneguiticerias falcuatum</i> (Steuer) [m]
<i>O. perglabra</i> Steuer	AC-I	I	<i>Cieneguiticerias perlaevis</i> (Steuer) [m]
<i>Haploceras falcuatum</i> Steuer	AC-II	II	<i>Cieneguiticerias falcuatum</i> (Steuer) [M]
<i>Lytoceras cf. sutile</i> (Oppel)	-	V	<i>Lytoceras</i> sp.

Remarks.- Abundant material which is mostly fragmentary shows exactly the shell shape and ribbing of this species, especially of the older transient α as seen in the type locality, Picún Leufú. Well-preserved large specimens were seen in the field, but they are very hard or impossible to extract if not in several small pieces with loss of the inner whorls and the bodychamber.

Occurrence and distribution.- As discussed in PGSS (2011).

***Lithacoceras* n. sp. aff. *picunleufuense* Parent, Garrido, Schweigert & Scherzinger, 2011**
Figs. 4-5

Material.- A complete adult microconch (MCNAM 24395) from bed AC-6 and a juvenile (macroconch?) phragmocone (MCNAM 24418/2) from bed AC-7. The mould of a complete adult macroconch with peristome was photographed in the field, this specimen comes from the bed AC-7.

Description.- The microconch is evolute with wide umbilicus; the whorl section is rounded in the inner whorls, but subrectangular in the outer whorls as also in the bodychamber. Ribbing moderately dense and strong, bifurcating on the upper half or upper third of the flank, secondaries are somewhat finer and cross the venter

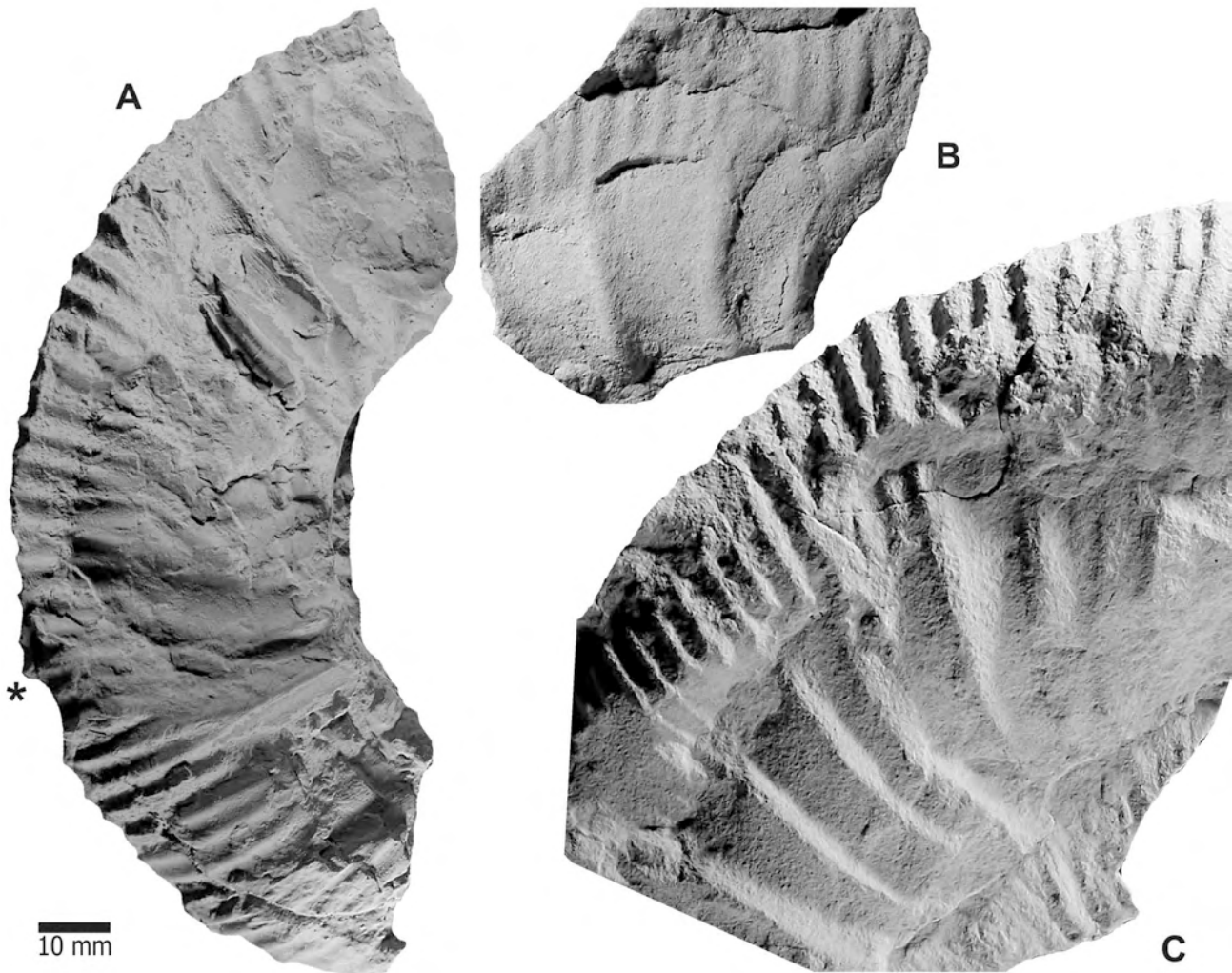


Figure 3. *Lithacoceras picunleufuense* Parent, Garrido, Schweigert & Scherzinger, Arroyo Cieneguita, bed AC-1 (Picunleufuense Z., *picunleufuense* α hz.). **A:** portion of adult macroconch phragmocone with beginning of bodychamber (MCNAM 24363). **B-C:** portions of adult bodychambers showing typical ribbing of the species (MCNAM 24362, 24364). All natural size. Asterisk indicating position of the last septum.

unchanged. The bodychamber is less than half a whorl long, the peristome is indistinct and bears short and wide lappets at a diameter of 124 mm.

The macroconch is larger, about $D = 215$ mm at peristome. Inner whorls like the microconch. The last whorl of the phragmocone is compressed with high-subrectangular whorl section; the sculpture is composed by prosocline primaries starting on the umbilical wall and bifurcating on the upper half of the flanks with some intercalatory ribs and two or three prosocline constrictions. At ca. $D = 130$ mm a short not very well-defined, stage of trifurcate virgatotomic ribbing can be observed. From there begins a variocostation. The first half of the bodychamber is covered by stronger and more distant primaries which trifurcate on mid-flank; the terminal part of the bodychamber is covered by strong, apparently undivided prosocline primaries which fade just behind the peristome. Bodychamber is 300° long.

Remarks.- The best resemblance of this species is with the lower Tithonian *L. picunleufuense*, a species widely distributed throughout the NMB. The differences are the somewhat stronger ribbing of the inner whorls tending to vanish on the bodychamber of the present macroconch; the microconch is larger and the lappets are shorter and wider

with respect to *L. picunleufuense*. The present material from AC demonstrates that the Andean lineage ranges up into the Middle Tithonian Proximus Z., and possibly gave rise to *Zapalia* Leanza & Zeiss, 1990 (TS: *Zapalia fascipartita* Leanza & Zeiss, 1992) known from the Internispinosum Z. of Los Catutos. *Zapalia* differs from the present species by the ribbing of the adult phragmocone which is composed by strong primaries subdivided in sheaves of finer secondaries.

Perisphinctes kokeni Behrendsen, 1891, from an indeterminate horizon of the Tithonian of Rodeo Viejo, is very similar to the microconch described, showing the same size, sculpture and coiling.

Occurrence and distribution.- The material described comes from beds of the *falculatum* hz. of the Proximus Z. of AC.

Genus *Choicensisphinctes* Leanza, 1980

Type species.- *Perisphinctes choicensis* Burckhardt, 1903; by OD.

Remarks.- The genus was reviewed recently (PGSS 2011). The material studied herein gives support to an apparent pattern of the macroconch morphology observed in the

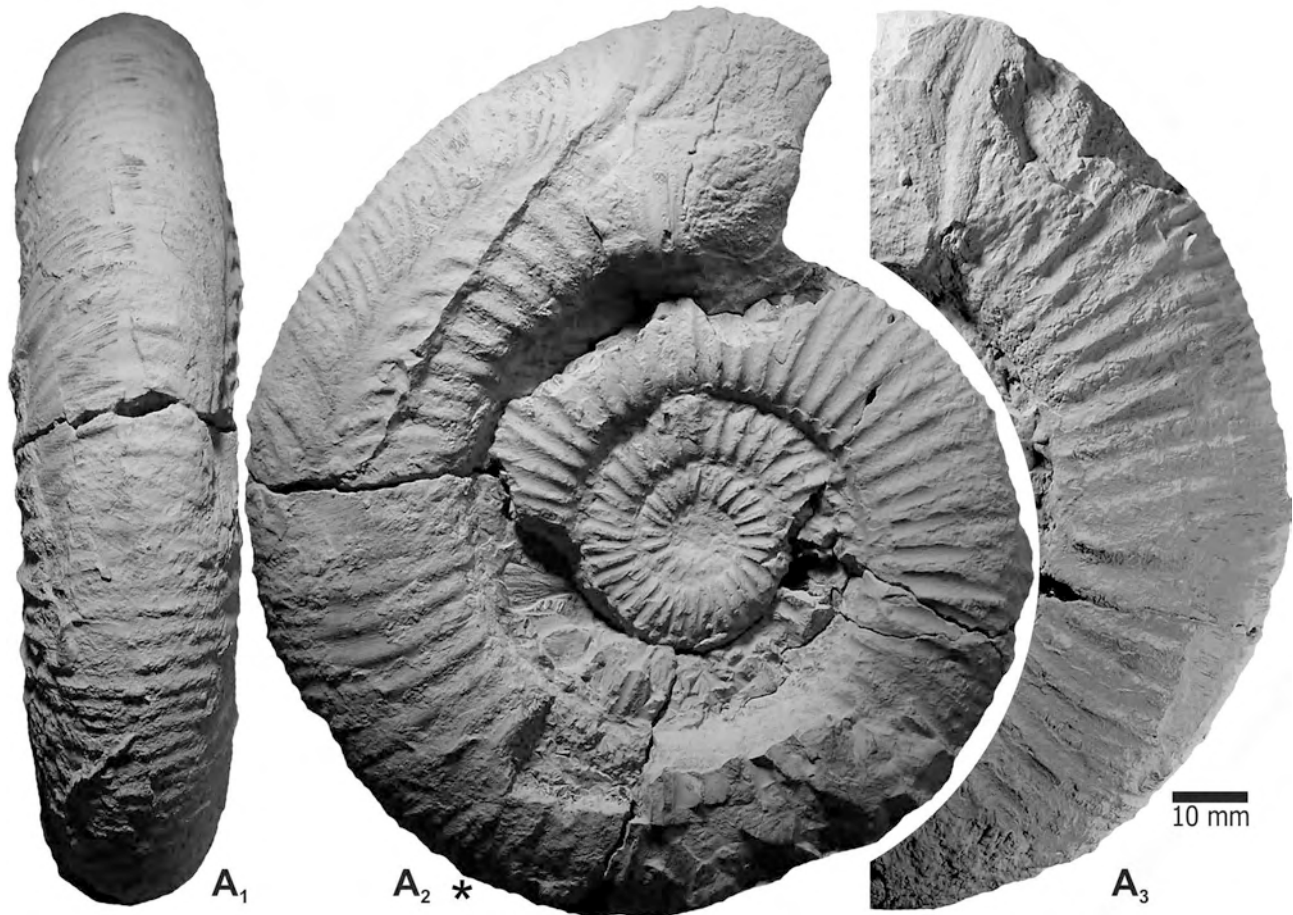


Figure 4. *Lithoceras* n. sp. aff. *picunleufuense* Parent, Garrido, Schweigert & Scherzinger. Arroyo Cieneguita, bed AC-6 (Proximus Z.). Adult microconch with lappets (MCNAM 24395). A₁: ventral view; A₂: lateral view showing a repaired injury in the left flank (frontal apertural view) not affecting the venter; A₃: lappet preserved on the right flank. Natural size. Asterisk indicates the last septum.

faunal successions of Picún Leufú, Cerro Lotena, Cerro Granito and Pampa Tril. The largest specimens with short, stout raised primaries (in the form of periumbilical bullae or tubercles) on the end of the phragmocone and bodychamber appear for first time in stratigraphic levels where *Pseudolissoceras zitteli* occurs. In the Picunleufuense Z., below the first occurrences of *P. zitteli*, the representatives of the genus have, on the adult bodychamber, primaries strong but acute and reaching the mid-flank, and also have smaller adult sizes. If this pattern is proved to be consistent after description of material under study it might be a good biostratigraphic marker.

***Choicensisphinctes platyconus* Parent, Garrido,
Schweigert & Scherzinger, 2011**
Fig. 6A-B

Synonymy.- See PGSS (2011).

Remarks.- In the bed AC-1 this species is very abundant but mainly occurs as impressions; collection of complete specimens is very difficult or impossible. The specimens collected and those observed in the field match with the type material, and especially with the morphotypes from the basal Tithonian *picunleufuense* α. hz.

Occurrence and distribution.- As discussed in PGSS (2011).

***Choicensisphinctes* cf./aff. *platyconus* Parent, Garrido,
Schweigert & Scherzinger, 2011**
Fig. 6C-E

2003a *Choicensisphinctes choicensis* (Burckhardt).- Parent: 154, fig. 8A-C.

2007 *Choicensisphinctes* cf. *windhausenii* (Weaver).- Parent & Cocca: 26.

2011 *Choicensisphinctes* cf./aff. *platyconus* n. sp.- Parent et al.: fig 23B-E.

Material.- Abundant material from bed AC-2 but mostly crushed; three specimens were collected.

Description.- Medium sized, the largest [M] is about 160 mm in diameter (Fig. 6D) at the end of the bodychamber. Moderately narrowly umbilicate on the phragmocone, with closely spaced primary ribs which split into three to six secondaries on the mid-flank, producing a fine and dense ventral ribbing (Fig. 6E). Near the end of the phragmocone there is a constriction bounded by inflate primaries in the form of varices, from which the primaries become progressively stronger and more widely spaced. The bodychamber is uncoiled, extends for at least three quarters of a whorl, and the primary ribs divide in sheaves on the mid-flank; intercalatory ribs occur irregularly.

The smaller adult specimen (Fig. 6C) has the

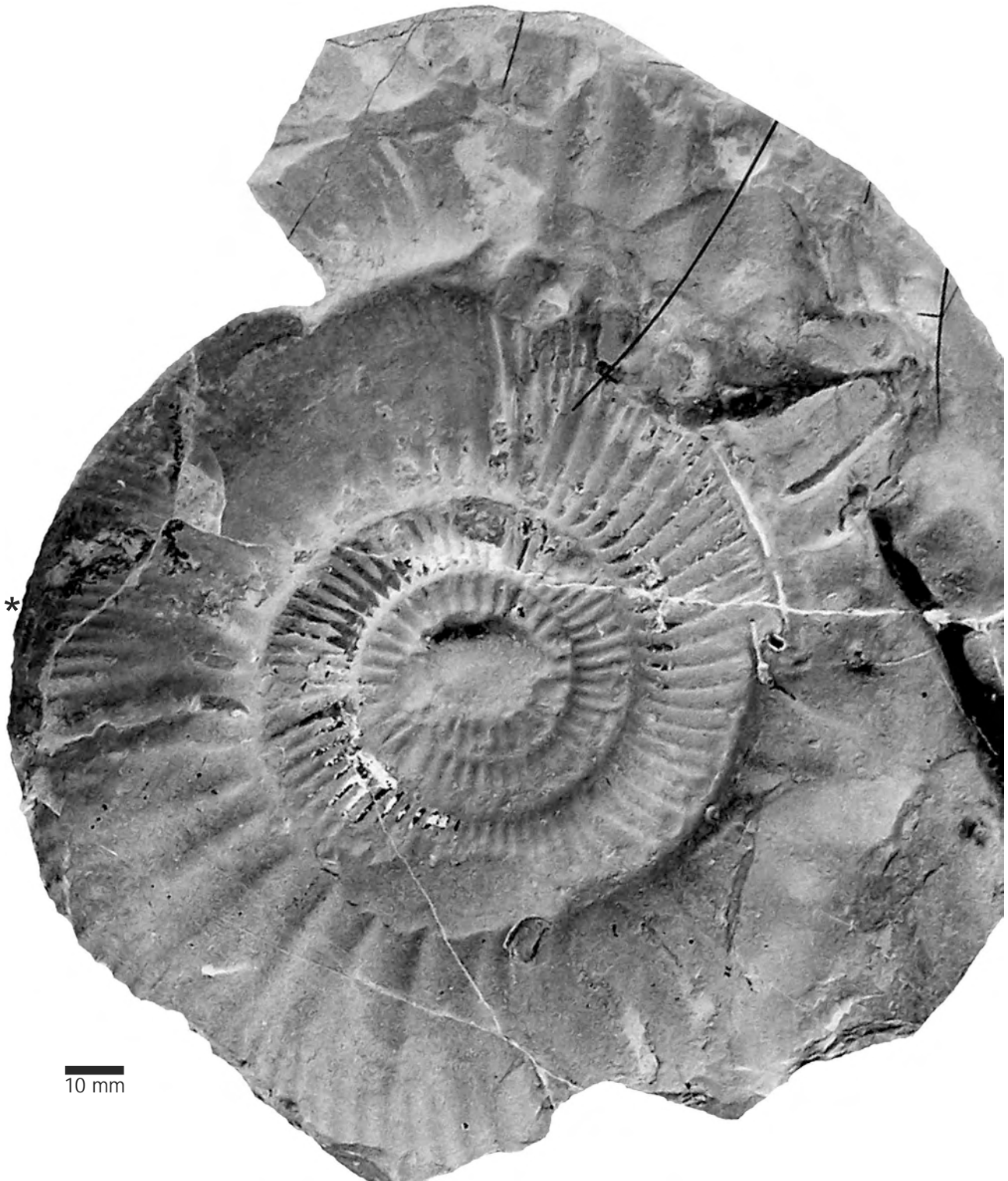


Figure 5. *Lithoceras* n. sp. aff. *picunleufuense* Parent, Garrido, Schweigert & Scherzinger. Arroyo Cieneguita, bed AC-7 (Proximus Zone). Adult macroconch with aperture (negative photograph of a mold not collected). Natural size. Asterisk indicates position of the last septum.

bodychamber partially preserved, showing strong acute primary ribs which fade off from the middle of the flank, producing a smooth ventral area.

Remarks.- This material shows a rather conspicuous ribbing and involution comparable with the material from the upper Picunleufuense Z. in Picún Leufú (PGSS 2011: fig. 23B-E).

Choicensisphinctes burckhardti (Douvillé, 1910) is

very similar to the specimen in Fig. 6E, but the bodychamber of that species is not known, thus constraining the comparison to the phragmocones. These early *Choicensisphinctes* can be differentiated mainly from the bodychamber since the phragmocones seem to be very similar. Within the earliest representatives of the lineage (*C. platyconus*) there are some morphotypes which already show similar aspects in shell shape and sculpture with *C.*



Figure 6. A-B: *Choicensisphinctes platyconus* Parent, Garrido, Schweigert & Scherzinger, Arroyo Cieneguita, bed AC-1 (Picunleufuense Z., picunleufuense α hz.); A: fragmentary phragmocone (MCNAM 2436); B: fragmentary bodychamber (MCNAM 24366). C-E: *Choicensisphinctes* cf./aff. *platyconus* Parent, Garrido, Schweigert & Scherzinger, A. Cieneguita, bed AC-2 (Picunleufuense Z.); C: adult macroconch bodychamber with remains of phragmocone (MCNAM 24367); D: adult macroconch (MCNAM 24370/1) with almost complete bodychamber; E: portion of adult phragmocone (MCNAM 24368). All natural size. The asterisk indicates the last septum.

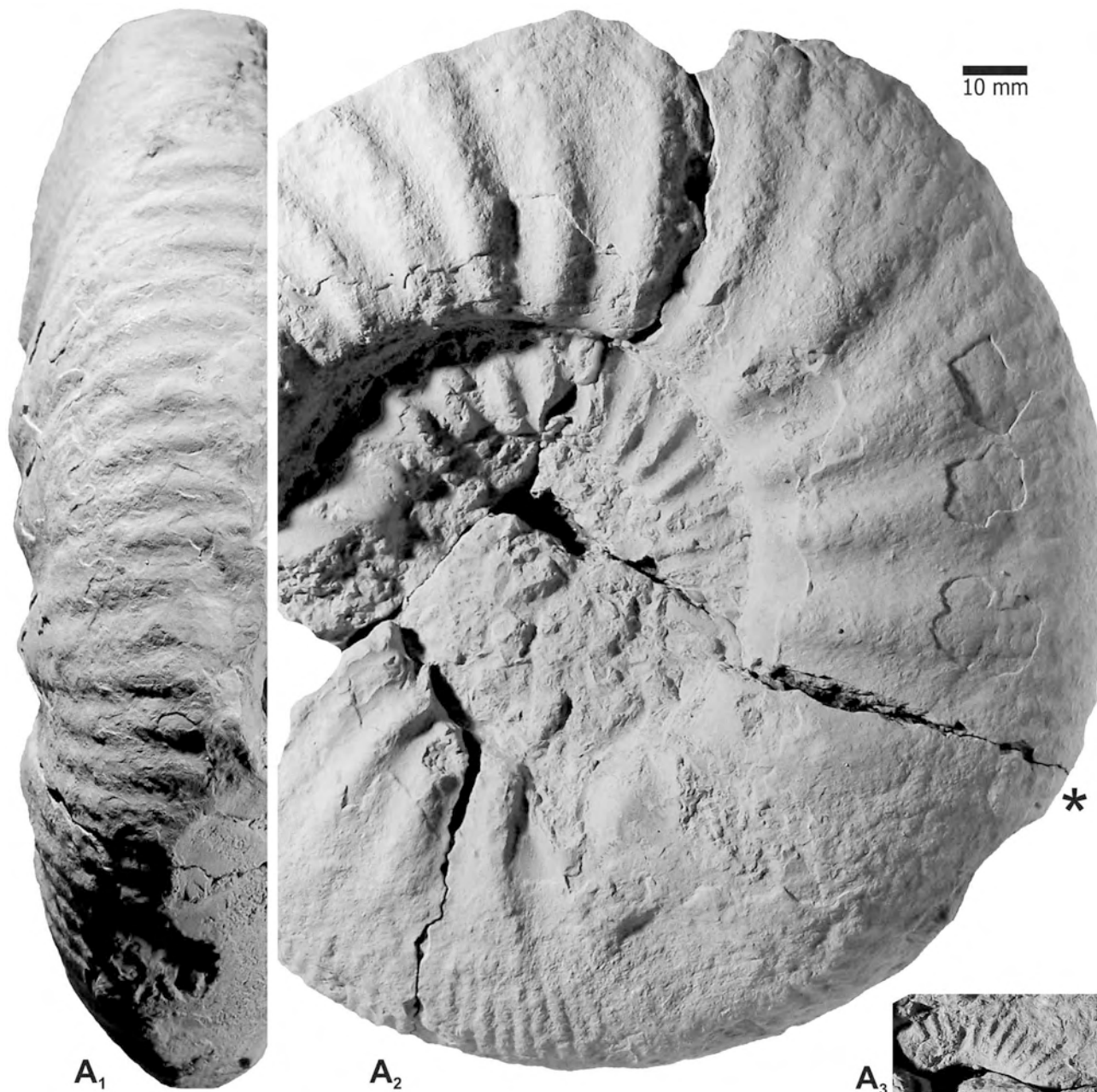


Figure 7. *Choicensisphinctes* n. sp. aff. *erinoides* (Burckhardt), Arroyo Cieneguita, bed AC-4 (Zitteli Z., *perlaevis* hz.), adult macroconch with incomplete bodychamber (MCNAM 24374). A₁; detail of the lateral ribbing of inner whorls at about $D = 40$ mm. Natural size. Asterisk indicates the position of the last septum.

burckhardti (e.g. PGSS 2011: figs. 15A-C and 16F).

Occurrence and distribution.- The present material is almost identical to, and occurs in a close stratigraphic position as the material from Picún Leufú (PGSS 2011), between the *picunleufuense* β hz. and the *malarguense* hz. Moreover, the close similarity between the HT of *Choicensisphinctes burckhardti* (Douvillé, 1910) and the specimen in Fig. 6E suggests a similar or the same horizon.

In Casa Pincheira (Parent 2003a: fig. 8) and in Portada Covunco (Parent & Cocca 2007: 26) this species occurs in the same stratigraphic position. From these localities much better preserved specimens were recorded, including specimens of *Catutosphinctes* which are identical to those figured from Picún Leufú (PGSS 2011: fig. 30B, 31A-E).

The specimens described under different species of

Virgatosphinctes Uhlig by Howlett (1989: pl. 2: 4, pl. 3: 1-3) from Eastern Alexander Island, Antarctica seem to fit closely to the present species. These specimens from Antarctica are very similar, especially in conspicuous characters, like the varices bounding a constriction and the aspect of ribbing.

***Choicensisphinctes* n. sp. aff. *erinoides*
(Burckhardt, 1903)**

Fig. 7, 8A-B, App. 1

Material.- Two macroconchs (MCNAM 24374-24375) from bed AC-4 (Zitteli Z.).

Description.- Suboxycone moderately involute. The two last whorls of the phragmocone are suboval in whorl section,

higher than wide, and covered by strong, acute, prosocline primary ribs which bi- or trifurcate on the mid-flank. The last half whorl of the phragmocone shows a change in the ribbing which gradually turns to be composed by stronger primaries divided in sheaves of four to six secondaries which cross the venter unchanged. The adult bodychamber begins at $D = 150$ mm and half of a whorl is preserved.

Remarks.- The new species differs from *C. cf. erinoides* and *C. cf. limits* (described below, bed AC-5) in the compressed form of the shell covered by strong primaries which persist on the bodychamber with no formation of bullae on the lower part of the flank, and the ventral ribbing strong. There is close similarity with the specimen of *C. cf. limits* (Fig. 12).

Occurrence and distribution.- The specimens described occur in bed AC-4, *perlaevis* hz., associated with *P. zitteli* in its lower occurrence in AC. More or less similar material is known from the Zitteli Z. of La Amarga-Cerro Granito (PSSE2008).

***Choicensisphinctes cf. erinoides* (Burckhardt, 1903)**

Figs. 8A-B, 9-10A, App. 1

Material.- Two poorly preserved specimens and one well preserved, complete adult [M] phragmocone (MCNAM 24385); abundant material seen in the field, bed AC-5 (Zitteli Z.).

Description.- Macroconch. Inner whorls ($D = 10-40$ mm) evolute, widely umbilicate with rounded whorl section and dense prosocline primaries mostly biplicate on the upper flank (*perisphinctoid-stage*). From about $D = 40-50$ mm the whorl section becomes suboval, slightly higher than wide and so remains up to at least the base of the bodychamber. The ribbing turns to be composed by primary ribs ($P = 25$) divided in three to, progressively, five secondaries from the middle of the flank. Some few primaries are polyschizotomic, they first bifurcate close to the umbilical shoulder and then trifurcate in virgatotomic style on the upper half of the flank (*mendozanus-stage*). From about $D = 90$ mm the ribbing ($P = 15-20$) is composed of more widely spaced, stronger and rounded primary ribs which are raised on the lower flank with bullae aspect (*bullate-stage*). They divide in sheaves of finer secondaries on the middle of the flank; the secondaries and some intercalatories of the same strength all cross the venter evenly spaced and with no changes.

The bodychamber in the specimen of Fig. 9 (field-photograph), begins at about $D = 170-190$ mm, it is strongly uncoiled and seems to have extended over a complete whorl, likely ending at about $D_p = 300-350$ mm. In the last portion of the adult phragmocone and, especially, on the beginning of the bodychamber the primary ribs ($P = 10$) tend to become triangular (cuneiform-like), and divided in sheaves of secondaries which fade away towards the peristome. The other [M] described are larger than this specimen.

Remarks and comparison.- The ontogeny of *C. cf. erinoides* shows three morphological/sculptural stages: (1) the *perisphinctoid stage* between $D = 10-40$ mm (Fig. 10A₁), (2) the *mendozanus stage* between $D = 50-90$ mm (Fig. 10A₂) and (3) the *bullate stage* mostly comprising the last half whorl of the phragmocone and the first half of the adult bodychamber, about $D = 90-200$ mm (Figs. 9, 10A₁). The *mendozanus stage* for this part of the ontogeny is so named

because it is identical to the last whorl of the LT of *Choicensisphinctes mendozanus* (Burckhardt, 1911; originally figured by a photograph in Burckhardt 1900a: pl. 25: 7).

C. cf. erinoides is very similar to the HT of *C. erinoides*, differing by their somewhat later and more gradual variocostation. Nevertheless, although it could be part of the intraspecific variation, the adult features are not preserved in the HT.

Differentiation between *C. cf. erinoides* and *C. cf. limits* (described below) is based on two morphological traits: the involution-umbilical width, and the ribbing density on the phragmocone; the whorl section cannot be fully evaluated because most material is crushed. Differences of this kind are, in modern ammonite taxonomy, merely morphotypical and could be biologically insignificant. Nevertheless, for the time being it is impossible to realize the morphological and stratigraphical relationships –so the taxonomy– between the holotypes of *C. erinoides* and *C. limits* on their TL and TH. Under these constraints, we describe our samples with tentative assignments to the closest nominal species although they most likely belong to a single species.

The specimens from Picún Leufú described in PGSS (2011) are identical but the inner whorls are not preserved, and their bodychamber is poorly known from fragmentary material.

The macroconch of *C. platyconus*, of the lowermost Tithonian Picunleufuense Z., is smaller and more compressed throughout the ontogeny, and the ribbing is slower variocostate on the adult stage.

Occurrence and distribution.- The material described is associated, in the bed AC-5 (*cf. erinoides* hz.), with *P. zitteli* and other species of the Zitteli Z. (see Fig. 2). In Picún Leufú (PGSS 2011) and Pampa Tril identical specimens occur in the same stratigraphic position.

***Choicensisphinctes cf. limitis* (Burckhardt, 1930)**

Figs. 8A-B, 10B-C, 11-12, 13A, App. 1

Material.- Several specimens more or less well preserved (MCNAM 24382-24384, 24387-24389) from bed AC-5.

Description.- Suboxycone, compressed and involute with narrow umbilicus throughout the phragmocone and beginning of the bodychamber. The inner whorls (about $D = 30-50$ mm) are very finely ribbed with primaries divided on the middle of the flanks, or lower, in sheaves of even finer secondaries which cross the venter without changes. From $D = 50-60$ mm the primaries become gradually stronger and more widely spaced, divided on the middle of the flank in sheaves of five to more than ten secondaries. Polyschizotomic ribbing (or pair of twinned primaries on the umbilical shoulder) is visible at $D = 90$ mm, where it is shortly developed the sculpture of the *mendozanus stage*. The last whorl of the phragmocone and the beginning of the bodychamber show strong, rounded primaries, raised on the umbilical shoulder forming bullae in the form of gross cuneiform primaries. Ventral ribbing retains almost the same strength from the inner whorls, and only from about $D = 250$ mm they become stronger.

The largest specimens (max $D = 330$ mm) available are phragmocones.

Remarks and comparison.- The *perisphinctoid stage* is not

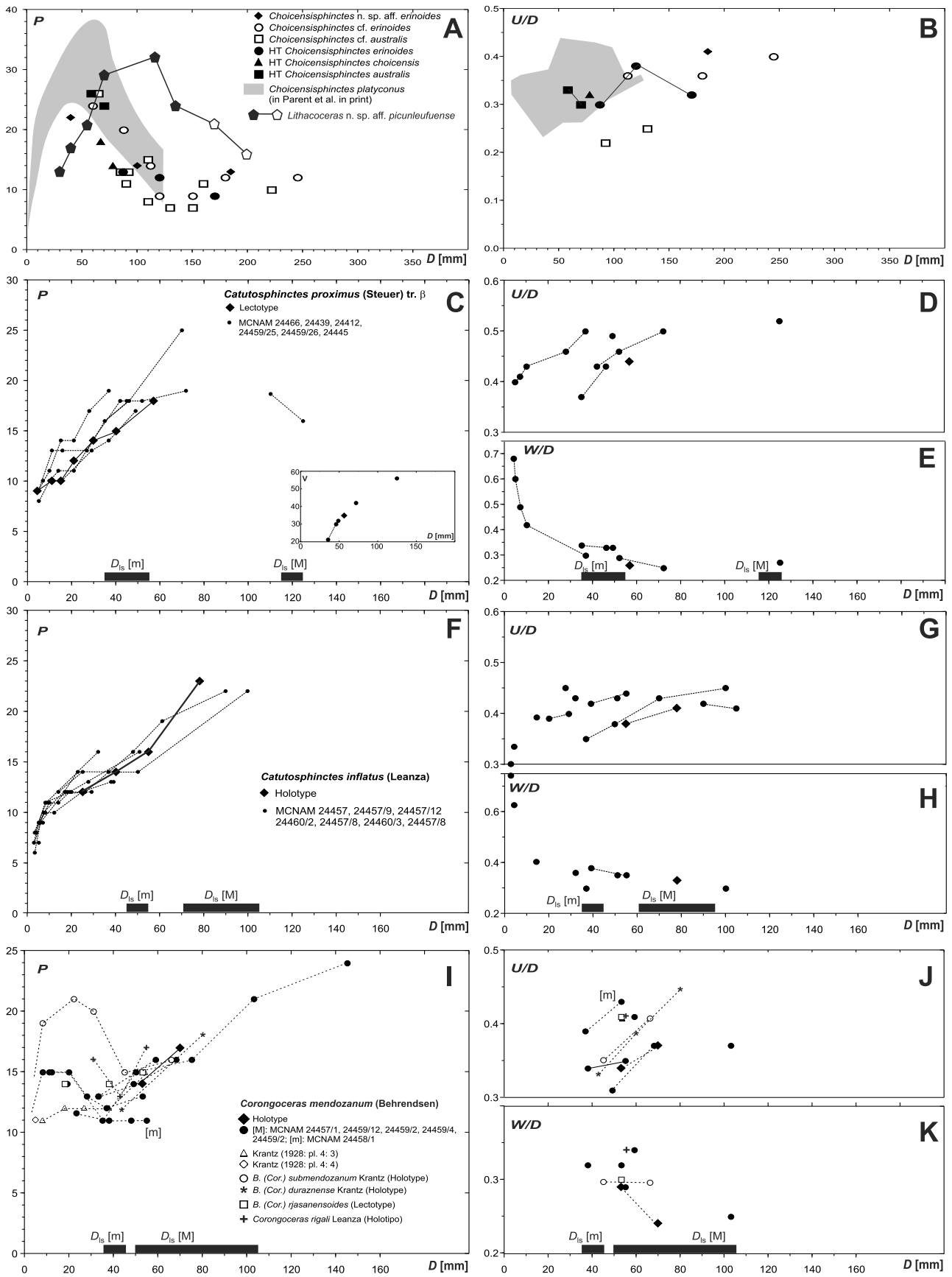


Figure 8. Biometry of *Choicensisphinctes* (A-B), *Catutosphinctes proximus* (C-E), *Catutosphinctes inflatus* (F-H) and *Corongoceras mendozanum* (I-K) based on the number of primary ribs per half-whorl (*P*), umbilical diameter relative to diameter (*U/D*) and whorl wide relative to diameter (*W/D*). Sequential measurements on single specimens linked by broken straight lines for showing ontogeny and general trends. References to the specimens plotted indicated in the left hand graph. Thick black bars on *D*-axis indicate the range of observed diameter at last septum for adult [M] and [m].

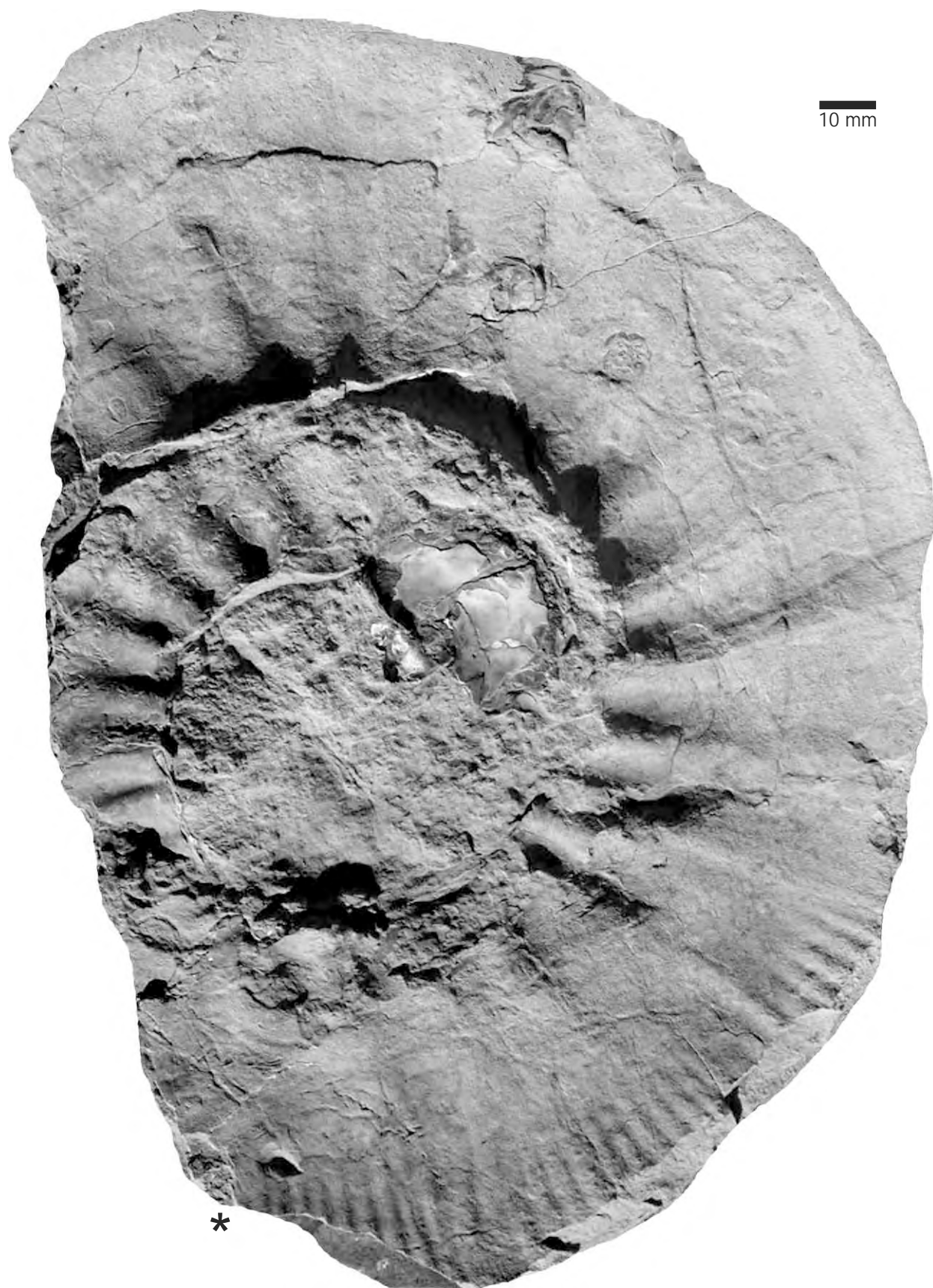


Figure 9. *Choicensisphinctes* cf. *erinoides* (Burckhardt). Almost complete adult macroconch of an evolute variant (negative field-photograph of a cast, natural size). Arroyo Cieneguita, bed AC-5 (Zittel Z., cf. *erinoides* hz.). Natural size. Asterisk indicates the last septum.

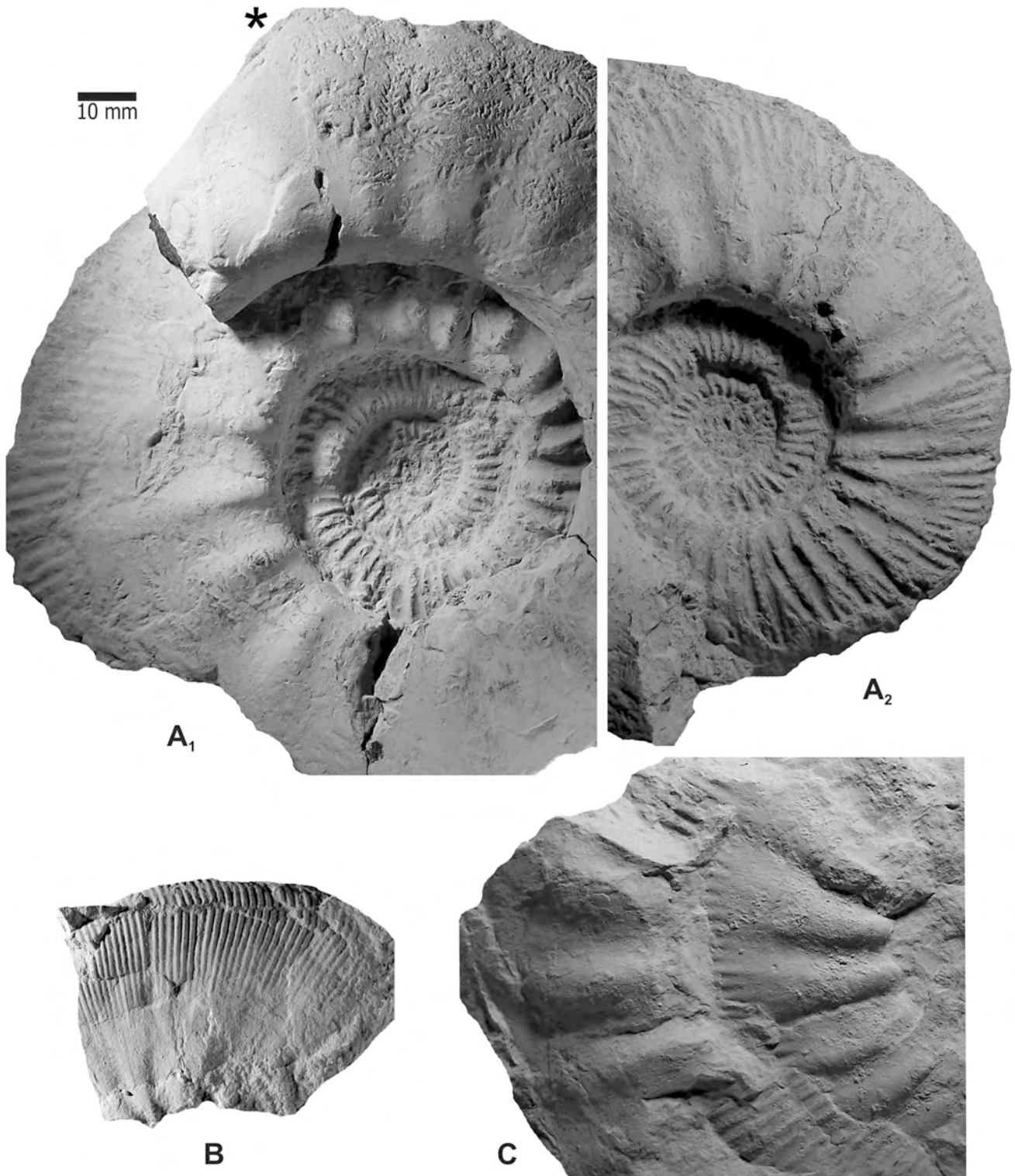


Figure 10. A: *Choicensisphinctes* cf. *erinoides* (Burckhardt), complete adult macroconch phragmocone with beginning of bodychamber (MCNAM 24385), Arroyo Cieneguita, bed AC-5 (Zitteli Z., cf. *erinoides* Hz.); **A₂:** lateral view after removing the last whorl of phragmocone shown in **A₁**. **B-C:** *Choicensisphinctes* cf. *limitis* (Burckhardt), A. Cieneguita, bed AC-5 (Zitteli Z., cf. *erinoides* Hz.); **B:** fragment of bodychamber (MCNAM 24387) showing the characteristic bundle of secondary ribs originated from a subtriangular wedge-like, short primary rib; **C:** crushed macroconch last whorl of phragmocone and portion of bodychamber (MCNAM 24384), the bundles of secondary ribs in advanced stages of growth are shorter and the primaries longer and stout. All natural size. Asterisk indicating the last septum.

visible in the present material although it seems to be present, restricted to the innermost whorls (Fig. 11A₅). The *mendozanus* stage is shortly expressed at about 90 mm in diameter (Fig. 11B) but somewhat different to what is seen in *C. cf. choicensis*. Indeed, the shell at that size is more

involute with more compressed whorl section and the ribbing although have the same design, is denser and finer. The *bullate* stage is well developed but on more tightly coiled whorls (Fig. 10C, 11B₂, 12). The meaning of these differences is discussed above, under *C. cf. choicensis*.

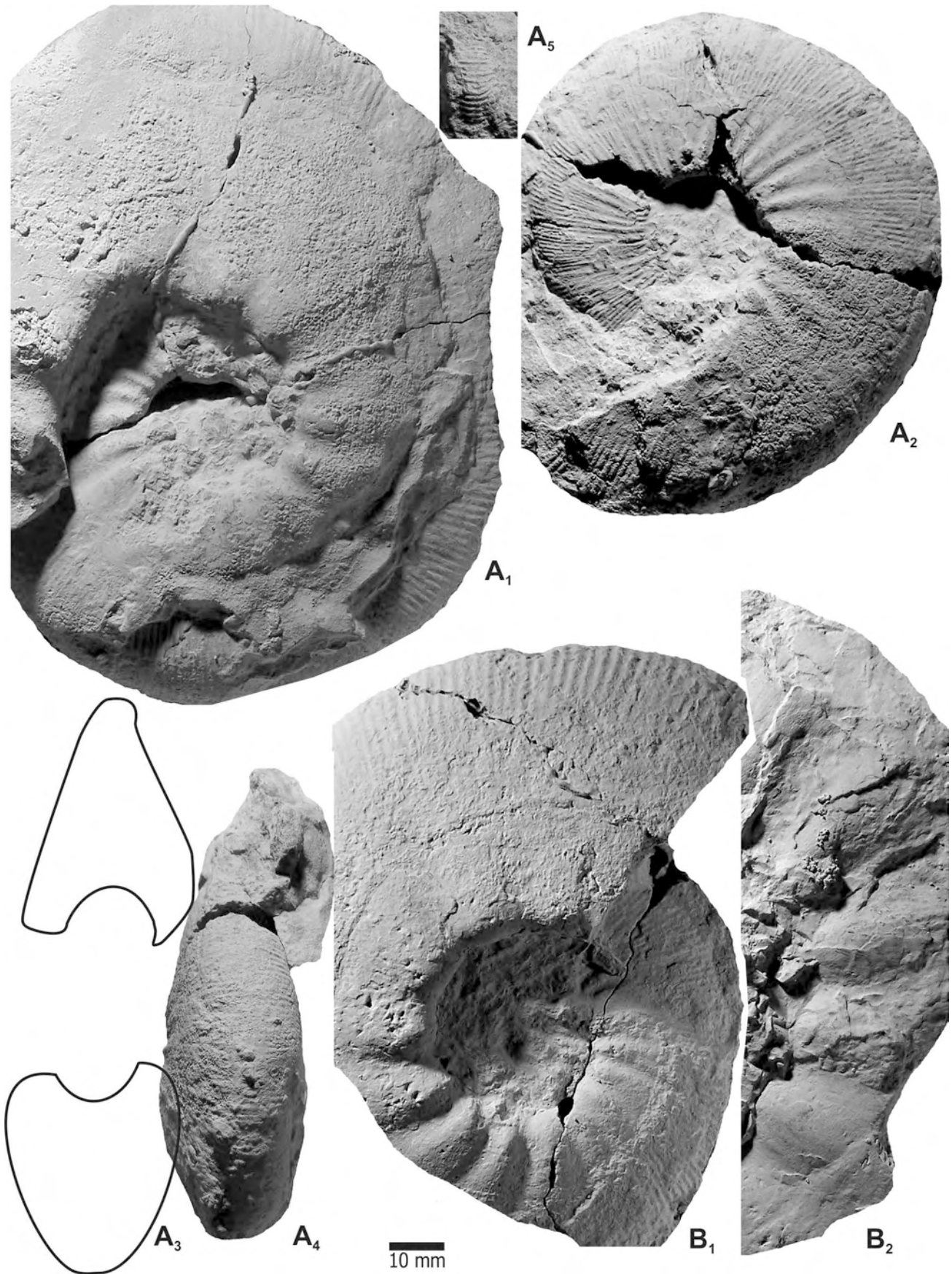


Figure 11. *Choicensisphinctes* cf. *limitis* (Burckhardt), A. Cieneguita, bed AC-5 (Zitteli Z., cf. *erinoides* hz.). **A:** adult macroconch phragmocone (MCNAM 24383), last whorl (**A₁**) crushed; **A₂**, **A₃**, **A₄**: left side, lateral and ventral views of the precedent whorl; **A₅**: whorl section at about $D = 100$ mm; **A₆**: detail of the ventral ribbing of the inner whorls (x1) at about $D = 25$ mm. **B:** macroconch phragmocone (**B₁**) with part of the bodychamber (**B₂**) preserved on the opposite face (MCNAM 24382). All natural size.

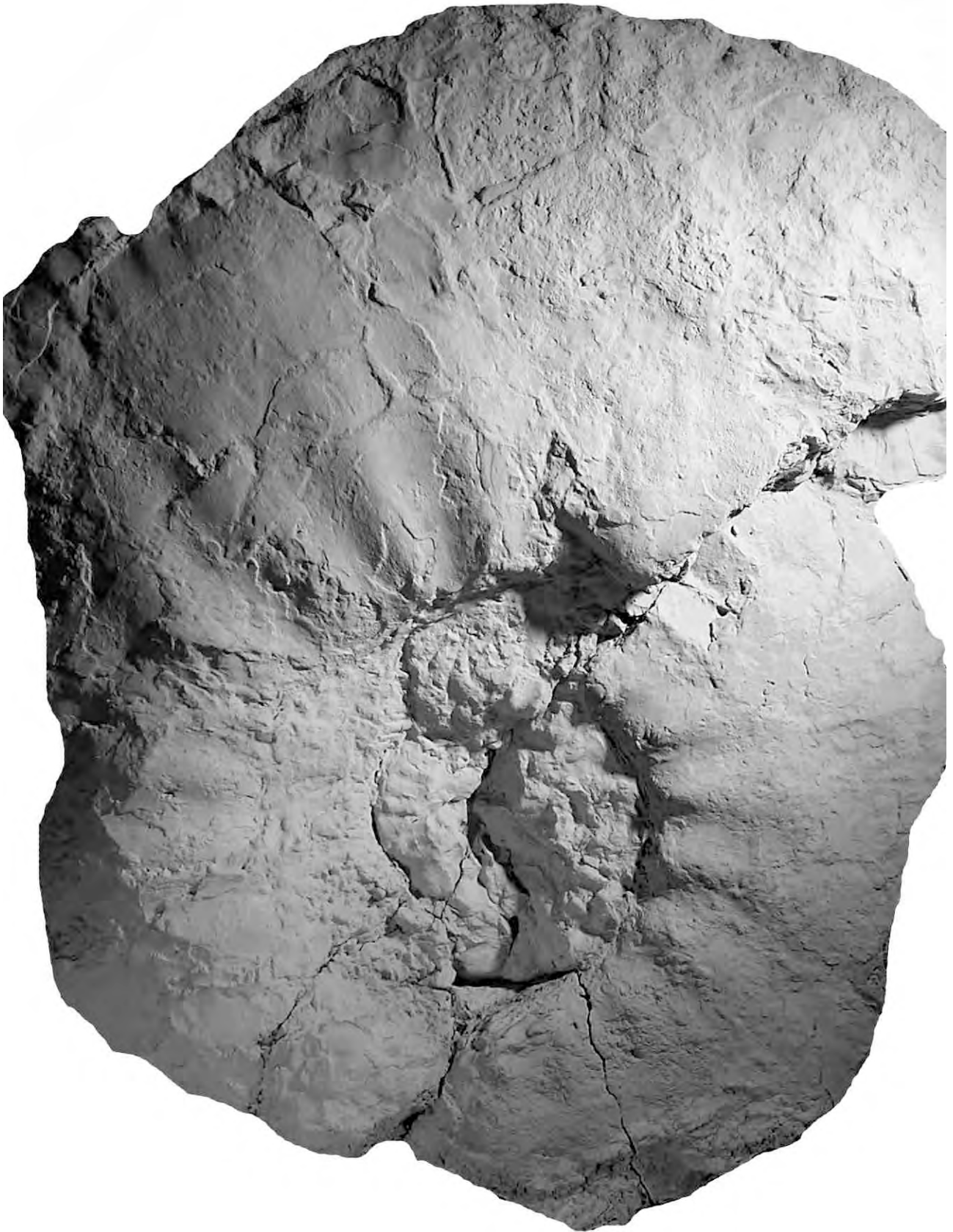


Figure 12. *Choicensisphinctes* cf. *limitis* (Burckhardt), crushed adult phragmocone (MCNAM 24389), Arroyo Cieneguita, bed AC-5 (Zitteli Z., cf. *erinoides* hz.). Reduced to three quarters of the actual size (x0.75).

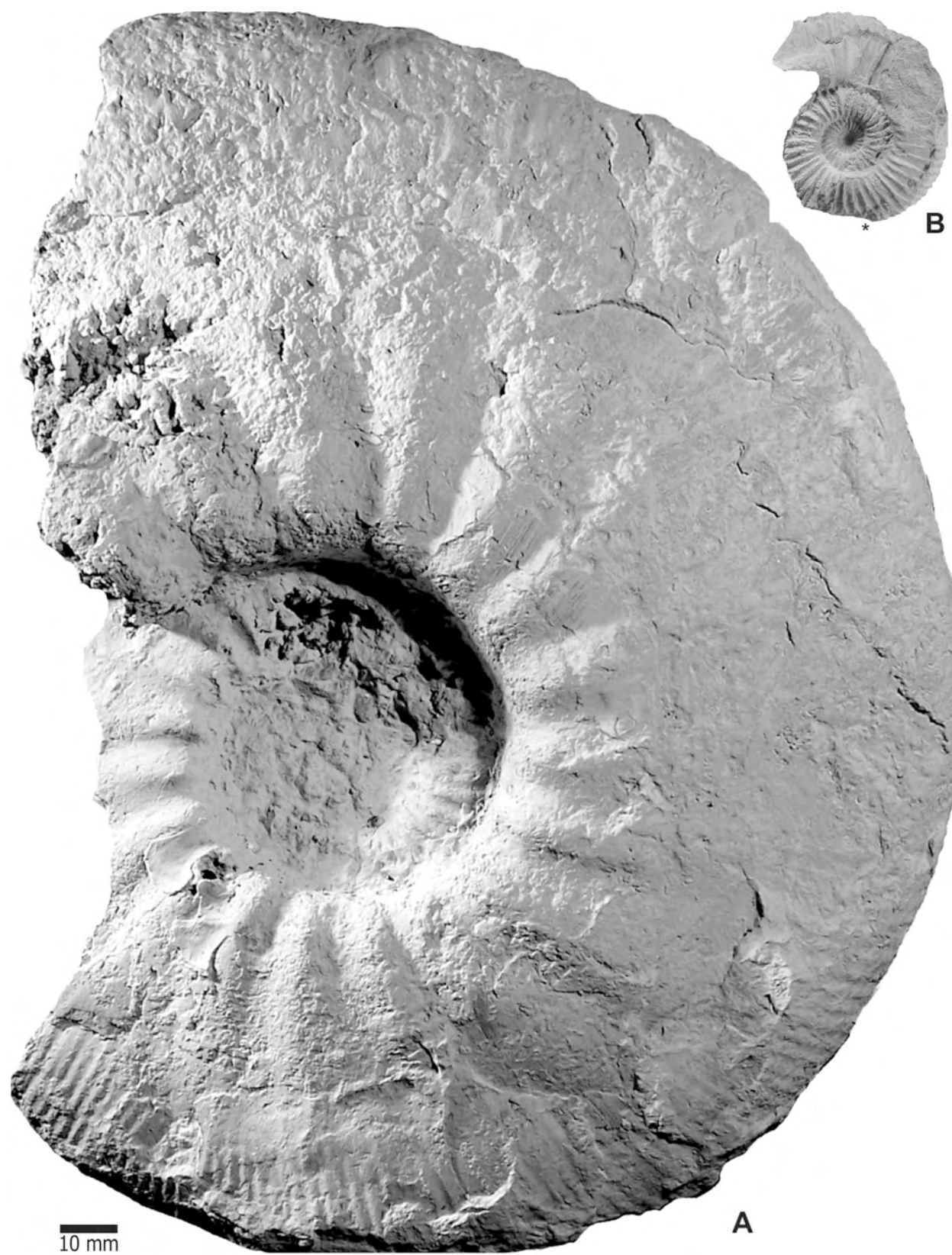


Figure 13. A: *Choicensisphinctes* cf. *limitis* (Burckhardt), crushed adult phragmocone (MCNAM 24388), Arroyo Cieneguita, bed AC-5 (Zitteli Z., cf. *erinooides* hz.). **B:** *Choicensisphinctes* sp. A, complete adult microconch with lappets (MCNAM 24445/2), A. Cieneguita, bed AC-7 (Proximus Z., *falculatum* hz.). All natural size. Asterisk indicating the last septum.

The HT of *C. limits* is a large phragmocone comparable with the largest specimens described herein, but a complete comparison is not possible because in that specimen the umbilical window is obscured by matrix and the inner whorls are not known.

The inner whorls shown in Fig. 11A are almost identical at comparable size with the HT of *Choicensisphinctes burckhardti* (Douvill , 1910).

Occurrence and distribution.- Bed AC-5 (cf. *erinoides* hz.), Zitteli Z. Large specimens from the upper Zitteli Z. of C. Lotena-C. Granito (PSSE 2008: 24, level 3) show their inner whorls identical to the specimen in Fig. 13A at the same diameter. These specimens are adult (uncoiled) phragmocones, larger than $D = 500$ mm, and could have been about $D = 1000$ mm at peristome.

***Choicensisphinctes* sp. A**

Fig. 13B

Description and remarks.- A small, complete adult microconch with lappets (MCNAM 24445/2) from bed AC-7 (*falculatum* hz., Proximus Z.). Moderately involute serpenticone with rounded to slightly subrectangular whorl section; densely ribbed by prosocline primaries which born on the umbilical wall and biplicate on the upper third of the flank. The bodychamber is half whorl long and the lappets are subtriangular as typical in the genus. This morphology corresponds to the perisphinctoid stage described above.

At a similar stratigraphic position in Cerro Lotena a macroconch *Choicensisphinctes* of moderate adult size occurs. The inner whorls of this specimen are similar to the present microconch, and the adult whorls have high and rather flat flanks and moderately narrow umbilicus.

***Choicensisphinctes striolatus* (Steuer, 1897)**

Fig. 14A-D

Synonymy.- See Parent (2003a).

Material.- Two microconchs and four macroconchs (MCNAM 24464/1-5), bed AC-17.

Description.- Innermost whorls globose, moderately involute, whorl section rounded wider than high. Ribbing begins at $D = 4$ mm as closely spaced plications on the lower third of the flank and umbilical shoulder. From $D = 6$ mm the whorl section turns to almost as high as wide; the lateral ribbing becomes dense, composed by fine primary ribs, mostly bifurcate on the lower third of the flank and the secondaries crossing the venter evenly spaced and unchanged. From $D = 12$ mm and through all the phragmocone the shell is more evolute, the whorl section slightly higher than wide with nearly flat flanks and rounded venter; the ribbing is very fine and dense, tending in most specimens to be weak on the lower part of the flanks.

In the macroconchs the bodychamber begins at about $D = 40$ mm; it is suboval in whorl section and covered by very fine and dense lateral ribbing, the primary ribs are moderately flexuous and divide in sheaves of secondaries on the lower half of the flanks.

In the microconchs the bodychamber begins at about $D = 22$ mm and extends through half a whorl with a more or less marked uncoiling near the peristome. It is compressed and very finely and densely ribbed by primaries which bi- or trifurcate on the middle of the flanks. The peristome remains

very finely ribbed and bears long subtriangular lappets.

Remarks.- The microconchs of the species are described for first time; the specimen figured by Leanza (1945: pl. 2: 7, 9) most likely is a microconch. The present macroconchs perfectly match with the LT and, especially, with the more involute and finely ribbed specimens which Steuer (1897) described as *Reineckeia striolatissima*.

This species was provisionally included in *Paraulacosphinctes* Schindewolf, 1925 by Parent (2003a) following Krantz (1928: 44), but the new material allows relocating the species in *Choicensisphinctes*. Inclusion in this genus is based on the shell shape and sculpture of the inner whorls and the form of the sexual dimorphism, which closely compare with *C. platyconus* and *C. densistriatus*. Indeed, the globose and finely ribbed innermost whorls (Fig. 14D) and the remaining phragmocone are identical to those of *C. platyconus* (see PGSS 2011: fig. 16B-D). The microconchs (Fig. 14A-B) are entirely comparable, including the form of the lappets (cf. PGSS 2011: fig. 15A-B). The stratigraphic gap between the *Choicensisphinctes* of the Zitteli Z. and *C. striolatus* is partially filled by *Choicensisphinctes* sp. A (described above) and material recently collected from Cerro Lotena (new species of the Proximus and Internispinosum zones) and Pampa Tril (undescribed forms from the Internispinosum and Alternans zones).

Steueroceras steueri Gerth (1925: 86, pl. 5: 4-4a, lectotype designated herein) from the Koeneni Z. of A. Durazno is indistinguishable from the specimens described above. Gerth (1925: 86-87) stressed the insignificant differences indicating that his species is very similar to *Steueroceras striolatissimum* (Steuer, 1897 = *C. striolatus*, see Parent 2003a), differing by the slightly denser ribbing and higher whorl section, suggesting the transitional variation between them through different localities but assuming the same age.

Occurrence and distribution.- The LT comes from the middle-upper Tithonian level Cieneguita-II of AC and was additionally described by Steuer (1921) from A. La Manga and Rodeo Viejo-III (nominally including the guide assemblage of ammonites of the *vetustum* hz., Alternans Z.). The present material was collected from a higher stratigraphic position, in the Koeneni Z., similar to the records of Leanza (1945). In C. Pincheira and P. Tril a succession of very similar forms occurs from the Internispinosum to the Alternans zones.

Genus *Krantziceras* n. gen.

Type species.- *Krantziceras compressum* n. sp.

Diagnosis.- Macroconchs. Compressed and evolute with shallow and wide umbilicus, more or less flat flanks and rounded to flattened venter; ribbing wiry, dense, narrowly biplicate on the upper half of the flank, few simple ribs; a narrow ventral groove may occur in the phragmocone; bodychamber isocostate to slightly variocostate.

Derivation of the name.- After Fritz Krantz (1859-1926).

Species included.- Some perisphinctoid ammonites with *Paraulacosphinctes*-like morphology occur in the interval of the Alternans to Noduliferum zones of the NMB, although they are apparently scarce accounting for the published

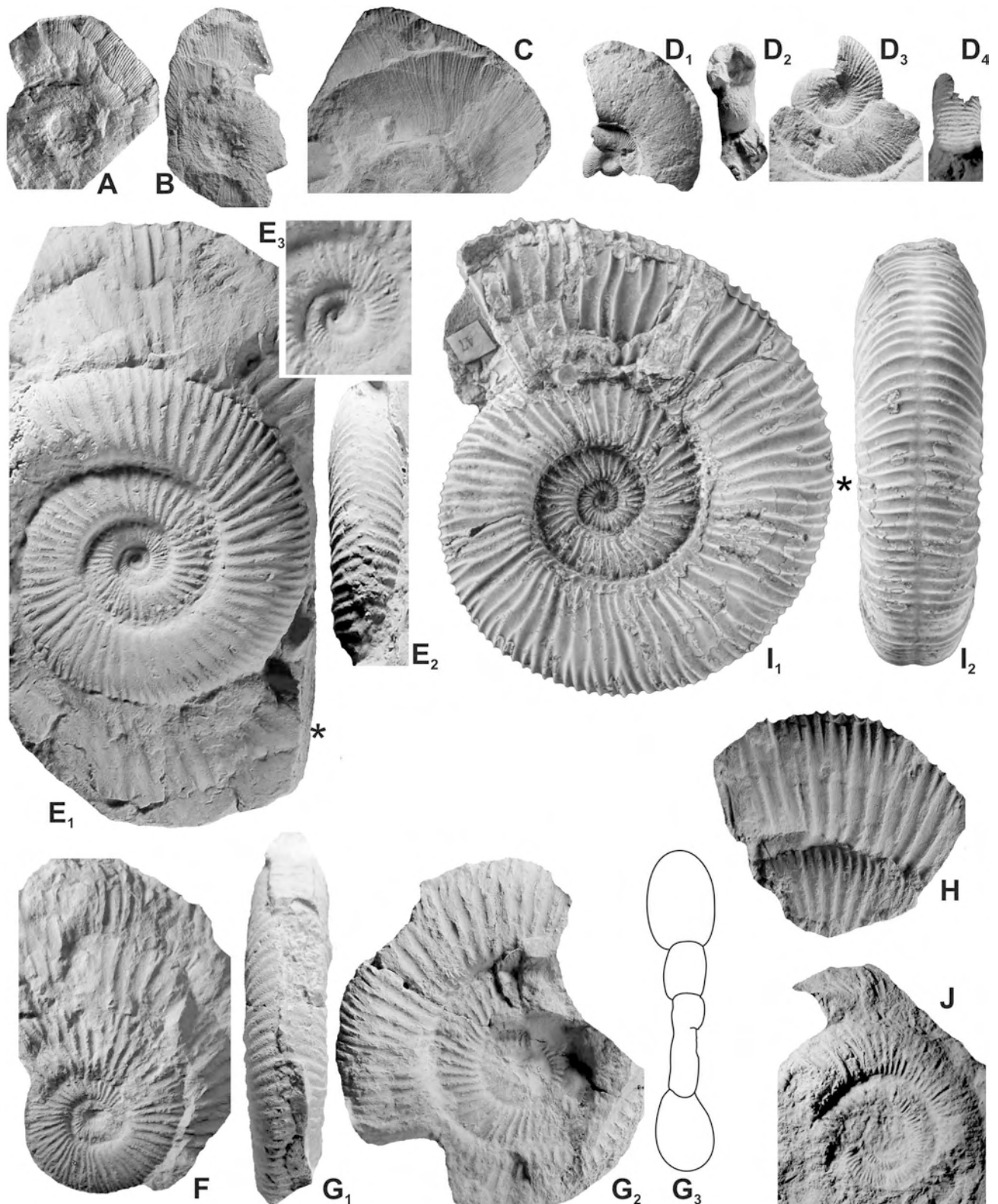


Figure 14. **A-D:** *Choicensisphinctes striolatus* (Steuer), Arroyo Cieneguita, bed AC-17 (Koeneni Zone, *striolatus* hz.); **A:** almost complete crushed adult microconch (MCNAM 24464/2) with base of lappets preserved. **B:** complete, crushed adult microconch with lappets (MCNAM 24464/1). **C:** portion of a macroconch bodychamber (MCNAM 24464/3). **D:** phragmocone (MCNAM 24464/5); **D₁-D₄:** apertural, lateral and ventral views of the inner whorls (x2). **E-H:** *Krantziceras compressum* n. gen. et n. sp., Arroyo Cieneguita, bed AC-19 (Noduliferum Zone, *compressum* hz.); **E:** holotype, adult macroconch with half whorl of bodychamber (MCNAM 24468/1); **E₃:** detail of the innermost whorls (x2); **F:** portion of phragmocone and bodychamber showing details of the sculpture (MCNAM 24468/5); **G:** paratype, phragmocone with beginning of the bodychamber (MCNAM 24468/7); **G₃:** whorl section at $D = 60$ mm. **H:** fragmentary specimen (MCNAM 24468/8) showing well preserved inner whorls. **I:** *Krantziceras wanneri* (Krantz, 1926), lectotype of *Aulacosphinctes wanneri* Krantz, 1926; adult specimen with a quarter whorl of bodychamber; Arroyo de La Manga, upper Tithonian, Alternans Zone; refigured from Krantz (1928: pl. 2: 6). **J:** *Malagasites?* sp. A, phragmocone (MCNAM 24454/3), A. Cieneguita, bed AC-12 (Internispinosum Zone). All natural size otherwise indicated. Asterisk indicating the last septum.

material, they could be included in the new genus as follows:

(1) *Aulacosphinctes wanneri* Krantz, 1926, Alternans Z. of Arroyo de la Manga. The HT by MT (Krantz 1928: pl. 2: 6) is refigured photographically herein (Fig. 14I) and discussed below.

(2) *Aulacosphinctes hebecostatus* Krantz, 1926 (1928: pl. 3: 8, HT by MT), C. Pincheira. The ammonites listed by Krantz (1928: 48) include nominal species of the interval Alternans-Damesi zones.

(3) *Krantziceras compressum* n. gen. et n. sp. (TS).

(4) *Krantziceras* cf. *compressum* n. gen. et n. sp.: the specimen figured as *Reineckeia transitoria* (Oppel) by Steuer (1897, 1921: pl. 15: 6, A. de la Manga; refigured in Parent 2003a: fig. 9E-F) and cited from level Cieneguita-III.

(5) *Substeueroceras disputabile* Leanza, 1945, Noduliferum Z. of M. Redondo. There was no type designation, thus the large macroconch specimen figured by Leanza (1945: pl. 7: 3, pl. 9: 1) is herein designated as the lectotype. The paralectotype (Leanza 1945: pl. 8: 3) is very different in its shell shape and sculpture respect to the LT, but shows the typical features of *Substeueroceras*.

(6) *Odontoceras ellipsostomum* Steuer, 1897, Noduliferum Z. of AC. The syntype series included several specimens, and no type was designated. The large phragmocone figured by Steuer (1921: pl. 21: 1-2) from his level Cieneguita-V is designated as lectotype and refigured in App. 2-A.

(7) *Krantziceras* cf. *compressum*: the specimen from AC figured as *Odontoceras theodorii* Oppel by Steuer (1897, 1921: pl. 20: 5, 7) from his level Cieneguita-V, Noduliferum Z. The original description indicates resemblance with the inner whorls of *K. compressum* n. gen. et n. sp.

Remarks.- There are some similarities in the ribbing style of *Krantziceras* n. gen. and *Andiceras* Krantz, 1926 (TS: *Andiceras trigonostomum* Krantz, 1926; by SD: Arkell 1957), but there are significant differences in the subtriangular whorl section and the persistent ventral depression with uninterrupted ribbing in *Andiceras*. However, the LT (herein designated) of *A. trigonostomum* (Krantz 1926, transl. 1928: pl. 2: 1) was isolately collected in the succession of Arroyo Paraguay and supposed to be of Tithonian age, but with no published evidence. These conditions turn impossible to assess the significance of the superficial similarities between these genera. Moreover, *Andiceras* should be considered a nomen dubium.

***Krantziceras compressum* n. sp.**

Fig. 14E-H

Type locality and horizon.- A. Cieneguita, bed AC-19, *compressum* hz., Noduliferum Z.

Derivation of the name.- After the compressed shell of the species.

Material.- Type series: Holotype [M], Fig. 14E (MCNAM 24468/1) and two paratypes: PT-I [M], Fig. 14F (MCNAM 24468/5); PT-II [M?], Fig. 14G (MCNAM 24468/7). Additional material: three fragmentary specimens. All from

bed AC-19, *compressum* hz., Noduliferum Z.

Description.- Innermost whorls ($D = 3-5$ mm) evolute, rounded in whorl section, at first smooth and then with fine prosocline primary ribs. From about $D = 7$ mm the whorl section becomes subrectangular with subvertical umbilical wall and rounded but clear-cut shoulder passing to the flat flanks; ribbing is composed by fine and dense primary ribs ($P = 22$), many of them bifurcating just below the involution line. The adult phragmocone, very evolute and with rounded venter, is ribbed by wiry and prosocline primary ribs ($P = 20$) narrowly biplicate on the upper third of the flanks. Ventral ribbing (secondary ribs plus very rare, isolated intercalatories) cross evenly space the venter with no changes in strength. The umbilical width tends to be wider and the lateral ribbing is denser towards the bodychamber, passing from $U/D = 0.39$, $P = 20$ (for $D = 33$ mm) to $U/D = 0.43$, $P = 25$ (for $D = 65$ mm).

In the HT the phragmocone ends at $D = 80$ mm. The bodychamber is crushed but shows clearly that the ribbing does not change (isocostate). The preserved portion of bodychamber extends along a half whorl; the adult size at the peristome is estimated at about $D = 110$ mm.

Remarks and comparison.- Material of this species from the Noduliferum Z. of P. Tril, identical to the type series, shows some complementary features: (1) the adult [M] may reach at the peristome a diameter of 190 mm, (2) the complete adult [M] bodychamber is $L_{bc} = 270-360^\circ$, and (3) in the juvenile phragmocone ($D = 30-50$ mm) of certain specimens occurs a well marked narrow ventral groove or smooth band, formed by the interruption of the ventral ribbing.

The LT of *Krantziceras disputabile* (Leanza) is similar to *K. compressum* n. gen. et n. sp. in the generic features, but differs significantly by its larger involution and sculpture and by reaching a bigger adult size. The ribbing of the phragmocone is more irregular, with polyfurcations and regular occurrence of intercalatory ribs, the bifurcation occurs at different heights of the flank with the secondaries detached from the primary. On the last whorl (bodychamber?) the specimen becomes variocostate from $D = 120$ mm, the primaries are somewhat engrossed and more spaced on the umbilical shoulder and the lower part of the flanks, and divide irregularly in three or more secondaries, there are several intercalatory ribs.

Krantziceras wanneri (Krantz) is stratigraphically older (Alternans Z.), the whorls are wider, the ribbing has more simple ribs associated to narrow constrictions, and the ventral ribbing is more consistently interrupted beside a narrow groove.

The cited occurrence of *Andiceras* between the Koeneni and Noduliferum zones in Real de las Coloradas (Mendoza) by Aguirre & Alvarez (1999) most likely corresponds to specimens of the present species.

Occurrence and distribution.- *compressum* hz., Noduliferum Z. of AC and P. Tril. In this latter locality the species was recorded from a narrow horizon just underlying the main occurrence of *Argentiniceras noduliferum* (Steuer, 1897).

Genus *Platydiscus* n. gen.

Type species.- *Platydiscus beresii* n. sp. Middle Tithonian.

Diagnosis.- Macroconch: innermost whorls rounded,

ribbing prosocline, strong on flanks, faint on the venter; middle whorls rounded, moderately involute, densely ribbed. Adult bodychamber three quarters to one whorl long, platycone, compressed, umbilicus wide and shallow; densely ribbed by acute flexuous primaries bifurcated on the middle of the flank and intercalating with some simple ribs, mostly grouped in pairs, all interrupted on venter on a persistent groove which fades off near the peristome. Microconch: phragmocone as in the macroconch; adult bodychamber half a whorl long, compressed, unevenly ribbed and bearing short lappets.

Derivation of the name.- After the compressed platycone shell morphology.

Remarks.- *Platydiscus* n. gen. differs from *Catutosphinctes* by its well marked and persistent ventral groove or smooth band, the compressed platycone aspect, the fine and dense ribbing on the inner whorls with a different sculptural style with low points of furcation (cf. Figs. 15B₃ and 19D₃-D₄). The macroconchs of *Catutosphinctes* become much larger in size. *Catutosphinctes* n. sp. A described below resembles *P. beresii* n. gen. et n. sp. by the inner whorls which are also finely ribbed with a faint smooth ventral band, but the subsequent ribbing is very different, typical of *Catutosphinctes*.

Species included.- The specimen from the lower Internispinosum Z. of Cerro Lotena figured as *Parapallasiceras* aff. *recticosta* Olóriz, 1978 by Leanza (1980: pl. 8: 6) could be assigned to *Platydiscus* n. gen., differing from the TS by the ribbing of the bodychamber which is more regular with higher point of furcation and cross the venter with no interruption. These differences are represented similarly in some specimens of AC (Fig. 15C-D, F). The specimen figured by Leanza (1945: pl. 3: 1-2) as *Aulacosphinctes mangaensis* (Steuer), from bed f of Arroyo del Yeso, is practically identical to the HT of *P. beresii* n. gen. et n. sp., slightly differing in the last whorl where the ventral groove is narrow and fades off through the peristome, but showing the characteristic shell shape and sculpture. This undoubted record of the genus in the Koeneni Z. indicates the genus has a rather long stratigraphic range. It is worth to note that the HT of *Reineckeia mangaensis* Steuer, 1897 (refigured photographically in Parent 2003a: fig. 9G-H) is a *Micracanthoceras*-like ammonite, evolute serpenticon with simple and bifurcate primary ribs with small tubercles on the furcation point.

***Platydiscus beresii* n. sp.**

Fig. 15A-J

Material.- 10 specimens [M], 2 [m] and 3 juvenile not sexed, all from beds AC-7 and AC-8. Type series (bed AC-7): Holotype [M], Fig. 15A (MCNAM 24450) and four paratypes: PT-I [M], Fig. 15B; PT-II [M], Fig. 15C; PT-III [m], Fig. 15G; PT-IV [m], Fig. 15J.

Type locality and horizon.- The type series was collected in AC (Fig. 1), bed AC-7, *fulcatum* hz., Proximus Z. (Fig. 2).

Derivation of the name.- After Matilde Sylvia Beresi (CRICyT, IANIGLA, Mendoza), specialist in fossil sponges.

Description.- Macroconchs: innermost whorls ($D < 8$ mm)

subospherocone with rather wide umbilicus, low flanks and widely rounded venter; ribbing strong and prosocline on the flanks but faint on the venter. The juvenile phragmocone at $D = 8-20$ mm is moderately involute to evolute with a rounded, rarely subrectangular, whorl section; ribbing fine and dense, prosocline, the primaries starting on the umbilical seam and bifurcating on the upper half or upper third of the flanks, simple undivided ribs may be more or less frequent, sometimes they are joined at the umbilical shoulder with the adjacent primary. The adult phragmocone ends, with low variation, at $D = 30-40$ mm. The adult bodychamber is compressed, higher than wide, subrectangular in whorl section. Ribbing composed by acute primaries which start at the upper umbilical wall and cross the flanks slightly and unevenly flexuous, mostly bifurcating on the mid-flank; there are some simple ribs, most of them in closely spaced pairs. All ribs are strongly interrupted on the venter, besides a narrow groove which persists up to close the peristome. Adult diameter at peristome is estimated as $D_p = 45-60$ mm. The length of the bodychamber is three quarters to a complete whorl long. Microconchs: the adult phragmocone ends at $D = 20-30$ mm showing the morphology and sculpture described for the macroconch. From $D = 20$ mm macro- and microconchs diverge slightly in morphology, the [m] is more compressed and retains the juvenil aspect of the sculpture up to the peristome, which bears short lappets.

Remarks.- Difference in the adult size between macro- and microconchs is weak, comparing adult phragmocone diameters and diameters at peristome of [M] and [m]. This uncommon phenomenon in perisphinctid ammonites is due to the fact that both sexual dimorphs, macro- and microconch, have similar adult phragmocone diameters, 20-30 mm in microconchs and 30-40 mm in macroconchs, and the lengths of the bodychamber differs in less than a half whorl.

Occurrence and distribution.- The material described was collected in beds AC-7 (*fulcatum* horizon) and AC-8, Proximus Zone. For the time being the species was not recorded in other localities in comparable stratigraphic position.

Subfamily Virgatosphinctinae Spath, 1923a

Genus *Malagasites* Enay, 2009

Type species.- *Perisphinctes (Virgatosphinctes) haydeni* Uhlig, 1910; by OD.

***Malagasites?* sp. A**

Fig. 14J

Remarks.- A single specimen from bed AC-12 (Internispinosum Z.) with a conspicuous morphology and ribbing style not seen in any other Andean perisphinctid. A well rounded serpenticon shell, very evolute with gently rounded flanks covered by densely arranged radial primary ribs which are mostly undivided, rarely bifurcated.

Subfamily Torquatisphinctinae Tavera, 1985

Genus *Catutosphinctes* Leanza & Zeiss, 1992

Type species. *Catutosphinctes rafaelli* Leanza & Zeiss, 1992 by OD. Middle Tithonian.

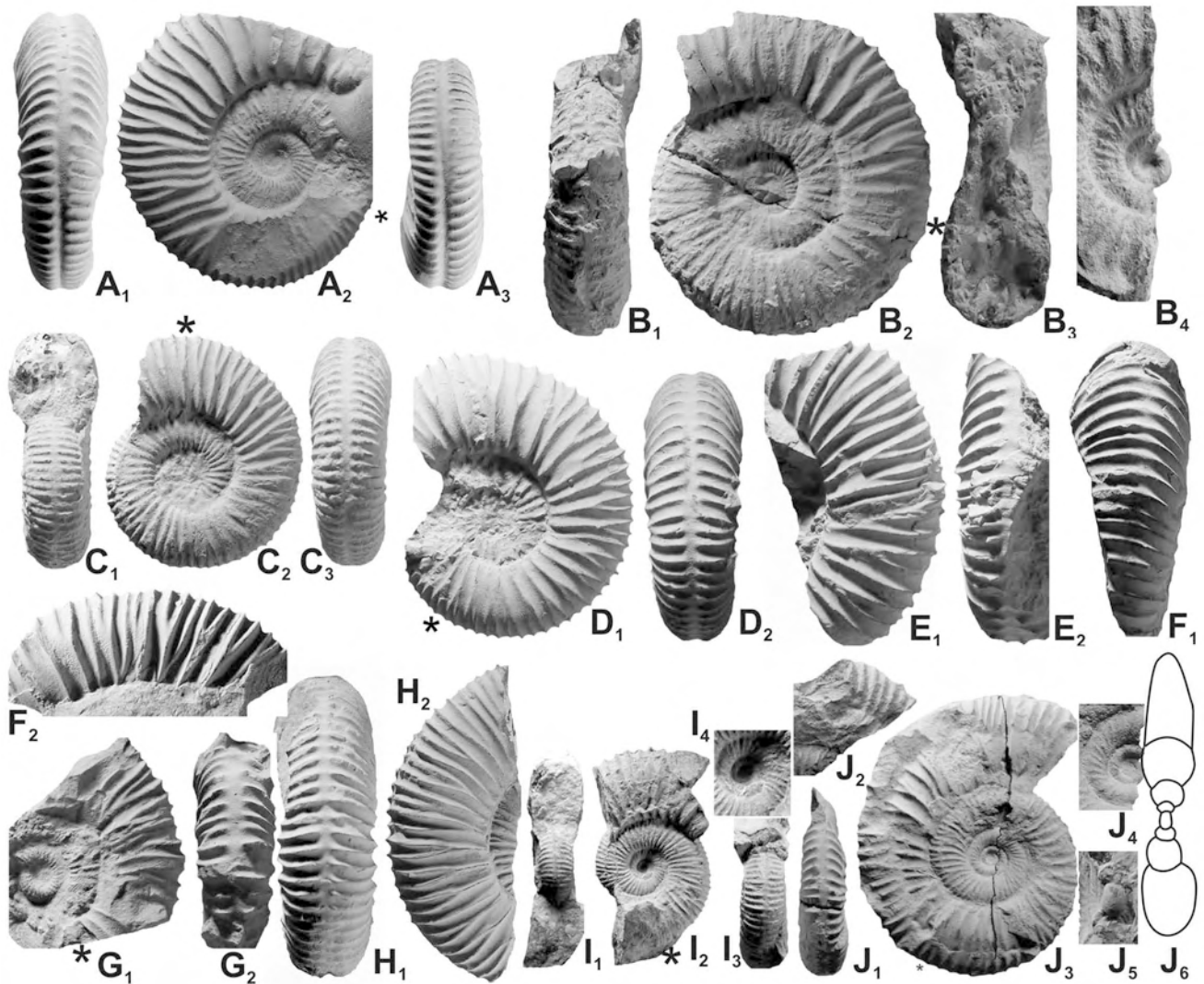


Figure 15. *Platydiscus beresii* n. gen. et n. sp. [M&m], A. Cieneguita, beds AC-7 (Proximus Z., *falculatum* hz.) and AC-8 (Proximus Z.). **A:** holotype, nearly complete adult macroconch (MCNAM 24450), bed AC-7. **B:** paratype I, nearly complete adult macroconch (MCNAM 24415/1), bed AC-7. **C:** paratype II, adult macroconch with beginning of the bodychamber (MCNAM 24416/2), bed AC-7. **D:** nearly complete macroconch (MCNAM 24416/1), bed AC-8. **E-F:** portions of adult macroconch bodychambers (MCNAM 24440 and 24448), bed AC-7. **G:** paratype III, nearly complete adult microconch (MCNAM 24415/4), bed AC-7. **H:** portion of adult macroconch bodychamber (MCNAM 24433), bed AC-7. **I:** nearly complete adult showing the innermost whorls (I, x2), the remaining phragmocone whorls and portions of bodychamber (MCNAM 24449/1), bed AC-8. **J:** paratype IV, complete adult microconch (MCNAM 24447), bed AC-7; **J₁:** ventral view at the end of phragmocone; **J₂:** lateral view of the lappet of the right side (apertural view); **J₃:** lateral view of left side; **J₄-J₅:** lateral and ventral views of the innermost whorls (x2). All natural size otherwise indicated. Asterisks at last septum.

Remarks. - The genus *Catutosphinctes* (recently reviewed in PGSS 2011) is currently known throughout the Tithonian of the NMB showing a lineage composed of rather slowly changing successions of species (see Parent 2001, 2003a). Herein new material of interesting species is described, one of them from the Zitteli Z., partially filling the gap in this zone. Much material from a large number of horizons has been collected in Pampa Tril, Cerro Granito and Cerro Lotena (to be published elsewhere) including several new species or transients of this lineage.

Catutosphinctes guenenakenensis Parent, Garrido, Schweigert & Scherzinger, 2011

Fig. 16A

Synonymy. - See PGSS (2011).

Remarks. - In bed AC-1 abundant but poorly preserved and

incomplete material of this species occurs. The best specimen (Fig. 16A) is a phragmocone with beginning of the bodychamber, apparently adult. This specimen is comparable with the phragmocone of the HT and other specimens figured by PGSS (2011: fig. 27A).

This morphotype of the species is characteristic of the *picunleufuense* α horizon of the Picunleufuense Zone. The wide geographic distribution throughout the basin is described in PGSS (2011).

Catutosphinctes cf. *guenenakenensis* Parent, Garrido, Schweigert & Scherzinger, 2011

Fig. 17

Material. - Two large macroconch specimens (MCNAM 24373), bed AC-4 (*perlaevis* hz., Zitteli Z.).

Description. - Stout, involute serpenticone with

subtrapezoidal, wider than high whorl section. Adult macroconchs with estimated max $D = 210$ mm, probably with peristome. The last septum is at $D_{ls} = 130$ mm; the bodychamber is at least $L_{bc} = 270^\circ$ and slightly uncoiled. The inner whorls are not preserved. The last whorl of the phragmocone shows, in the first half, prosocline polyschizotome ribs which bifurcate on the lower half of the flank and one of the secondaries bifurcates again on the upper part of the flank. In the last half whorl of phragmocone the ribbing turns to more widely spaced and stronger composed by acute primary ribs which born on the umbilical shoulder and bi- or trifurcate on the upper half of flanks in secondaries of reduced strength with the point of furcation slightly swollen. The subdivision is subvirgatotome with scarce intercalatories. The ventral ribbing is evenly spaced and weak on the mid-venter. The bodychamber is moderately variocostate, showing strong blade-like, prosocline primary ribs which start on the umbilical shoulder and bi- or trifurcate on the upper third of the flank. Some few ribs associated to constrictions are polyschizotome.

Remarks.- The most similar species is *C. guenenakenensis*. The differences are the greater involution, the stouter whorl section and the shorter stage of blade-like primaries divided in several secondaries in the present material. This form of the Zitteli Z. is very important for composing the *Catutosphinctes* lineage, but the available material is scarce for evaluating the taxonomic significance of the differences respect *C. guenenakenensis*.

Catutosphinctes windhausenii (Weaver, 1931)

- 1900a *Perisphinctes colubrinus* Reinecke.- Burckhardt: 44, pl. 24: 5-6.
 1903 *Perisphinctes* aff. *pseudocolubrinus* Kilian.- Burckhardt: 39, pl. 5: 1-2.
 *1931 *Aulacosphinctes windhausenii* n. sp.- Weaver: 412, pl. 44: 300 [HT].
 n1980 *Subdichotomoceras windhausenii* (Weaver).- Leanza: 36, pl. 8: 2.
 *2011 *Catutosphinctes windhausenii* (Weaver).- Parent et al.: fig. 25A [HT refigured].

Remarks.- This species was recently revised (PGSS 2011). It is characterized by an evolute serpenticone coiling throughout the ontogeny, with rounded or compressed (microconchs) whorl section and acute ribbing which cross the venter unchanged. Inner whorls are the most distinctive, very evolute with rather distant strong, acute, slightly prosocline primary ribs, bifurcate on the upper half or third or the flanks; secondary ribs are widely splayed and, in the microconchs, they cross the venter evenly arched forwardly.

This morphotype is mainly recorded from the *malgarguense* hz., and in Cerro Granito is recorded abundantly (including large [M]) in a level where occur the first *P. zitteli*. Below occurs, according to our records, the well defined and different *C. guenenakenensis* (see PGSS 2011) and above *C. cf. guenenakenensis* (described above), which is followed by the earliest or close representatives of *C. proximus* (transient α in Parent 2001, 2003a) illustrated by specimens like that figured by Steuer (1921: pl. 15: 11 = Parent 2003a: fig. 9K-L) and Parent (2003a: fig. 13A and B).

New information is now available from new collections in other parts of the NMB. An early record of *C. windhausenii* was presented by Burckhardt (1900a and 1903) with three

specimens from his M6-assemblage of Casa Pincheira, named *malgarguense* hz. by PGSS (2011).

The specimen from the Internispinosum Z. of C. Lotena figured by Leanza (1980: pl. 8: 2) is a microconch with the base of the lappet preserved. Besides the very different age, it differs from *C. windhausenii* by its narrower umbilicus, a wider whorl section, a more radial ribbing with well marked swellings shaping lamellar tubercles on the point of furcation of the ribs. We consider this specimen from C. Lotena as a [m] closely allied to *Catutosphinctes araucanense* (Leanza, 1980).

The ammonite from A. de la Manga figured by Steuer (1921; refigured herein in App. 2-G) as *Reineckeia* cf. *stephanoides* (Oppy) shows superficial resemblance with the HT of *C. windhausenii* but differences are more important and significant. The specimen from A. de la Manga shows a depressed, wider than high whorl section with a characteristic wide and subflattish venter, and has well define tubercles from which the primaries trifurcate, indicating it is clearly a representative of *Windhauseniaceras* Leanza, 1945 (see discussion below).

Catutosphinctes cf. windhausenii (Weaver, 1931)

Fig. 16B-D

Material.- Three more or less well preserved specimens from bed AC-2 (MCNAM 24392 and 24394) and bed AC-3 (MCNAM 24393). Picunleufuense Zone.

Remarks.- The available material includes macroconchs (Fig. 16B-C) and a lappeted microconch (Fig. 16D). The inner whorls are not preserved but the outer whorls of the macroconchs are evolute and covered with strong, wiry ribbing resembling the HT of *C. windhausenii*. The microconch is interesting for it shows the strong irregular ribbing close to the peristome and the lappet that was unknown yet in this species.

Catutosphinctes proximus (Steuer, 1897)

Figs. 8C-E, 18A-F, 19A-C, App. 1

- *1897 *Reineckeia proxima* nov. sp.- Steuer: 160, pl. 22 : 7-8 [LT].
 n1897 *Reineckeia proxima* nov. sp.- Steuer: 160, pl. 22 : 10-11 [paralectotype].
 1921 *Reineckeia proxima* n. sp.- Steuer: 61, pl. 8: 7-8 [LT refigured].
 n1921 *Reineckeia proxima* n. sp.- Steuer: 61, pl. 8: 10-11 [paralectotype refigured].
 1980 *Aulacosphinctes proximus* (Steuer).- Leanza: 44, pl. 6: 2, 4-5.
 2001 *Torquatisphinctes proximus* (Steuer).- Parent: 30, fig. 8D-H.
 *2003a *Torquatisphinctes proximus* (Steuer).- Parent: 159, figs. 9I-J [LT refigured], 13A-B.
 n2009 *Aulacosphinctes proximus* (Steuer).- Aguirre & Vennari: 39, fig. 5r-t.
 n2011 *Catutosphinctes proximus* (Steuer).- Parent et al.: fig. 25B [paralectotype refigured].

Material.- Eighteen more or less well preserved specimens (6 [M], 4 [m], 8 juveniles or incomplete) and several fragmentary ones from beds AC-7 to AC-11.

Description.- This species has a rather long stratigraphic range (about upper Zitteli to lower Internispinosum zones),

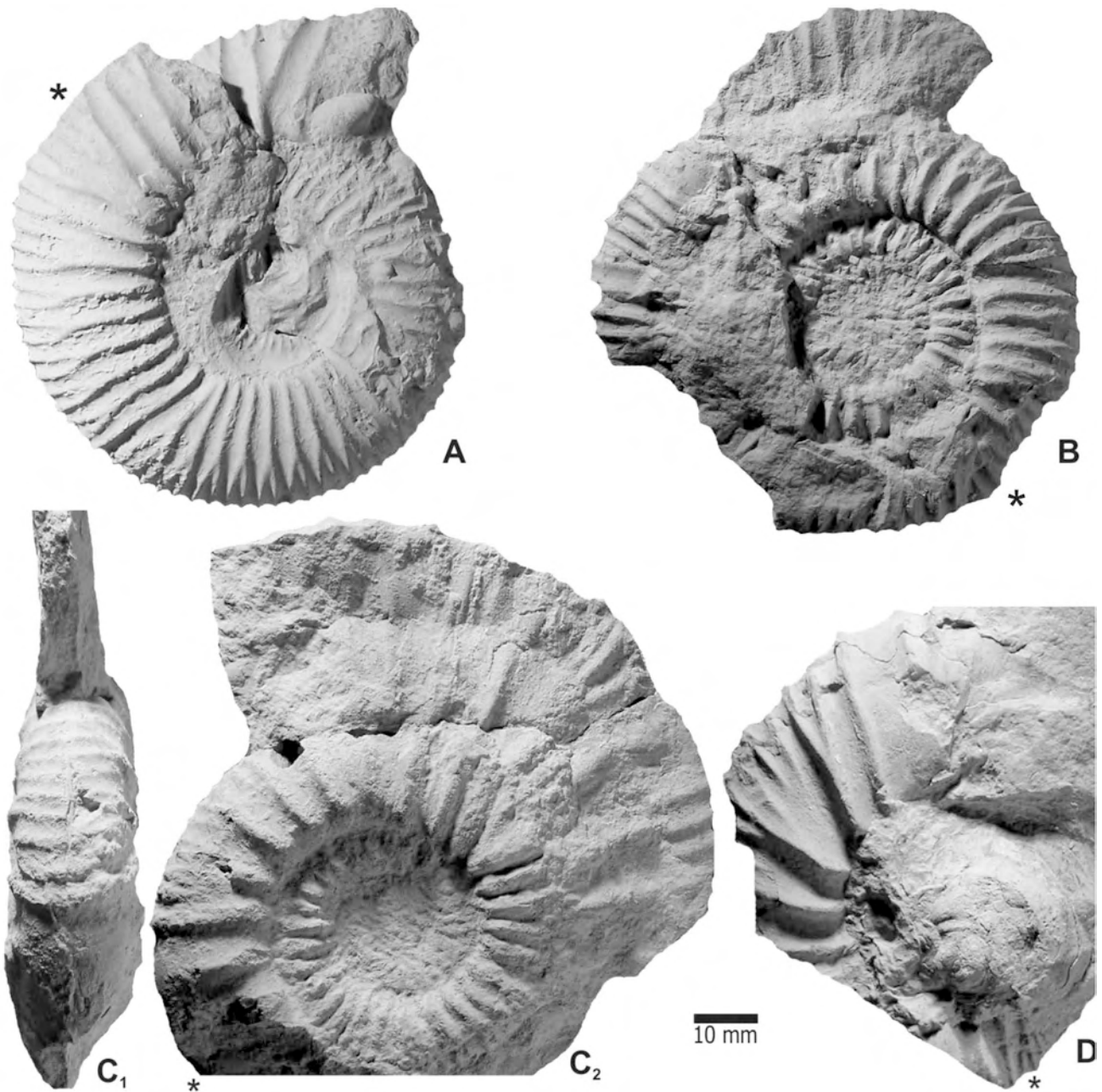


Figure 16. **A:** *Catutosphinctes guenakenensis* Parent, Garrido, Schweigert & Scherzinger, macroconch phragmocone with beginning of bodychamber (MCNAM 24403), A. Cieneguita, bed AC-1 (Picunleufuense Z., *picunleufuense* α hz.). **B-D:** *Catutosphinctes* cf. *windhausei* (Weaver), A. Cieneguita; **B:** phragmocone with crushed portion of bodychamber (MCNAM 24392), bed AC-2 (Picunleufuense Z.); **C:** phragmocone with crushed portion of bodychamber (MCNAM 24393), bed AC-3 (Picunleufuense Z.); **D:** adult microconch bodychamber with lappets and remains of phragmocone (MCNAM 24394), bed AC-2 (Picunleufuense Z.). All natural size. Asterisks indicating the last septum.

along which can be distinguished at least two successive mean morphotypes called transients α and β (Parent 2001: 30). The typical morphology of the transient α was already described in detail by Parent (2003a: 160). The material described below corresponds to late representatives of the transient β to which the lectotype belongs.

Macroconchs: At $D = 2.5$ mm the shell is evolute ($U/D = 0.40$) with wide depressed whorl section ($W/D = 0.70$); venter smooth, flanks covered by prosocline primary ribs. The shell remains very evolute with moderately wide umbilicus and depressed whorl section up to about $D = 7$ mm; ventral ribbing is faint and primaries acute and prosocline. The remaining whorls of the phragmocone turns to a more serpenticonic morphology, evolute with wide

umbilicus and suboval to subrectangular whorl section, may be slightly wider than high or vice versa. The sculpture consists of strong, acute, prosocline bifurcate primary ribs raising on the point of furcation; very few ribs remain simple and few others trifurcate after a constriction; ventral ribbing cross the venter evenly spaced with no changes out of a slight forward arching which follows a forward projection of the secondaries on the uppermost flank. The number of primary ribs follows increasing regularly with short breaks in which the number of ribs remains constant, but rapidly returning to the continuous increments with the growth. The bodychamber begins at about $D_{is} = 60$ and 110 mm in the two larger specimens studied; the largest one has widely spaced and strong primaries with abundant intercalatory ribs.

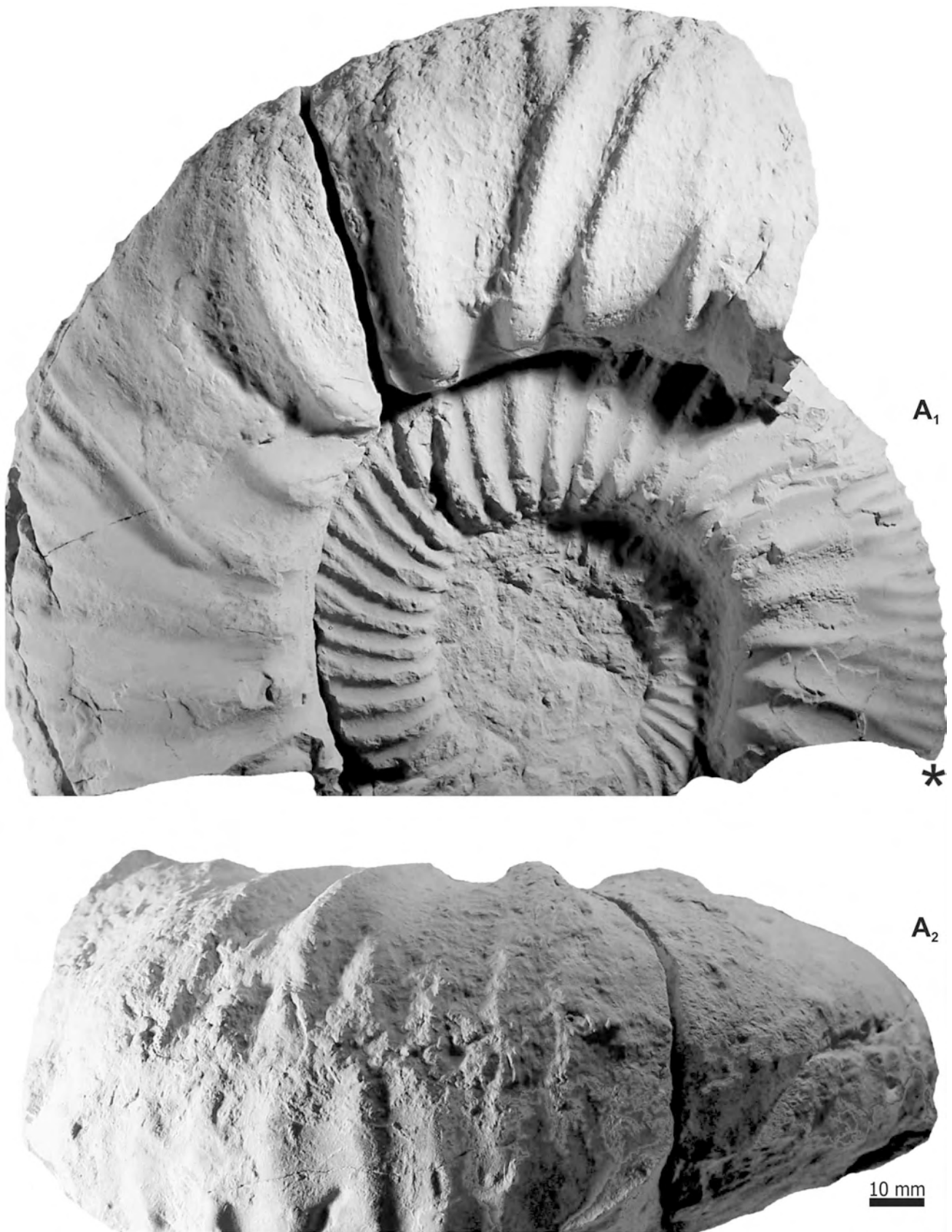


Figure 17. *Catutosphinctes* cf. *guenenakenensis* Parent, Garrido, Schweigert & Scherzinger, adult macroconch with almost complete bodychamber (MCNAM 24373), Arroyo Cieneguita, bed AC-4 (Zitteli Z., *perlaevis* hz.). Natural size. Asterisk indicating the last septum.

Microconchs: phragmocone like in the [M]. The bodychamber begins at $D = 35\text{--}55$ mm depending on the specimens. Whorl section is variable, more or less inflates to slender, evolute to very evolute. Ribbing remains unchanged up to the peristome. The peristome bears short and wide lappets.

Remarks.- After the description of both sexual dimorphs it can be assumed that the LT (see Parent 2003a: fig. 9I-J) is a [m] and, moreover, its morphology is intermediate between the specimens shown in Figs. 18C and 18D. The adult bodychamber of the [M] remains incompletely known from our material. The [M] morphotype shown in Fig. 18B persists, at least, up to the bed AC-11 (*Internispinosum* Z.) where also occur specimens closer to *C. inflatus* (Fig. 20A). The large [m] morphotype shown in Fig. 18E persists, at least, up to the bed AC-10 (*Internispinosum* Z.).

Ribbing curves show a remarkable feature in the present species and in *C. inflatus*. The number of primary ribs per half whorl (P) has a sustained trend of increasing from the innermost whorls. Within the interval $D = 10\text{--}40$ mm all specimens retain for a short stage exactly the same number P producing transitory breakings in the trend, seen as short horizontal segments of the growth curves in Fig 8C (and in Fig. 8F for *C. inflatus*). This process is seen in the specimens as a short stage in which the ribs are more widely spaced after which they resume quickly the increments. This process recalls the segmental growth observed by Howarth (1998: 46) in late Kimmeridgian *Torquatisphinctes*, and, certainly, could be a modification of these changes in growth rates in *Catutosphinctes* which is considered a local Andean lineage derived directly from the Indo-Madagascan *Torquatisphinctinae* (PGSS 2011).

The slender and very evolute specimen shown in Fig. 19C is interesting because it is an extreme morphotype in terms of shell shape but the sculpture ontogeny seems closely comparable to that of the remaining material described above. On the other hand, this morphotype occurs in abundance in a well defined horizon of the upper *Proximus* Z. in Cerro Lotena.

The paralectotype (PGSS 2011: fig. 25B) shows a sculpture composed by acute ribs which reach the venter and are interrupted, with formation of lamellar tubercles or bullae, besides a well marked ventral groove. This sculpture is diagnostic of *C. inflatus* (see description below) but not typical of *C. proximus*.

Occurrence and distribution.- Beds AC-7-AC-11, *Proximus* to *Internispinosum* zones.

***Catutosphinctes* sp. A**

Fig. 19E-F

Remarks and comparison.- Two specimens, from beds AC-7 and AC-8 (*Proximus* Z.) respectively, which show a characteristic sculpture, especially in the inner whorls. Up to $D = 20$ mm they are moderately involute and densely ribbed, changing later to strong, acute primaries bifurcated on the uppermost part of the flank with a subrectangular whorl section. This form intergrades with *C. proximus* via *C. cf. proximus* from bed AC-7 (Fig. 19D).

These specimens are important for biostratigraphy since in C. Lotena this form is abundant in beds of the upper *Proximus* Z., or less probably of the lowermost *Internispinosum* Z., below the horizon where occur specimens comparable with that in Fig. 19C.

***Catutosphinctes colubrinoides* (Burckhardt, 1903)**

*1900a *Perisphinctes colubrinus* Reinecke.- Burckhardt: 46, pl. 26: 4 (LT).

*1903 *Perisphinctes colubrinoides* n. sp.- Burckhardt: 57, pl. 10: 9, 10 (LT refigured).

Lectotype.- Burckhardt (1903: 57) based this species on at least three specimens from the Tithonian of C. del Burro – Río Choicas, but with no designation of a type. The specimen figured by Burckhardt (1903: pl. 10: 10) is designated herein as the lectotype. This specimen, a microconch, was formerly figured photographically in Burckhardt (1900a: pl. 26: 4) as *P. colubrinus*.

Remarks.- The LT and figured paralectotype are identical to *C. rafaelli* Leanza & Zeiss, 1992 [m] as illustrated in Parent & Cocca (2007: fig. 3A-B). Although these later are [m] with a shorter ontogeny respect to their [M], it can be seen that they differ clearly from *C. proximus* by the more evolute and slender shell with consistent alternation of an undivided primary each one biplicate. Nevertheless, it is interesting to note that the occurrence of few undivided primary ribs is already seen in some specimens of that species (e.g. Fig. 18C-D), but it is very rare in the older *C. guenenakenensis*. Finally, in the latest known representative of the genus, *C. inflatus* (see below), the undivided primary ribs are frequent, sometimes predominating, especially on the adult macroconch bodychamber.

***Catutosphinctes inflatus* (Leanza, 1945)**

Figs. 8F-H, 20-21, App. 1

1897 *Reineckeia proxima* n.sp.- Steuer: 160, pl. 22: 10-11.

1921 *Reineckeia proxima* n. sp.- Steuer: 61, pl. 8: 10-11.

1928 *Riasanites* aff. *swistowianus* Nikitin.- Krantz, p. 27, pl. 4: 8.

*1945 *Berriassella fraudans* (Steuer) var. *inflata*.- Leanza, p. 31, pl. 1: 1 [HT].

2009 *Aulacosphinctes proximus* (Steuer).- Aguirre & Vennari: 39, fig. 5r-t.

2011 *Catutosphinctes inflatus* (Leanza).- Parent et al.: 81.

2011 *Catutosphinctes proximus* (Steuer).- Parent et al.: fig. 25B [Paralectotype of *C. proximus* refigured].

Material.- 33 more or less complete macro- and ?microconchs from beds AC-14-16.

Description.- Macroconch: innermost whorls ($D = 3$ mm) globose, moderately evolute with lateral plications and a pair of rows of swellings on the venter. At $D = 4$ mm the shell is cadicone ($W/D = 0.80$) moderately involute ($U/D = 0.30$), completely ribbed by dense primary ribs starting on the umbilical margin and with a well marked ventral interruption. The shell remains very evolute up to the bodychamber. From $D = 13$ mm the whorl section is rounded to subrectangular ($W/D = 0.60$), somewhat wider than high but variable, and compressing towards the peristome. Primary ribs strong and acute, they born on the low umbilical wall and some of them remain simple, but mostly bifurcate on the upper third of the flank, widely splayed, with the point of furcation raised forming an incipient lamellar tubercle. Secondary ribs are as strong and acute as the primaries, reaching the venter where they die out more or less abruptly, sometimes with swellens or lamellar tubercles aside a groove. From the last whorl of the phragmocone, about $D =$

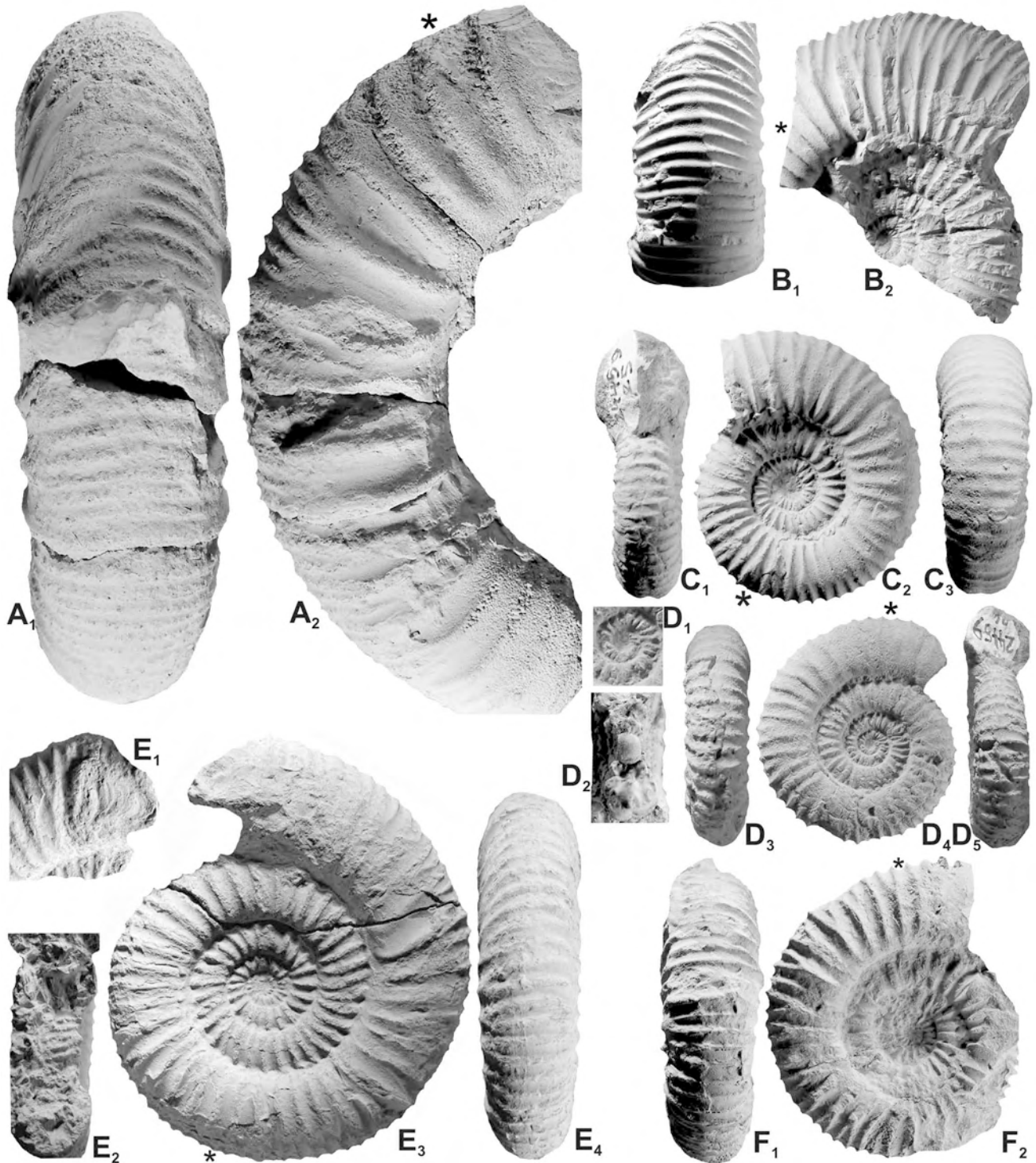


Figure 18. *Catutosphinctes proximus* (Steuer), A. Cieneguita, Proximus Zone. **A:** half whorl of macroconch phragmocone with beginning of bodychamber (MCNAM 24466), bed AC-7. **B:** macroconch phragmocone with portion of bodychamber (MCNAM 24412), bed AC-7. **C:** almost complete adult microconch (MCNAM 24459/25), involute-stout variant, bed AC-8. **D:** adult microconch phragmocone with beginning of bodychamber (24459/26), compressed-evolute variant, bed AC-8; **D₁-D₅**: lateral and ventral views of innermost whorls (x2). **E:** complete adult microconch with lappets (MCNAM 24439), bed AC-7; **E₁**: detail of the lappet, left face apertural view; **E₂**: detail of inner whorl showing continuous ribbing through the venter. **F:** adult microconch with a quarter whorl of bodychamber (MCNAM 24445), bed AC-7. All natural size otherwise indicated. Asterisks indicating the last septum.

50 mm, up to the bodychamber the shell has the aspect of a stout serpenticonic ($U/D = 0.40$, $W/D = 0.40$) and the ventral groove vanished. The phragmocone ends at about $D = 100$ mm. The adult bodychamber, moderately uncoiled, extends for more than a half whorl (there are no specimens with peristome in present samples). The whorl section is rounded to subrectangular, as high as wide; primary ribs acute and

high, some bifurcate but others remain simple, all crossing the venter without interruption. The maximum size of the most complete specimen (Fig. 21A) is estimated as $D = 170$ mm. However, large fragments of bodychambers suggest sizes larger than 200 mm in diameter. Microconch: in the present material there are some few specimens which could be considered microconchs but none of them has the lappets

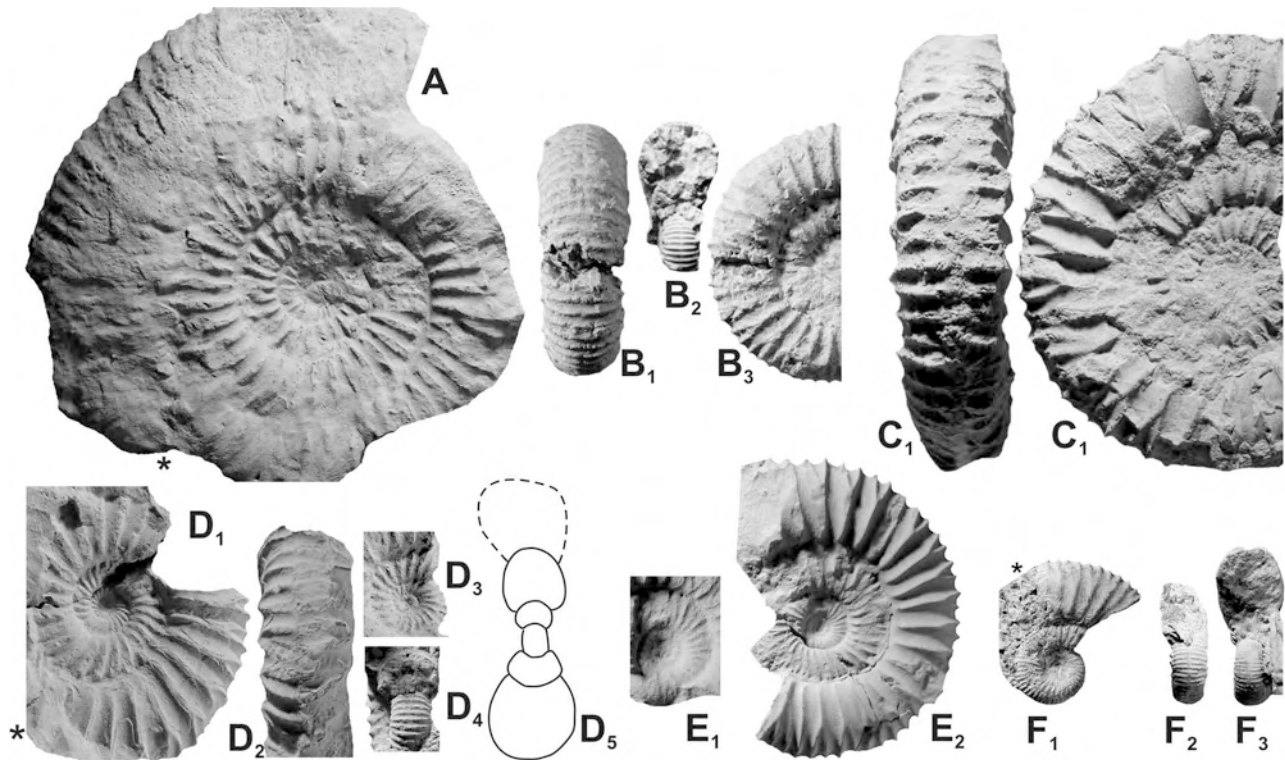


Figure 19. A-C: *Catutosphinctes proximus* (Steuer), A. Cienegueta; A: macroconch with portion of bodychamber crushed (MCNAM 24455/1), bed AC-10 (Internispinosum Z.); B: phragmocone (MCNAM 24455/2), bed AC-10; B₂: detail of inner whorls in apertural view; C: almost complete specimen (MCNAM 24416/3), bed AC-8 (Proximus Z.). D: *Catutosphinctes* cf. *proximus* (Steuer), phragmocone with beginning of bodychamber (MCNAM 24463/2), A. Cienegueta, bed AC-7 (Proximus Z.); D₁-D₄: lateral and apertural views of the inner whorls; D₅: whorl section at about $D = 35$ mm. E-F: *Catutosphinctes* sp. A, A. Cienegueta; E: phragmocone with more than half whorl of bodychamber (MCNAM s/n), bed AC-7; E₁: detail of the inner whorls (x2); F: phragmocone with beginning of the bodychamber (MCNAM 24448), bed AC-8 (Proximus Zone); F₁-F₃: ventral and apertural views of the last whorl of phragmocone. All natural size otherwise indicated. Asterisk indicating the last septum.

preserved. The inner whorls are identical to the macroconch. The bodychamber begins at $D = 40$ -50 mm with moderate uncoiling ($U/D = 0.45$). The lateral ribbing remains unchanged and the venter shows the groove persisting from the inner whorls. The ventral ribs end somewhat raised in small lamellar tubercles, more or less marked depending on the specimens.

Remarks.- The described sculpture on the phragmocone of *C. inflatus* is very conspicuous with some differences from the older representatives of the *Catutosphinctes* lineage. Indeed, *C. inflatus* differs from *C. proximus* by (1) the somewhat narrower umbilicus (see Fig. 8D, G), (2) stronger and more acute primary ribs, in some cases flared on the bodychamber (see Fig. 21A, E), (3) the widely splayed secondaries ending on mid-venter besides a well marked ventral groove with frequent formation of small tubercles on septate whorls (see Fig. 20B-C, 21A, D), and (4) the more densely ribbed adult bodychamber with finer primaries. The onset of a faint ventral tuberculation is seen very early in the ontogeny, from about $D = 3$ mm, shortly after the nepionic constriction.

The HT comes from beds of the Alternans or Koeneni zones of A. del Yeso (Leanza 1945, see PGSS 2011 for discussion). The specimen from Arroyo Alamillo-Chacay (between A. Durazno and AC) figured by Krantz (1928: pl. 4: 8) as *Riasanites* aff. *swistowianus* Nikitin clearly belongs to the present species. This latter was cited in association with *Riasanites rjanensoides* Krantz (1928: pl. 4: 7; this is the only figured specimen, herein designated as the

lectotype) which can be safely attributed to *Corongoceras mendozanum* (see description below) which is associated with *C. inflatus* in beds AC-14-AC-15.

The two specimens illustrated by Aguirre & Vennari (2009: fig. 5r-t) as *Aulacosphinctes proximus* clearly belong to the present species; they are identical in shell shape and sculpture to the specimens in Fig. 21B-E and differ significantly from *C. proximus* as compared above.

C. inflatus is the latest known representative of the *Catutosphinctes* lineage.

Occurrence and distribution.- For the time being, based on the synonymy list and recent collections, the species has been recorded from the upper Tithonian of AC, A. del Yeso, A. Alamillo-Chacay, Pampa Tril and Paso Piquenques.

Genus *Mazatepites* Cantú, 1967

Type species.- *Mazatepites arredondense* Cantú, 1967; by monotypy. Tithonian.

Diagnosis (emended).- Phragmocone serpenticonic evolute, subrectangular whorl section with rounded venter; constricted, primary ribs widely spaced, blade-like. Adult bodychamber more compressed, slightly uncoiled, at least three-quarters whorl long; short acute primary ribs divided in sheaves of finer secondaries, venter evenly ribbed or almost smooth.

Remarks.- The diagnosis proposed above is based on the HT

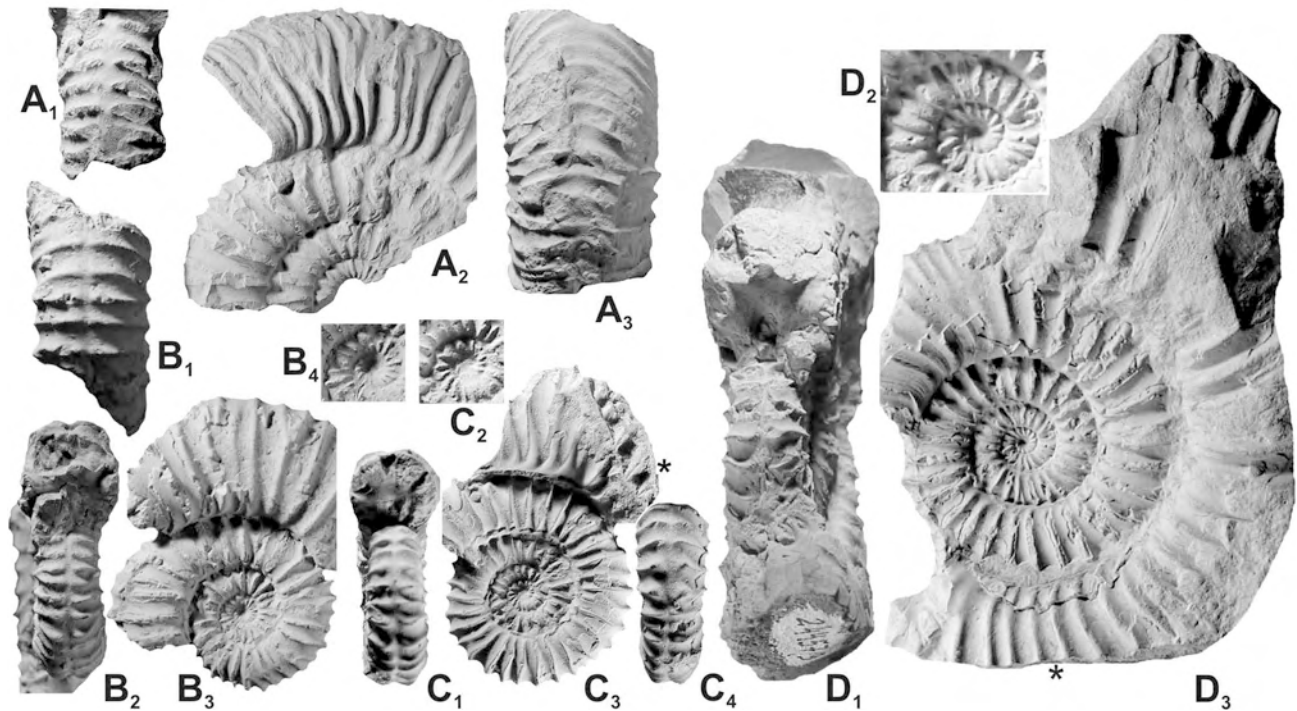


Figure 20. **A:** *Catutosphinctes* cf. *inflatus* (Leanza), adult macroconch? (MCNAM 24456/1), A. Cieneguita, bed AC-11 (Internispinosum Z.). **B-D:** *Catutosphinctes inflatus* (Leanza), A. Cieneguita, bed AC-14 (Alternans Z.). **B:** phragmocone (24457/12), **B₄**: detail of the innermost whorls (x2). **C:** microconch? with portion of bodychamber (MCNAM 24457); **C₂**: detail of the innermost whorls (x2). **D:** adult macroconch with incomplete bodychamber (MCNAM 24457/9); **D₂**: detail of the innermost whorls (x2). All natural size otherwise indicated. Asterisk indicating the last septum.

and PT of the TS, and should allow to distinguish *Mazatepites* from other Ataxioceratidae of similar age.

The conspicuous morphology of these ammonites shows similarities with certain simoceratids like *Virgatosimoceras* Spath, but the resemblance was resolved as pure homoeomorphy (Scherzinger et al. 2010). The adult primary ribs dividing in sheaves is a feature typical of the Ataxioceratidae. The serpenticonic aspect of the phragmocone and the strong primaries raised on the umbilical shoulder suggest inclusion into the Torquatisphinctinae better than in the Lithacoceratinae. Thus, considering we have no evidence about the origin of *Mazatepites*, the only available classification is purely morphological and preliminary, into the Torquatisphinctinae.

The record of the genus in well-horized Andean Tithonian ammonite assemblages as described below is very important for time-correlation with the Caribbean area, and possibly providing additional information for time-correlation with the Tethyan standard (discussed below).

Mazatepites arredondense Cantú, 1967

Fig. 22A-B

*1967 *Mazatepites arredondense* n. sp.- Cantú: 7, pl. 1: 1 [Paratype], 4 [HT].

1967 *Tithopeltoceras* sp.- Cantú: 12, pl. 7: 6.

1993 *Mazatepites arredondense* Cantú.- Stinnesbeck et al.: pl. 3: 2-3.

Material.- Two more or less well preserved specimens: an adult phragmocone with the beginning of the bodychamber from bed AC-6 (MCNAM 24369) and a juvenile specimen with its bodychamber from bed AC-7 (MCNAM 24418/3); Proximus Z.

Description.- Phragmocone serpenticonic, evolute, strongly ribbed; sculpture composed by blade-like primaries which fade-out on the ventrolateral shoulder, a few of them are flared and cross the venter with slow weakening. The bodychamber is not preserved.

Remarks.- The HT is an almost complete adult macroconch, the bodychamber begins at about $D = 95$ mm and extends along 300° . The varicostation begins at the end of the last whorl of the phragmocone, passing from the widely spaced, strong blade-like primaries (like in the PT, an almost complete juvenile specimen with bodychamber of a whorl long) to the more densely spaced primaries divided into three to five weaker secondaries, then progressing to the final stage, higher than wide in whorl section, and covered by shorter primaries polyfurcating in sheaves.

The present specimens are identical to the phragmocones of the HT and the PT. The specimen in Fig. 22B could be an adult microconch with bodychamber. This latter specimen shows a flared rib, a feature not seen in the type specimens, but very similar sculpture is observed in the specimen which Cantú (1967: pl. 7: 6) figured as *Tithopeltoceras* sp.

A comparable phragmocone specimen from bed AC-7, figured as *Mazatepites* cf. *arredondense* in Fig. 22C, is somewhat different in that the inner whorls are not so strongly ribbed as in the type specimens, and the furcation of the primary ribs of the adult phragmocone is somewhat higher on the flanks.

The type horizon of *M. arredondense* lies in the Middle Tithonian, 6 m thick set of limestone beds, biostratigraphic unit called "Unidad con *K. victoris* y *P. zitteli*" in the type locality "Afloramiento 4", Mazatepec (Cantú 1967: 7, 21). The guide assemblage, as illustrated by Cantú (1967), includes *Pseudolissoceras zitteli* (Burckhardt, 1903) and a

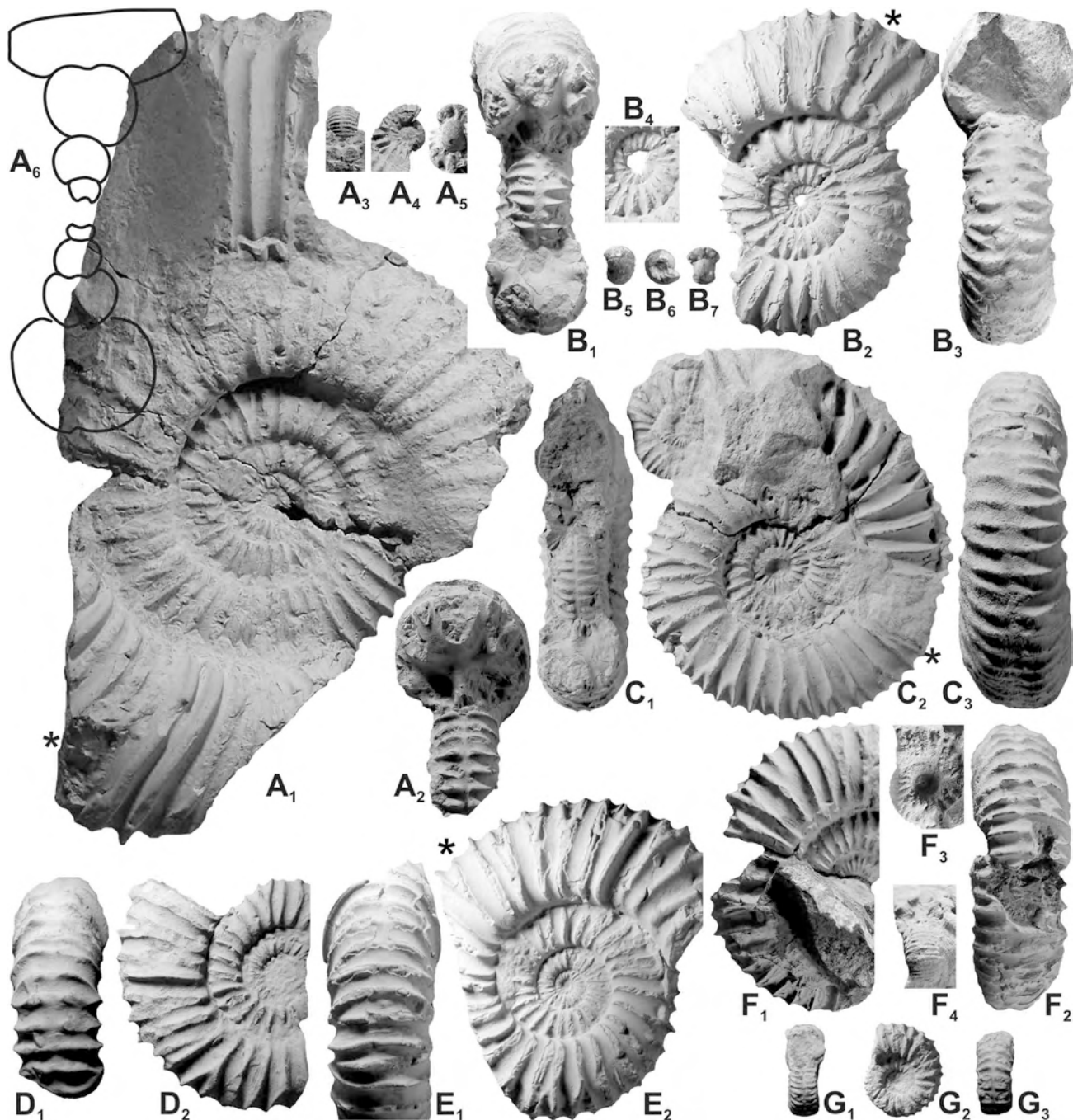


Figure 21. *Catuosphinctes inflatus* (Leanza, 1945). A. Cieneguita, beds AC-15 (Alternans Z., *vetustum* hz.) and AC-16 (Alternans Z.). **A:** complete adult macroconch (MCNAM 24460/2, bed AC-16), showing the venter of juvenil phragmocone (**A₂**) and innermost whorls at the onset of lateral ribbing and slightly later the ventral ribbing (**A₃-A₅**, x2); **A₆**: whorl section at about $D = 80$ mm. **B:** adult microconch? phragmocone with the beginning of the bodychamber (MCNAM 24457/8, bed AC-15), showing venter of juvenil phragmocone (**B₁**), inner whorls (**B₄**, x2) and innermost whorls (detached) at the onset of lateral ribbing (**B₅-B₇**, x2). **C:** juvenile macroconch with incomplete bodychamber (MCNAM 24457/6), bed AC-15, showing the venter of the juvenil phragmocone (**C₁**). **D:** adult microconch? phragmocone (MCNAM 24460/3), bed AC-16. **E:** adult microconch? with incomplete bodychamber (MCNAM 24457/8), bed AC-16. **F:** adult microconch? phragmocone (MCNAM 24460/1), bed AC-16, showing the inner whorls densely ribbed (**F₁-F₄**, x2). **G:** juvenil specimen (MCNAM 24457/20), bed AC-15, with beginning of bodychamber. All natural size otherwise indicated. The asterisks indicate the position of the last septum.

specimen, figured as *Aulacosphinctoides* sp. (Cantú 1967: pl. 2: 2) which could be assigned to the genus *Catuosphinctes*. The other ammonites are not identifiable, especially the deformed fragments assigned to *Kossmatia victoris* (Burckhardt, 1906) and *K. subzacatecana* Cantú, 1967. Moreover, after the revision by Enay (2009) it is clear that they should not belong to the Tithonian ammonite genus *Kossmatia*. The ammonites figured by Stinnesbeck et al. (1993) belong to the same assemblage, but include a

specimen figured as *Proniceras* sp.

Within these ammonites "*Aulacosphinctoides*" sp. occurs consistently associated with *M. arredondense* in different samples (Cantú 1967: pl. 2: 2; Stinnesbeck et al. 1993: pl. 4: 5). This ammonite is very similar to early representatives of *C. proximus*. For instance, very similar forms occur in the Zitteli to lower *Proximus* zones of Cerro Lotena (e.g. Leanza 1980: pl. 6: 4-5) and Cerro Granito, so that the Mexican ammonite could likely be a closely related

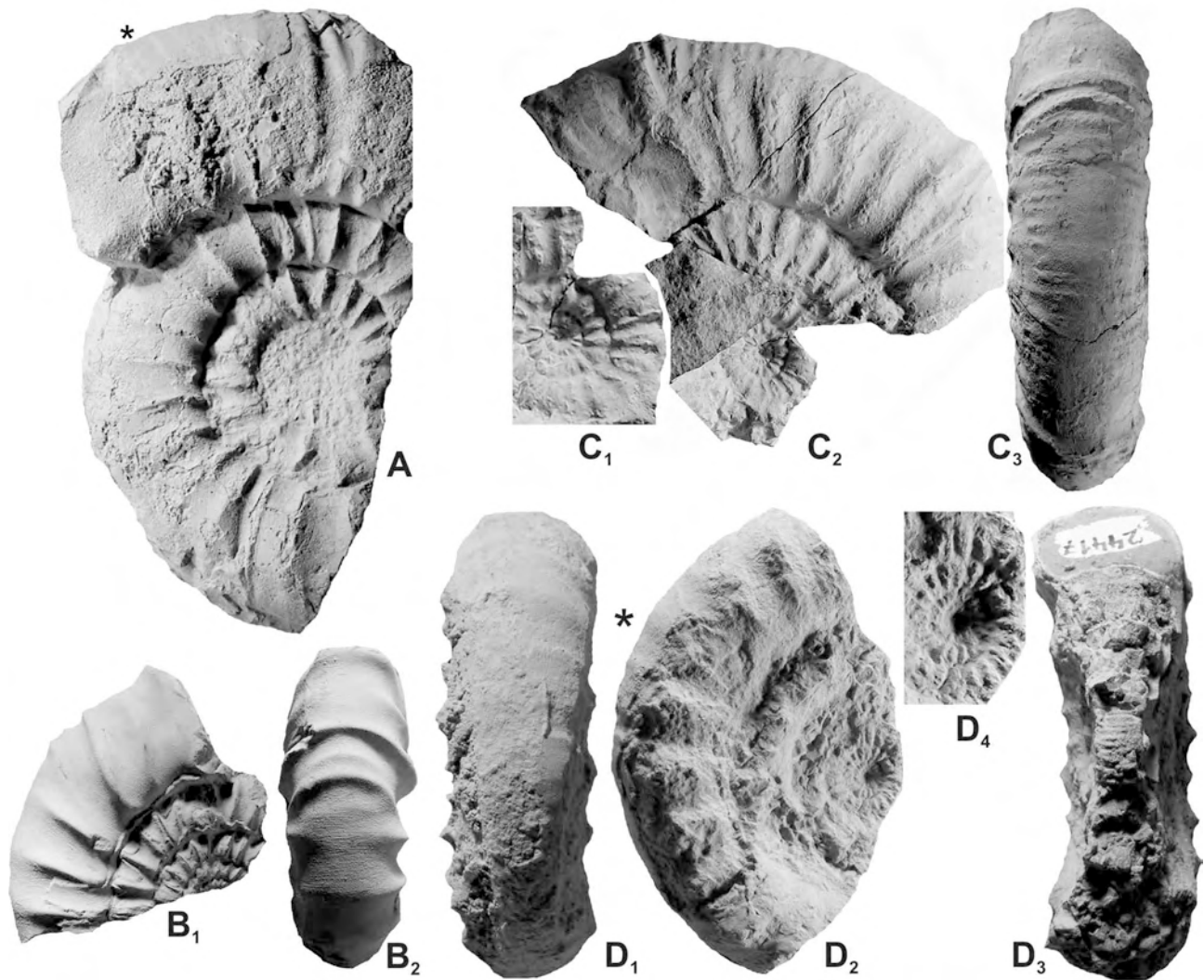


Figure 22. A-B: *Mazatepites arredondense* Cantú, A. Cieneguita. A: macroconch with beginning of bodychamber (MCNAM 24396), bed AC-6 (Proximus Z.). B: adult microconch? with a quarter whorl bodychamber (MCNAM 24418/3), A. Cieneguita, bed AC-7 (Proximus Z., *falculatum* Hz.). C: *Mazatepites* cf. *arredondense*, adult? phragmocone (MCNAM 24438), bed AC-7 (Proximus Z., *falculatum* Hz.); C₁: detail of inner whorls (x2). D: *Mazatepites* sp. A., macroconch, complete phragmocone with beginning of bodychamber (MCNAM 24417), A. Cieneguita, bed AC-8 (Proximus Z.); D₄: detail of the inner whorls (x2). All natural size otherwise indicated. Asterisks indicating the last septum.

form, and of similar age (cf. López et al. 2007: fig. 2). It is remarkable that this fragmentary material was used to assign a late Tithonian age to the assemblage of the type horizon of *M. arredondense* by Imlay (1980, see also Callomon 1992). The specimen figured as *Proniceras* sp. is very different in comparison to the LT of the TS, *Ammonites pronus* Oppel (see Fig. 28A), but very similar to the microconchiate *Proniceras idoceroides* Burckhardt (1919: 15: 2-4). This fact points to an older age of the assemblage of *Proniceras* from Mexico described by Burckhardt (1919) as already suggested by Callomon (1992: 268); further discussion below, under Spiticeratinae.

Mazatepites sp. A

Fig. 22D

Material.- A moderately well-preserved specimen (MCNAM 24417), bed AC-8 (Proximus Z.).

Description.- Shell shape uniform from the innermost whorls up to the beginning of the bodychamber at $D = 70$

mm: depressed serpenticone, evolute, widely umbilicate with low and convex flanks passing to a widely rounded venter. Inner whorls ($5 < D < 15$ mm) covered by radial acute primaries ($P = 10$ to 12) which bifurcate in weaker secondaries which cross unchanged the venter. From $D = 20$ mm up to the bodychamber the number of primary ribs remain constant and more widely spaced and stronger, but fading from the ventrolateral shoulder, leaving the venter smooth or with faint, wide undulations.

Remarks.- This ammonite shows resemblance with *Mazatepites* in the strong lateral ribbing from the inner whorls. However, it differs significantly from *M. arredondense* by the lack of variocostation on the bodychamber and the more depressed whorl section. The inner whorls are identical to those of the specimen determined as *M. cf. arredondense* (Fig. 22C) from the underlying stratigraphic level AC-7. From the material currently available is hard to evaluate if the morphological differences are related to their apparently slightly different age or actually belongs to a different species.

Family Neocomitidae Salfeld, 1921
Subfamily Berriasellinae Spath, 1922

Remarks.- The most representative berriasellids of the Andean upper Tithonian are those assigned to the genera *Parodontoceras* Spath, 1923b (TS: *Hoplites calistoides* Behrendsen, 1921; by OD) and *Substeuerocheras* Spath, 1923b (TS: *Odontoceras koeneni* Steuer, 1897; by OD). Wright et al. (1996) considered *Parodontoceras* a junior synonym of *Berriasella* Uhlig, 1905. Nevertheless in the present paper they are considered as separate genera, mainly because of the wide variation found in the type species which includes some extreme morphotypes, suggesting *Parodontoceras* is a local specialized lineage within the Berriasellinae.

On the other hand, differences of *Parodontoceras* with respect to *Substeuerocheras*, as represented by their type species, are significant enough for precluding the proposal of Verma & Westermann (1973) that they are synonyms. For supporting this argument three selected macroconchs from close localities are figured: an adult phragmocone of *P. calistoides* from bed G-9 (Koeneni Z.) of Casa Pincheira (Fig. 25A; Parent 2003a: fig. 1B); a complete adult phragmocone and a complete adult macroconch of *S. koeneni* from the Koeneni Z. of Chacay Melehué and Mallín Quemado, respectively (Fig. 23D, F and Fig. 24). These specimens of *S. koeneni* are identical but more complete than the type specimens herein refigured in App. 2-B-C.

P. calistoides [M] is involute, platycone with compressed, higher than wide whorl section and tabulate venter from the inner whorls, passing to more evolute and inflate on the adult phragmocone (Fig. 25A; cf. Leanza 1945: pl. 5: 5-6). Ribbing ontogeny is regular with a persistent smooth ventral band from inner whorls; dense, flexuous-subfalcate, prosocline primaries bifurcate at mid-flank with a more or less marked inflection, secondaries and intercalaries fade out on the venter, sometimes slightly rose besides the smooth ventral band (Fig. 25A).

S. koeneni is similar in shell shape but more involute and with more rounded venter which becomes narrower on the bodychamber; ribbing is uneven, composed by flexuous primaries which bifurcate indistinctly on the umbilical shoulder or around the mid-flank, and frequently in both points; on inner whorls ventral ribbing may be very narrowly interrupted on the depressed venter (Fig. 23D₄), weakened on the venter of adult phragmocone (Fig. 23D₁, D₃) and not interrupted on the narrow venter of the adult bodychamber (Fig. 23F). The last whorl of the adult [M] phragmocone in *S. koeneni* shows flared primary ribs with finer secondaries branching at different heights (Fig. 24).

We have recently collected in the upper Tithonian of Pampa Tril a specimen of *S. koeneni* which shows some differences in sculpture ontogeny and stratigraphic position respect the typical material. However, the specimen was collected in beds which could belong to the upper Alternans or less probably lower Koeneni Z. Its shell shape and sculpture recall the recently described features of *Stevensia* Enay, 2009. Our specimen is apparently an adult macroconch with the bodychamber crushed and incomplete. The inner whorls up to about 25 mm in diameter are narrow compressed, highly whorled with a well marked interruption of the ventral ribs forming a narrow smooth band. From $D = 50$ mm, last whorl of phragmocone, the groove vanishes completely and the venter changes to rounded as typical in the species. The shell morphology changes to discoidal, coiling moderately involute with more or less convex flanks

and widely rounded to flattish venter. Ribbing gently flexuous, primaries originate deep on the umbilical wall, divided into two, less commonly three secondaries on the upper half of the flanks; intercalatory ribs are rather frequent but unevenly distributed and as long as the secondaries, sometimes loosely connected with the primary on the point of furcation. Some primaries bifurcate on the umbilical shoulder, and the anterior secondary branches again on the upper half of the flank. All secondaries and the intercalatories cross evenly spaced the venter describing an adorally oriented curve like a rounded chevron, they are weak or interrupted faintly, and raising slightly on the ventrolateral shoulders forming a small lamellar tubercle.

These specimens provide evidence for two alternative hypothesis about the origin of *S. koeneni*: (1) it could derive from early *P. calistoides* which occurs from a deeper stratigraphic position, clearly in the Alternans Z. (e.g. the material from AC described below and Pampa Tril) and/or the Internispinosum Z. (*Odontoceras nodulosum* Steuer, 1897, from his level Cieneguita-II); or (2) it could derive from, or belong to the Kimmeridgian-Tithonian lineage *Stevensia-Kossmatia-Nepalites* as described from Nepal by Enay (2009) and partially from New Zealand by Stevens (1997). This latter hypothesis of a Subaustral origin of *S. koeneni* would be supported by records of related forms in Antarctica. Krantz (1926) has described a conspicuous representative of *S. koeneni* as, significantly, *Kossmatia pseudodesmidoptycha* Krantz, 1926 (1928: pl. 1: 4, lectotype herein designated; pl. 1: 5, paralectotype) from the Koeneni Z. of A. Durazno. The inner whorls figured by Krantz are very similar to a small specimen of *Substeuerocheras* aff. *koeneni* (Fig. 23C) from the Alternans Z., bed AC-15. Both specimens are inflate, moderately involute perisphinctoid shells; at $D = 5-10$ mm the lateral ribbing consists of moderately distant prosocline primaries which bifurcate on the upper half of the flanks and reach the venter with formation of a well defined smooth ventral band bounded by small lamellar tubercles which are at the end of the ventral ribbing; from $D = 10-12$ mm the lateral ribbing of the specimen of AC becomes denser and more flexuous with the furcation point at variable heights; ventral sculpture is unchanged and persists the wide smooth band bounded by small tubercles. The LT of *K. pseudodesmidoptycha* is a specimen very similar to the specimen from C. Melehué (Fig. 23D) but the flanks are flat and ventral interruption of the ribs persists up to a larger diameter, forming on the adult whorls a weak forward inclination on the venter. This species overlies a horizon with *Andiceras acuticostatum* Krantz, 1926 (1928: pl. 2: 2, HT by MT), an evolute variant or transient of *S. koeneni* as indicated by its ribbing style and shell shape.

Genus *Parodontoceras* Spath, 1923b

Type species.- *Hoplites calistoides* Behrendsen, 1891; by OD

***Parodontoceras calistoides* (Behrendsen, 1891)**

Figs. 23A-B, 25A

Synonymy.- See Leanza (1945) and Klein (2005).

Material.- An adult macroconch (MCNAM 24459/1), bed AC-15; three fragmentary phragmocones, bed AC-16; a phragmocone (MCNAM 24457/21), bed AC-17.

Description.- The larger specimen is a macroconch with the bodychamber crushed. The phragmocone is platycone,

moderately involute, with high flat flanks and rather deep umbilicus. In the inner whorls the ribbing is fine and dense, flexuous, bifurcated on the upper half of flanks. In the last whorl of the phragmocone ribbing becomes somewhat stronger and widely spaced with the bifurcation point on the upper third of the flank; the secondaries with scarce, short intercalaries fade out on the venter slightly engrossed besides a smooth band. The bodychamber is uncoiled, slightly variocostate with primary ribs more widely spaced, less flexuous and wider.

The smaller specimens are phragmocones from a higher stratigraphic position. These are compressed, involute platycones with the same ribbing as the macroconch described above but finer and denser.

Remarks.- The inner whorls of the macroconch from bed AC-15 (Fig. 23A) are almost identical to the HT and the typical specimen shown in Fig. 25A; the last whorl of the phragmocone shows differences because the ribbing is stronger, with primaries bifurcating upper on the flank. On the other hand its occurrence in the Alternans Z. seems to be lower than the few specimens shown in the literature.

The specimens from bed AC-17 (e.g. Fig. 23B) are more involute and narrower umbilicate ($U/D = 0.17$ respect to 0.31 in the HT at similar size) and finely ribbed. The best match is with *Thurmannia discoidalis* Gerth, 1925 which is herein considered a compressed variant of a later transient of *P. calistoides*. The HT by MT (Gerth 1925: 98, pl. 5: 3) comes from a stratigraphic level in Bardas Blancas associated with *C. striolatus*, below a level yielding *Reineckeia egregia* Steuer, 1897 and "*Berriasella multipartita*" (Gerth 1925: 92, 122, unfigured, nomen nudum). The description and comparisons given by Gerth for this latter species suggest a tuberculate form close to *Hoplites quadripartitus* Steuer, 1897 which, likely, is a synonym of *R. egregia*, both from the Berriasian (see below). Moreover, Gerth in his own copy changed in handwritten the assignment of the species to *Corongoceras*.

The species seems to be moderately variable along its stratigraphic range. This pattern is suggested by the similar specimens figured by Steuer (1921), under different names, which seem to be no more than variants of *P. calistoides*. Indeed, the species of Steuer (1897): *Odontoceras nodulosum* (LT herein designated and refigured in App. 2-K), *Odontoceras beneckeii* (LT refigured in App. 2-L; a paralectotype refigured in App. 2-M), *Odontoceras gracile*, *Odontoceras kayseri* and *Odontoceras tenerum*, all show nothing but small differences between them which do not support the separation in different species. In P. Tril these morphotypes can be collected in abundance in different combinations from certain stratigraphic levels of the succession, ranging from the Alternans Z. to the Koeneni Z.

Occurrence and distribution.- In beds AC-15-AC-17, M. Redondo (Leanza 1945: 90, pls. 3: 11, 5: 5-6) and Bardas Blancas (Krantz 1928) the species ranges from the Alternans to the Koeneni zones. In Bardas Blancas (Krantz 1928: 49) pointed out the long stratigraphic range of the species and described this range as the succession from *P. calistoides* to "*Neocomites*" *kayseri* (= *P. calistoides*).

Genus *Blanfordiceras* Cossmann, 1907

Type species.- *Ammonites wallichi* Gray, 1832; by OD

Remarks.- The genus has been recently discussed in detail by

Enay (2009) who established a late Tithonian age for the representatives of the Spiti-Shales of Thakkhola, Central Nepal. The genus *Boehmiceras* Grigorieva, 1938 (TS: *Hoplites boehmi* Uhlig, 1905) is considered herein a junior synonym of *Blanfordiceras*.

Blanfordiceras vetustum (Steuer, 1897)

Figs. 26C-F, 27A-B, App. 2-D-E

- 1897 *Hoplites wallichi* Gray sp.- Steuer: 184, pl. 30: 1-3.
 *1897 *Hoplites vetustus* nov. sp.- Steuer: 183, p. 30: 4-10.
 1897 *Reineckeia turgida* nov. sp.- Steuer: 155, pl. 28: 3-4 [HT].
 ?1908 *Berriasella patagoniensis* n. sp.- Favre: 622, pl. 33: 5 [LT].
 1910 *Blanfordiceras steueri* n. sp.- Uhlig: 188.
 1921 *Hoplites wallichi* Gray.- Steuer: 87, pl. 16: 1-2.
 *1921 *Hoplites vetustus* n. sp.- Steuer: 85, pl. 16: 4-5 [LT], 7, 8-9.
 1921 *Reineckeia turgida* n. sp.- Steuer: 56, pl. 14: 3-4 [HT].
 1926 *Berriasella subprivasensis* Krantz- Krantz: 438.
 1928 *Berriasella subprivasensis* n. sp.- Krantz: 20, pl. 3: 4.
 1931 *Berriasella subprivasensis* Krantz.- Weaver: 443, pl. 56: 356-357.
 ?1937 *Blanfordiceras patagoniensis* (Favre).- Feruglio: 62, pl. 6: 4-6, 8, pl. 7: 1-2.
 n1945 *Micracanthoceras vetustum* (Steuer).- Leanza: 45, pl. 5: 9-10, 11
 1960 *Berriasella privasensis* Pictet.- Collignon: fig. 670.
 1960 *Blanfordiceras* cf. *wallichi* Gray.- Collignon: fig. 679.
 1960 *Blanfordiceras delgai* n. sp.- Collignon: figs. 680 [HT], 681.
 1960 *Blanfordiceras* aff. *rotundidoma* Uhlig.- Collignon: fig. 684.
 1960 *Blanfordiceras rotundidoma* Uhlig var. *venusta* n. var.- Collignon: fig. 685.
 1960 *Blanfordiceras tenuicostatum* n. sp.- Collignon: fig. 686 [HT].
 1960 *Aulacosphinctes mörickeri* Opperl var. *alta* n. var.- Collignon: fig. 720.
 1960 *Aulacosphinctes laxicosta* Steuer.- Collignon: fig. 721.
 1960 *Aulacosphinctes laxicosta* Steuer var. *simplex* n. var.- Collignon: fig. 722.
 1960 *Aulacosphinctes laxicosta* Steuer var. *ankitokensis* n. var.- Collignon: fig. 724.

Lectotype.- Designated by Spath (1934: 13), the specimen from AC figured by Steuer (1921: pl. 16: 4-5) from his level Cieneguita-II. It is worth to remark that the figure caption of the fig. 4 of pl. 16 indicates level Cieneguita-IV, nevertheless, in the text (p. 85 and table of p. 44) it is indicated the occurrence of the type specimens in levels Cieneguita-II and III. In level Cieneguita-II Steuer (1921: 88) also cited the occurrence of *C. mendozanum* with *Blanfordiceras*, like in the bed AC-15 of the present study. It can be assumed that the type horizon of *B. vetustum* lies in some part of the level Cieneguita-II.

New material from Arroyo Cieneguita.- Ten more or less complete specimens (MCNAM 24461/1-4, 24459/4, 10, 12-15, 17) and large fragments, all from bed AC-15; additionally some few specimens have been collected from bed AC-16.

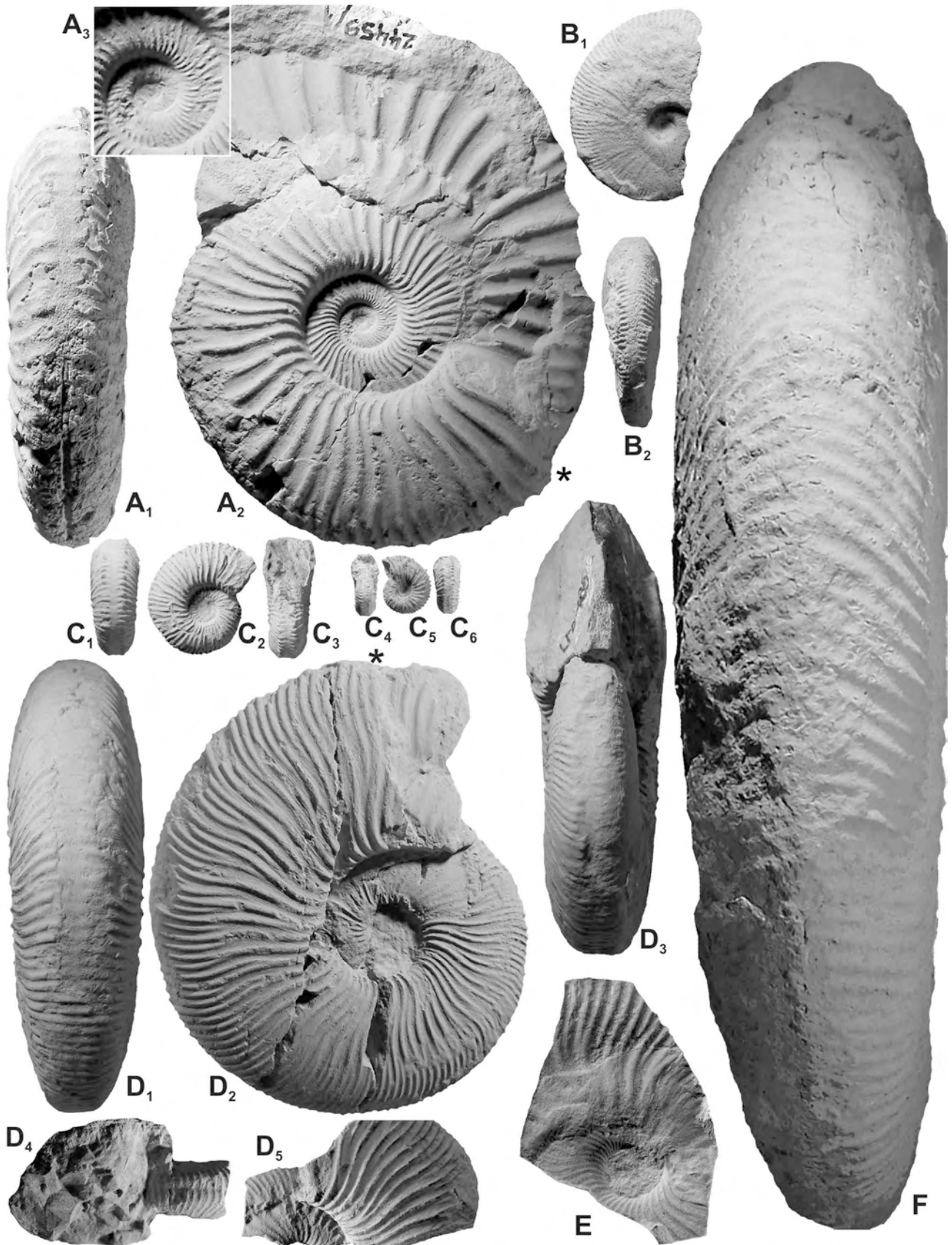


Figure 23. A-B: *Parodontoceras calistoides* (Behrendsen), A, Cieneguita; A: adult macroconch (MCNAM 24459/1) of an early transient, bed AC-15 (Alternans Z., *vetustum* hz.), A₃: inner whorls (x2); B: phragmocone (MCNAM 24457/21) of an involute later transient, bed AC-17 (Koeneni Z., *striolatus* hz.). C: *Substeuerocheras* aff. *koeneni* (Steuer), juv. phragmocone (MCNAM 24461/3), A, Cieneguita, bed AC-15 (Alternans Z., *vetustum* hz.); C₄-C₆: apertural, lateral and ventral views after removal of the last whorl. D-F: *Substeuerocheras koeneni*; D: adult macroconch with beginning of bodychamber (LPB 485), Koeneni Z., Chacay Melehué; lateral, ventral and apertural views of the last whorl of phragmocone; D₁-D₅: ventral and lateral views of the inner whorls at D = 30 mm. E: fragmentary specimen (MCNAM 24464/4), A, Cieneguita, bed AC-17 (Koeneni Z., *striolatus* hz.); F: ventral view of a complete adult macroconch (MOZPI 3438), Koeneni Z., Mallín Quemado [lateral view in Fig. 24]. All natural size except A₃. Asterisk indicating the last septum.



Figure 24. *Substeueroceras koeneni* (Steuer), complete fully grown adult macroconch (MOZPI 3438) showing the peristome, upper Tithonian, Mallín Quemado [ventral view in Fig. 23F]. Natural size. Asterisk indicating the last septum.

Description.- All the available specimens seem to be macroconchs. Innermost whorls at $D = 4-10$ mm, evolute to moderately involute depending on the specimens, whorl section rounded to suboval, with widely rounded venter; ribbing composed by fine prosocline primaries which

vanish completely on the ventro-lateral shoulder.

The subsequent whorls of the phragmocone are moderately involute with subrectangular to suboval whorl section, the venter is rounded with flat aspect because of ventral ribbing. Ribbing becomes acute and stronger;

primary ribs are prosocline to subradial, straight to slightly flexuous, starting on the uppermost portion of the umbilical shoulder and bifurcating, rarely trifurcate, on the upper third of the flank; simple and intercalatory ribs are infrequent; all ribs reach the ventro-lateral shoulder more or less raised, in some cases forming small lamellar tubercles, and become weak on the mid-venter. In the studied sample the adult phragmocone ends within $D=70-90$ mm.

The bodychambers observed differ from the last whorl of the phragmocone by being uncoiled and the ventral ribbing mostly interrupted besides a well marked groove, but gradually become uninterrupted. There is not evident process of variocostation.

The large but fragmentary specimens available (not figured) show a whorl section subrectangular to subtrapezoidal, with gently curved flanks and rounded venter at an estimated size of $D=130-160$ mm. As usual, the whorl section nude of the acute ribbing is suboval or rounded subtrapezoidal. Ribbing is strong and acute, most primaries undivided or biplicate on the upper half of the flank, some flared. Ventral ribbing weakened on the mid-venter.

Remarks.- The sample described comes from a single faunal level, bed AC-15, named *vetustum* hz. Additional specimens come from the lower part of bed AC-16, but these are incomplete and do not show any perceptible difference respect the sample described. The morphology and sculpture ontogeny show a variation of juvenile and adult whorls intergrading through evolute variants (relatively low flanks) with straight, prosocline primaries bifurcating on the upper part of the flank with formation of a slight swollen (Figs. 26F, 27B), and the more involute variants with higher flanks covered by slightly flexuous primaries bifurcating on the middle or uppermost part of the flanks (Fig. 26C-E); the specimen shown in Fig. 27A shows an intermediate morphology. The inner whorls do not show variations, supporting definitely the coeval age of the sample. The specimens originally figured by Steuer (1897) already showed this pattern of variation (Steuer 1921: pl. 16: 4-5, 7 and 8-9). *Reineckeia turgida* Steuer (1897, transl. 1921: pl. 14: 3-4, HT by MT, faunal level Loncoche-III) is at the extreme of the inflate variants. This specimen with comparable sculpture ontogeny is somewhat larger in adult size and its wide whorl section is associated with the strengthening of the ribbing with a prominent bullae-like portion on the point of furcation. The specimen described as *Hoplites wallichi* Gray by Steuer (1897, transl. 1921: pl. 16: 1-2), later renamed *Blanfordiceras steueri* by Uhlig (1910: 188), is identical with the specimen from AC in Fig. 26F.

Within this range of continuous variation can be easily accommodated, as a compressed and evolute, slender variant, *Berriasella subprivasensis* Krantz, 1926 described on material from closely similar or identical stratigraphic position. This species was proposed for a single specimen (Krantz 1926: 438), giving a short information about the differences in comparison with *Berriasella privasensis* Pictet, the measurements of the shell (recalled in Krantz 1928: 20) and the type locality Arroyo Durazno, but with no figuration. It was later that this specimen, the HT by MT, was figured (Krantz 1928: pl. 3: 4). The type horizon lies within beds that can be assigned to the Alternans Z., containing in that locality, according to Krantz (1928: 49): *P. calistoides*, *Corongoceras mendozanum* Behrendsen, *Blanfordiceras argentinum* Krantz (additional material described below) and *Aspidoceras andinum* Steuer. The ammonites of this ensemble are very similar to the ammonite assemblage on

which is defined the *vetustum* hz. (see below). The specimen figured by Weaver (1931: figs. 356-357; herein refigured in App. 2-D) from Arroyo Curacó, matches closely with the more compressed variants of *B. vetustum*.

Micracanthoceras vetustum (Steuer) in Leanza (1945: pl. 5: 9-10), from the Koeneni Z. of Arroyo del Yeso, is clearly a himalayitid ammonite, unrelated with *B. vetustum*. However, the other specimen from the same bed figured by Leanza (1945: pl. 5: 11) can be attributed to *Blanfordiceras*.

Blanfordiceras bardense (Krantz, 1926) was based on five specimens but apparently without designation of a type; the figured specimen (Krantz 1928: pl. 1: 7) from Bardas Blancas is herein designated as the lectotype and refigured (Fig. 25B). This specimen resembles the more involute specimens of *B. vetustum* (cf. Fig. 26C-E) but shows differences which seem significant enough for retaining it as a separate species. Indeed, it has narrower umbilicus and higher flanks covered by irregular, flexuous ribbing with abundant intercalatory ribs and the height of the bifurcation point variable around the mid-flank. Although these differences could be considered as simply originated in the greater involution as a pattern of covariation with ribbing, this morphotype exceeds the limits of all the remaining material, and on the other hand it seems to have a stratigraphic position somewhat higher than the *vetustum* hz. The ensemble of ammonites of the type horizon of *B. bardense* as listed by Krantz (1928: 47), consists of *P. calistoides*, *Choicensisphinctes striolatus* and *Chigaroceras gerthi* (Krantz), suggesting correlation with the bed AC-17 which we have assigned to the Koeneni Z. *B. bardense* was described by Leanza (1945: pl. 2: 3-4) from the bed 1762 of Mallín Redondo, as conforming the guide assemblage of the *bardense* hz. defined below, older than the type horizon of the species. Thus, we conclude that *B. bardense* is a later form of *Blanfordiceras* ranging the Alternans and Koeneni zones in the upper Tithonian of the NMB.

The material of *Blanfordiceras patagoniense* Favre, 1908 described by Feruglio (1937) from the region of Lago Argentino (southern Patagonia) is very poorly preserved for sound comparison but has the appearance of *B. vetustum*. The specimens were collected by A. de Agostini from beds which Feruglio (1937) assigned to his Horizonte 1. The list of species attributed to this horizon includes nominally species which suggest a stratigraphical interval from the upper Tithonian to the lower Valanginian, although judging from the figured specimens the fauna of Horizonte 1 points to different stratigraphic horizons within the upper Tithonian-upper Berriasian interval.

Blanfordiceras weaveri Howlett, 1989 is very hard to compare for it is based on two poorly preserved or incomplete specimens from the Tithonian of the Himalia Ridge in Antarctica. However, it is very similar to *Blanfordiceras laxicosta* (Steuer, 1897) as discussed below.

The large number of nominal species described by Collignon (1960) from the Hollandi Z. which are listed in the synonymy list above, share all the same morphological patterns of variations described for *B. vetustum* when considered as an ensemble. On the other hand it is very important the fact that they occur with the same morphotypes of *Coronogoceras mendozanum* (Behrendsen) which are described below.

The abundant material of *Blanfordiceras* described by Enay (2009) from the Tithonian of Nepal was classified in a large number of morphospecies, distributed in at least three horizons (Enay 2009: pls. 49-52). The bulk of his material

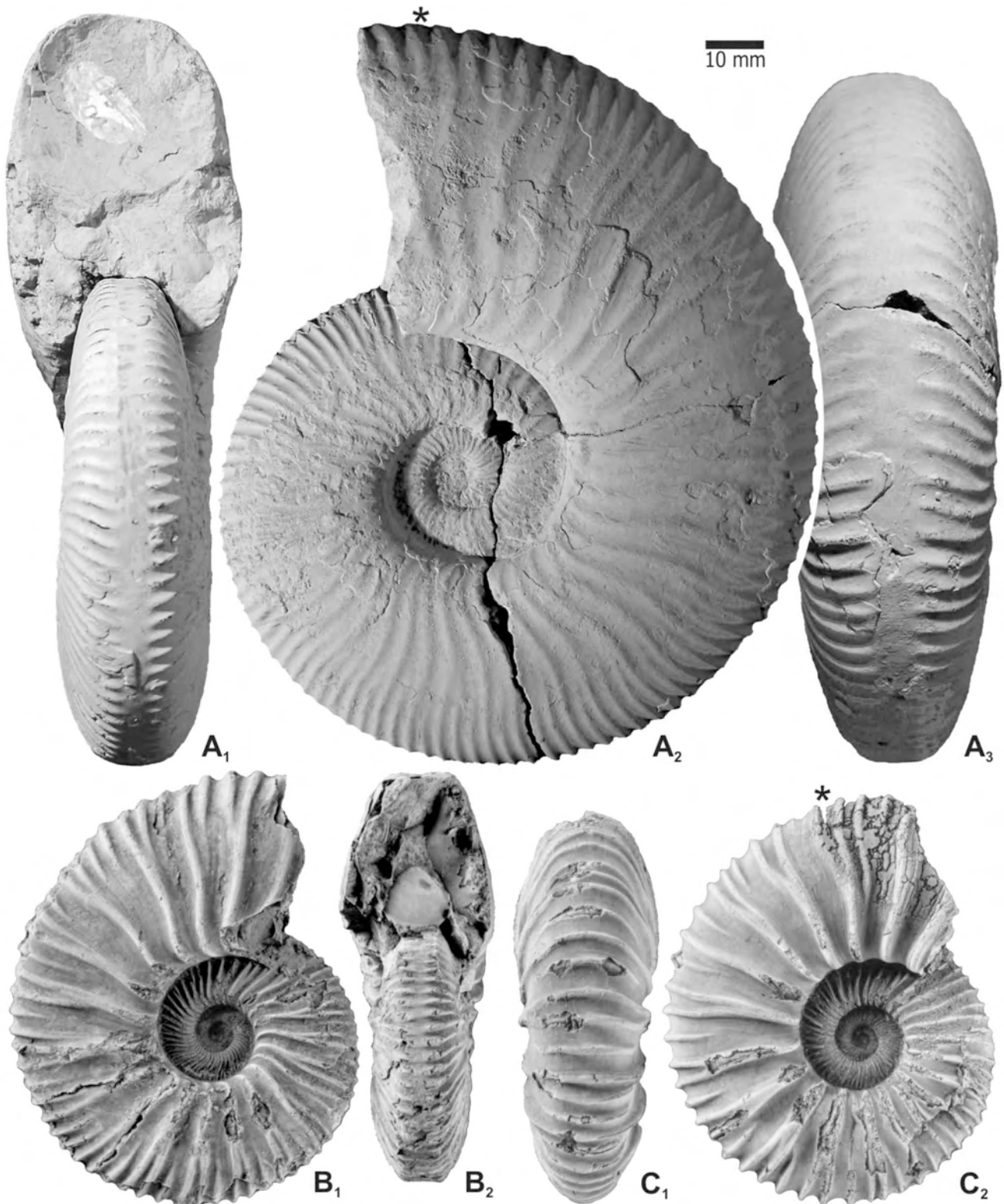


Figure 25. A: *Parodontoceras calistoides* (Behrendsen), adult phragmocone with beginning of bodychamber (LPB 204), Casa Pincheira (bed G9 in Parent 2003: fig. 1B), upper Tithonian, Koeneni Z. B: *Blanfordiceras bardense* (Krantz), holotype, phragmocone; Bardas Blancas, upper Tithonian, Alternans Z.; refigured from Krantz (1928: pl. 1: 7). C: *Chigaroceras gerthi* (Krantz), holotype, adult phragmocone with beginning of bodychamber; Bardas Blancas, Alternans Z.; refigured from Krantz (1928: pl. 1: 8). All natural size. Asterisk indicating the last septum.

comes from the *Blanfordiceras*-horizon (lower? Upper Tithonian) where *Corongoceras helmstaedti* Enay, 2009 and *C. fibuliferum* Enay, 2009 occur. Considering this *Blanfordiceras* assemblage as a whole some general

similarities are observed which are no more than those features of the genus, but also occur significant differences in shell morphology and sculpture ontogeny respect to *B. vetustum*. Ribbing of the mentioned Nepali *Blanfordiceras*

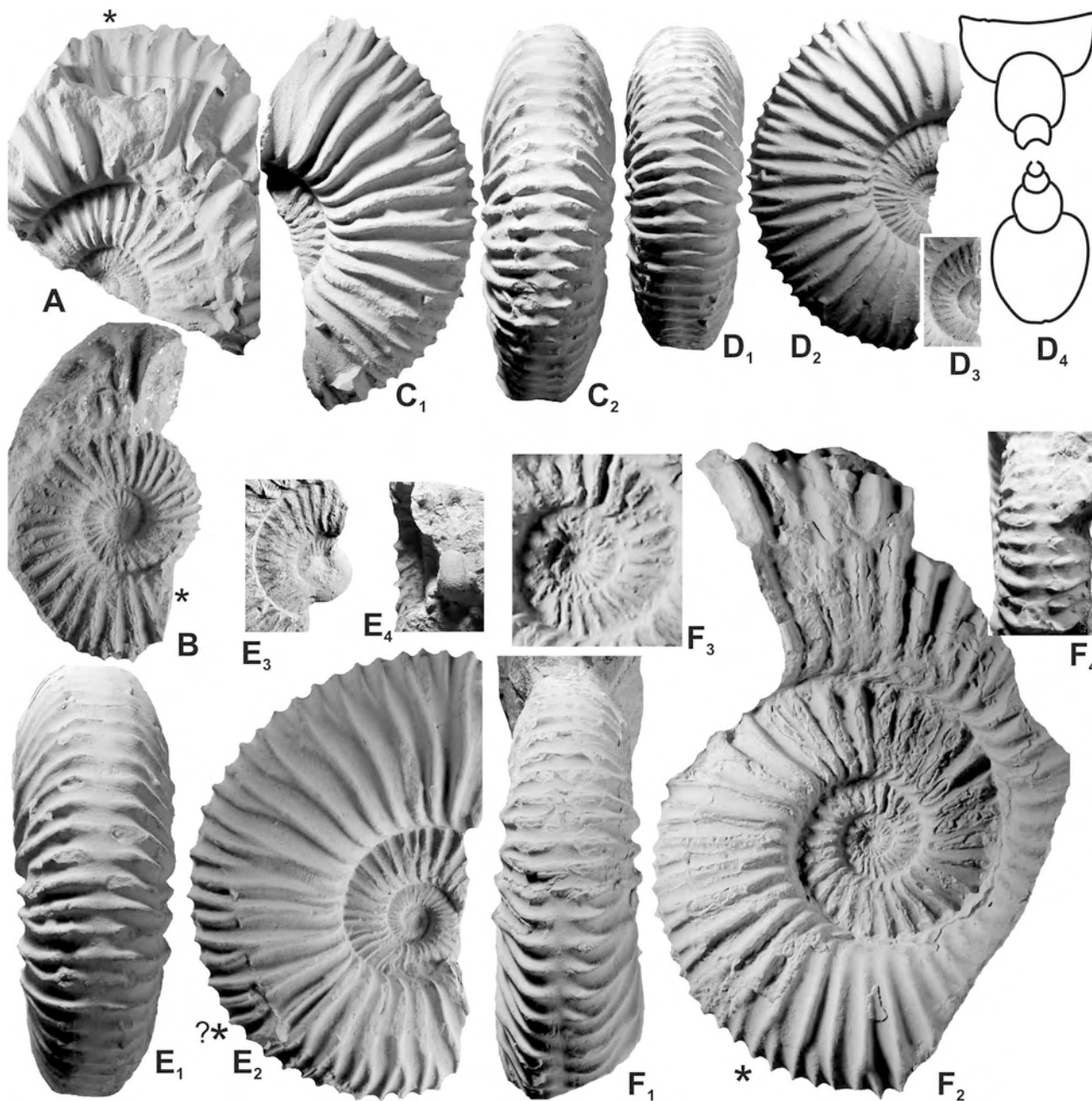


Figure 26. **A:** *Chigaroceras gerthi* (Krantz), ?macroconch phragmocone with beginning of bodychamber (MCNAM 24461/2), A, Cieneguita, bed AC-15 (Alternans Z., *vetustum* hz.). **B:** *Blanfordiceras* sp. A (MCNAM 24463/4), complete phragmocone with a portion of bodychamber, A, Cieneguita, bed AC-8 (Proximus Z.). **C-F:** *Blanfordiceras vetustum* (Steuer), Arroyo Cieneguita, bed AC-15 (Alternans Z., *vetustum* hz.). **C:** fragmentary macroconch (MCNAM 24461), involute morphotype. **D:** macroconch with incomplete bodychamber (MCNAM 24461/4), involute variant; **D₃**: detail of the innermost whorls (x2); **D₄**: whorl section at $D = 57$ mm. **E:** adult macroconch with incomplete bodychamber (MCNAM 24461/1), moderately inflate evolute variant with incipient ventral spines on phragmocone; **E₃-E₄**: detail of the innermost whorls, lateral and ventral views (x2). **F:** almost complete adult macroconch (MCNAM 24459/4), compressed variant; **F₃**: detail of the innermost whorls (x2); **F₄**: ventral view of the beginning of the last whorl. All natural size otherwise indicated. Asterisk indicating the last septum.

is more flexuous with a lower point of furcation, and the ventral sculpture does not show any sign of tubercles on the termination of the ventral ribs; there is a rather persistent smooth ventral band which is wide in the pre-adult phragmocone; and the ventral ribbing of the adult macroconchs describes a rounded chevron.

Occurrence and distribution.- Beds AC-15-AC-16, Alternans Z. As discussed following the synonymic list, the species is widely recorded through the southern Gondwana,

including the NMB, the Austral Basin, Antarctica and Madagascar. Considering the assemblage composed by *B. vetustum* and *C. mendozanum*, with similar distribution, the *vetustum* hz. allows an intercontinental time-correlation as discussed below.

***Blanfordiceras argentinum* (Krantz, 1926)**

Fig. 27C

Material.- A single specimen (MCNAM 24459/22) loose

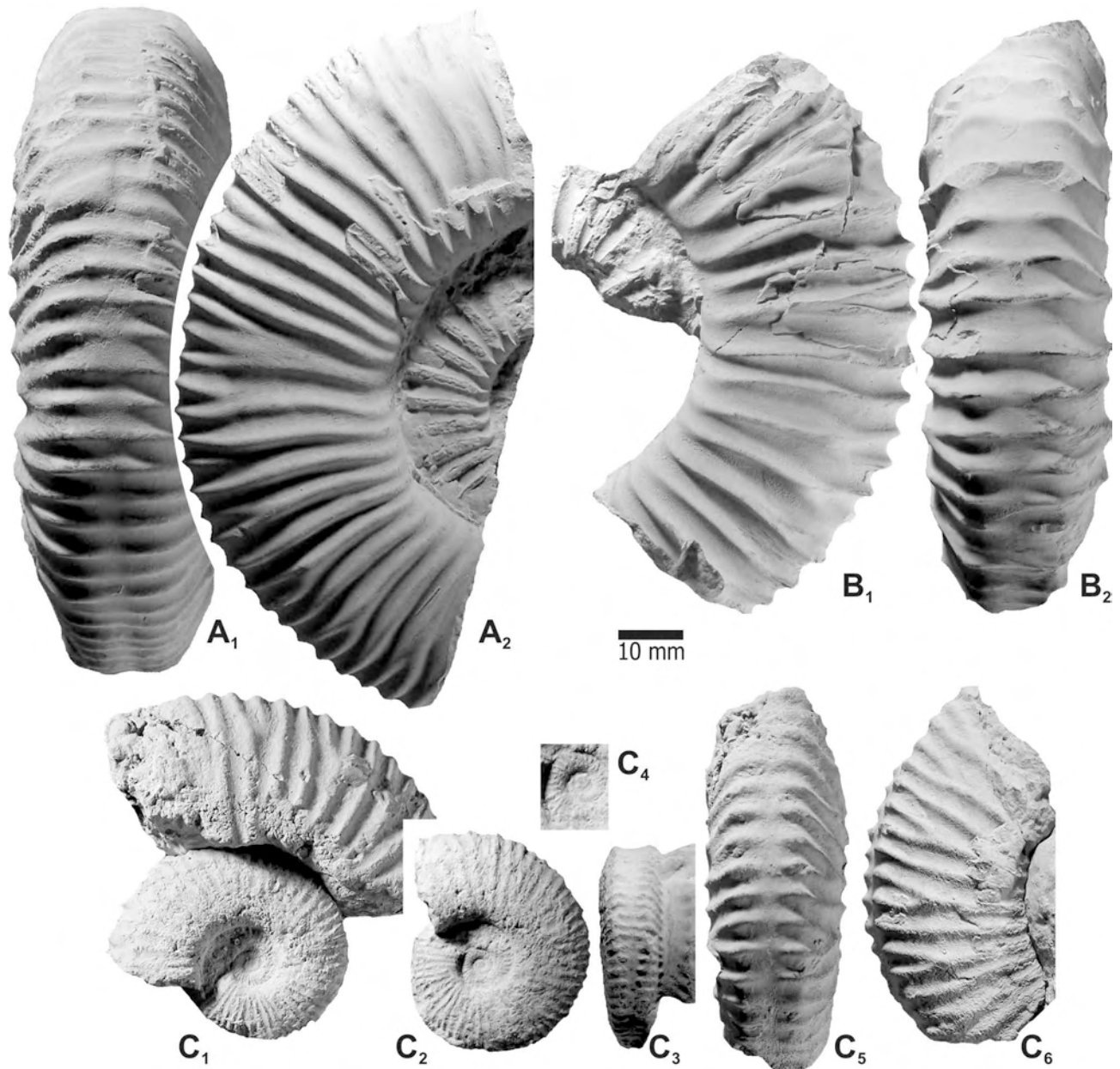


Figure 27. A-B: *Blanfordiceras vetustum* (Steuer), Arroyo Cieneguita, bed AC-15 (Alternans Z., *vetustum* hz.). **A:** adult macroconch with incomplete bodychamber (MCNAM 24459/10), moderately involute platyconic variant. **B:** macroconch bodychamber with portion of phragmocone (MCNAM 24459/17), coarsely ribbed evolute variant. **C:** *Blanfordiceras argentinum* (Krantz), phragmocone of an adult? specimen (MCNAM 24459/22), A. Cieneguita, loose from beds AC-15 or AC-16. **C₁**: right side (apertural view), **C₂-C₃**: lateral and ventral views with last whorl removed, **C₄**: inner whorls (x2), **C₅-C₆**: ventral and lateral (left in apertural view) views of the last whorl. All natural size otherwise indicated.

from bed AC-15 or AC-16.

Description.- The specimen is completely septate. The outermost whorl is evolute, subtrapezoidal in whorl section, covered by strong prosocline primaries of which one each two bifurcates on the upper half of the flank with the formation of a small tubercle; ventral (secondaries plus undivided primaries) ribs reach the venter after rising on the ventrolateral shoulder and fade off besides a well defined, moderately narrow smooth band. The inner whorls are platyconic, involute, with high flanks and flat or concave venter; the ribbing is much finer and denser than in the outermost whorl; primaries prosocline which bifurcate on the upper third of the flank, but many of them remain undivided; all ribs rise notoriously on the ventrolateral

shoulder in the form of small lamellar tubercles, then fade off or weaken besides a smooth band. As can be observed in Fig. 27C the innermost whorls are more rounded and densely ribbed.

Remarks.- The only Andean ammonite comparable with the above described one is *Berriasella argentina*. This species was based on two specimens without designation of a type; thus, the specimen figured by Krantz (1928: pl. 3: 3) is herein designated as the lectotype. This specimen in an adult with a portion of the bodychamber clearly uncoiled, apparently a macroconch, collected from the Alternans Z. of Arroyo de La Manga. The ammonite ensemble of the type horizon includes most of the species which conform the guide assemblage of the *vetustum* hz. They are (Krantz 1928: 50),

under current taxonomy: *B. argentinum*, *Corongoceras? steinmanni* Krantz, 1926 (additional material described below), *C. mendozanum*, *P. calistoides* [including *Parodontoceras kayseri* (Steuer)], *Steueria? mangaensis* [*Steueria* n. gen., Andean himalayitid described below], *C. proximus* and *Krantziceras wanneri* n. gen. (discussed above). However, it cannot be safely assigned to a special horizon since the specimens of the Krantz's list come from several beds of limestones with levels of concretions.

Phragmocones comparable to inner whorls of the present species have been collected from the Internispinosum Z. of Cerro Granito and from the upper Internispinosum or Alternans Z. of Cerro Lotena.

***Blanfordiceras* sp. A**

Fig. 26B

Description and remarks.- A single specimen (MCNAM 24463/4) from bed AC-8 (Proximus Z.) consisting of a phragmocone with remains of bodychamber. The phragmocone is platyconic with subrectangular whorl section, flat flanks and well rounded venter. Ribbing composed of slightly procline primaries which mostly bifurcate on the upper half or third of the flank. The ventral ribs are not interrupted on the venter, only slightly weakening.

This specimen shows clearly the shell morphology and sculpture which characterizes the genus *Blanfordiceras* and shows resemblance with *B. vetustum* (cf. Fig. 26D) which has the inner whorls with rounded venter covered by uninterrupted ribbing, although somewhat finer. It is the oldest known representative of the genus and also somewhat similar to *C. cf. proximus* (Fig. 19D).

***Blanfordiceras laxicosta* (Steuer, 1897)**

Remarks.- In the bed AC-19 (*compressum* hz.) we have collected crushed fragmentary specimens which are similar to *Blanfordiceras laxicosta* (Steuer, 1897, transl. 1928: pl. 18: 4-5, the HT by MT). The HT comes from the level Cieneguita-IV, the type horizon of *S. koeneni*, which also includes: *P. calistoides* (incl. *P. beneckeii*, LT designated by Enay et al. 1996: 228), *Choicensisphinctes? intercostatus* (Steuer, 1897), *Odontoceras fasciatum* Steuer, 1897 (? = *Choicensisphinctes striolatus*) and *Parodontoceras? subfasciatum* (Steuer, 1897). This association indicates an age within the Koeneni Z., somewhat below the *compressum* hz. The specimen figured by Leanza (1945: pl. 6: 9-10) from the bed 1768 of M. Redondo is very close to the HT.

It is worth to note that this species closely matches to *B. weaveri* because of the strong, acute primaries with low point of furcation covering the high flanks of an involute ammonite which shows the bifurcation points of the inner whorls through the umbilical window; the whorl section is compressed with subflatish venter and the ventral ribbing very narrowly interrupted or weakened.

Genus *Chigaroceras* Howarth, 1992

Type species.- *Chigaroceras banikense* Howarth, 1992; by OD.

Remarks.- *Chigaroceras* differs from *Blanfordiceras* by the evenly rounded venter, covered by uninterrupted and more flexuous, irregular ribbing with primaries bi- or trifurcate with a swollen (or lamellar tubercle), indistinctly on the umbilical shoulder or on the mid-flank.

***Chigaroceras gerthi* (Krantz, 1926)**

Figs. 25C, 26A

Description and remarks.- A single specimen (MCNAM 24461/2) from bed AC-15 (Alternans Z., *vetustum* hz.) with part of the bodychamber which is uncoiled indicating it belongs to an adult.

The species had been only known by a single specimen, its HT by MT (Krantz 1928: pl. 1: 8). It was collected in Bardas Blancas, from beds of the Koeneni Z. (discussed above). Additional discussion about the HT and its assignment to *Chigaroceras* has been formerly given by Leanza (1996).

Family Olcostephanidae Haug, 1910 **Subfamily Spiticeratinae Spath, 1924**

Remarks.- The diagnosis of *Proniceras* Burckhardt, 1919 (TS: *Ammonites pronus* Oppel; SD Roman 1938) given by Wright et al. (1996: 43) indicates the lack of tubercles on the inner and middle whorls, and later whorls with curved umbilical bullae and simple to triplicate ribs. However, the LT of *Ammonites pronus* (herein refigured photographically: Fig. 28A) shows the development of stout, rounded moderately elongate umbilical tubercles from about $D = 15$ mm, which are retained up to the end of the last preserved whorl without signs of any kind of lateral tubercles. The shell is compressed, moderately involute, covered by sheaves of ribs branching from the tubercles. Ventral ribbing is strong and dense, projected forward forming a chevron. These features fit with the diagnosis of *Negrelliceras* Djanélidzé, 1922 given by Wright et al. (1996: 43). In contrast, the Mexican *Proniceras* specimens described by Burckhardt (1919) are perisphinctid-like, evolute, compressed forms, densely ribbed from the inner whorls; in middle or outer whorls primary ribs are reinforced on the umbilical shoulder forming elongated swellings (bullae) which could be described as tubercles in some cases. *P. subpronum* Burckhardt, 1919 is the species with earlier development of umbilical tubercles, from $D = 20-25$ mm. The adult specimen of *P. idoceroides* Burckhardt (1919: pl. 15: figs. 2-4) is a compressed, evolute and densely ribbed microconch with lappets which shows that the genus is sexually dimorphic. The *Proniceras* of Burckhardt are early late Tithonian in age (Callomon 1992) and they seem to conform the earliest part of the lineage leading to *Negrelliceras* and most likely also to *Spiticerates* Uhlig, 1903 (including *Kilianiceras* Djanélidzé, 1922).

The LT stands from an unfortunate designation which has led to some confusion in combination with the wide intraspecific variation of the Spiticeratines claimed everywhere but never evaluated. The diagnoses of Wright et al. (1996) for *Spiticerates* Uhlig, 1903, *Kilianiceras* Djanélidzé, 1922 and *Negrelliceras* are based on the occurrence and ontogenetic persistence of the row of lateral tubercles. Differentiation between *Spiticerates* and *Kilianiceras* is in many cases confused by the sizes at which the onset and/or vanishment of the lateral tubercles are observed. However, these differences seem to be nothing more than variation based on heterochronic phenotypic plasticity in the developmental pathways. Assuming this variation as intraspecific and considering that both subgenera have the same stratigraphic distribution (Upper Tithonian? - Berriasian, Wright et al. 1996: 43), we adopt herein a simple taxonomy considering the genus *Spiticerates*

undivided.

Negrelliceras, commonly compressed and finely ribbed, without lateral tubercles all through its ontogeny, could likely be an independent lineage. Nevertheless, differentiation in respect to *Spiticeras* is completely artificial and unclear. For example, Djanélidzé (1922: pl. 5 and 7) illustrated six macroconchs, including a large well-preserved specimen as *N. negreli*, distributed in five different species of *Spiticeras* and *Negrelliceras*, and, on the other hand, five lappeted microconchs distributed in three different species of *Negrelliceras* and *Proniceras* (pl. 6: 1-5). All these specimens are identical in coiling and sculpture, only differing in the more or less inflated shell, and the microconchs by possessing lappets, thus strongly suggesting they all belong to a single, sexually dimorphic species of the Berriasian.

Genus *Spiticeras* Uhlig, 1903

Type species.- *Ammonites spitiensis* Blanford, 1863;
by SD Roman, 1938.

Spiticeras fraternum (Steuer, 1897)

Fig. 28C

- *1897 *Holcostephanus fraternus* nov. sp.- Steuer: p. 192, pl. 29: 1 [LT].
- 1897 *Holcostephanus (Astieria) Bodenbenderi* nov. sp.- Steuer: 191, pl. 28: 5-6 [LT].
- *1921 *Holcostephanus fraternus* n. sp.- Steuer: 95, pl. 15: 1 [LT refigured].
- 1921 *Holcostephanus bodenbenderi* n. sp.- Steuer: 94, pl. 4: 5-6 [LT refigured].
- 1925 *Spiticeras damesi* (Steuer) forma planulata nueva forma.- Gerth: 67, pl. 3: 2.
- 1945 *Spiticeras (Negrelliceras) singulare* n. sp.- Leanza: 79, pl. 17: 1, 6-7, 9.
- 1945 *Spiticeras (Kilianiceras) damesi* (Steuer).- Leanza: 73, pl. 20: 7.
- 1951 *Spiticeras limaensis* n. sp.- Rivera: 46, pl. 6: 5 [HT].

Lectotype.- The species was based on a number of specimens from Arroyo Alberjillo and Rodeo Viejo but with no designation of type specimen, and it seems that there has not been any later formal designation. Thus, we designate the specimen figured by Steuer (1921: pl. 15: 1) as the lectotype. The type locality is A. Alberjillo but unfortunately the stratigraphic position within the section is unknown.

Material.- Two specimens, macroconch phragmocones more or less well preserved (MCNAM 24469/1, 24468/4), bed AC-19.

Description.- The best preserved specimen (Fig. 28C) is a phragmocone (max $D = 85$ mm), probably adult and rather complete for it seems to be uncoiled at the end. Inner whorls ($D < 15$ mm) evolute, depressed, whorl section oval, flanks covered by acute, radial primary ribs and with prosocline constrictions. Middle whorls ($20 < D < 60$ mm) moderately evolute with wide umbilicus. The lateral ribbing gradually enlarges and swells up on the umbilical shoulder and on the flank. This bituberculate stage persists along two or three whorls, then umbilical swollens convert in well marked, radially elongated periumbilical tubercles from which branch two to four secondaries which reach the venter evenly spaced; ventral ribbing forming an angular chevron,

weakened or interrupted besides a narrow smooth band; there can be seen about two constrictions per whorl. The last whorl becomes subtriangular, higher than wide, venter rounded; the ribbing vanishes, the umbilical tubercles are placed on the umbilical shoulder properly, and occur a well marked and strongly prosocline constriction.

The other specimen available is more compressed with the primary ribs swollen as elongated umbilical tubercles, which divide on the half of the flank in bundles of projected secondaries crossing the venter uninterrupted.

Remarks.- The described specimen is identical to the LT in every detail of its morphology, sculpture and size. The other specimen available preserves part of its bodychamber, which has lateral ribs, but it is smaller and more compressed, with wider spaced periumbilical tubercles.

The LT comes from an unspecified horizon. This usually precludes a meaningful use of the name. However, the list of ammonites given by Steuer (1897, transl. 1921: 43-45) for the section of this locality consists of several well-known species which have been figured, and moreover, most of specimens are HT by MT known associated with other ammonites in other localities in Berriasian beds:

(1) *Reineckeia egregia* Steuer, 1897 (1921: pl. 9: 1-2, HT by MT). An identical specimen was figured by Leanza (1945: pl. 5: 1-2) from the Noduliferum Z. of M. Redondo. Other material of this species was collected in Pampa Tril, in beds of the Noduliferum Z. with *Negrelliceras* sp. and *Cuyaniceras*? sp., overlying a bed with abundant *A. noduliferum* (Steuer) and underlying a horizon with abundant *Subthurmannia* cf. *boissieri* and similar forms. This indicates a late Berriasian age for its type horizon.

(2) *Reineckeia mutata* Steuer, 1897 (1921: pl. 13: 1, HT by MT). This ammonite is very similar to the HT by MT of *Argentiniceras bituberculatum* Leanza, 1945 from the lower Noduliferum Z. Inner whorls are identical, but the outer whorl is more subrectangular with two rows of tubercles. However, the description given by Steuer (1921: 53) mentions a short bituberculate stage.

(3) *Reineckeia koellikeri* (Oppel).

(4) *Reineckeia planuslistra* Steuer, 1897. After the description given by Steuer (1921: 65) it seems that the HT by MT corresponds to the inner whorls of *R. incerta*.

(5) *Reineckeia incerta* Steuer, 1897. The last whorl of the HT by MT recalls, in shape and sculpture, the adult bodychamber of *S. koeneni* (see Fig. 23F and 24), but the phragmocone is different, bearing stronger and more widely spaced primaries. An identical specimen to that figured by Steuer was collected in the upper Koeneni to lower Noduliferum z. of C. Pincheira (Parent 2003: fig. 1B).

(6) *Odontoceras transgrediens* Steuer, 1897. The specimen from A. Alberjillo is the HT by MT of the TS of *Cuyaniceras* Leanza, 1945 (SD Arkel 1952). *C. transgrediens*, and other seven species which seem to be merely intraspecific variants, were described by Leanza (1945) from a single bed included in the lower Damesi Z. (Berriasian) of A. del Yeso.

(7) *Holcostephanus fraternus* Steuer.

(8) *Stephanoceras damesi* Steuer, 1897. A single specimen,

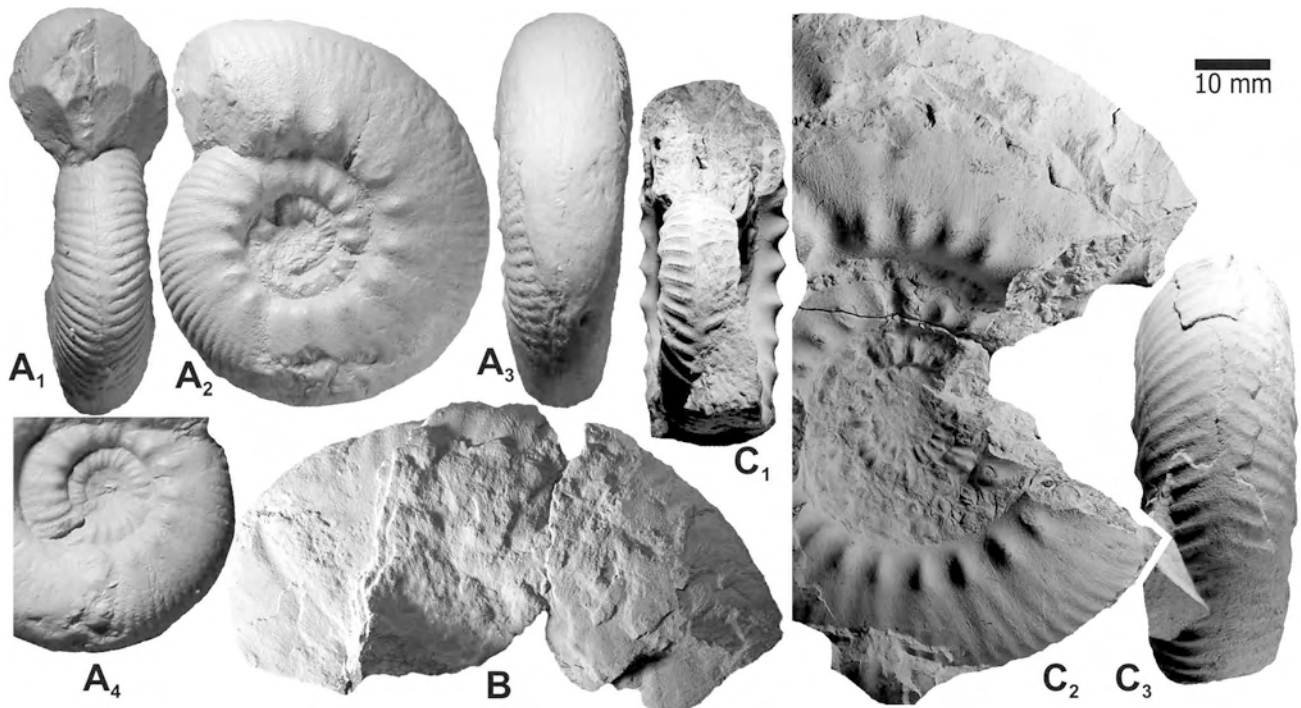


Figure 28. **A:** *Proniceras pronum* (Oppel). Cast (LPB M122) of the lectotype of *Ammonites pronus* Oppel, 1865 (BSPG AS III 211); Tithonian; Koniaków, West Carpathian Mountains, Poland; apertural (A₁), lateral (A₂) and ventral (A₃) views of the right face (apertural view); A₄: detail of the inner whorls (left face) showing the onset of periumbilical transformation of the primary ribs into radially elongate bullae with fasciculate secondaries. **B:** *Groebericeras bifrons* Leanza, portion of bodychamber (MCNAM 24469/2), A. Cieneguita, bed AC19 (Noduliferum Z., *compressum* hz.). **C:** *Negrelliceras fraternum* (Steuer), adult phragmocone (MCNAM 24469/1), A. Cieneguita, bed AC-19 (Noduliferum Z., *compressum* hz.). All natural size.

the HT by MT of the TS of *Kilianiceras* Djanélidzé, 1922 (SD by Roman, 1938). Leanza (1945) described material assigned to this species from a bed of the Damesi Z., associated with *Spiticeras singulare* (= *S. fraternum*).

In conclusion, the stratigraphic interval where these ammonites occur in other localities is demonstrated by Leanza (1945) to be a relatively narrow interval of the Noduliferum Z. It can be assumed with little risk that the type horizon of *S. fraternum* lies in rocks of the upper Vaca Muerta Fm., belonging to the Noduliferum Z.

The type series of *S. singulare* consisted of six specimens from beds of the Damesi Z. of M. Redondo and A. del Yeso (Leanza 1945: 80), but none of them was designated as type. The best preserved specimen from A. del Yeso figured by Leanza (1945: pl. 17: 1 and 7) is herein designated as the lectotype. This specimen slightly differs from the specimen of AC by a somewhat fainter sculpture, but otherwise shows striking resemblance in its overall shell shape and sculpture ontogeny at similar sizes, vanishing on both the flanks and venter towards the peristome. The paralectotypes are all strongly similar to each other, with variations in the sizes at which the lateral and ventral ribbing fade off. The smaller paralectotype (Leanza 1945: pl. 15: 1, 6) bears very faint umbilical tubercles and clearly shows the same aspect of ventral ribbing of the inner whorls as observed in the specimen from AC (Fig. 28C). Considering that both morphologically indistinguishable species occur more or less in the same stratigraphic horizon, *S. singulare* is considered a junior synonym of *S. fraternum*. Furthermore, the specimen figured as *S. (Kilianiceras) damesi* by Leanza (1945: pl. 20: 7) shows the same sculpture (with a single row of tubercles) and shell shape, only differing by somewhat stronger umbilical tubercles. We therefore interpret this

specimen as an extreme variant of the species in the opposite end of the variation compared with the smaller paralectotype of *S. singulare* mentioned above.

The more compressed and strongly ribbed specimen of the sample from bed AC-19 is very similar in the essential features to the LT of *S. singulare* and shows close similarity with the HT of *Spiticeras limaensis* Rivera, 1951 from the upper Tithonian or lower Berriasian of Puente Inga, Perú.

Occurrence and distribution.- Bed AC-19, *compressum* hz., Noduliferum Z. As discussed above the species occurs in the Noduliferum Z. of several other localities besides the type locality: P. Tril, M. Redondo, A. del Yeso. Gerth (1925: 123, 124) cited the species from C. Pincheira and Quebradas del Mollar, and Leanza & Hugo (1977: 255) from Mallín Quemado and Bajada del Agrio.

Genus *Groebericeras* Leanza, 1945

Type species.- *Groebericeras bifrons* Leanza, 1945; by OD

Groebericeras bifrons Leanza, 1945

Fig. 28B

Description and remarks.- Two portions of bodychamber (MCNAM 24469/2), bed AC-19. The specimens are crushed, but the characteristic features of the genus are observable: compressed, involute with coarse, rounded ribs on the upper flank and venter, prosocline wide and shallow constrictions.

The species is typical of the Noduliferum Z. and has been recently revised by Aguirre & Alvarez (1999). These authors collected their material from a level just above an interval containing ammonites they called *Andiceras-*

faunule. It is most likely that the ammonites from that horizon belong to *Krantziceras compressum* n. gen. et n. sp.

Family Himalayitidae Spath, 1925

Remarks.- The concept of the family adopted herein mainly follows Donovan et al. (1981) with additions by Tavera (1985), Boughdiri et al. (1999) and Enay et al. (1998a, b). The family includes a group of Andean forms likely rooted in the Torquatisphinctinae, perhaps in *Catutosphinctes proximus* or some close, yet undescribed species of the late Middle Tithonian (late Proximus to early Internispinosum zones) morphologically similar to "*Burckhardticeras*" Olóriz (name pre-occupied). *Windhausenicer* *internispinosum* (Krantz) could likely be one of the earliest members of the Andean representatives of the family (see Parent 2001, 2003a, b). Classification of the Andean forms at the subfamily level could be convenient under the biogeographically-based criterium of a group of lineages or genera originated and developed in the NMB, as part of the local biota (sensu Dommergues & Marchand 1988).

Genus *Windhausenicer* Leanza, 1945

Type species.- *Perisphinctes internispinosus* Krantz, 1926; by OD. Middle Tithonian.

Windhausenicer internispinosum (Krantz, 1926)

Fig. 29F-G, App. 2-G-H

Synonymy.- See Parent (2003b).

Material.- A juvenile with part of the bodychamber (MCNAM 24418/6) from bed AC-9 and a portion of a phragmocone (MCNAM 24453) from bed AC-11.

Description.- The juvenile specimen (bed AC-9), max $D = 30$ mm, is evolute ($U/D = 0.45$ to 0.53) with depressed whorl section ($W/H_1 = 1.05$ to 1.25) throughout the ontogeny. The ribbing is rather uniform from the innermost whorls, composed by acute, prosocline primary ribs bifurcated on the upper part of the flank. At about $D = 8$ mm there is a short stage with a distinctive sculpture: it begins with a deep constriction followed by a blade-like, undivided, prosocline primary which is then followed by primaries that bifurcate on the umbilical shoulder and the secondaries are looped on the upper flank. The last whorl of the phragmocone is evenly ribbed by acute primaries divided in two secondaries of reduced strength with the point of division swollen forming a incipient lamellar tubercle; ventral ribbing evenly spaced and interrupted on the mid-venter forming a continuous groove. The bodychamber is not preserved except for a short portion of a poorly preserved whorl after the last septum showing no changes in whorl section or sculpture.

The other specimen is a portion of phragmocone of a larger individual (bed AC-11). It is well-preserved showing the characteristic morphology and sculpture of the species: evolute and depressed with strong and acute primaries reaching the ventrolateral shoulder where bifurcate ribs form a marked lamellar tubercle; there is a strong constriction developed on the flanks and venter; ventral ribbing is less strong than primaries, unevenly spaced and ending on a small tubercle besides a narrow groove.

Remarks.- The species has been recently revised (Parent

2003b, Parent et al. 2007). The specimen from bed AC-11 is typical for the species, indicating clearly some part within the *Internispinosum* (total range) Biozone, thus within the conjugated Internispinosum (non standard chrono-) Zone.

The smaller specimen from bed AC-9, at the base of the local Internispinosum Z., is an early representative of the species, showing the short sculptural stage with looped secondaries as the lectotype (see Parent 2003b: fig. 1B) but at smaller diameter. The tubercles are weaker in the specimen of AC than in the lectotype at comparable diameters. On the other hand it shows close resemblance with *C. proximus*, especially specimens from bed AC-10 (Fig. 19A-B). This succession of different transients of *W. internispinosum*, where the older ones are very similar to specimens of the late transients of *C. proximus* (transient β in Parent 2003a) strongly supports the hypothesis of a derivation of *Windhausenicer* from *Catutosphinctes* (see Parent 2001). More abundant and complete material from Pampa Tril (still unpublished) illustrates this pattern more confidently.

Genus *Steueria* n. gen.

Type species.- *Berriasella alternans* Gerth, 1921. Tithonian.

Derivation of the name: After Alexander Steuer (1867-1936).

Diagnosis: Mid-sized to large adult macroconchs. Innermost whorls stout and involute, ribbing dense, weakened or interrupted on mid-venter. Middle whorls platycone more or less evolute, whorl section suboval to subtrapezoidal with venter rounded; ribbing dense with more or less marked lateral and ventral lamellar tubercles each two or four of the primaries, appearing later in ontogeny when finer and denser the ribbing and with a persistent smooth ventral band or groove. Adult phragmocone and bodychamber suboval to subtrapezoidal in whorl section; coarse primaries of which one each two, three or four bifurcates on the upper part of the flank on a tubercle; secondaries rarely looped; long ventral spines, as rounded tubercles or bullae on the inner mold resembling parabolic nodes. Microconchs smaller, with small lappets.

Remarks and comparison.- In Gerth's own copy of his paper (1925), he made manuscript annotations which provide valuable information about view points attained after publication. In the title "*Berriasella alternans* spec. nov." (p. 89) he made one of those annotations reassigning the species to *Neocosmoceras* Blanchet, 1922. This annotation is a good indication of the difficulties in classifying that species which shows a conspicuous himalayitid-like bodychamber but with densely ribbed *Berriasella*-like inner whorls. Moreover, it is in accord with his reference (Gerth 1925: 90) to the similarities between *B. alternans* and *Ammonies koellikeri* Oppel. On the other hand, in p. 89, Gerth has stressed the slight differences between *B. alternans* and *B. inaequicostata* Gerth, 1921 consisting only in the rib density of the inner whorls. Taking into account the material described below and the type specimens of *B. alternans*, *B. inaequicostata* and *B. spinulosa* it can be realized that when denser the ribbing the later in the ontogeny appear the tubercles, especially the ventral ones, as stressed in the diagnosis above.

Corongoceras show some similarities with *Steueria* n.

gen., but predominate consistent differences, mainly on the inner whorls. In *Corongoceras* the inner whorls have flat venter and strong tubercles on the point of furcation and on the venter or ventro-lateral shoulder. In *Steueria* the venter is well rounded, ribbing is fine and dense with less frequent puntiform tubercles. In *Corongoceras* adult ribbing is not dense but strong, acute and widely splayed on spiniform tubercles, and almost all of the ventral ribs end on ventro-lateral tubercles.

Steueria n.gen. differs from the typically serpenticone *Micracanthoceras* by the densely ribbed inner whorls with two rows of lamellar tubercles and on the adult phragmocone covered by more or less flexuose primary ribs with a high-lateral tubercle or lamellae. These differences are best realized by comparison with *Micracanthoceras koellikeri* (Oppel) since the LT of *M. microcanthum* (see Geyssant 1997: pl. 26: 1) is preserved at a smaller size which does not show the sculpture of the adult phragmocone and the bodychamber. *Ammonites koellikeri* was based on 2 specimens according to Zittel (1868), one of which is only a fragment. The specimen figured by Zittel (1868: pl. 18: 1) is designated herein lectotype and refigured by a cast (Fig. 32). Its inner whorls are very evolute with strong lateral tubercles on one each three or four primaries; the last whorl preserved, yet septated at $D = 162$ mm, is subrectangular to suboval in whorl section whereas in *Steueria alternans* is subtrapezoidal to subrectangular, higher than wide. The sculpture is different as mentioned above, consisting of strong and distant primary ribs which almost all bifurcate on the upper half of the flanks and cross the venter slightly weakened with an indistinct raising on the ventro-lateral shoulder. *Ammonites koellikeri* has been cited frequently in the Andean Tithonian, e.g. Behreidsen (1891), Steuer (1897), Krantz (1926). This latter author figured the plaster cast of a small specimen (Krantz 1928: pl. 3: 1) indicating this is the "type", but this specimen actually does not belong to the original type series.

Wichmanniceras Leanza, 1945 was based on the single species *Wichmanniceras mirum* Leanza (1945: pl. 1: 4-5, HT by MT). The HT ($D = 48$ mm) is a very evolute and widely umbilicate ($U/D = 0.52$) serpenticonic ammonite with rather strong, radial ribbing and very sparse small lateral tubercles on the phragmocone, a short stage of ribs looped on the ventro-lateral shoulder and the bodychamber with two rows of closely spaced ventral tubercles. The differentiation from *Steueria* n. gen. is in that (1) rib density increases with growth, reaching the maximum on the bodychamber whereas *Steueria* shows the opposite trend, (2) the sculpture includes two or three rows of tubercles in *Steueria* n. gen. but a single one in *Wichmanniceras*, and (3) the shell shape is consistently inflated to compressed platyconic, higher than wide whorl section in *Steueria* n. gen. but very evolute serpenticonic with rounded whorl section in *Wichmanniceras*. In spite of its small adult size the HT of *W. mirum* seems to be adult as suggested by the change in the sculpture and the uncoiling on the last half whorl. It is interesting to note that the phragmocone of *W. mirum* has no differences respect *Micracanthoceras microcanthum*, and could likely be a species of this genus.

Species included.- *Berriasella spinulosa*, *Berriasella inaequicostata*, *Berriasella groeberi* Leanza, 1945, *Corongoceras rigali* Leanza, 1945, *Berriasella delhaesi* Leanza, 1945, *Berriasella pastorei* Leanza, 1945, *Micracanthoceras lamberti* Leanza, 1945, *Micracanthoceras tapiai* Leanza, 1945 and *Neocosmoceras*

cf. *sayni* (Simionescu, 1899) in Aguirre & Charrier (1990: pl. 1: 1-2).

Berriasella spinulosa, *B. alternans* and *B. inaequicostata* were introduced by Gerth (1921: 147) based on specimens collected by himself but with neither full descriptions nor figuration; only later (Gerth 1925) the three species were described and figured. However, this was done before the formal introduction of nomenclatural rules in 1930. Gerth (1921) mentioned the three species coming from a specific stratigraphical interval ("Zona de *Steuroceras koeneni*") and provided brief comparisons with similarly morphological taxa. Therefore, although not illustrated, the introduction of these species seems to be valid, and only the year of publication must be changed. *B. spinulosa* was based on at least six specimens but with no designation of a type specimen, and apparently it has not been designated a lectotype. The specimen figured by Gerth (1925: pl. 6: 1), a complete adult macroconch phragmocone with the beginning of the bodychamber crushed, is herein designated as lectotype and refigured (Fig. 29A). The only paralectotype figured by Gerth (1925: pl. 6: 2, 2a), an incomplete or juvenile phragmocone, is also refigured (Fig. 29B). The type locality and horizon is at Arroyo Durazno, Mendoza (Fig. 1), bed 31g in Gerth (1925: 126), *Alternans* Z., upper Tithonian. *B. inaequicostata* was defined with at least two specimens at hand; that illustrated by Gerth (1925: pl. 6: 4) from the same bed 31g is herein designated lectotype and refigured (Fig. 29D), as well as the figured paralectotype (Gerth 1925: pl. 6: 4a) refigured in Fig. 29C.

Steueria alternans (Gerth, 1921)

Figs. 29A-D, 30-31

- 1900b *Reineckeia Koellikeri* Oppel.- Burckhardt: 16, pl. 20: 14-15, pl. 21: 1.
 1900b *Reineckeia microcantha* Oppel.- Burckhardt: 16, pl. 25: 16-17.
 1921 *Berriasella alternans* n. sp.- Gerth: 117.
 1921 *Berriasella spinulosa* n. sp.- Gerth: 117.
 1921 *Berriasella inaequicostata* n. sp.- Gerth: 117.
 *1925 *Berriasella alternans* nov. sp.- Gerth: 89, pl. 6: 3-3a [HT by MT].
 1925 *Berriasella spinulosa* nov. sp.- Gerth: 91, pl. 6: 1 [LT], 2-2a [paralectotype].
 1925 *Berriasella inaequicostata* nov. sp.- Gerth: 90, pl. 6: 4 [LT], 4a [paralectotype].
 ?1937 *Berriasella spinulosa* Gerth.- Feruglio: 65, pl. 8: 7-13.
 1945 *Berriasella inaequicostata* Gerth.- Leanza: 34, pl. 4: 2.
 1945 *Berriasella groeberi* n. sp.- Leanza: 37, pl. 4: 1 [HT by MT].
 1945 *Berriasella delhaesi* n. sp.- Leanza: 39, pl. 6: 1-2 [LT].
 1945 *Berriasella pastorei* n. sp.- Leanza: 33, pl. 3: 12-13 [LT].
 1945 *Corongoceras alternans* (Gerth).- Leanza: 47, pl. 1: 2-3.
 1945 *Corongoceras rigali* n. sp.- Leanza: 48, pl. 6: 3-4 [HT].
 1945 *Himalayites concurrens* n. sp.- Leanza: 46, pl. 3: 5-6 [HT].
 ?1960 *Berriasella* aff. *spinulosa* Gerth.- Bürgl: 194, pl. 4: 13.
 1967 *Berriasella spinulosa* Gerth.- Leanza: 145.
 1972 *Micracanthoceras spinulosa* (Gerth).- Enay: 375.
 *2001 *Corongoceras alternans* (Gerth, 1925).- Parent: 32,

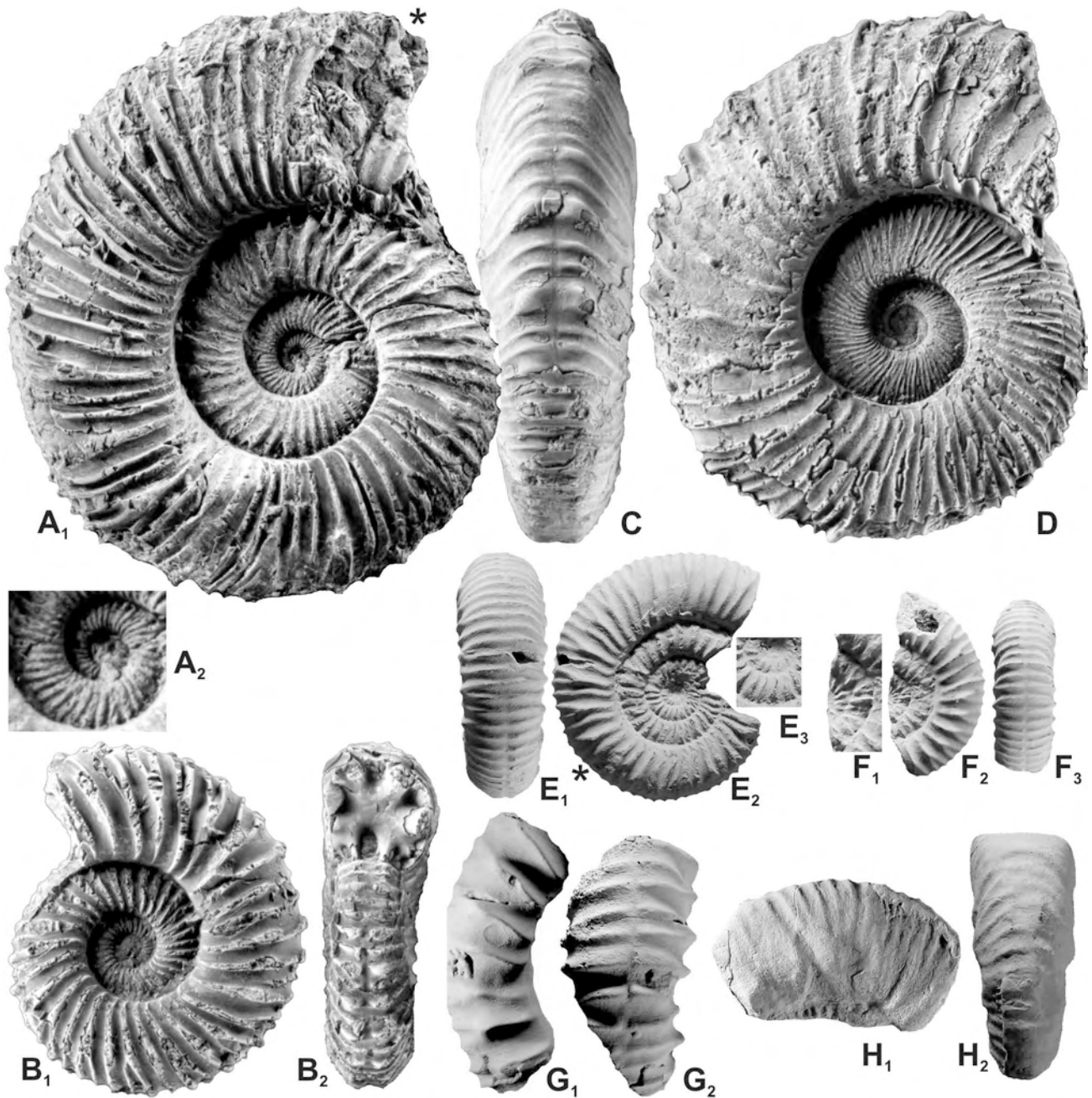


Figure 29. A-B: *Steueria alternans* (Gerth, 1921), Arroyo Durazno, Alternans Z.; **A**: lectotype of *Berriasella spinulosa* Gerth, 1921 herein designated, refigured from Gerth (1925: pl. 6: 1), adult macroconch with beginning of bodychamber crushed; **A₂**: inner whorls enlarged (x2); **B**: paralectotype refigured from Gerth (1925: pl. 6: 2), phragmocone. **C-D**: *Berriasella inaequicostata* (Gerth, 1921), A. Durazno, Alternans Z.; **C**: ventral view of a paralectotype refigured from Gerth (1925: pl. 6: 4a); **D**: lectotype herein designated, refigured from Gerth (1925: pl. 6: 4), adult macroconch phragmocone. **E**: *Micracanthoceras* sp. A, almost complete specimen (MCNAM 24418/4), bed AC-9 (Internispinosum Z.); **E₂**: detail of the inner whorls (x2). **F-G**: *Windhausenicerus internispinosum* (Krantz), A. Cieneguita; **F**: juvenil specimen with beginning of bodychamber (MCNAM 24418/6) of an early representative of the species, bed AC-9 (Internispinosum Z.), **F₁**: detail of the inner whorls (x2); **G**: portion of phragmocone (MCNAM 24453) of a typical representative of the species, bed AC-11 (Internispinosum Z.). **H**: *Himalayites* cf. *andinus* Leanza, portion of bodychamber (MCNAM 24465), loose from bed AC-18. All natural size otherwise indicated. The asterisks indicate the last septum.

fig. 9D-E [HT refigured].

n2001 *Corongoceras* cf. *alternans* (Gerth, 1925).- Parent: 32, fig. 8K-L.

2005 *Micracanthoceras?* *spinulosum* (Gerth, 1925).- Klein: 20.

n2005 *Berriasella inaequicostata* Gerth.- Klein: 170.

2005 *Corongoceras alternans* (Gerth).- Klein: 25.

Holotype.- The HT by MT of *B. alternans* was already refigured and discussed in Parent (2001: 32, fig. 9D-E), bed

31g (TH), Arroyo Durazno (TL).

Material from AC.- Four specimens: an almost complete adult macroconch (MCNAM 24402), bed AC-14; a subadult macroconch (MCNAM 24459/19) and two juvenile specimens (MCNAM 24459/X1, 24459/X2), bed AC-15.

Description of new material from AC.- Inner whorls ($D < 10$ mm) stout depressed, suboval whorl section with wide rounded venter; ribbing prosocline, mostly bifurcate on the

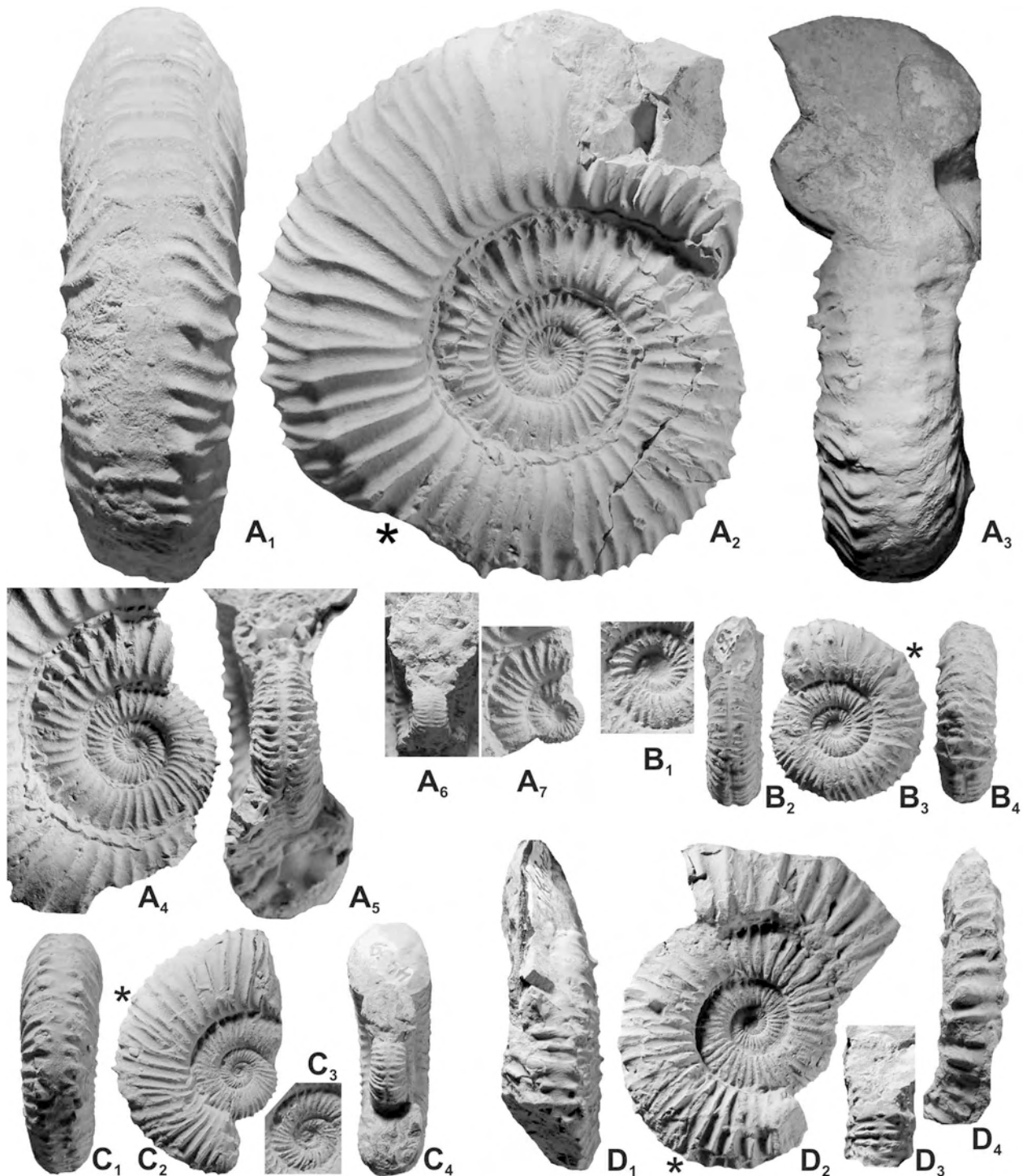


Figure 30. *Steueria alternans* (Gerth, 1921), A. Cieneguita, beds AC-14 (A) and AC-15 (B-D), Alternans Zone. **A:** almost complete adult macroconch (MCNAM 24402), showing details of the inner whorls (A₆-A₇, x2). **B:** juvenil specimen with beginning of bodychamber (MCNAM 24459/X2), **B₁**: details of the innermost whorls (x2). **C:** juvenil specimen with beginning of bodychamber (MCNAM 24459/X1), **C₁**: details of the innermost whorls (x2). **D:** subadult macroconch with almost complete bodychamber (MCNAM 24459/19); **D₁**: ventral view of the last whorl of the phragmocone, **D₂**: lateral view, **D₃**: ventral view at the beginning of the bodychamber, **D₄**: ventral view of the last preserved part of the bodychamber. All natural size otherwise indicated. Asterisks indicating the last septum.

ventrolateral shoulder and vanishing ventrally besides a narrow smooth band; one to three constrictions per whorl.

Middle whorls (about $10 < D < 50$ mm) more compressed and involute, suboval to subtrapezoidal in whorl section with the venter rounded to nearly flat; ribbing dense, primaries prosocline to subradial, most of them undivided, each three of four ribs only one of them is bi- or trifurcate on a lateral lamellar tubercle but all ribs reach the venter evenly

spaced and fade out aside a well marked smooth band resembling a groove; the anterior secondary rib originated from the lateral tubercle ends on a ventral lamellar tubercle which is stouter and rounded in some specimens.

The last whorl of the adult phragmocone (about $D > 50$ mm) evolute and the bodychamber moderately uncoiled, suboval to subtrapezoidal in section with flat to rounded venter. Ribbing is more irregular and acute, most primaries

bifurcate others remain simple and few others trifurcate or bifurcate lower on the flank and again upwards; the point of furcation is on the upper third of the flank with formation of a lamellar tubercle which sometimes is only a raising on the point of furcation. Secondary and undivided primaries reach the venter and fade out aside a smooth band. On the first half of the bodychamber some few secondaries loop on the ventrolateral lamellar tubercle; towards the peristome the ribbing remains strong and acute but the tubercles disappear. Remains of the bodychamber on the preceding whorl indicates at least $L_{BC} = 220^\circ$.

Description of the lectotype of B. spinulosa (Fig. 29A). - The inner whorls are densely ribbed by fine, prosocline, primary ribs which start on the umbilical wall and bifurcate irregularly above the mid-flank. From about $D = 7$ mm some ribs swell close to the ventrolateral shoulder in the shape of a lamellar tubercle. From $D = 25$ mm there is one each two or four primaries which bifurcate at irregular height and with the formation of a radially elongate, lamellar tubercle. The last whorl of the phragmocone is more evolute, the whorl section suboval, slightly higher than wide; the ribbing remains irregular, about one or two singles each one bifurcate, and the tubercles are more rounded and notorious but less frequent. The bodychamber is not preserved, only the very beginning crushed which suggests that ribbing is slightly stronger and more widely spaced. The diameter at last septum is $D_s = 94$ mm, $U/D = 0.43$, $W/H_1 = 1$, $P = 32$, $V = 50$. The beginning of the last phragmocone whorl is at $D = 73$ mm showing $U/D = 0.40$, $H_1/D = 0.34$, $P = 25$, $V = 37$.

Remarks and comparison. - The material from AC is practically identical to the LT of *B. spinulosa*, matching in shell shape and sculpture; the only difference is in the more subtrapezoidal whorl section of the adult of AC (Fig. 30A).

Burckhardt (1900b: pl. 20: 14-15 and pl. 21: 1) figured two fragments of large macroconch bodychambers from the upper Tithonian of Liu-Cullín, Río Agrío whose ornamentation is identical, at larger size, to the HT of *B. alternans*. Another specimen from the upper Tithonian of Sierra Vaca Muerta (Burckhardt 1900b: pl. 25: 16-17) consists of a small specimen ($D = 31$ mm) with a portion of bodychamber. This specimen seems to be juvenil for there is no signs of uncoiling; its shell shape and sculpture are comparable with the specimen shown in Fig. 30B but with weaker tubercles. The last whorl is also superficially similar to *Micracanthoceras* sp. A (described below, Fig. 29E), but the inner whorls are different.

The specimens described by Feruglio (1937: pl. 8: 7-13) as *B. spinulosa* do not seem to belong to the present species which includes that nominal species as a variant. Although the material consists of impressions of small specimens, it can be observed that all of them are loosely ribbed from the innermost whorls by wiry primaries which bifurcate irregularly on middle of the flank and occur more or less frequently small tubercles on the points of furcation.

There is a consistent pattern of co-variation between fine and dense ribbing with small or imperceptible tubercles and coarser and less dense ribbing with larger and more rounded tubercles. This pattern can be observed even in a single sample as the material described and those specimens of the bed 31g of Gerth (1925). Considering this intergradation of morphologies and the co-occurrence in a single horizon at several localities (A. Durazno, Mallín Redondo and AC), *B. inaequicostata*, *B. spinulosa* and *B. alternans* are assumed as intraspecific variants of a single

species, *Steueria alternans* n. gen. The selection of *S. alternans* as the specific name preserved is in terms of nomenclatural stability for it is the index of the Alternans Z.

Berriasella pastorei Leanza was based on four specimens from bed 1762 of the section of Mallín Redondo, Alternans Z. (Leanza 1945: 90). There was no designation of a type; the only figured specimen (Leanza 1945: pl. 3: 12-13) is a small adult because of the clearly uncoiled bodychamber and herein designated as the lectotype. This specimen exhibits a bodychamber indistinguishable from the HT of *S. alternans*, and the sculpture of the phragmocone is identical to the HT of *B. inaequicostata* at comparable diameter. *Corongoceras rigali* Leanza (1945: pl. 6: 3-4, HT by MT), from the same horizon of Mallín Redondo is a small adult with the diagnostic sculpture of *Steueria* n. gen. which differs from the specimen figured by Leanza (1945: pl. 1: 2-3) as *Corongoceras alternans* only by the stronger ventral tubercles. *Berriasella delhaesi* Leanza was based on four specimens from beds 1762 and 1762a of the same locality. A type specimen was not designated; the only specimens figured by Leanza (1945: pl. 6: 1-2) is hence designated here as the lectotype. This specimen is an adult with a part of its bodychamber preserved, uncoiled; its sculpture and shell shape is typical of *Steueria* n. gen. These variants of *S. alternans* show the range of variation of this transient of the species that is used below for characterization and definition of the *bardense* hz.

The large adult phragmocone shown in Fig. 31, from the Alternans Z. of Cajón de Almaza, is very close to the LT of *B. spinulosa* but larger, its size at the peristome is estimated as at least $D = 240$ mm. The inner whorls are moderately dense ribbed with lateral and ventral tubercles like in the specimen of Fig. 30D and the LT of *B. spinulosa*, but the outermost whorl is almost identical, although larger, to the last whorl of the HT of *B. alternans*.

The pattern of variation of *S. alternans* is a good example of the changes in duration of sculpture ontogenetic stages (developmental heterochronies) which produce mosaics of different variants which are commonly assigned to different species if isolated specimens are considered. The sculpture stages during ontogeny are the same but expressed at variable diameters and for different intervals. For instance, considering the specimens of *S. alternans* of the bed 31g of Gerth (1925) the finely and densely ribbed stage is developed on almost the whole phragmocone of the LT of *B. inaequicostata* (Fig. 29D), but this stage is shorter in the LT of *B. spinulosa* (Fig. 29A) and in the HT of *B. alternans*, where it is restricted to the inner whorls. Thus, the next sculpture stage of bituberculate ribs with two or four simple, intercalated primaries begins at different sizes.

Occurrence and distribution. - Beds AC-14-AC-15, Alternans Z. Other records: the type locality (A. Durazno), M. Redondo and C. Almaza (Fig. 31). There are several citations without illustration in the literature (e.g. Leanza & Hugo 1977, among others) which cannot be evaluated and thus not included in the synonymy list.

Genus *Corongoceras* Spath, 1925

Type species. - *Corongoceras lotenoense* Spath, 1925; by OD. Middle-upper Tithonian.

Remarks. - *C. lotenoense* was unfortunately based on a small specimen (the HT by MT), from an unknown horizon of Cerro Lotena, which represents only a nucleus (Parent 2001:

fig. 9A-B). Therefore, the aspect of the mature whorls remain unknown. Haupt (1907) figured two specimens as *Hoplites koellikeri* (Oppel) collected in Cerro Lotena, but Spath (1925) included for his definition of the species only one of the two specimens figured by Haupt (1907: fig. 7a-b). Thus, this specimen is the monotypic holotype of *C. lotenoense*, whereas Enay (2009: 204) erroneously supposed this specimen being the lectotype.

Corongoceras has been used for classification of innumerable ammonites of Tethyan affinities and the Indo-Madagascan Realm. However, the original definition of the genus based on poor material precludes any meaningful discussion of most of those nominal occurrences.

Considering the limitations to the interpretation of the genus that the type species impose, we adopt for the following descriptions a concept for the genus restricted to the Andean forms *C. lotenoense*, *C. mendozanum* (Behrendesen), and preliminarily *C. ? steinmanni* (Krantz) and *C. ? filicostatum* Imlay, 1942.

In the upper Proximus Z. (bed AC-8) occurs a conspicuous ammonite, *Corongoceras?* sp. A (Fig. 33A), with strong, acute and widely spaced primary ribs bifurcate on the upper third of the flank producing equally strong secondaries which tend to vanish on mid-venter. This specimen recalls the aspect of the outermost whorl of the HT of *C. lotenoense* (Parent 2001: fig. 9A-B), but the specimen of *Corongoceras?* sp. A has more flexuous ribs lacking the small tubercles as seen in *C. lotenoense*. On the other hand, *C. proximus* and *P. beresii* n. gen. et n. sp., coming from the same level, are different, especially by their sculptures. The HT of *Corongoceras involutum* Biró, 1980 is very similar as discussed below. In these terms *Corongoceras?* sp. A could be an early representative of the genus in which the tubercles are not yet fully developed.

***Corongoceras mendozanum* (Behrendesen, 1891)**

Figs. 8I-K, 33B-D, 34, App. 1, App. 2-F

- *1891 *Hoplites mendozanus* n. sp.- Behrendesen: 399, pl. 25: 2 [HT].
- 1897 *Reineckeia Koellikeri* Oppel sp.- Steuer: 157, pl. 22: 5.
- *1921 *Hoplites mendozanus* n. sp.- Behrendesen: 181, pl. 2: 4 [HT refigured].
- 1921 *Reineckeia koellikeri* Oppel.- Steuer: 31, pl. 8: 5.
- 1926 *Berriasella (Corongoceras) duraznensis* Krantz.- Krantz: 445
- 1926 *Berriasella (Corongoceras) mendozana* Behrendesen.- Krantz: 446
- 1926 *Berriasella (Corongoceras) submendozanum* Krantz.- Krantz: 446
- 1926 *Berriasella (Riasanites) rjasanenoides* Krantz.- Krantz: 441, pl. 17: 1-2
- 1928 *Berriasella (Corongoceras) duraznense* n. sp.- Krantz: 29, pl. 4: 1 [HT refigured] (as *Corongoceras duraznense* n. sp. in caption).
- 1928 *Berriasella (Corongoceras) mendozanum* Behrendesen.- Krantz: 29, pl. 4: 3-4 (as *Berriasella mendozanum* in caption).
- 1928 *Berriasella (Corongoceras) submendozanum* n. sp.- Krantz: 30, pl. 4: 6 [HT refigured] (as *Corongoceras submendozanum* n. sp. in caption).
- 1928 *Berriasella (Riasanites) rjasanenoides* n. sp.- Krantz: 25, pl. 4: 7 [LT refigured, as *Riasanites rjasanenoides* n. sp.].
- 1945 *Aulacosphinctes* sp. indet.- Leanza: 22, pl. 3: 7-8.

- 1960 *Blanfordiceras acuticosta* Uhlig.- Collignon: figs. 682-683.
- 1960 *Corongoceras irregulare* n. sp.- Collignon: fig. 690.
- 1960 *Corongoceras fibulatum* n. sp.- Collignon: figs. 703 [LT], 704.
- 1960 *Corongoceras bifurcatum* n. sp.- Collignon: fig. 706 [HT].
- 1967 *Berriasella (Corongoceras) mendozana* (Behrendesen).- Leanza: 145, pl. 2: 1.
- ?1973 *Corongoceras mendozanum* (Behrendesen).- Verma & Westermann: 247, pl. 54: 2.
- p1979 *Blanfordiceras* aff. *wallichi* (Gray).- Thomson: 27, pl. 7: c.
- ?1980 *Corongoceras involutum* n. sp.- Biró: 233, pl. 7: 7 [HT], 8-9 [paratypes].
- ?1985 *Micracanthoceras (Corongoceras) mendozanum* (Behrendesen).- Tavera: 186, pl. 25: 3
- 1989 *Blanfordiceras acuticosta* (Uhlig).- Howlett: 28, pl. 1: 3.
- ?2004 *Corongoceras* sp. C.- Yin & Enay: fig. 10(8).

Holotype and type locality and horizon.- The only specimen figured by Behrendesen (1891) is the holotype by monotypy, collected from the Tithonian of Rodeo Viejo.

Material.- 20 [M] and [m] specimens from beds AC-14 and AC15 (Alternans Z.).

Description.- Sexually dimorphic. Platycone, moderately involute with a more or less narrow umbilicus. Strongly ribbed by procline primary ribs mostly bifurcate, widely splayed from a raised point or tubercle on the upper third of the flank, and interrupted on the venter by formation of a spiniform tubercle aside of a more or less wide smooth band. Simple, undivided primaries scarce, sometimes unclearly connected with a normal primary rib at the umbilical shoulder. Whorl section subrectangular, typically higher than wide, with flatten or slightly convex flanks and tabular venter.

Macroconchs: Innermost whorls at $D < 4$ mm globose and smooth. At about $D = 4-5$ mm remains globose but finely ribbed. From $D = 8$ mm (Fig. 34C) the ventral ribbing is stronger and interrupted on the venter after formation of a lamellar tubercle aside a smooth ventral band; lateral ribbing is simple, apparently undivided and procline; the whorl section is subrectangular with flat venter and more or less convex to the flat flanks, and remains in this style during the juvenile and adult ontogeny. From $D = 15-20$ mm the whorl section may be subrectangular to subtrapezoidal or suboval, with sustained trend throughout the ontogeny to become more and more compressed and higher (Fig. 8I-K, 34C). Ribbing stronger and less dense, first bifurcations appear on the mid-flank with formation of a lateral tubercle at the point of furcation. From $D = 25-30$ mm almost all primaries bifurcate on the upper third of the flank with formation of a well defined spiniform tubercle which on the adult phragmocone may be more elongated in some specimens. Secondary ribs reach the venter and die-out on a elongated spiniform tubercle besides a smooth band. The adult bodychamber begins at a variable size within $D = 45-100$ mm; the whorl section is compressed. Primary ribs bifurcate without formation of lateral tubercles. On the venter the ribs are mostly weaken, not interrupted but raised on the ventrolateral shoulder thus forming a ventral depression (in the exact form that is seen in the inner whorls of the HT of *Corongoceras lotenoense*). Bodychamber

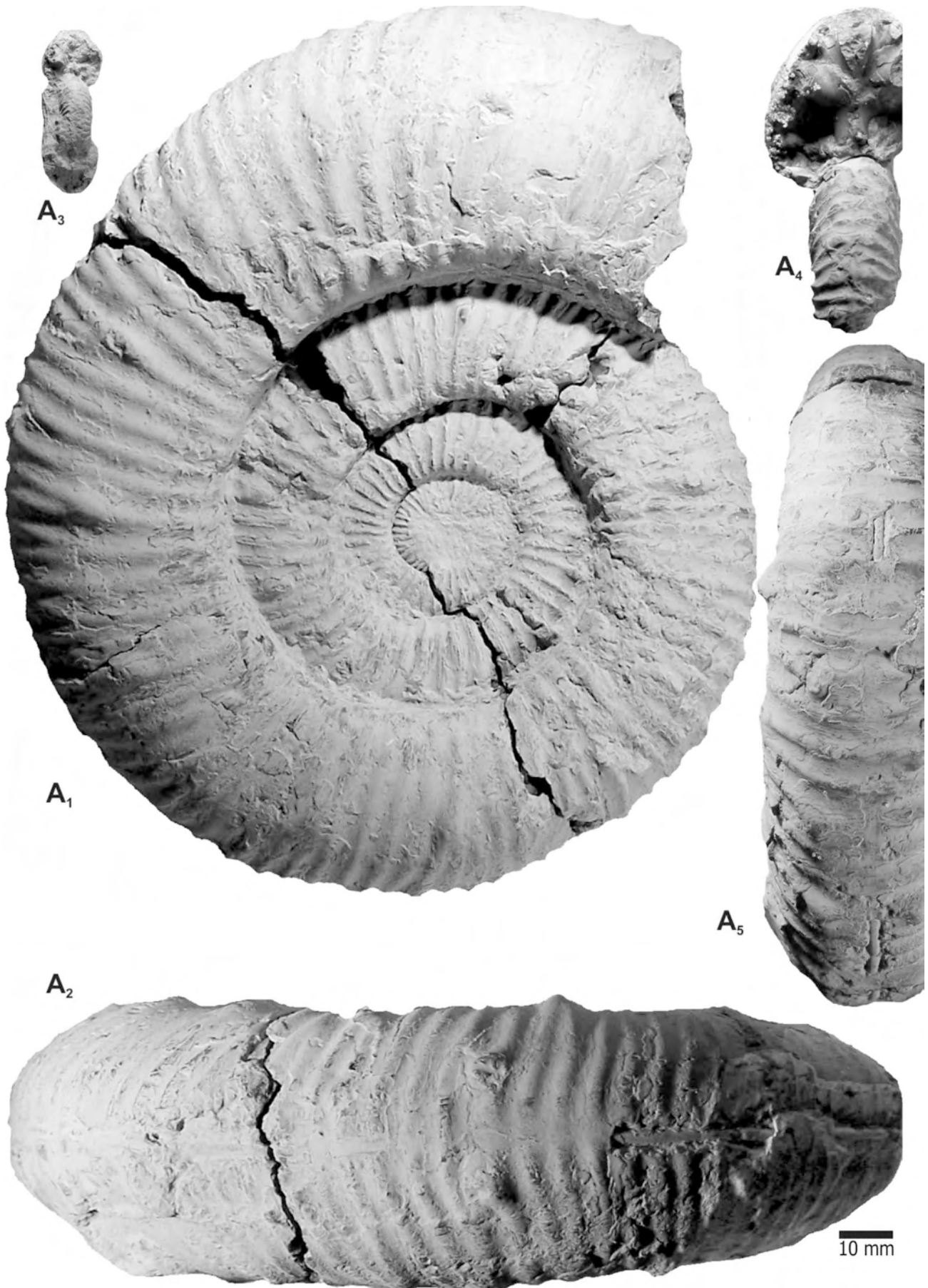


Figure 31. *Steueria alternans* (Gerth, 1921), Cajón de Almaza, Alternans Z.. Adult macroconch phragmocone (MOZPI 6654). A₁: ventral view of inner whorls at $D=25$ mm; A₂: ventral view of inner whorls at $D=50$ mm. All natural size.

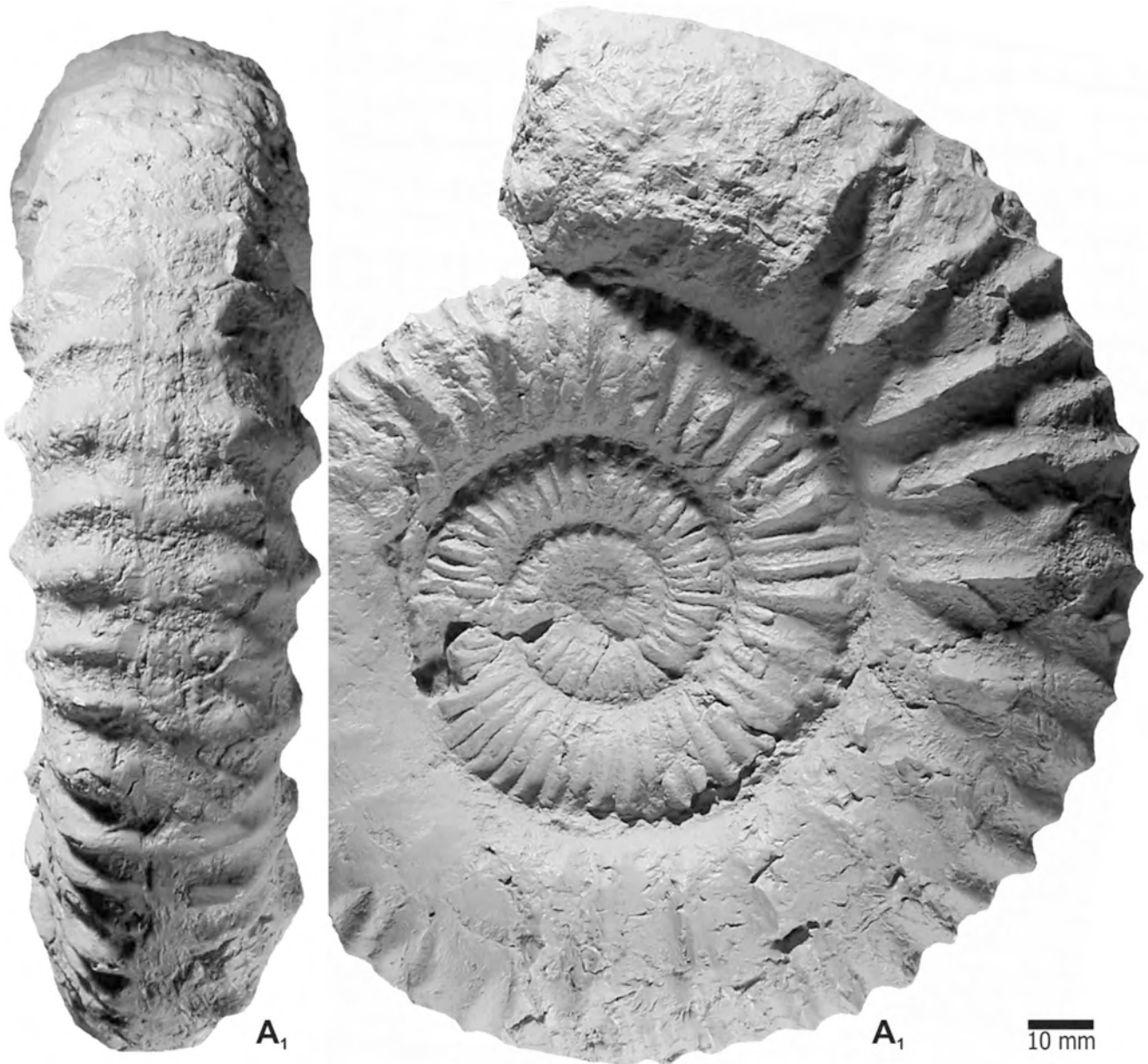


Figure 32. A: *Micracanthoceras koellikeri* (Oppel). Cast (LPB M128) of the holotype of *Ammonites koellikeri* Oppel, 1865 (BSPG AS III 468); Tithonian; Stramberg, Mähren, Czech Republic. Ventral (A_1) and lateral (A_2) views. Natural size.

length is at about 180-270°.

Microconchs: The inner whorls, up to $D = 20-30$ mm, are identical to that of the macroconchs. The bodychamber begins, in the only complete adult specimen available, at $D = 35$ mm. It is evolute, subrectangular in whorl section which can be as wide and high. Sculpture composed by coarse primary ribs developed from the umbilical seam, forming a lamellar tubercle on the umbilical shoulder, run prosocline the flank and raise on a spiniform tubercle in the uppermost part of the flank; from this tubercle the primaries split in two widely splayed secondaries or remain simple, and all fade out on a more or less marked tubercle aside a ventral groove (on the internal mould). Bodychamber length is 240°.

Remarks. - The present specimens are considered to conform a monospecific assemblage with a moderately wide and continuous range of infrasubspecific morphological variation around the HT of *C. mendozanum*.

The outermost whorl of the HT of *C. lotenoense* (perhaps the only specimen figured) is close to the described material of *C. mendozanum* at comparable diameter – very typical himalayitids. This resemblance is the only objective fact which leads us to the inclusion of *Hoplites mendozanus* in *Corongoceras*. However, in the HT of *C. lotenoense* the inner whorls are covered by more flexuous primary ribs and the secondaries cross the venter without interruption. It is very significant that the largest adult macroconch described above shows a sculpture identical to that observed in the inner whorls of the HT of *C. lotenoense* in the adult phragmocone (at $D = 60-100$ mm). However, some specimens recently collected in Cerro Lotena which are almost identical to the holotype of *C. lotenoense* come from levels which probably belong to the upper part of the Internispinosum or lower part of the Alternans zones, thus suggesting a slightly older age for *C. lotenoense* in comparison to *C. mendozanum*, which is well-located in the

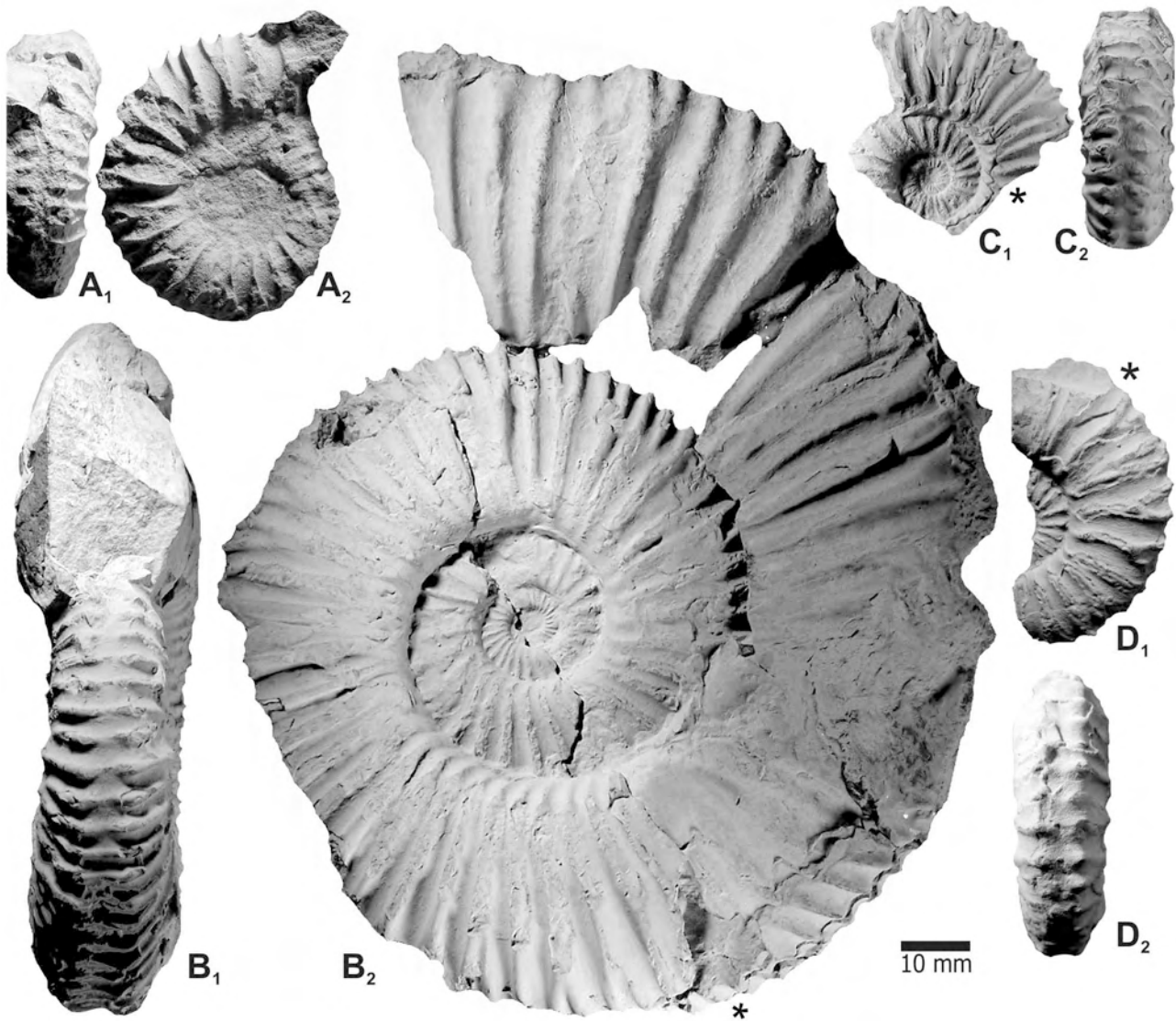


Figure 33. **A:** *Corongoceras?* sp. A, complete adult microconch (MCNAM 24431), A. Cieneguita, bed AC-8 (Proximus Z.). **B-D:** *Corongoceras mendozanum* (Behrendsen), A. Cieneguita, Alternans Z.; **B:** almost complete adult macroconch (MCNAM 24457/1), bed AC-14. **C:** juvenil macroconch with a quarter whorl of bodychamber (MCNAM 24459/7), bed AC-15. **D:** macroconch (MCNAM 24459/2) with beginning of the bodychamber, bed AC-15. All natural size. Asterisks indicate the last septum.

Alternans Zone. Leanza (1980: pl. 6: 6) figured a specimen from the Internispinosum Z. of Cerro Lotena as *C. lotenense*, which differs clearly from the HT of this species and from the present material of *C. mendozanum* in being more evolute with a rounded-depressed whorl section and a stronger prorsiradiate ribbing in the inner whorls. The venter of the outermost whorl is very similar to the inner whorls of *C. mendozanum* (see Fig. 34C-D). For morphotypical reasons this specimen could be assigned to *C. ?filicostatum*.

The monotypic HT of *Berriasella* (*Corongoceras*) *submendozanum* Krantz, 1926 (1928: pl. 4: 6) is almost identical to the macroconch shown in Fig. 34F, a compressed variant with fine ribbing on the inner whorls. *B. (C.) duraznense* Krantz, 1926 is known by a single specimen from the Alternans Z. of A. Durazno, and differs only in having a wide and low, rounded whorl section (cf. Fig. 34G).

B. (Riasanites) rjasanenoides Krantz, 1926 shows the typical shell morphology and sculpture of the species, with moderately dense ribbed inner whorls, as in the specimen shown in Fig. 34F. However, the rounded venter with uninterrupted ribs is a difference hard to evaluate since it is

not observed in any of the studied specimens. Nevertheless, Krantz (1928: 25-26) indicated that in the inner mould the ribs are depressed and form a groove.

The specimen figured by Leanza (1945: pl. 3: 7-8) as *Aulacosphinctes* sp. indet., although small, can be confidently attributed to the species. Indeed, the compressed subrectangular whorl section, higher than wide, the strong acute primary ribs divided on a small tubercle on the upper half of the flanks, and the ventral ribs ending on small bullae aside a well marked groove conform a typical *C. mendozanum*. On the other hand, the whorl section higher than wide and the tubercles on the point of furcation exclude this specimen from *Aulacosphinctes*.

Corongoceras involutum Biró, 1980, from the Alternans Z. of Chile, shows a shape and sculpture very similar to the compressed specimens of *C. mendozanum* (e.g. Fig. 34F). The ventral sculpture of one of the paratypes (Biró 1980: pl. 7: 9) on which the ventral rows of tubercles are very closely spaced bounding a ventral groove, matches the specimens in Fig. 33C-D. The HT (Biró 1980: pl. 7: 7) is very similar to the specimen of *Corongoceras?* sp. A (Fig.

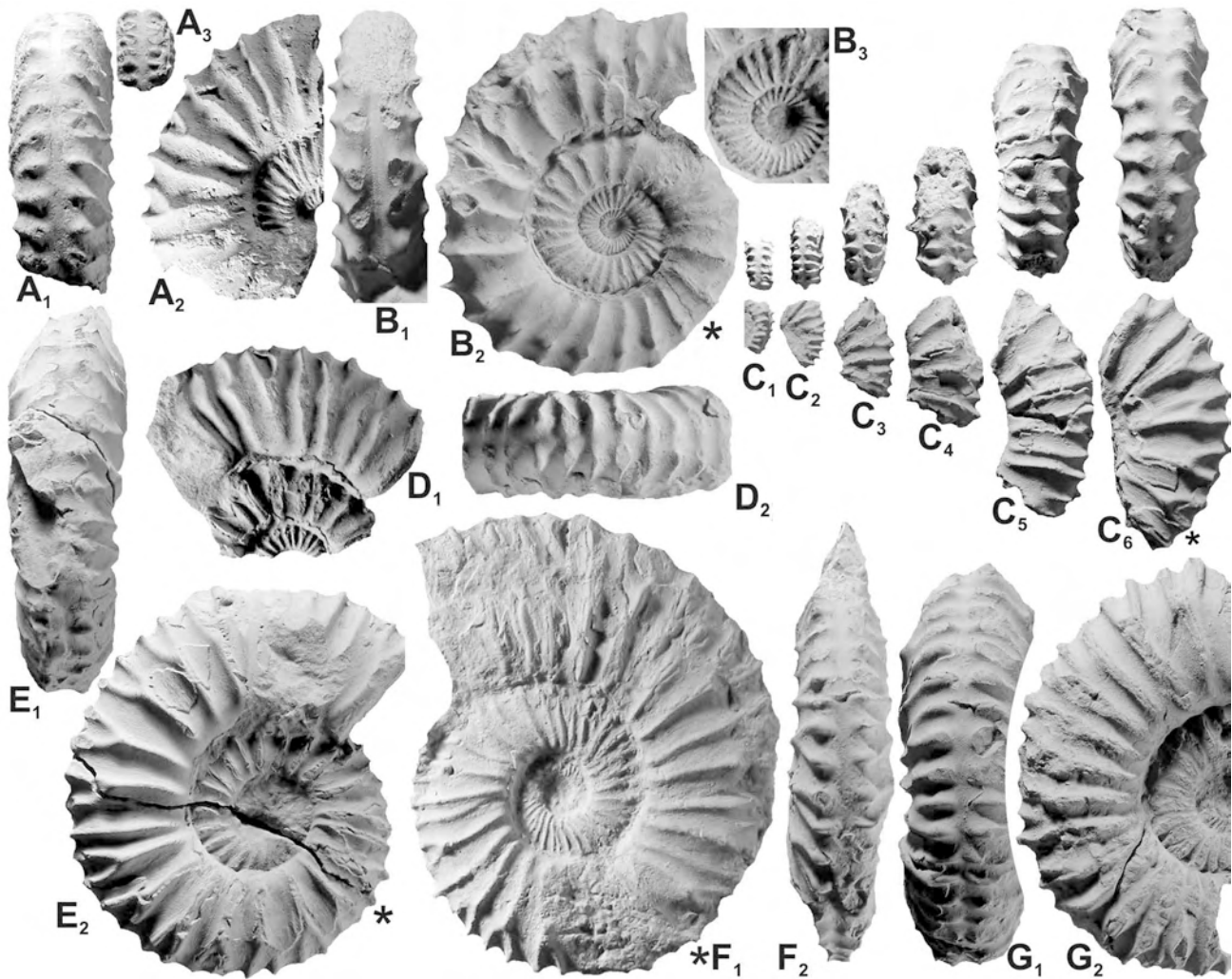


Figure 34. *Corongoceras mendozanum* (Behrendsen). **A.** Cieneguita, beds AC-14 and AC-15 (Alternans Zone). **A₁**: incomplete ?macroconch phragmocone (MCNAM 24459); **A₂**: detail of the venter of the penultimate whorl. **B:** complete adult macroconch with lappets (MCNAM 24458/1); **B₂**: detail of the innermost whorls (x2). **C:** juvenil macroconch dissected for showing the ontogeny in ventral (upper row) and corresponding lateral (lower row) views (MCNAM 24459/24) at about $D = 8-10$ mm (**C₁**), $D = 13$ mm (**C₂**), $D = 20$ mm (**C₃**), $D = 25$ mm (**C₄**), $D = 35$ mm (**C₅**) and $D = 41$ mm (**C₆**, bodychamber). **D:** adult macroconch with lappets (MCNAM 24459/11). **E:** macroconch with incomplete bodychamber (MCNAM 24459/2). **F:** adult macroconch with incomplete bodychamber (MCNAM 24459/4), compressed variant. **G:** macroconch phragmocone with incomplete bodychamber (MCNAM 24459/2), stout variant. All natural size except **E₃** (x2). All natural size (x1) otherwise indicated. Asterisk indicating the last septum.

33A) in size, shape and sculpture, differing in the ventral aspect which shows prominent lamellar tubercles on the ventrolateral shoulder. Thus, *C. involutum* could be an early transient of *C. mendozanum*.

Occurrence and distribution.- The material described comes from beds AC-14 and AC-15, *vetustum* horizon, Alternans Z. The HT of the species comes from an unknown horizon at Rodeo Viejo; our material includes a large macroconch (Fig. 33B) which, at comparable diameter, is almost identical, suggesting the HT might come from beds of very similar age of that of beds AC-14-AC-15. Other localities: Arroyo del Yeso (Leanza 1945), Arroyo Durazno (Gerth 1925) and Casa Pincheira (Krantz 1928, Parent 2003a).

***Corongoceras? steinmanni* (Krantz, 1926)**

Fig. 35, App. 1

1926 *Berriasella Steinmanni* Krantz.- Krantz: 439, pl. 14: 3-4 [LT designated herein].

1928 *Berriasella steinmanni* n. sp.- Krantz: 22, pl. 1: 3 [LT refigured].

Material.- A single adult macroconch specimen with the bodychamber incomplete (MCNAM 24457/A) from bed AC-14 (Alternans Z.).

Description.- Innermost whorls wide and depressed, involute, finely and densely ribbed, the ventral ribbing evenly spaced and not interrupted on the venter. From about $D = 10$ mm the shell is more evolute. The lateral ribbing is strong and acute with strong constrictions; the ventral ribs, evenly spaced are interrupted besides a narrow groove. From about $D = 30$ mm the whorl section is suboval, slightly higher than wide with a flat venter. The ribbing is less prosocline, slightly curved forward; most primary ribs bifurcate on the upper third of the flank in equally strong secondaries which reach the ventrolateral shoulder slightly raised and becoming weaker towards the middle of the venter where they fade off aside a moderately wide ventral groove. Through $D = 70$ to 90 mm most ventral ribs have a

rounded or sometimes lamellar tubercle located near the ventrolateral shoulder and then continue without interruption on the venter. The bodychamber begins at $D = 93$ mm; the short portion preserved is strongly uncoiled and does not show changes in sculpture beyond the lost of the ventral tubercles.

Remarks.- *B. steinmanni*, from Arroyo de la Manga (most likely Alternans Z.), was based on at least two specimens without designation of a type specimen. The specimen figured by Krantz (1928: pl. 1: 3) is herein designated as the lectotype. This species seems to be very scarce and had never been cited after its original description. The present specimen is very similar in shell shape and sculpture, including the conspicuous short stage of bituberculate venter at the end of the adult phragmocone, then vanishing on the bodychamber. The drawing of the LT (Krantz 1928: pl. 1: 3) shows some pairs of secondary ribs looped on the ventrolateral ending on the tubercle, but not in the present specimen. The secondary ribs looped on a ventrolateral, rounded tubercle (spine on the shell) are known in *Steueria* n. gen. (described below) and rarely in *Wichmanniceras mirum* Leanza, 1945.

The inner and the outermost whorls are very similar to those of *C. mendozanum* (cf. Figs. 34C and 35B respectively).

Genus *Micracanthoceras* Spath, 1925

Type species: *Ammonites microcanthus* Oppel in Zittel, 1868; by OD.

Remarks.- Following Donovan et al. (1981) we consider that *Micracanthoceras* included a group of macroconchs whose corresponding microconchs are commonly placed in *Aulacosphinctes* Uhlig, 1910 (type species: *Ammonites moerikeanus* Oppel, 1863).

Micracanthoceras sp. A

Fig. 29E

Material.- A single, well-preserved specimen (MCNAM 24418/4), bed AC-9 (Internispinosum Z.).

Description and remarks.- The specimen consists of a complete phragmocone ($D_{is} = 33$ mm) with half a whorl of the bodychamber. Evolute serpentine coiling throughout its ontogeny, widely umbilicate with a suboval whorl section, slightly wider than high. Phragmocone: lateral ribbing coarse, subradial (prosocline in the innermost whorl visible at about $D = 5$ mm) with one each two primaries bifurcate on the upper part of the flank. In the last two whorls the point of furcation is raised as a small tubercle. Bodychamber: lateral ribbing is similar at the beginning (the swellings at the point of furcation are well marked in the form of lamellar tubercle), the ventral ribbing is raised on a small tubercle and fades out aside a narrow ventral groove. The last quarter of whorl of the bodychamber is slightly uncoiled; the ribbing remains unchanged except that the tubercles fade out and the ventral ribs cross the venter unchanged, so that the venter is only slightly depressed without forming a groove. The peristome seems to be not preserved, however, the last rib is curved forward with a medial projection which could indicate the base of a lappet. In this case the specimen was considered representing an adult microconch.

Remarks and comparison.- The generic assignment is difficult because the specimen is a microconch or an incomplete or juvenile macroconch. It differs from the early *W. internispinosum* described above in a different ribbing, and the tiny ventral tubercles which are unknown in *Windhauseniceras*. The occurrence of mid-ventral rows of minute tubercles leads to comparison with *C. ? steinmanni* but, although the inner whorls are similar, the ventral tubercles are different and occur at different sizes. However, they could belong to the same genus, representing different sexual dimorphs or, well, different species of different ages. But for the time being the scarce material does not allow advancing closer identifications.

The specimen from Arroyo Loncoche (level Loncoche-I) figured by Steuer (1921: pl. 7: 3-4) as *Reineckeia microcantha* (Oppel) matches perfectly with the described specimen, showing the same serpentine shell shape with strong lateral ribbing forming a tubercle on the upper flank and two closely spaced rows of minute tubercles on the venter. The stratigraphic position of the level Loncoche-I seems to be in the lower Upper Tithonian.

Assignment to *Micracanthoceras* is based on the overall shape of the shell and the sculpture formed by an alternation of simple, undivided primary ribs with others divided on the upper flank forming a tubercle. In this sense it compares very closely with some Tethyan morphotypes of *M. microcanthum* from Sierra Gorda, Spain (e.g. Tavera 1985: pl. 22: 3-5; note the specimen in fig. 3 which shows the minute tubercles on the venter). *Micracanthoceras* and *Aulacosphinctes* are typical of the Microcanthum Z in the western Tethys. Tavera (1985: pl. 22: 2) figured a lappeted microconch which strongly resembles the present specimen which could likely be a microconch. The resemblance of the present specimen with those Spanish specimens seems enough for a specific assignment, but we have only a single specimen and, on the other hand, the difference in age may be important (see chapter on biostratigraphy below).

Genus *Himalayites* Uhlig in Boehm, 1904

Type species.- *Himalayites treubi* Boehm, 1904; by SD R. Douvillé 1912.

Himalayites? cf. *andinus* Leanza, 1975

Figs. 29H

Material.- A fragmentary specimen (MCNAM 24465), loose from bed AC-18.

Description and remarks.- The specimen seems to consist of a portion of bodychamber with remains of the last whorl of the phragmocone. The whorl section is compressed subrectangular, with high flanks and rounded venter. The fragment shows a change of ribbing which is at first composed by acute primaries bi- or trifurcate on the mid-flank, turning to a tuberculate stage. From a stout tubercle placed close to the umbilical shoulder, merge about five secondary ribs which cross the venter evenly spaced and without changes in strength. Strong narrow constrictions occur associated with the tubercles. The preceding whorl shows a dense lateral ribbing close to the umbilical seam of the subsequent whorl.

The compressed whorl section with stout lateral tubercles, from which several secondaries branch, and the moderately dense ribbed venter are the diagnostic features of *Himalayites*, especially of *H. treubi* (see Arkell et al.

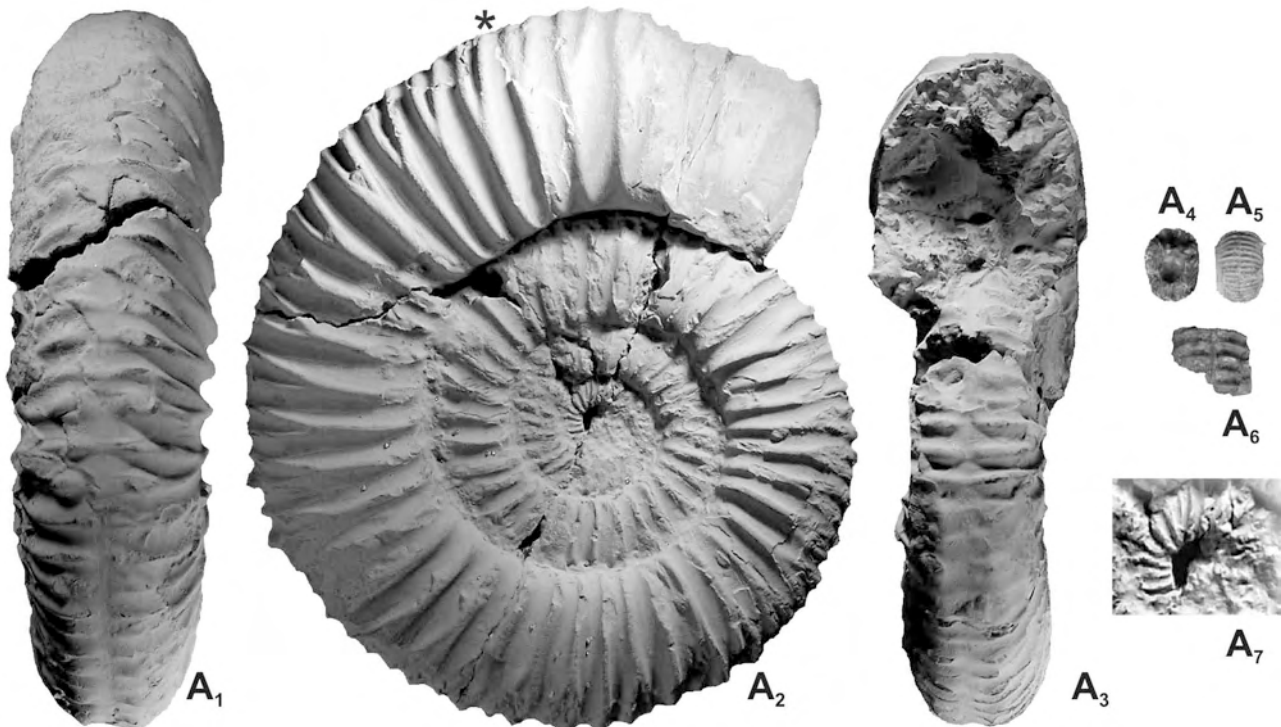


Figure 35. *Corongoceras? steinmanni* (Krantz), adult macroconch phragmocone with beginning of the bodychamber (MCNAM 24457/A), A. Cieneguita, bed AC-14 (Alternans Z.); **A₁-A₃**: apertural and ventral views (x2) of the innermost whorls at $D = 5$ mm; **A₄-A₇**: ventral and lateral views (x2) of inner whorls at $D = 13$ mm. All natural size otherwise indicated. Asterisk indicating the last septum.

1957: fig. 468, 5) and *H. ventricosus* Uhlig (1910: pl. 38: 4).

H. andinus from the upper Tithonian of Mallín Quemado is similar at a larger size when the lower row of lateral tubercles appear (Leanza 1975: fig. 3b, paratype). Assignment to *Himalayites* is doubtful for the configuration of the sculpture which has small ventral tubercles, similar to *S. alternans*, and the lateral ones are small.

Family Aspidoceratidae Zittel, 1895
Subfamily Aspidoceratinae Zittel, 1895

Genus Aspidoceras Zittel, 1868

Type species: Ammonites rogoznicensis Zejsner, 1846; by monotypy.

***Aspidoceras cf. euomphalum* Steuer, 1897**
 Figs. 36A-C

Synonymy. - See Parent et al. (2007).

Description. - As typical for aspidoceratids, complete and/or well-preserved specimens are very scarce or almost impossible to extract from the limestones and marls. Despite of this situation, we have composed an ensemble of fresh fragmentary specimens which allow to associate most material from beds AC-7-AC-11 with the species described from samples of the lower part of the Internispinosum Z. of Barda Negra in Parent et al. (2007).

The best preserved specimen is a small phragmocone (Fig. 36C) with the test preserved. Max $D = 38$ mm, globose, narrowly umbilicate, depressed with widely rounded and smooth venter. On the flanks there are two rows of tubercles; the periumbilical ones are small with a subcircular base. The lateral ones are stout, each of them forms the base of a

hollow, long spatulate spine.

The portions of a bodychamber shown in Fig. 36A-B are rather typical for this species: whorl section wider than high with a widely rounded venter covered with wide ribs. Lateral and periumbilical tubercles are connected by a short rib, most of them radially elongate (bullae sensu Arkell 1957) or less frequently with a subcircular base. All these tubercles are the bases on the internal moulds of hollow spines of the test (Fig. 36A).

Fragments of large bodychambers (bed AC-7) show two rows of unconnected, rounded tubercles; one of them on the umbilical shoulder and the second one on the upper flank; the part of the flank between the rows is flat. The adult macroconch size is estimated to 500-600 mm.

From bed AC-15 (partially equivalent with the level Cieneguita-III of Steuer 1921) was collected a crushed portion of a macroconch phragmocone (MCNAM 24459/9), about $D = 150$ mm, which is directly comparable with the LT of *E. euomphalum*. This specimen differs from the material described above from beds AC-7 – AC-11 in that its venter shows no ribs but only growth lines like the LT.

Remarks. - *A. euomphalum* was recently revised and the LT refigured photographically (Parent et al. 2007: fig. 8). The material from Barda Negra described in that paper seems conspecific with the herein described, which was collected from the upper Proximus to Internispinosum zones. Therefore it is somewhat older than the horizon of the LT which comes from the Alternans-Koeneni zones. There are no doubts that the present material from beds AC-7-AC-11 belongs to a different transient morphologically distinguishable from the LT. With more and better preserved material a separation at the specific level seems possible.

Aspidoceras cieneguitense Steuer, 1897 was based on a single specimen from the level Cieneguita-II of AC, herein

refigured in Fig. 38B for comparison. It differs from *A. cf. euomphalum* in a more evolute coiling at comparable sizes (cf. Figs. 36C and 38B).

Occurrence and distribution.- Upper Proximus to (lower) Internispinosum zones throughout the NMB: Barda Negra (Parent et al. 2007), Cerro Lotena (Leanza 1980: pl. 8: 1), Los Catutos (Leanza & Zeiss 1990: pl. 36: 3), Pampa Tril, and AC.

Genus *Physodoceras* Hyatt, 1900

Type species.- *Ammonites circumspinosus* Oppel, 1863 (= *Ammonites circumspinosus* Quenstedt, 1849); by OD.
Late Oxfordian-early Kimmeridgian.

Remarks.- Steuer (1897, 1921: pl. 6: 5) figured a complete adult [M] with peristome from AC, level Cieneguita-I, as *Aspidoceras cyclotum* Oppel, a subjective synonym of *Physodoceras neoburgense* (Oppel). This specimen (refigured herein in Fig. 38A) is identical to another [M] which we have collected in the upper Zitteli Z. of C. Granito, associated with *P. zitteli*, *Physodoceras* sp. [m], *Cieneguiticeras perlaevis* [m] and very large macroconchs of *Choicensiphinctes* (PSSE 2008: 24, level 3), among other ammonites under study.

Physodoceras sp. A in Parent, Garrido, Schweigert & Scherzinger (2011)

Figs. 37E

Description and remarks.- A small specimen (MCNAM 24406/1), from bed AC-8 (Proximus Z.). It is apparently a juvenile macroconch with a portion of the bodychamber. The shell is compressed and involute, narrowly umbilicated with a narrow and well-rounded venter. The phragmocone is slightly higher than wide, turning on the bodychamber to high-whorled, much higher than wide, with gently rounded umbilical shoulders. At least from $D = 5$ mm the shell is almost smooth, only faint growth lines occur on the flanks.

The present specimen is identical with the material from the *perlaevis* hz. of Picún Leufú described in PGSS (2011: fig. 32C).

Aspidoceras aff. *haynaldi* Herbich (in Steuer 1921: pl. 5: 11; herein refigured in App. 2-I), from the level Cieneguita-II, belongs to the genus *Physodoceras* as indicated by the sculpture ontogeny consisting of small lateral tubercles on the inner whorls, lateral and periumbilical on the outer whorls, and the lateral ones vanishing at the end of the phragmocone or beginning of the bodychamber. This specimen, from a similar stratigraphic position in the section, differs from *Physodoceras* sp. A by possessing tubercles from the inner whorls and by being much more inflates and evolute at similar diameters.

Genus *Toulisphinctes* Sapunov, 1979

Type species.- *Toulisphinctes zieglerei* Sapunov, 1979; by OD.

Toulisphinctes cf. *rafaeli* (Oppel, 1863)

Fig. 36D-E

Material.- Two poorly preserved phragmocones (MCNAM 24418/1) from bed AC-8 and material recorded in the field form bed AC-7, Proximus Z.

Description and remarks.- The phragmocone is rather

involute, the whorl section is suboval depressed, slightly wider than high; a row of periumbilical tubercles from which a strong primary rib arise, with two intercalary ribs crossing the venter.

The largest specimen observed (photograph taken in the field shown in Fig. 36E) represents the last portion of the phragmocone and a part of the bodychamber of an adult [M]. Its diameter was probably 300 mm at the beginning of the bodychamber. The whorl section is subrectangular, with flat flanks and rounded venter. There are two rows of tubercles: the periumbilical ones situated on the umbilical shoulders, unevenly spaced, with rounded bases and connected with the lateral tubercles; the lateral ones are situated on the mid-flank; they are unevenly spaced and mostly correspond with the periumbilicals. They have a bullate aspect and are connected with the periumbilicals by a more or less marked rib which persists up to the venter. Intercalary ribs are abundant, especially between the more widely spaced tubercles.

Morphologically, this lineage appears quite conservative. The specimen shown in Fig. 36D is almost indistinguishable from the late Kimmeridgian *Toulisphinctes garibaldii* (Gemmellaro, 1868), e.g. Schlegelmilch (1992: pl. 71: 1) and another specimen from Swabia in the collections of the Staatliches Museum für Naturkunde (Stuttgart).

Toulisphinctes? sp. A [m]

Fig. 37D

Description.- Inner whorls at $D = 7-12$ mm are evolute and depressed with low flanks and widely rounded venter. On the umbilical shoulder densely spaced bullae occur which are directed both forwardly and towards the umbilicus. The bodychamber begins at $D = 26$ mm and expands three quarters of a whorl (but is incomplete) and is moderately uncoiled on the last part. The whorl section is suboval, depressed, with a flat venter. The sculpture consists of dense primary ribs which link three rows of tubercles: (1) on the almost undefined umbilical shoulder, very small and faint, (2) on the upper part of the flanks, and (3) on the ventrolateral shoulder. Some few primaries bifurcate on one of the lateral tubercles on the upper half of the flank, and the secondaries end on tubercles as the simple ribs. On the venter the ribs are very weak and become interrupted thus forming a wide smooth band. The last third part of the bodychamber is smooth.

Remarks.- This ammonite is very similar to specimens described as *Simocoscoceras simum* (Oppel), *S. adversum* (Oppel) or *S. catulloi* (Zittel) –e.g., Kutek & Wierzbowski (1986: pl. 2: 4-10), Fözy et al. (1994: pl. 2: 4-5, 8-9), or Schweigert (1997: pl. 1: 2). However, there are important differences: (1) our specimen is two or three times larger, and (2) the inner whorls are different. The differences in adult size are not to be considered, for there may be less important considering that the expression of sexual dimorphism can widely differ in different environments or latitudes. However, the inner whorls are widely depressed, globose, with a smooth venter and acute flanks with periumbilical tubercles different from those in *Simocoscoceras*. The latter genus is a group of microconchs related to *Pseudhimalayites*.

The specimen is a microconchiate aspidoceratid. The [m] of *P. subpretiosus* is a different ammonite described above, so that it could be the dimorph of any of the other

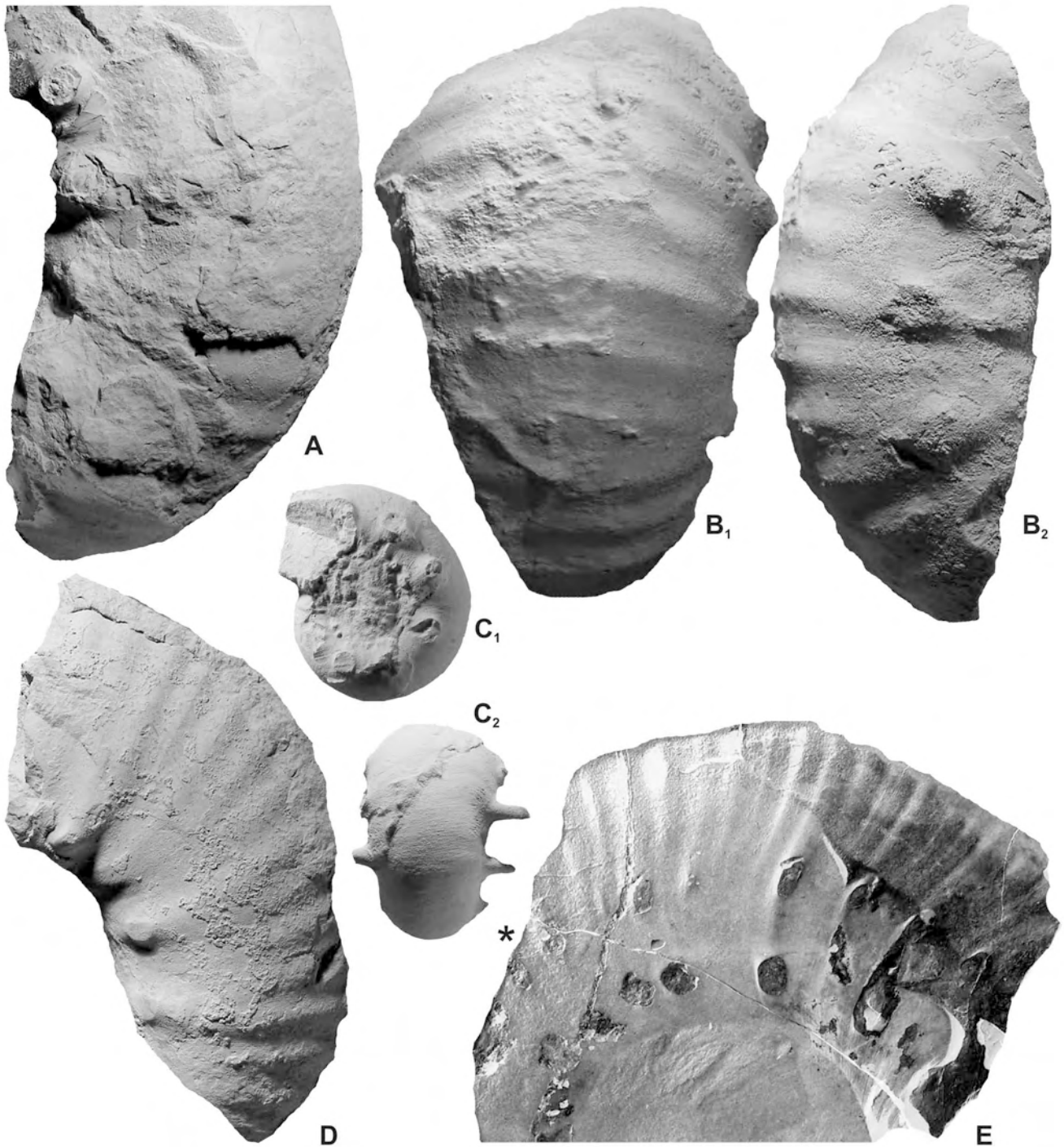


Figure 36. **A-C:** *Aspidoceras* cf. *euomphalum* Steuer, A. Cieneguita; **A:** portion of macroconch bodychamber (MCNAM 24424), bed AC-7 (Proximus Z., falculatum Hz.) with test preserved showing the tubercles of internal mold below hollow spines with subcircular base; **B:** portion of macroconch bodychamber (MCNAM 24415/7), bed AC-7; **C:** juvenil macroconch phragmocone (MCNAM 24456/2), bed AC-11 (Internispinosum Z.) with test preserved showing the tubercles of internal mold below long spatulate, hollow spines with subcircular base. **D-E:** *Toulisphinctes* cf. *rafaeli* (Oppel), A. Cieneguita; **D:** portion of macroconch phragmocone (MCNAM 24418/1), bed AC-8 (Proximus Z.); **E:** adult macroconch bodychamber with terminal portion of phragmocone (negative field-photograph of a cast not collected, x0.5), bed AC-7. All natural size otherwise indicated. Asterisks at last septum.

aspidoceratids which occur in the same bed AC-7: *Aspidoceras* (*A.* cf. *euomphalum*), or *Toulisphinctes* (*T.* cf. *rafaeli*). The early development of well-marked umbilical tubercles on acute flanks, like in the present specimen, is a morphological trait observed in the inner whorls of *Toulisphinctes* (see Schweigert 1997), to which could likely belong the present specimen.

Genus *Pseudhimalayites* Spath, 1925

Type species.- *Aspidoceras steinmanni* Haupt, 1907
(= *Cosmoceras subpretiosum* Uhlig, 1878);
by OD; Middle Tithonian.

Remarks.- The genus has been recently revised by Schweigert (1997) who presented a succession of species which clearly conform a lineage ranging from the Oxfordian

to the Tithonian.

***Pseudhimalayites subpretiosus* (Uhlig, 1878)**

Fig. 37A-C

Synonymy.- See Parent (2001).

Material.- Three adult [M] (MCNAM 24420/5, 24421, 24426) and one [m] (MCNAM 24420/1), bed AC-7.

Description.- Macroconchs: Evolute and depressed during the whole ontogeny. Inner whorls at $D = 15-25$ mm rounded to subpolygonal in whorl section (nude of sculpture is suboval slightly wider than high with flat venter). Sculpture composed by three rows of tubercles and primary ribs which link the three tubercles and cross the venter. The faint umbilical tubercles are incipiently developed from $D = 15$ mm, presented as swellings just above the umbilical shoulder; the lateral ones are well-developed, located close to the ventrolateral shoulder; and the ventral ones have the shape of well-marked bullae. In the last whorl of the phragmocone ($D = 25-60$ mm) the whorl section becomes subrectangular, more or less rounded. All tubercles are strong and well-developed, the ventral ones are lamellar, elongate transverse to the venter, well separated from each other by a smooth band; on the flanks the umbilical and ventrolateral tubercles are rounded, and are the bases of long spatulate spines. The bodychamber is partially preserved in one specimen (Fig. 37B), showing a wider than high whorl section; the ventral tubercles fade away and the ventral ribs are somewhat weak close to the end of the phragmocone, whereas the tubercles on the flanks remain well developed.

Microconch: The inner whorls at $D = 6-11$ mm are globose with wide umbilicus, low flanks and widely rounded, smooth venter. On the flanks occurs a row of densely distributed tubercles. Later, from about $D = 15$ mm, a row of faint, incipient umbilical tubercles and a row of ventrolateral spiniform tubercles appear. At $D = 22$ mm the adult bodychamber begins which expands less than a half whorl ($L_{bc} = 160^\circ$) and is strongly uncoiled near the peristome. It is suboval in whorl section with flat venter. The trituberculation persists up to the peristome with faint, falcate ribs linking the three rows. The peristome bears a pair of long straight lappets.

Remarks.- The LT of *P. steinmanni* has the inner whorls closely comparable with the HT of *Pseudhimalayites subpretiosus*, which is a small, incomplete specimen (Schweigert 1997: pl. 1: 4). The adult macroconch in Fig. 37A is shown dissected for exhibiting the inner whorls at the same size. The similarity is complete giving strong support to the conespecificity.

Occurrence and distribution.- The palaeobiogeographic distribution in the Tethys and in America was recently discussed (Schweigert 1997, Parent 2001). The vertical range in the NMB is now better known, longer than previously assumed, at least from the upper Zitteli up to the upper Proximus zones, and in Pampa Tril and Cerro Lotena it has been recorded even in the lower Internispinosum Z.

Superfamily Haploceratoidea Zittel, 1884

Family Haploceratidae Zittel, 1884

Genus *Pseudolissoceras* Spath, 1925

Type species.- *Neumayria zitteli* Burckhardt, 1903; by SD Roman, 1938. Middle Tithonian.

***Pseudolissoceras zitteli* (Burckhardt, 1903)**

Figs. 39B

Synonymy.- See Leanza (1980), Parent (2001) and recent additions in PGSS (2011).

Material.- An adult macroconch (MCNAM 24375) and several juvenile or incomplete specimens from beds AC-4-AC-5 and fragments from the lower part of bed AC-6.

Remarks.- The largest specimen (Fig. 39B), from bed AC-4, is an adult macroconch with the bodychamber incomplete. From the last whorl of the phragmocone the umbilical shoulder is acute and the umbilical wall flat and inclined. In the few specimens from bed AC-5 the umbilical shoulder and wall are rounded.

The species occurs throughout the NMB. Its stratigraphic range defines the total range of the *Zitteli* Bz.

Family Oppediidae H. Douvillé, 1890

Subfamily Taramelliceratinae Spath, 1928

Genus *Cieneguiticeras* Parent, Myczinski, Scherzinger & Schweigert, 2010

Type species.- *Haploceras falcatum* Steuer, 1897; by OD. Middle Tithonian.

***Cieneguiticeras perlaevis* (Steuer, 1897)**

Figs. 39G-H

Synonymy.- See PMSS (2010: 457).

Material.- A sample of crushed specimens (MCNAM 24370/2) in a single concretion from bed AC-2 including a fragmentary adult macroconch and four microconchs; a juvenile macroconch (MCNAM 24377) from bed AC-5, and fragments from bed AC-4.

Remarks.- The new material is easily comparable with the specimens from the Picunleufuense Z. of Picún Leufú described in PGSS (2011: fig. 35). The lectotype of the species comes from the level Cieneguita-I of Steuer (1921) which approximately corresponds to our set of beds AC-2 - AC-6. This assumption indicates that the species has a vertical range from the earliest Picunleufuense Z. (*picunleufuense* α horizon) to the most part of the *Zitteli* Z., bed AC-5 (specimen in Fig. 39G).

Occurrence and distribution.- Beds AC-2-AC-5, Picunleufuense to *Zitteli* zones. See also PMSS (2010).

***Cieneguiticeras falcatum* (Steuer, 1897)**

Fig. 39I-N

Synonymy.- See PMSS (2010: 459).

Material.- Several [M] and [m] specimens from bed AC-7: MCNAM 24404/1-15, 24405/1-7, 24406/1-7, 24407/1-11, 24410/1-3, 24421-24441.

Remarks.- The species was fully described in PMSS (2010) considering the type material of the species and abundant material from bed AC-7, including the present specimens. Some additional specimens are figured herein for illustrating the variability in the sculpture of the

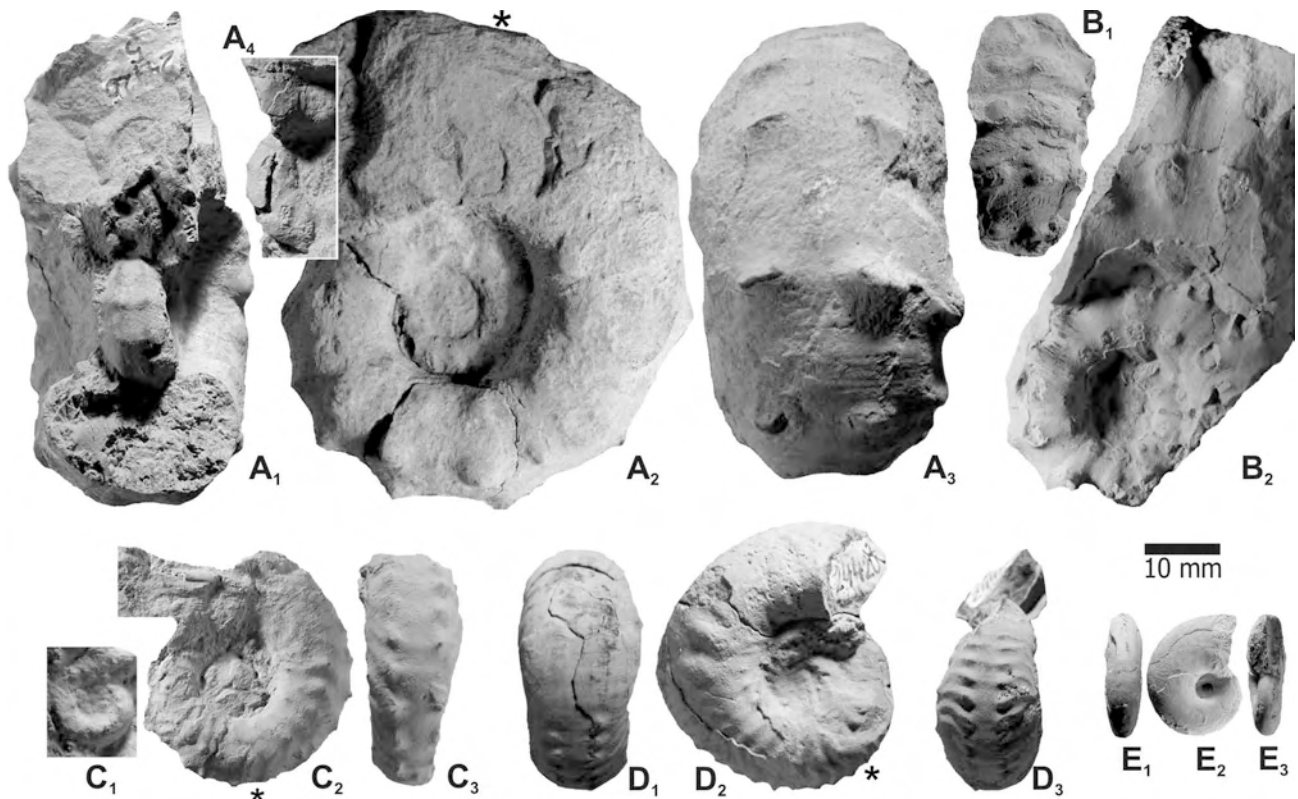


Figure 37. A-C: *Pseudhimalayites subpretiosus* (Uhlig), A. Cieneguita, bed AC-7 (Proximus Z., *falculatum* hz.). A: adult macroconch with beginning of bodychamber (MCNAM 24420/5); A₁: half whorl removed showing inner whorls, A₂-A₃: lateral and ventral views, A₄: lateral view of inner whorls shown in A₁. B: adult macroconch with a portion of bodychamber (MCNAM 24426), B₁: ventral view of the last whorl of the phragmocone. C: complete adult microconch with lappets (MCNAM 24420/1); C₁: inner whorls seen from the opposite side shown in C₂. D: *Toulisphinctes?* sp. A, adult microconch with almost complete bodychamber (MCNAM 24428) showing a marked asymmetry on the bodychamber (pathologic), bed AC-7. E: *Physodoceras* sp. A, phragmocone with part of the bodychamber (MCNAM 24406/1), A. Cieneguita, bed AC-8 (Proximus Z.). All natural size. Asterisk at last septum.

macroconchs which may be strong (Fig. 39I, N; see also Parent et al. 2010: fig. 5E) or weaker (Fig. 39J) from its onset on the adult phragmocone. The microconchs are also variable in expression of the lateral sculpture (Fig. 39K-M). However, the adult size seems to be rather constant.

All the specimens come from bed AC-7 which can be considered the type horizon of the species, partly equivalent to the level Cieneguita-II of Steuer (1921). This assumption is based on the fact that after detailed collection in the type locality we have found very abundant macro- and microconchs of *C. falculatum* confined to the bed AC-7, including some specimens identical in size and morphology to the LT. Upwards in the section, in bed AC-8 a small specimen was collected which is more compressed and suboxycone than typical macroconchs of *C. falculatum*. In addition, it shows well-marked ventrolateral lunuloid ribs from about $D=20$ mm. This specimen was described as *C. cf. falculatum* (PMSS 2010: fig. 5F), awaiting more material from this bed.

Occurrence and distribution.- In AC the species is confined to the *falculatum* hz., Proximus Z. but a cf.-specimen from bed AC-8 is the youngest known record. In Pampa Tril we have recently collected some specimens which can not be assigned to the present species, they come from a bed with an abundant fauna which suggests an age of the uppermost Proximus or lowermost Internispinosum zones. In Cerro Lotena, a well-preserved specimen co-occurs with ammonites which could be equivalent to, or later than the *falculatum* hz. Material from Cañadón de los Alazanes was

described in Parent (2001: fig. 8A-C).

Cieneguiticeras? sp. A

Fig. 39F

Description and remarks.- A well-preserved, complete adult phragmocone with the beginning of the bodychamber showing incipient but marked uncoiling, from bed AC-5 (Zitteli Z.). The specimen is an involute and compressed opeliid, with a sharp umbilical shoulder and steep umbilical wall. Short prosocline primary ribs appear on the lower third of flank. The aspect of the umbilicus is similar to that in the microconchs of *Pasottia andina*, however, the ribbing is unknown in the [M] of *Pasottia* which are completely smooth throughout its ontogeny. On the other hand, the present specimen does not show the lateral sulcus with linguiform structures typical of *P. andina* [m].

Genus *Pasottia* Parent, Schweigert, Scherzinger & Enay, 2008

Type species.- *Pasottia andina* Parent, Schweigert, Scherzinger & Enay, 2008; by OD. Middle Tithonian.

Pasottia andina Parent, Schweigert, Scherzinger & Enay, 2008

Fig. 39A

Remarks.- An incomplete adult [M] phragmocone, typical specimen collected in bed AC-4, rather the same



Figure 38. A: *Physodoceras neoburgense* (Oppel), complete adult macroconch with peristome (GZG-499-17), A. Cieneguita, level Cieneguita-I, refigured from Steuer (1921: pl. 6: 5). **B:** *Aspidoceras cieneguitiense* Steuer, holotype by monotypy, macroconch phragmocone (GZG-499-14), A. Cieneguita, level Cieneguita-II, refigured from Steuer (1921: pl. 5: 8-9). All natural size. Asterisk indicating the last septum.

stratigraphic position than the type material from La Amarga (section Cerro Granito-I).

Genus *Parastreblites* Donze & Enay, 1961

Type species.- *Oppelia circumnodosa* Fontannes, 1879; by OD. Middle Tithonian.

***Parastreblites?* cf. *comahuensis* Leanza, 1980**
Fig. 39C

Material.- A single specimen (MCNAM 24399) from bed AC-4 (Zitteli Z.).

Description and remarks.- The specimen is an involute and moderately inflate phragmocone. Whorl section oval, higher than wide, with well-rounded venter. The last whorl preserved is practically smooth, only the last quarter is covered by an irregular ribbing composed of widely rounded, flexuous primaries which appear on the umbilical shoulder and become wider on the upper half of flank, then crossing the venter somewhat weakened. Some primaries divide indistinctly on the lower half of the flank. The specimen seems to be a juvenile because there is no indication of uncoiling.

This specimen is comparable with the smaller part visible in the holotype of *P.?* *comahuensis*, but they cannot be compared at similar sizes. The type species of *Parastreblites* and others described by Donze & Enay (1961) show a well-defined falcooid ribbing with the outer half of the primaries strong and lunuloid in shape on the phragmocone; the adult bodychamber usually becomes smooth. In contrast, the holotype of *P.?* *comahuensis*, a large phragmocone, shows only growth lines (Leanza 1980: 22) which describe a sigmoidal trajectory, and the upper half of

phragmocone is smooth. It is therefore somewhat doubtful if the Andean species actually belongs to the genus *Parastreblites*.

Subfamily Streblitinae Spath, 1925

Genus *Uhligites* Kilian, 1907

Type species.- *Streblites krafftii* Uhlig, 1903; by SD Roman, 1938.

***Uhligites?* sp. A**
Fig. 39E

Description and remarks.- A single specimen (MCNAM 24406/2) from bed AC-8. It consists of a small adult phragmocone with a quarter of a whorl belonging to the bodychamber which is clearly uncoiled. Compressed and involute with a rounded, grooved venter which suggests the provisory assignment to *Uhligites*.

Genus *Semiformiceras* Spath, 1925

Type species.- *Ammonites fallauxi* Oppel, 1865; by OD. Middle Tithonian.

***Semiformiceras?* sp. A**
Fig. 39D

Material.- A single specimen (MCNAM 24405) from bed AC-5.

Description and remarks.- The only specimen available is smaller but similar to the phragmocone of a *Semiformiceras*

semiforme (Oppel, 1865) figured by Cecca & Enay (1991: pl. 2: 18) from the Semiforme Z. of Le Pouzin, France.

BIOSTRATIGRAHY

In a typical section a zone or subzone spans a range of beds, only some of which are fossiliferous. In some cases, in which fossils are relatively abundant, different assemblages occur which are distinguishable in taxonomic composition and morphology from the overlying and underlying assemblages. This condition may be used for further subdivision of the stratigraphic scale below the subzonal level. This procedure should be based on the smallest faunal change detectable that is the closest stratigraphical levels that can be palaeontologically distinguished. A faunal horizon is a bed or series of beds, characterized by a fossil assemblage, within which no further stratigraphical differentiation of the fauna can be discerned. These horizons are defined or identified in a particular local section; later they can be recognized in other sections by means of the typical fossil assemblage or parts of it as seen in the TL. Moreover, within any pair of horizons can be inserted other new ones defined in other sections. These concepts and procedures, so adopted in this paper, have been fully discussed and applied by Gabilly (1971), Callomon (1985, 1995), Scherzinger & Schweigert (1999) and Schweigert (2007) among many others; further discussion and application to the Andean upper Callovian-Oxfordian have been worked out in Parent (2006). The adopted zonal subdivision of the Andean Tithonian is based on Leanza (1981a, b) and Parent et al. (2007); the Andean Berriasian was subdivided into two zones by Leanza (1945) what is followed herein.

Biostratigraphy of the studied section (Figs. 2, 40)

Picunleufuense (standard) Zone – Beds AC-1-AC-3.- This zone was defined in the section of Picún Leufú with its base marked at the *picunleufuense* α hz. (PGSS 2011: 95). This horizon becomes the standard base of the Andean Tithonian.

***picunleufuense* α hz. (bed AC-1):** *Lithacoceras picunleufuense* transient α , *Chicensisphinctes platyconus*, *Catutosphinctes guenenakenensis* and *Cieneguiticeras perlaevis* (impressions). This assemblage allows recognizing the lowermost horizon of the zone. There are few specimens well-preserved but the material is abundant, allowing to identify the diagnostic features.

Bed AC-2: *C. guenenakenensis* persists into this bed associated with *C. cf./aff. platyconus*, *Catutosphinctes cf. windhauseni* and *Cieneguiticeras perlaevis*. This assemblage is very similar to that of Picún Leufú which occurs between the *picunleufuense* β hz. and the *perlaevis* hz. (Zitteli Z.), and could correspond to the *marguense* hz. (see PGSS 2011: fig. 38), but it remains to be investigated.

Bed AC-3: The isolated occurrence of *C. cf. windhauseni* is not far informative biostratigraphically than to suggest the Picunleufuense Z. This assignment is based on the fact that the first occurrence of *P. zitteli* comes from the overlying bed AC-4, but remains tentative for *C. windhauseni* is a species which ranges in its TL (Cerro Granito) and in Cerro Lotena through the Picunleufuense Zone up to the lower beds of the Zitteli Zone.

Mendozanus/Zitteli zones – Beds AC-4-AC-5.- The beds AC-4 and AC-5 are assigned to the Mendozanus and/or Zitteli zones undifferentiated, since undoubted *P. zitteli* occurs along with ammonites which are closely comparable with those of the guide assemblage of the Mendozanus Z., preventing distinction of the zones. Overlapping of the ranges of the characteristic ammonites of these two zones was already recorded from Picún Leufú (and other localities) and described in PGSS (2011). The situation is faced again in AC, pending a solution from new collections in the type locality at Cajón del Burro-Río Choicas or another locality with a more detailed record and abundant material from these levels.

***perlaevis* hz. (bed AC-4):** *C. perlaevis*, *Pasottia andina*, *Parastrebitis? cf. comahuensis*, *Choicensisphinctes* n. sp. aff. *erinoides*, *C. cf. guenenakenensis* and *P. zitteli*. Within this assemblage the morphotypes of *C. perlaevis*, *P. andina* and *P. zitteli* are closely comparable with those described from the *perlaevis* hz. in Picún Leufú.

***cf.-erinoides* hz., new (bed AC-5):** This bed yields an interesting ammonite assemblage composed of *P. zitteli*, *Choicensisphinctes cf. erinoides*, *C. cf. limits*, *Cieneguiticeras? sp. A*, and *Semiformiceras? sp. A*. These ammonites are considered a distinctive assemblage for the introduction of the *cf.-erinoides* horizon.

Proximus Zone – Beds AC-6-AC-8.- Assignment of these beds to the Proximus Z. is suggested by the occurrence of *Catutosphinctes proximus*, including specimens almost identical to the LT. However the beds are sandwiched by beds with *P. zitteli* below and *Windhauseniceras internispinosum* above, which is the usual biostratigraphical criterium, as described by Leanza (1981a: 80), for recognition of the Proximus (non-standard) Zone.

Bed AC-6: In this bed occur two interesting species: *Lithacoceras* n. sp. aff. *picunleufuense* and *Mazatepites arredondense*, both of which persist into the next overlying bed.

***falculatum* hz., new (bed AC-7):** A rich and variable assemblage of ammonites (and gastropods) including *L.* n. sp. aff. *picunleufuense*, *M. arredondense*, *M. cf. arredondense*, *Cieneguiticeras falculatum*, *Choicensisphinctes* sp. A (Fig. 13B), *Catutosphinctes proximus* (long ranging), *Catutosphinctes* sp. A (Fig. 19E-F), *Platydiscus beresii* n. gen. et n. sp., *Pseudhimalayites subpretiosus*, *Physodoceras* sp. A, *Toulisphinctes cf. rafaelli*, *A. cf. euomphalum* and *Catutosphinctes cf. inflatus*. These ammonites are considered a significant assemblage for the introduction of the *falculatum* horizon. Some of these species range up into the overlying bed, but the horizon is restricted to bed AC-7; higher up, slight to moderate morphological changes are observable in most species.

Bed AC-8: The ammonites from this bed are poorly preserved: *C. cf. falculatum*, *C. proximus*, *Catutosphinctes* sp. A, *Corongoceras? sp. A*, *Platydiscus beresii* n. gen. et n. sp., *T. cf. rafaelli*, *A. cf. euomphalum*, *Uhligites? sp. A*, and *Mazatepites? sp. A*.

Internispinosum Zone – Beds AC-9-AC-13.- This zone is usually hard to recognize in the northern part of the NMB for the index-guide species *W. internispinosum* is very scarce, even not yet recorded in many localities. The best development of the zone is known in its TL, Cerro Lotena, where several meters of limestones and marls show a succession of morphotypes of the species associated with several other ammonites.

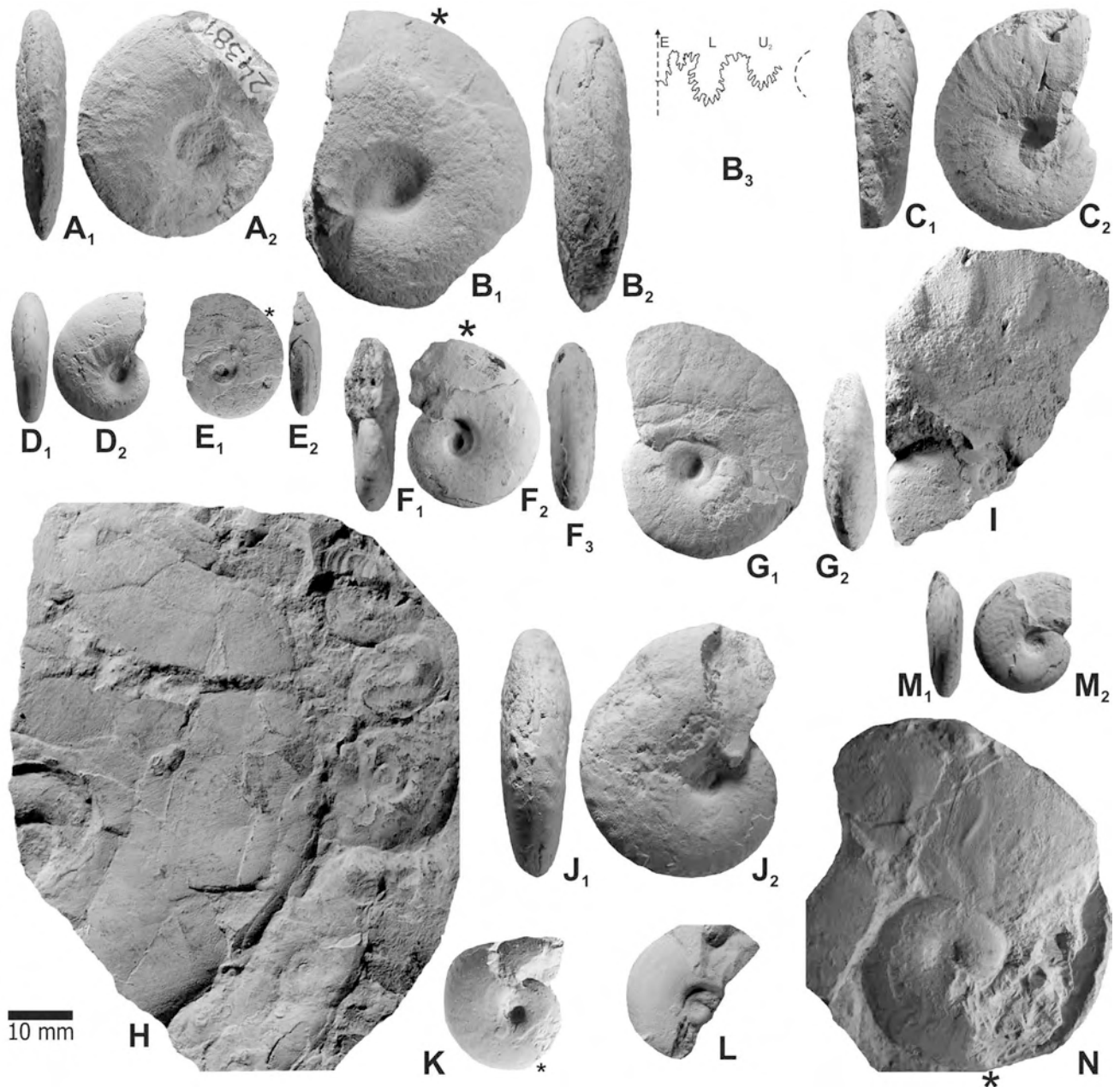


Figure 39. **A:** *Pasottia andina* Parent, Schweigert, Scherzinger & Enay, macroconch phragmocone (MCNAM 24381), bed AC-4 (Mendozanus-Zitteli zones). **B:** *Pseudolissoceras zittelli* (Burckhardt), adult macroconch with a portion of bodychamber (MCNAM 24375), bed AC-5 (Zitteli Zone); **B₃**: septal suture line(x1) at $D = 41$ mm. **C:** *Parastreblites?* cf. *comahuensis* Leanza, phragmocone (MCNAM 24399), bed AC-4 (Zitteli Zone). **D:** *Semiformiceras?* sp. A, phragmocone (MCNAM 24405), bed AC-5 (Zitteli Zone). **E:** *Uhligites?* sp. A, adult specimen with a quarter whorl bodychamber (MCNAM 24406/2), bed AC-8 (Proximus Zone). **F:** *Cieneguiticeras?* sp. A., apparently adult phragmocone with beginning of the bodychamber (MCNAM 24399/1), bed AC-5 (Zitteli Zone). **G-H:** *Cieneguiticeras perlaevis* (Steuer), A. Cieneguita; **G:** juvenil macroconch with beginning of bodychamber (MCNAM 24377), bed AC-5 (Zitteli Zone); **H:** adult macroconch and adult microconchs (MCNAM 24370/2) associated in a concretion with *Choicensisphinctes* cf./aff. *platyconus* (MCNAM 24370/1 in Fig. 6D), bed AC-2 (Picunleufuense Zone). **I-N:** *Cieneguiticeras falculatum* (Steuer), bed AC-7 (Proximus Zone, *falculatum* hz.); **I:** adult macroconch (MCNAM 24404/6); **J:** macroconch phragmocone (MCNAM 24405); **K:** adult microconch (MCNAM 24404/10); **L:** adult microconch (MCNAM 24404/7); **M:** adult microconch (MCNAM 24407/4) with most part of bodychamber; **N:** almost complete adult macroconch (MCNAM 24404/15). All specimens from Arroyo Cieneguita. All natural size. Asterisk indicating the last septum.

After extensive collection in A. Cieneguita we could find just two incomplete specimens of *W. internispinosum*, and one of which is used to mark the base of the zone. The lowermost occurrence of *W. internispinosum* is associated with a specimen classified as *Micracanthoceras* sp. A. Most of the ammonites which occur in beds AC-9-AC-11 range from the Proximus Z.: *C. proximus*, *A. cf. euomphalum*, *Catutosphinctes* cf. *inflatus*. Bed AC-12 with *Malagasites?* sp. A and bed AC-13 lacking fossils are included in this zone

merely because the bed AC-14 is considered as belonging to the Alternans Zone.

Alternans Zone – Beds AC-14-AC-16.- In the studied section the base of this zone has been conventionally marked by a bed yielding *Steueria alternans* n. gen., *Corongoceras mendozanum* and *Catutosphinctes inflatus*.

Bed AC-14: Three species were recorded from this bed: *S. alternans*, *C. mendozanum* and the earliest representatives

of *C. inflatus* which locally persists upwards into the Koeneni Z. like in A. Yeso (Leanza 1945: 89). The occurrence of *C. mendozanus* is usually cited as indicative of the Alternans Z. (Leanza 1981a: 79). The bed c of A. Yeso with *C. australis* and the specimen of *C. mendozanus* figured by Leanza (1945: pl. 3: 7-8) as *Aulacosphinctes* sp. was originally included in the definition of the Alternans Z. by Leanza (1945).

vetustum hz., new (bed AC-15): a rich and varied assemblage composed by *A. cf. euomphalum*, *C. inflatus*, *C. mendozanus*, *P. calistoides*, *Chigaroceras gerthi*, *Blanfordiceras vetustum*, *Steueria alternans* n. gen. and *Substeueroceras* aff. *koeneni*. These ammonites are considered as the guide assemblage for the introduction of the *vetustum* horizon.

Bed AC-16: In this bed *C. inflatus*, *P. calistoides* and *B. vetustum* persist.

Koeneni Zone – Bed AC-17.- This bed is attributed to the Koeneni Z., in first place, by the association of ammonites which were all included in this zone by Leanza (1945); on the other hand the bed AC-17 overlies the uppermost occurrence of *Corongoceras* and underlies, after a gap in bed AC-18, the Noduliferum Zone (Andean lower Berriasian).

striolatus hz., new (bed AC-17): *Parodontoceras calistoides* (a later, compressed and involute morphotype described as *Thurmannia discoidalis* by Gerth, 1925), *S. koeneni* and abundant *Choicensisphinctes striolatus*. This assemblage is conspicuous and distinctive enough to be considered the guide assemblage of a new faunal horizon.

The bed AC-18 is mostly covered. A single specimen of *H. cf. andinum* probably comes from this bed.

Noduliferum Zone – Bed AC-19.- The assignation of this bed to the Noduliferum Z. is based on the consideration of the stratigraphic position of the *compressum* hz. as discussed below.

compressum hz., new (bed AC-19): *Krantziceras compressum* n. gen. et n. sp. and *Spiticeras fraternum* are considered as the guide assemblage for the introduction of the *compressum* horizon. The horizon occurs in isolation in the sampled section, so that its stratigraphic position is not directly observed, but there are two independent hints which indicate its position in the lower part of the Noduliferum Z.: (1) the occurrence of *S. fraternum* in M. Redondo and A. Yeso is in the Damesi Z. and below, and (2) the ammonite succession in the richly fossiliferous locality Pampa Tril proliferated abundant adult specimens of *K. compressum* n. gen. et n. sp. in a bed just underlying the *noduliferum* hz. (defined below), a stratigraphic horizon with abundant and well-preserved, large adult macroconchs of *Argentiniceras noduliferum*. The occurrence of this latter species in P. Tril is in the same form as in M. Redondo. It is the only abundant ammonite in a single, thin stratigraphic level. The *compressum* hz. could be at least partially equivalent to the "Andiceras trigonostomum Zone" of Aguirre (2001); see discussion under *Krantziceras compressum* n. gen. et n. sp.

?Damesi Zone – Bed AC-20.- The zonal assignation of this bed is tentative, based on the fact that the collected ammonites were exclusively described from the Damesi Z. (Gerth 1921) by Leanza (1945).

Bed AC-20: In the lower part of this thick bed of limestone were collected fragmentary specimens of *Cuyaniceras* cf. *transgrediens* (Steuer, 1897) and *Groebericeras bifrons*

(Leanza, 1945). This association indicates the Damesis Z., most likely the *transgrediens* hz. (defined below).

Regional biostratigraphic time-correlation

In this chapter time-correlation below the subzonal level, between different areas of the NMB is presented. It is based on the recognition of ammonite horizons out of their type locality by means of the recognition of the guide assemblages. By these means time-planes proving synchronicity between beds of different localities become available. These time-planes are the narrowest and most accurate ones that can be obtained in stratigraphy (see Gabilly 1971, Callomon 1985, 1995). They would allow to refine the current correlations on which the geological history of the basin is based. The results are represented in the chart of Fig. 40 where the order of localities is through the South-North transect indicated in Fig. 1. Additional explanations and/or information from other localities is provided in the caption of Fig. 40. On the basis of the ammonite descriptions above and the well-controlled successions of M. Redondo and A. Yeso described by Leanza (1945), three additional ammonite horizons can be conveniently defined, which, on the other hand, can be recognized in other localities as indicated in Fig. 40:

bardense hz., new (Alternans Z.).- Bed 1762 of M. Redondo (Leanza 1945: 90), 0.25 m of bituminous marls with concretions yielding *Blanfordiceras bardense* (Krantz, 1926), *Steueria alternans* n. gen. in a wide range of variants (see synonymy above) and "Berriasella" *krantzii* Leanza, 1945. Leanza (1945: 34, 35) used alternatively the names "Horizonte con *B. inaequicostata*" or "Horizonte con *C. alternans*" indistinctly for the bed 1762 or the beds 1762-1763. This inconsistent denomination prevents the interpretation and use of these "horizons", but in some cases the former could be equivalent to the *bardense* hz. introduced herein.

noduliferum hz., new (Noduliferum Z.).- Bed h of A. Yeso (Leanza 1945: 89), 0.40 m of sandy limestone yielding *Argentiniceras noduliferum* (Steuer, 1897) and *A. bituberculatum* Leanza (1945: pl. 8: 1-2, HT by MT). *A. noduliferum* differs from *A. bituberculatum* by the short stage of bituberculation and apparent smaller adult size. Specimens of *A. noduliferum* abundantly occur at P. Tril in the bed directly overlying the *compressum* hz..

transgrediens hz., new (Damesi Z.).- Bed l of A. Yeso (Leanza 1945: 89), 0.40 m of marls with calcareous concretions yielding *Spiticeras gigas* Leanza, 1945 and *Cuyaniceras transgrediens* (Steuer, 1897) with several morphospecies which most likely are merely intraspecific variants but, anyway, they show as described by Leanza (1945) the variation which characterizes the species in this horizon.

Time-correlation with the Primary Standard

Time-correlation of the Tithonian successions of the NMB with the International Primary Standard (Enay & Geyssant 1975, Geyssant 1997) is a matter of current adjustments and proposals. But the predominant endemic Andean character of the fauna makes it hard to find time-planes for

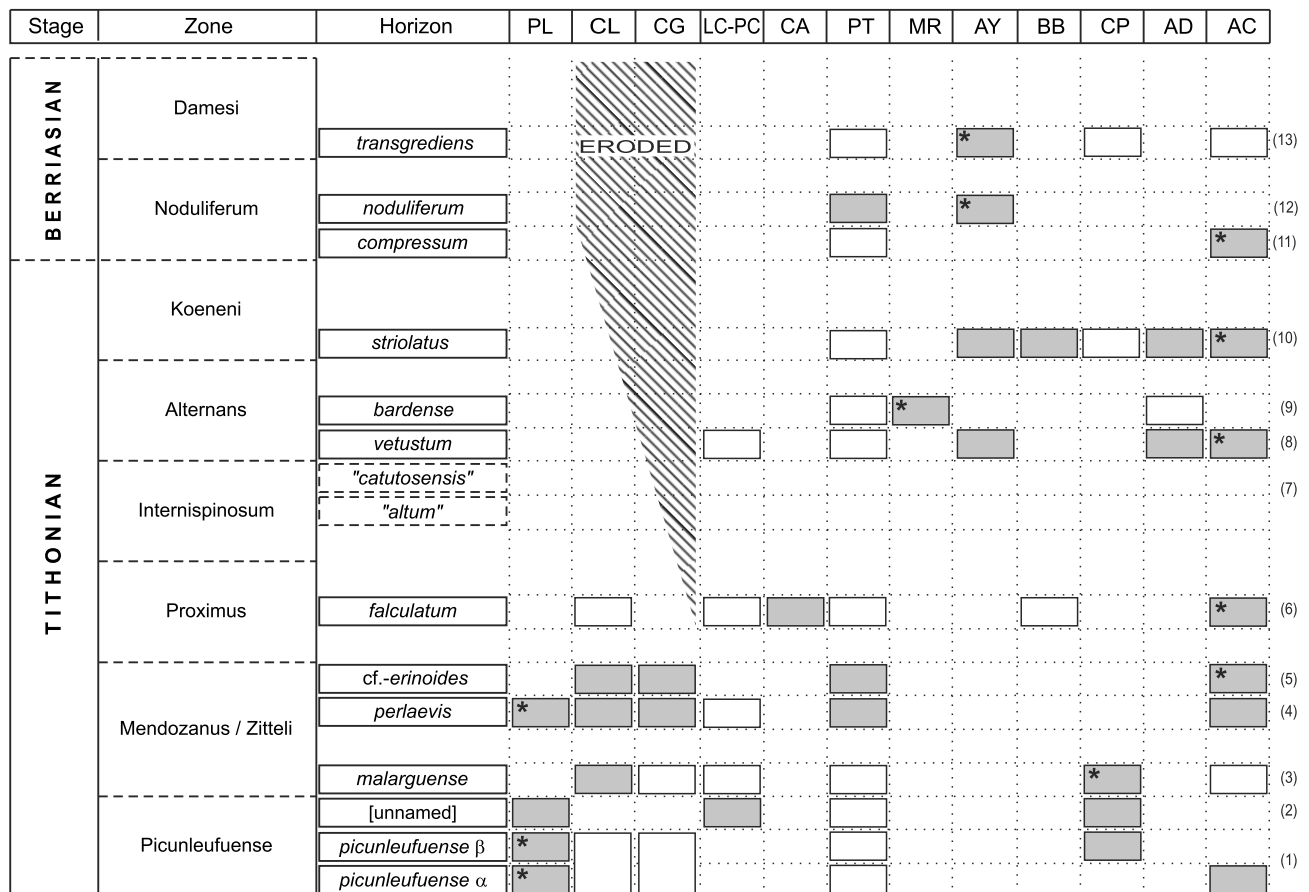


Figure 40. Regional biostratigraphic time-correlation chart for the Neuquén-Mendoza Basin. Correlations based on the recognition of ammonite horizons through the transect of selected localities indicated in Fig. 1 (see abbreviations). The height of the boxes of each zone does not indicate time-duration neither content of horizons, they are sized for convenience of design. Firm recognition of horizons indicated with gray boxes, tentative with white boxes. The asterisk indicates the type locality or section. The Mendozaanus and Zitteli zones are not separated because the impossibility of discrimination in AC and other studied localities (see discussion in text and in PGSS 2011). In most localities several levels with ammonites are known between the horizons indicated in this figure, but they are not indicated because they have not been evaluated for the adjustment to the criteria used in this study. The height of the horizon within each zone is arbitrary for other horizons could be established above and/or below (see details in text). Notes: (1): the *picunleufuense* α hz. and *picunleufuense* β hz. were defined in Picún Leufú and their recognition in other localities was already discussed (PGSS 2011). The *picunleufuense* α hz. is the base of the Picunleufuense Standard Zone. Abundant material of these two horizons was recently collected in PT. These horizons were defined in the southernmost portion of the NMB, their recognition in AC (northern part of the basin) and in several other intermediate localities indicates the horizon is a reliable marker for regional time-correlation. In LA-CG and CL both horizons occur undifferentiated in a basal conglomerate of the Vaca Muerta Fm. (2): this horizon is characterized by a conspicuous new species described preliminary as *Choicensisphinctes* cf./aff. *platyconus* (see Fig. 6C-E and PGSS 2011: fig. 23B-E), very close to *C. platyconus* and *C. burckhardtii*. In CP a good specimen was figured in Parent (2003: fig. 8) as *C. choicensis*. In AC it corresponds to bed AC-2. (3): the *malarguense* hz. has its type locality at CP (PGSS 2011). In PC could be represented by ammonites collected in the upper part of the bed PC-2 of the section described in Parent & Cocca (2007). (4): the *perlaevis* hz. (defined in PGSS 2011) was recently recognized in CL and CG and is represented by the bed AC-4. In PT the horizon is well represented by *C. perlaevis* abundant, *P. zitteli*, small *Physodoceras* and the same morphotype of *Choicensisphinctes* cf. *erinoides* than in PL. (5): the guide-assemblage of the cf. *erinoides* hz. includes specimens similar to the type specimens of *C. erinoides*, *C. australis* and *C. mendozanus* from Cajón del Burro-Río Choicas (Burckhardt 1900), suggesting very similar age with the guide-assemblage of the Mendozaanus Z. of Burckhardt (1903: 106). The type horizon of *C. limits* at Paso Montañas includes a specimen (Burckhardt 1900: pl. 25: 2) similar to *C. cf. guenakenensis* described above from bed AC-4 (*perlaevis* hz.). (6): the *falculatum* hz. introduced in this report yields a rich ammonite assemblage. In a thick succession of beds in CL-CG there occur a very abundant and rich fauna including *P. subpretiosus*, *C. falculatum*, *C. proximus* and *Toulisphinctes rafaeli*. This assemblage indicates very closely the *falculatum* hz., but the fauna is very abundant and probably after description could be discriminated different new ammonite horizons within the Proximus Z. which are commonly not recorded in the successions of southern Mendoza. (7): the "*altum*" and "*catutosensis*" horizons [after *Aspidoceras altum* Biró, 1980 and *Catutosphinctes catutosensis* (Leanza & Zeiss, 1990)] were introduced by Leanza & Zeiss (1992) for the Internispinosum Z. of the local succession of Los Catutos. Nevertheless, only three ammonite impressions were illustrated what prevents their use for comparison, and, on the other hand, similar ammonites are known from CL and LC but in different stratigraphic positions. For the time being these two horizons are not considered for correlation. (8): the *vetustum* hz. is recognized in AD (very close to AC) on the basis of the ammonite assemblage listed by Krantz (1928: 49), including different morphotypes of *C. mendozanum* as described above, *Blanfordiceras argentinum*, *B. vetustum* (as *Berriasella subprivasensis*), *P. calistoides* and *A. andinum* Steuer, 1897. The beds with these ammonites were denominated the "Berriasella calistoides Zone" by Krantz (1928: 49), which should be equivalent to the *vetustum* hz. In AY, the bed c of Leanza (1945: 89) yields *Corongoceras mendozanum* (as *Aulacosphinctes* sp., discussed above, under *C. mendozanum*) and *Catutosphinctes australis* (Leanza, 1945) which is indistinguishable from *C. inflatus* of the *vetustum* hz. (9): the type horizon of *S. alternans*, bed 31 g of the section of AD (Gerth 1925: 126), comprises ammonites very similar to those of the guide assemblage of the *bardense* hz. from MR, but it also includes *S. koeneni* and the range of variation of *S. alternans* is different as described in text. (10): the *striolatus* hz. is represented in AY by the bed f of Leanza (1945), in BB (Krantz 1928, Gerth 1925: 122) and in AD by the bed 31h (in Gerth 1925: 126, see discussion in text). In CP the specimens of *C. striolatus* (see Parent 2003) are similar to those of AC but the other species of the guide assemblage are not recorded. (11): the *compressum* hz. could be present in PT by the occurrence of the index in abundance but only microconch *Spiticeras* were collected that remain to be studied. (12): the *noduliferum* hz. could be used conveniently for standardization of the Noduliferum Z. For the time being it has been clearly recognized in PT. (13): the *transgrediens* hz. could be used conveniently for standardization of the Damesi Z. In CP (Parent 2003) have been collected few well preserved specimens almost identical with the HT (by MT) of *Cuyaniceras transgrediens* from the bed 6 of Gerth (1925: fig. 15).

reliable distant correlations with the Tethyan fauna. After the detailed revision presented by Leanza (1981a, b, with complete lists of references from the foundations), few advances were published later. The next detailed revision based on published data was presented by Callomon (1992) for the Circum-Pacific successions, but referring to the Andean successions as reviewed by Leanza (1981b). Other recent papers dealing with Tithonian-lower Berriasian biostratigraphy based on figured ammonites are Leanza & Zeiss (1990, 1992), Aguirre & Alvarez (1999), Aguirre & Vennari (2009), Aguirre et al. (2007). The results presented in the present paper with the mentioned references and the most recent studies in Parent & Capello (1999), Parent (2001, 2003b), Parent et al. (2006), PGSS (2011) and Schweigert et al. (2002) allow to propose some new advances. The conclusions by Zeiss & Leanza (2008) are based on two ammonites collected loose in the field, thus they cannot be discussed in the present context.

The base of the standard Picunleufuense Z., the *picunleufuense* α hz., has been proposed as the standard base for the Tithonian of the NMB (PGSS 2011). This does not imply precise correlation with the *eigeltungense* hz. of the Hybonotum Z. of the Submediterranean Tithonian (Schweigert 2007: tab. 1), however, it is possible that the lower part of the Picunleufuense Z. be late Kimmeridgian in age.

The conspicuous ammonite *Volanoceras krantzense* Cantú, 1990 which allows a reliable correlation with the complete representation of the lineage in the southern Tethys indicates the Semiforme Z., most likely the late part of this zone (Schweigert et al. 2002: 10). The HT was collected in B. Blancas (Krantz 1928); an additional specimen, associated with *Choicensisphinctes windhausenii*, *P. zitteli* and *Catutosphinctes windhausenii*, was recently collected in C. Granito, below the TH of *Pasottia andina*. Thus, considering this assemblage and the fact that *P. zitteli* is known to range in the Semiforme Z. of Europe, it can be concluded that at least the bed AC-3 is time equivalent to the Semiforme Z.

The *falculatum* hz. (bed AC-7) includes a wide variety of species, but most of them are known only in Andean regions or have long stratigraphic ranges like the aspidoceratids. The only conclusion to be drawn is that this horizon is sandwiched by the Semiforme Z. below and the earliest himalayitids known from the Andes (*Micracanthoceras* sp. A and *W. internispinosum*) above. It is therefore assumed to correlate within the Fallauxi Z. what is not new but in accordance with previous estimations (Parent 2001, Parent & Capello 1999). A possible time-correlation with the Caribbean region is suggested by the occurrence of *Mazatepites arredondense* in the section of AC.

The *vetustum* hz. (bed AC-15) also includes a rich assemblage. In this case, the bulk of ammonites of the guide assemblage, *C. mendozanum* and *B. vetustum*, are well-recorded from Madagascar (Collignon 1960, discussed above) where this horizon can be recognized in some part of the Hollandi Zone. Thus, close time-correlation can be assumed between the two basins.

Acknowledgements. - Matilde Beresi (IANIGLA/CRICYT, Mendoza) gave us valuable support for planning the field-work and Oscar D. Capello (Rosario) gave us valuable support during the field-work. Esperanza Cerdeño and Susana Devincenzi (Museo A. Moyano, Mendoza) have catalogued the material collected. G. Schairer, A. Nützel (Bayerische Staatss. für Paläontologie und Geologie, München), H. Jahnke and M. Reich (Georg-August-Univ. Göttingen),

and E.A. Nesbitt and R.C. Eng (Burke Museum, Seattle) have provided us with casts and/or photographs of type and figured specimens. A.C. Garrido (Museo Olsacher, Zapala) provided us full access to the collections. Diego Bosquet and Gustavo Lucero (Secretaría de Cultura, Mendoza) helped us for organizing the field-works. A.C. Garrido (Zapala), R. Enay (Lyon), R. Myczynski (Warsaw), V. Mitta and M Rogov (Moscow), S. Bengtson (Ofertersheim), A. Cantú (México), G. Delanoy (Nice), Nicola Pezzoni (Mantova) and Daniele Coltellacci (Rome) helped with literature, advice and discussions. The editors E.P. Peralta and A. Greco (Rosario) helped us in different ways. Facultad de Ingeniería, Universidad Nacional de Rosario partially funded the field-work. A.B. Villaseñor (Mexico, DF) and C. Sarti (Bologna) gave valuable suggestions for enhancing the manuscript as reviewer of the journal.

REFERENCES

- Aguirre-Urreta M.B., 2001. Marine Upper Jurassic-Lower Cretaceous stratigraphy and biostratigraphy of the Aconcagua-Neuquén Basin, Argentina and Chile. *Journal of Iberian Geology* **27**: 71-90.
- Aguirre-Urreta M.B. & Charrier R., 1990. Estratigrafía y amonites del Tithoniano-Berriasiano en las nacientes del Río Maipo, Cordillera Principal de Chile central. *Ameghiniana* **27**: 263-271.
- Aguirre-Urreta M.B. & Álvarez P.P., 1999. The Berriasian genus *Groebericeras* in Argentina and the problem of its age. *Scripta Geologica Special Issue* **3**: 15-29.
- Aguirre-Urreta M.B., Mourgues F.A., Rawson P., Bulot G. & Jaillard E., 2007. The Lower Cretaceous Chañarcillo and Neuquén Andean basins: ammonoid biostratigraphy and correlations. *Geological Journal* **42**: 143-173.
- Aguirre-Urreta B. & Vennari V., 2009. On Darwin's footsteps across the Andes: Tithonian-Neocomian fossil invertebrates from the Piuquenes Pass. *Revista de la Asociación Geológica Argentina* **64**: 32-42.
- Arkell W.J., 1952. Nomenclatural notes. Jurassic Ammonoidea. *Journal of Paleontology* **26**: 860-861.
- Arkell W.J., 1957. Jurassic ammonites. In Arkell W.J., Kummel B. and Wright C.W.: *Treatise on Invertebrate Paleontology*, (L) Mollusca 4, R.C. Moore (ed.). University of Kansas Press and Geological Society of America, Kansas and New York, 22+490 pp.
- Behrendsen O., 1891. Zur Geologie des Ostabhanges der argentinischen Cordillere. *Zeitschrift der Deutschen geologischen Gesellschaft* **44**: 369-420.
- Behrendsen O., 1921. Contribución a la geología de la pendiente oriental de la Cordillera argentina. *Actas de la Academia Nacional de Ciencias de la República Argentina* **7**: 155-227. [Spanish translation of Behrendsen O., 1921].
- Biró-Bagóczy L., 1980. Algunos ammonites nuevos en la Formación Lo Valdés, Tithoniano-Neocomiano, Provincia de Santiago (33°50' Lat. Sur), Chile. *Actas del Segundo Congreso Argentino de Paleontología y Bioestratigrafía* **1**: 223-242.
- Blanchet F., 1922. Sur un groupe d'ammonites éocretacées dérivées des *Cosmoceras*. *Compte Rendu Sommaire des Seances de la Société Géologique de France* **13**: 158-160.
- Boehm G., 1904. Beiträge zur Geologie von Niederländisch. Die Südküsten der Sula-Inseln Taliabu und Mangoli. 1. Grenzschieben zwischen Jura und Kreide. *Palaeontographica Supplement* **4**: 11-46.
- Boughdiri M., Enay R., Le Hégat G. & Memmi L., 1999. *Hegaraites* nov. gen. (Ammonitina): Himalayitidae nouveau du Tithonien supérieur de la coupe du Jebel Rhéouis (Axe nord-sud, Tunisie centrale). Précisions stratigraphiques, approche phylétique et signification biogéographique. *Revue de Paléobiologie* **18**: 195-121.
- Braccini O.I., 1970. Cuenca del Salado. In: Leanza A.F. (ed.): *Geología Regional Argentina*: 407-417. Academia Nacional de Ciencias de Córdoba.

- Burckhardt C., 1900a. Profils géologiques transversaux de la Cordillera Argentino-Chilienne. Stratigraphie et tectonique. *Anales del Museo de La Plata, Sección geológica y mineralógica* **2**: 1-136.
- Burckhardt C., 1900b. Coupe géologique de la Cordillere entre Las Lajas et Curacautin. *Anales del Museo de La Plata, Sección Geología y Minería* **3**: 1-102.
- Burckhardt C., 1903. Beiträge zur Kenntnis der Jura- und Kreideformation der Cordillere. *Palaeontographica* **50**: 1-144.
- Burckhardt C., 1906. Le faune Jurassique de Mazapil avec un appendice sur les fossiles du Cretacique inférieur. *Boletín del Instituto Geológico de México* **23**: 1-216.
- Burckhardt C., 1911. Bemerkungen über die russisch-borealen Typen in Oberjura und Kreide in Mexico. *Centralblatt für Mineralogie und Paläontologie* **15**: 477-483.
- Burckhardt C., 1919. Faunas jurásicas de Symon (Zacatecas) y faunas cretácicas de Zumpango (Guerrero). *Boletín del Instituto Geológico de México* **33**: 1-137.
- Burckhardt C., 1930. Étude synthétique sur le Mésozoïque Mexicain. *Mémoires de la Société Paléontologique Suisse* **49**: 1-280.
- Bürgl H., 1960. El Jurásico e Infracretácico del Río Batá, Boyaca. *Boletín Geológico* **6**: 169-211.
- Buckman S.S., 1919-1921. Yorkshire type ammonites. Vol 3: 5-64. Wesley & Son edit., London.
- Callomon J.H., 1985. The evolution of the Jurassic ammonite family Cardioceratidae. *Special Papers in Palaeontology* **33**: 49-90.
- Callomon J.H., 1992. In: von Hillebrandt, A., P. Smith, G.E.G. Westermann, J.H. Callomon: Upper Jurassic, especially of Mexico. Part 4: Biochronology. 12. Ammonite Zones of the Circum-Pacific Region. Westermann G.E.G. (ed.): *The Jurassic of the Circum-Pacific*: 247-272.
- Callomon J.H., 1995. Time from fossils: S.S. Buckman and Jurassic high-resolution geochronology. In: M.J. Le Bas (ed.): Milestones in Geology. *Geological Society London, Memoir* **16**: 127-150.
- Cantú C.A., 1967. Estratigrafía del Jurásico de Mazatepec, Puebla (México). *Instituto Mexicano del Petróleo, Monografía* **1**: 1-30.
- Cantu C.A., 1990. *Volanoceras chignahuapense* sp. nov., amonita del Titoniano Inferior de Puebla, Centro de México. *Revista Sociedad Mexicana de Paleontología* **3**: 41-45.
- Cecca F. & Enay R., 1991. Les ammonites des zones à Semiforme et à Fallauxi du Tithonique de l'Ardèche (Sud-Est de la France): stratigraphie, paléontologie, paléobiogéographie. *Palaeontographica* **A219**: 1-87.
- Collignon M., 1960. Atlas des fossiles caractéristiques de Madagascar. Fascicule 6 (Tithonique). Service Geologique de Madagascar, Tananarive. Plates 134-175.
- Cossmann M., 1907. Rectifications de Nomenclature. *Revue critique de Paléozoologie* **11**: 1-64.
- Djanélidzé A., 1922. Les *Spiticerus* du sud-est de la France. *Mémoires pour servir à l'explication de la Carte Géologique détaillée de la France* **1922**: 1-255.
- Dietze V., Callomon J.H., Schweigert G. & Chandler R.B., 2005. The ammonite fauna and biostratigraphy of the Lower Bajocian (Ovale and Laeviuscula zones) of E Swabia (S Germany). *Stuttgarter Beiträge zur Naturkunde* **B353**: 1-82.
- Dommergues, J.-L. & Marchand, D., 1988. Paléobiogéographie historique et écologique: Applications aux ammonites du Jurassique. In: Wiedmann, J. & Kullmann, J. (eds.): *Cephalopods – Present and Past*, 351-364. Schweizerbart, Stuttgart.
- Donovan D.T., Callomon J.H. & Howarth M.K., 1981. Classification of the Jurassic Ammonitina. In House M.R. & J.R. Senior (eds.): *The Ammonoidea. Systematics Association Special Volume* **18**: 101-155.
- Donze P. & Enay R., 1961. Les Céphalopodes du Tithonique Inferieur de la Croix-de-Saint-Concours pres Chambéry (Savoie). *Travaux Laboratoire Géologique de Lyon* **NS7**: 1-236.
- Douvillé H., 1890. Sur la classification des Cératites de la Craie. *Bulletins de la Société Géologique de France (serie 3)* **18**: 275-292.
- Douvillé R., 1910. Céphalopodes argentins. *Mémoires de la Société Géologique de France (Paléontologie)* **43**: 5-24.
- Doyle P., Poiré D.G., Spalletti L., Pirrie D., Brenchley P. & Matheos S.D., 2005. Relative oxygenation of the Tithonian-Valanginian Vaca Muerta-Chachao formations of the Mendoza shelf, Neuquén Basin, Argentina. *Geological Society London, Special Publication* **252**: 185-206.
- Enay R., 1972. Paléogéographie des ammonites du Jurassique Terminal et mobilité continentale. *Géobios* **5**: 355-407.
- Enay R., 2009. Les faunes d'ammonites de l'Oxfordien au Tithonien et la biostratigraphie des Spiti-Shales (Callovien supérieur-Tithonien) de Thakkhola, Népal Central. *Documents des Laboratoires de Géologie Lyon* **166**: 1-246.
- Enay R. & Geysant J., 1975. Faunes tithoniques des chaînes bétiques (Espagne méridionale). Colloque sur la limite Jurassique-Crétacé, Lyon, Neuchâtel, 1973. *Mémoires du Bureau de Recherche Géologique et Minières* **86**: 39-55.
- Enay R., Barale G., Jacay J. & Jaillard E., 1996. Upper Tithonian ammonites and floras from the Chicama Basin, Northern Peruvian Andes. *GeoResearch Forum* **1-2**: 221-234.
- Enay R., Boughdiri M. & Le Hegarat G., 1998a. *Durangites*, *Protacanthodiscus* et formes voisines du Tithonien supérieur-Berriasien dans la Téthys méditerranéenne (SE France, Espagne, Algérie et Tunisie). *Compte Rendus de l'Académie des Sciences, Paris* **327**: 471-477.
- Enay R., Boughdiri M. & Le Hegarat G., 1998b. *Toucasiella* gen. nov.: Himalayitidae nouveau du Tithonien supérieur de la Téthys occidentale (SE Espagne, Tunisie). Origine de *Durangites*. *Compte Rendus de l'Académie des Sciences, Paris* **327**: 425-430.
- Favre F., 1908. Die Ammoniten der unteren Kreide Patagoniens. *Neues Jahrbuch für Mineralogie, Geologie und Paläontologie, Beilage-Band* **25**: 601-647.
- Feruglio E., 1937. Palaeontographia Patagonica. *Memorie dell' Instituto Geologico della Reale Università di Padova* **11**: 1-384.
- Fontannes F., 1879. Description des ammonites des calcaires du Château de Crussol, Ardche (zones à *Oppelia tenuilobata* et *Waagenia beckeri*). Georget edit., p. 1-11 + 1-123. Lyon.
- Fözy I., Kázmér M. & Sente I., 1994. A unique Lower Tithonian fauna in the Gerecse Mts., Hungary. *Palaeopelagos Special Publication* **1**: 155-165.
- Gabilly J., 1971. Méthodes et modèles en stratigraphie du Jurassique. *Mémoire Bureau Recherche Géologique et Minière de France* **75**: 5-16.
- Gerth H., 1921. Fauna und Gliederung des Neocoms in der argentinischen Kordillere. *Centralblatt für Mineralogie, Geologie und Paläontologie* **1921**: 112-119, 140-148.
- Gerth H., 1925. Contribuciones a la estratigrafía y paleontología de los Andes Argentinos I: Estratigrafía y distribución de los sedimentos mesozoicos en los Andes Argentinos. *Actas de la Academia Nacional de Ciencias de la República Argentina* **9**: 7-55.
- Geysant J., 1997. Tithonien. In: Cariou E. & Hantzpergue P. (coord.): *Biostratigraphie du Jurassique ouest-européen et méditerranéen: zonations parallèles et distribution des invertébrés et microfossiles. Bulletins du Centre de Recherche Elf-Exploration et Production* **17**: 97-102.
- Grigorieva O.K., 1938. A Lower Valanginian ammonite fauna from the basin of the Belaya River on the northern slope of the Caucasus (Maikop area). *Azov and Black-Sea Geological Survey. Materials on the Geology and uses of fossils, Rostov-on-Don* **1**: 83-122.
- Gulisano C.A. & Gutiérrez-Pleimling A.R., 1995. The Jurassic of the Neuquén Basin. a) Neuquén Province. Field Guide: b) Mendoza Province. *Publicaciones de la Asociación Geológica Argentina* **E3**: 1-111.
- Hantzpergue P., 1989. Les ammonites Kimméridgiennes du Haut-

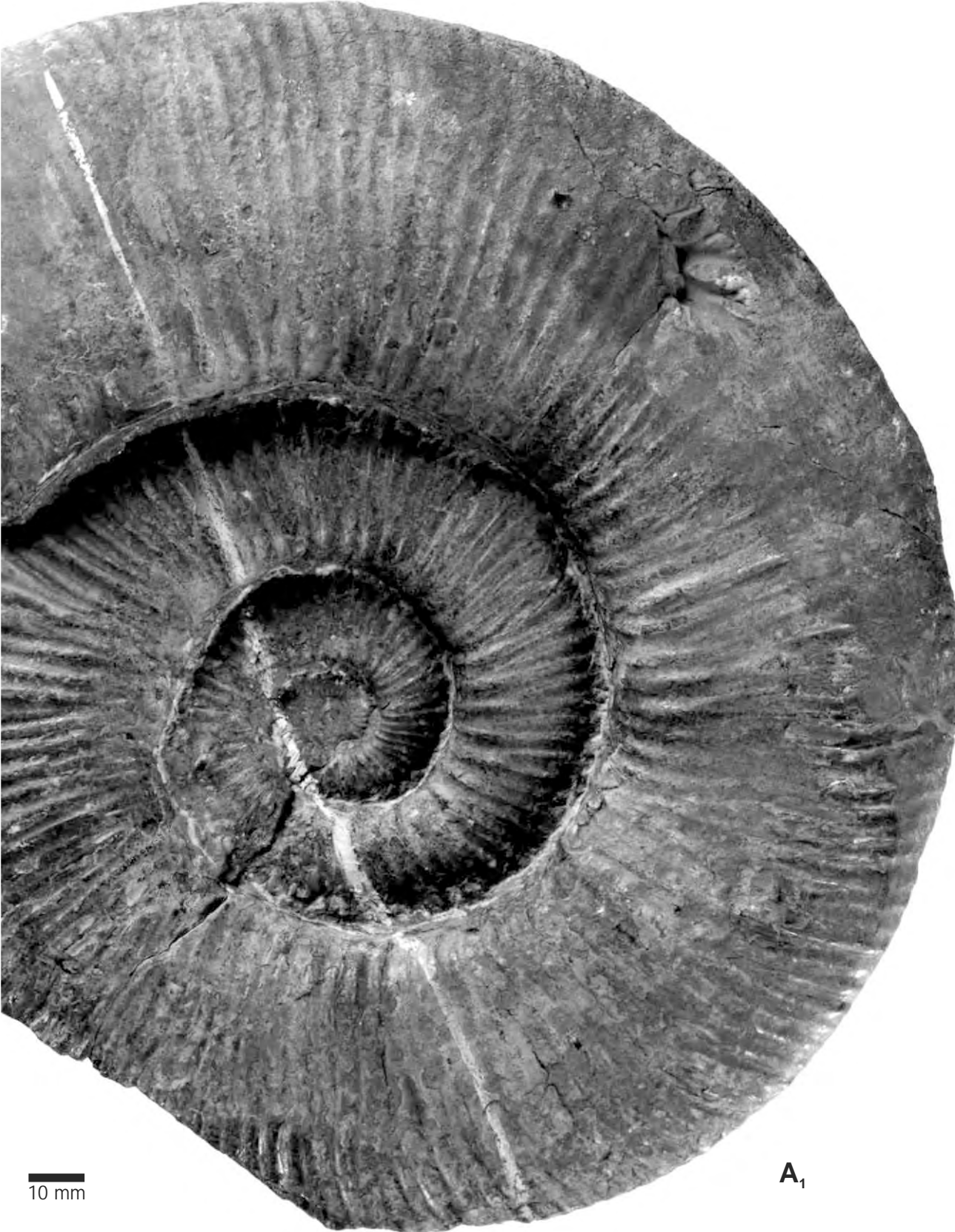
- Fond d'Europe occidentale. *Cahiers de Paléontologie*, p. 1-428. Paris.
- Haug E., 1910. Période Crétacée. In Emil Haug: *Traité de géologie*, vol. 2: 1153-1396. Les Périodes Géologiques, fascicle 2. Colin. Paris.
- Haupt O., 1907. Beiträge zur Fauna des oberen Malm und der unteren Kreide in der argentinischen Cordillere. *Neues Jahrbuch für Mineralogie, Geologie und Paläontologie, Beilage-Band 21*: 187-236.
- Howarth M.K., 1992. Tithonian and Berriasian ammonites from the Chia Gara Formation in northern Iraq. *Palaeontology* **35**: 597-655.
- Howarth M.K., 1998. Ammonites and nautiloids from the Jurassic and Lower Cretaceous of Wadi Hajar, southern Yemen. *Bulletin of the Natural History Museum London (Geology)* **54**: 33-107.
- Howlett P.J., 1989. Late Jurassic – Early Cretaceous cephalopods of eastern Alexander Island, Antarctica. *The Paleontological Association Special Papers in Palaeontology* **41**: 1-72.
- Hyatt A., 1900. Cephalopoda. In: Eastman's Zittel textbook of Paleontology, First edition, p. 502-604. New York.
- Imlay R.W., 1942. Late Jurassic fossils from Cuba and their economic significance. *Bulletin of the Geological Society of America* **53**: 1417-1478.
- Imlay R.W., 1980. Jurassic paleobiogeography of the conterminous United States in its continental setting. *United States Geological Survey Professional Papers* **1062**: 1-134.
- Kilian C.C.C.W., 1907-1913. Erste Abteilung: Unterkreide (Palaeocretacicum). Lieferung 1-3: 1-398. In F. Frech: *Lethaea Geognostica. II. Das Mesozoicum, Band 3 (Kreide)*. Schweizerbart. Stuttgart.
- Klein J., 2005. Lower Cretaceous Ammonites I. Perisphinctaceae 1. Himalayitidae, Olcostephanidae, Holcodiscidae, Neocomitidae, Oosterellidae. In Riegraf W. (ed.): *Fossilium Catalogus. I. Animalia (Pars 139): I-IX + 1-484*. Backhuys Publishers.
- Krantz F., 1926. Die Ammoniten des Mittel- und Obertithons. In: Jaworski E., Krantz F. & Gerth H. (eds.): *Beiträge zur Geologie und Stratigraphie des Lias, Doggers, Tithons und der Unterkreide im Süden der Provinz Mendoza (Argentinien)*. *Geologische Rundschau* **17a**: 427-462.
- Krantz F., 1928. La fauna del Tithono superior y medio de la Cordillera Argentina en la parte meridional de la Provincia de Mendoza. *Actas de la Academia Nacional de Ciencias de la República Argentina* **10**: 1-57. [Spanish translation of Krantz F., 1926].
- Kutek J. & Wierzbowski A. 1986. A new account on the Upper Jurassic stratigraphy and ammonites of the Czorsztyn succession, Pienny Klippen Belt, Poland. *Acta geologica Polonica* **36**: 289-316.
- Landman N.H., Kennedy W.J., Cobban W. & Larson N.L., 2010. *Scaphites* of the “*nodosus* group” from the Upper Cretaceous (Campanian) of the Western Interior of North America. *Bulletin of the American Museum of Natural History* **342**: 1-242.
- Leanza A.F., 1945. Ammonites del Jurásico superior y del Cretácico inferior de la Sierra Azul en la parte meridional de la provincia de Mendoza. *Anales del Museo de La Plata, Paleontología* **1**: 1-99.
- Leanza H.A., 1975. *Himalayites andinus* n. sp. (Ammonitina) del Tithoniano superior de Neuquén, Argentina. *Actas del Primer Congreso Argentino de Paleontología y Estratigrafía* **1**: 581-588.
- Leanza H.A., 1980. The Lower and Middle Tithonian ammonite fauna from Cerro Lotena, Province of Neuquén, Argentina. *Zitteliana* **5**: 3-49.
- Leanza H.A., 1981a. The Jurassic-Cretaceous boundary beds in West Central Argentina and their ammonite zones. *Neues Jahrbuch für Geologie und Paläontologie, Abhandlungen* **161**: 62-92.
- Leanza H.A., 1981b. Faunas de ammonites del Jurásico superior y del Cretácico inferior de América del Sur, con especial consideración de la Argentina. In: W. Volkheimer & E.A. Musacchio (eds.): *Cuencas Sedimentarias del Jurásico y Cretácico de América del Sur 2*: 559-598. *Comité Sudamericano del Jurásico y Cretácico*.
- Leanza H.A., 1996. The Tithonian ammonite genus *Chigaroceras* Howarth (1992) as a bioevent marker between Iraq and Argentina. *GeoResearch Forum* **1-2**: 451-458.
- Leanza H.A. & Hugo C.A., 1977. Sucesión de ammonites y edad de la Formación Vaca Muerta y sincrónicas entre los paralelos 35° y 40° l.s. Cuenca Neuquina-Mendocina. *Revista de la Asociación Geológica Argentina* **32**: 248-264.
- Leanza H.A. & Zeiss A., 1990. Upper Jurassic Lithographic Limestone from Argentina (Neuquén Basin): Stratigraphy and Fossils. *Facies* **22**: 169-186.
- Leanza H.A. & Zeiss A., 1992. On the ammonite fauna of the Lithographic Limestones from the Zapala region (Neuquén province, Argentina), with the description of a new genus. *Zentralblatt für Geologie und Paläontologie, Teil I, H. 6, 1991*: 1841-1850.
- López I.L., Villaseñor M.A.B. & Olóriz S.F., 2007. Sobre una asociación de ammonites del Jurásico superior (Tithonico) de Mazatepec, Puebla, México. In: Díaz E.M. & Rábano I. (eds.): *Fourth European Meeting on the Palaeontology and Stratigraphy of Latin América. Cuadernos del Museo Geominero* **8**: 245-249.
- Meister C., 1989. Canalisation intra-spécifique chez des Hildocerataceae du Domérien. In: Dommergues J.-L., Cariou E., Contini D., Hantzpergue P., Marchand D., Meister C. & Thierry J.: *Homéomorphies et canalisations évolutives: le rôle de l'ontogenèse. Quelques exemples pris chez les ammonites du Jurassique*. *Geobios* **22**: 5-48.
- Olóriz F., 1978. Kimmeridgiense-Tithonico inferior en el sector central de las Cordilleras Béticas. Paleontología, Bioestratigrafía. *Tesis Doctoral de la Universidad de Granada*, 758 p.
- Oppel A., 1862-1863. III. Ueber jurassische Cephalopoden. *Palaeontologische Mittheilungen* **1**: 127-262.
- Parent H., 1998. Upper Bathonian and lower Callovian ammonites from Chacay Melehué (Argentina). *Acta Palaeontologica Polonica* **43**: 69-130.
- Parent 2001. The Middle Tithonian (Upper Jurassic) ammonoid fauna of Cañadón de los Alazanes, southern Neuquén-Mendoza Basin, Argentina. *Boletín del Instituto de Fisiografía y Geología* **71**: 19-38.
- Parent H., 2003a. The Ataxioceratid ammonite fauna of the Tithonian (Upper Jurassic) of Casa Pincheira, Mendoza (Argentina). In: Parent H., Olóriz F. & Meléndez G. (eds.): *Jurassic of South America. Journal of South American Earth Sciences* **16**: 143-165.
- Parent H., 2003b. Taxonomic and biostratigraphic re-evaluation of *Perisphinctes internispinosus* Krantz, 1926 (Upper Jurassic, Ammonoidea). *Paläontologische Zeitschrift* **77**: 353-360.
- Parent H., 2006. Oxfordian and late Callovian ammonite faunas and biostratigraphy of the Neuquén-Mendoza and Tarapacá basins (Jurassic, Ammonoidea, Western South-America). *Boletín del Instituto de Fisiografía y Geología* **76**: 1-70.
- Parent H. & Capello O.D., 1999. Ammonites del Tithoniano inferior de Casa Pincheira, Mendoza (Argentina). *Revue de Paléobiologie* **18**: 347-353.
- Parent H., Scherzinger A. & Schweigert G., 2006. The earliest ammonite faunas from the Andean Tithonian of the Neuquén-Mendoza Basin, Argentina. Chile. *Neues Jahrbuch für Geologie und Paläontologie Abhandlungen* **241**: 253-267.
- Parent H., Scherzinger A., Schweigert G. & Capello O.D., 2007. Ammonites of the Middle Tithonian Internispinosum Zone from Barda Negra, Southern Neuquén-Mendoza Basin, Argentina. *Boletín del Instituto de Fisiografía y Geología* **77**: 11-24.
- Parent H. & Cocca S.E., 2007. The Tithonian (Upper Jurassic) ammonite succession at Portada Covunco, Neuquén-Mendoza Basin, Argentina. *Boletín del Instituto de Fisiografía y*

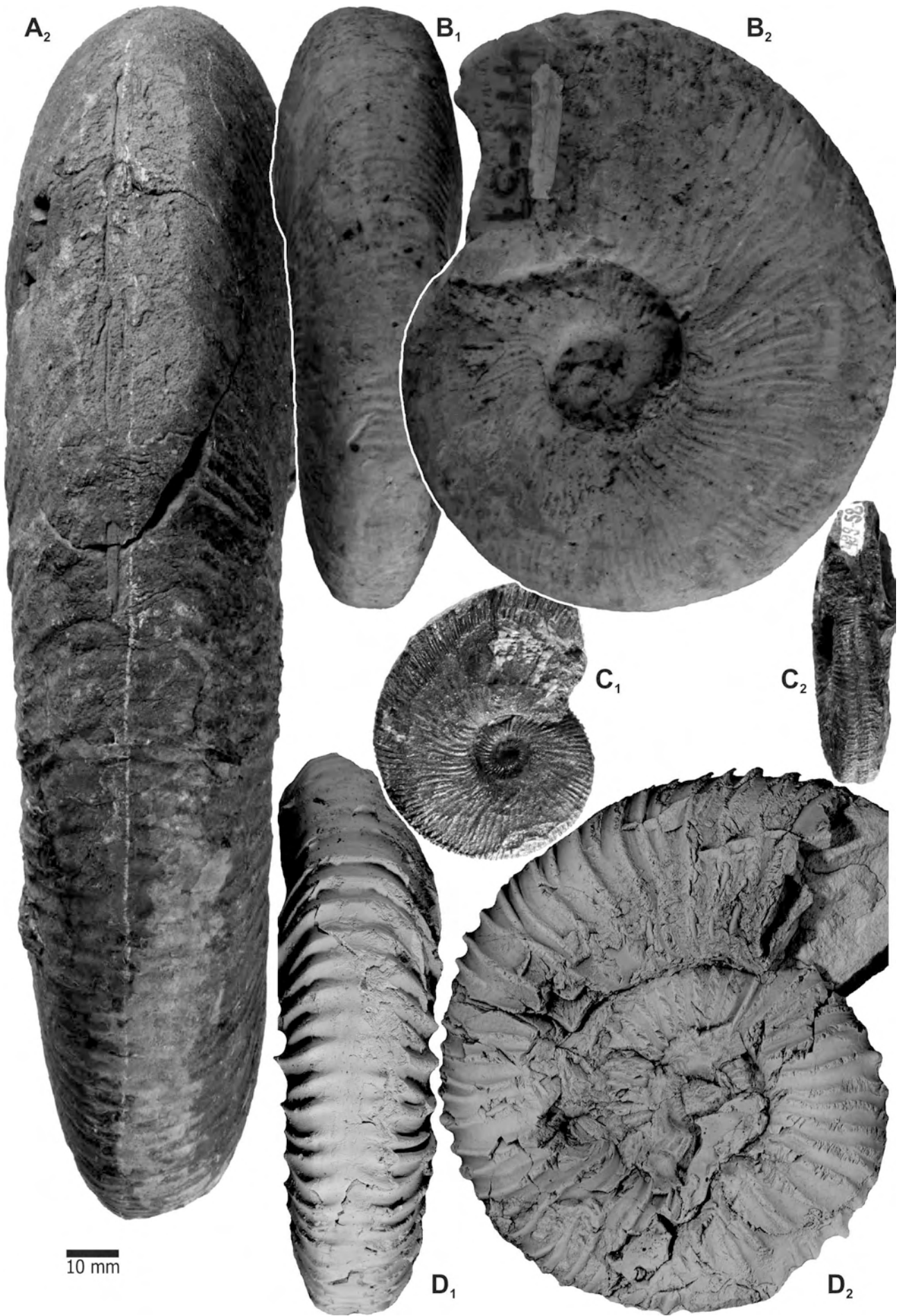
- Geología* **77**: 25-30.
- Parent H., Schweigert G., Scherzinger A. & Enay R., 2008. *Pasottia*, a new genus of Tithonian Opeleiid ammonites (Late Jurassic, Ammonoidea: Haploceratoidea). *Boletín del Instituto de Fisiografía y Geología* **78**: 23-30.
- Parent H., Myczynski R., Scherzinger A. & Schweigert G., 2010. *Cieneguiticeras*, a new genus of Tithonian opeleiid (Ammonoidea, Late Jurassic). *Géobios* **43**: 453-463.
- Parent H., Garrido A., Schweigert G. & Scherzinger A., 2011. The Tithonian ammonite fauna and stratigraphy of Picún Leufú, southern Neuquén Basin, Argentina. *Revue de Paleobiologie* **30**(1; June): 45-104.
- Paul C.R.C., Allison P.A. & Brett C., 2008. The occurrence and preservation of ammonites in the Blue Lias Formation (lower Jurassic) of Devon and Dorset, England and their palaeogeological, sedimentological and diagenetic significance. *Palaeogeography, Palaeoclimatology, Palaeoecology* **270**: 258-272.
- Quenstedt F.A., 1845-1849. Petrefaktenkunde Deutschlands, 1/1: Cephalopoden. Fues, Tübingen IV+580 p.
- Rivera R., 1951. La fauna de los estratos Puente Inga, Lima. *Boletín de la Sociedad Geológica del Perú* **22**: 1-53.
- Roman F., 1938. Les ammonites jurassiques et crétacées. Essai de genera. Masson, Paris, 554 p.
- Sapunov I.G., 1979. Les fossiles de Bulgarie. III.3. Jurassique supérieur, Ammonoidea. Academie Bulgare des Sciences, p. 1-263.
- Scherzinger A. & Schweigert G., 1999. Die Ammoniten-Faunenhorizonte der Neuburg-Formation (Oberjura, Südliche Frankenalb) und ihre Beziehungen zum Volgium. *Mitteilungen der Bayerischen Staatssammlung für Paläontologie und historische Geologie* **39**: 3-12.
- Scherzinger A., Fözy I. & Parent H., 2010. The Early Tithonian (Late Jurassic) ammonite genus *Virgatosimoceras* Spath (Ammonoidea: Simoceratidae) - revision and value for correlation. *Neues Jahrbuch für Geologie und Paläontologie Abhandlungen* **256**(2): 195-212.
- Schindewolf O.H., 1925. Entwurf einer Systematik der Perishinthen. *Neues Jahrbuch für Geologie und Paläontologie Abhandlungen Beilage* **52B**: 309-343.
- Schlegelmilch R., 1994. Die Ammoniten des süddeutschen Malms. VII + 297 pp.; Stuttgart, Jena & New York (Fischer).
- Schweigert G., 1997. Die Ammonitengattungen *Simocosmoceras* Spath und *Pseudhimalayites* Spath (Aspidoceratidae) im süddeutschen Oberjura. *Stuttgarter Beiträge zur Naturkunde* **B246**: 1-29.
- Schweigert G., 2007. Ammonite biostratigraphy as a tool for dating Upper Jurassic lithographic limestones from South Germany – first results and open questions. *Neues Jahrbuch für Geologie und Paläontologie Abhandlungen* **245**: 117-125.
- Schweigert G., Scherzinger A. & Parent H., 2002. The *Volanoceras* lineage (Ammonoidea, Simoceratidae) – a tool for long-distance correlations in the Lower Tithonian. *Stuttgarter Beiträge zur Naturkunde* **B326**: 1-43.
- Spath L.F., 1923a. On ammonites from New Zealand. *Quarterly Journal of the Geological Society* **79**: 286-312.
- Spath L.F., 1923b. A monograph of the Ammonoidea of the Gault, part 1: 1-72. *Monographs of the Palaeontological Society of London*.
- Spath L.F., 1924. On the Blake collection of Ammonites from Kachh, India. *Paleontographica Indica* **9**: 1-29.
- Spath L.F., 1925. The Collection of fossils and rocks from Somaliland made by B.N.K. Wyllie and W.R. Smellie. Part 7: Ammonites and aptychi. *Monographs of the geological Department of the Hunterian Museum* **1**: 111-164.
- Spath L.F., 1927-1933. Revision of the Jurassic Cephalopod Fauna of Kachh (Cutch). *Paleontographica Indica* N.S. **9**(2): 1-945.
- Spath L.F., 1934. The Jurassic and Cretaceous ammonites and belemnites of the Attock district. *Memoris of the Geological Survey of India, Palaeontologica Indica* NS **20**(4): 1-71.
- Steinmann G., 1890. Cephalopoda. In: G. Steinmann & L. Döderlein (eds.): *Elemente der Paläontologie*: 344-475, Leipzig (Engelmann).
- Steuer A., 1897. Argentinische Jura-Ablagerungen. Ein Beitrag zur Kenntnis der Geologie und Paläontologie der argentinischen Anden. *Palaeontologische Abhandlungen* **7**(N.F. 3): 129-222.
- Steuer A., 1921. Estratos Jurásicos Argentinos. Contribución al conocimiento de la Geología y Paleontología de los Andes Argentinos entre el río Grande y el río Atuel. *Actas de la Academia Nacional de Ciencias de Córdoba* **7**: 25-128. [Spanish Translation of Steuer A., 1897].
- Stevens G.R., 1997. The Late Jurassic Ammonite fauna of New Zealand. *Institute of Geology and Nuclear sciences Monograph* **18**: 1-217.
- Sturani C., 1971. Ammonites and stratigraphy of the "Posidonia alpine" beds of the Venetian Alps (Middle Jurassic, mainly Bajocian). *Memorie degli Istituti di Geologia e Mineralogia dell'Università di Padova* **28**: 1-190.
- Stinnesbeck W.S., Adatte T. & Remane J., 1993. Mazatepec (Estado de Puebla, México) – Reevaluación de su valor como estratotipo del límite Jurásico-Cretácico. *Revista Española de Micropaleontología* **25**: 63-79.
- Tavera J.M., 1985. Los ammonites del Tithónico superior-Berriasense de la Zona Subbética (Cordilleras Béticas). *Tesis doctorales Universidad de Granada* **587**: 1-381.
- Thomson M.R.A., 1979. Upper Jurassic and lower Cretaceous ammonite faunas of the Ablation Point area, Alexander Island. *British Antarctic Survey Scientific Reports* **97**: 1-37.
- Uhlig V., 1903. Himalayan Fossils. The Fauna of the Spiti Shales. *Memoirs of the Geological Survey of India. Palaeontologica Indica* **15**, **4**(1): 1-132.
- Uhlig V., 1910. Himalayan Fossils. The Fauna of the Spiti Shales. *Memoirs of the Geological Survey of India. Palaeontologica Indica* **15**, **4**(2): 133-306.
- Verma H.M. & Westermann G.E.G., 1973. The Tithonian (Jurassic) Ammonite Fauna and Stratigraphy of Sierra Catorce, San Luis Potosi, Mexico. *Bulletin of American Paleontology* **63**/277: 107-320.
- Weaver A., 1931. Paleontology of the Jurassic and Cretaceous of West Central Argentina. *Memoirs of the University of Washington* **1**: 1-496.
- Wilmsen M. & Mosavinia A., 2011. Phenotypic plasticity and taxonomy of *Schloenbachia varians* (J. Sowerby, 1817) (Cretaceous Ammonoidea). *Paläontologische Zeitschrift* **85**(2): 169-184.
- Wright C.W., Callomon J.H. & Howarth M.K., 1996. Cretaceous Ammonoidea. In: Kaesler R.L. (ed.). *Treatise on Invertebrate Paleontology, Part L, Mollusca 4* (revised). Geological Society of America and University of Kansas Press; 20+362 pp.
- Yin J. & Enay R., 2004. Tithonian ammonoid biostratigraphy in eastern Himalayan Tibet. *Géobios* **37**: 667-686.
- Zeiss A., 1968. Untersuchungen zur Paläontologie der Cephalopoden des Unter-Tithon der Südlichen Frankenalb. *Abhandlungen der Bayerischen Akademie der Wissenschaften, mathematisch-naturwissenschaftliche Klasse, neue Folge* **132**: 1-190.
- Zeiss A. & Leanza H.A., 2008. Interesting new ammonites from the Upper Jurassic of Argentina and their correlation potential: new possibilities for global correlation at the base of the Upper Tithonian by ammonites, calpionellids and other fossil groups. *Newsletters on Stratigraphy* **42**(3): 223-247.
- Zittel K.A.v., 1868. Die Cephalopoden der Stramberger Schichten. *Paläontologische Mittheilungen aus dem Museum des königlich Bayerischen Staates* **2**: 33-118.
- Zittel K.A.v., 1884. Cephalopoda, p. 329-522. In: Zittel K.A. (ed.): *Handbuch der Paläontologie*, vol. 1, Abt. 2 (3), Lief. 3. München & Leipzig (Oldenbourg).

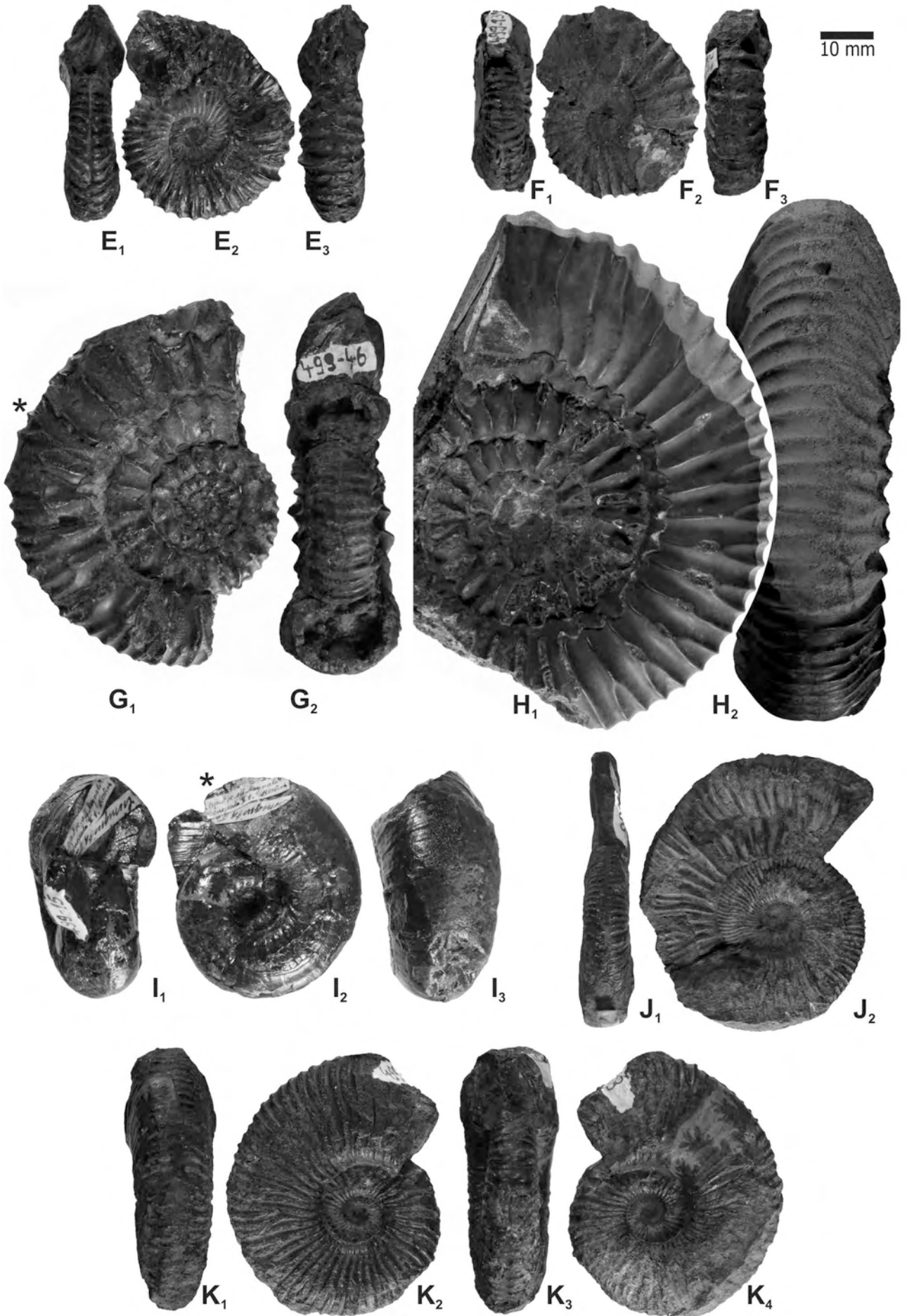
Appendix 1. Measurements of type and selected specimens. Dimensions and abbreviations explained in text.

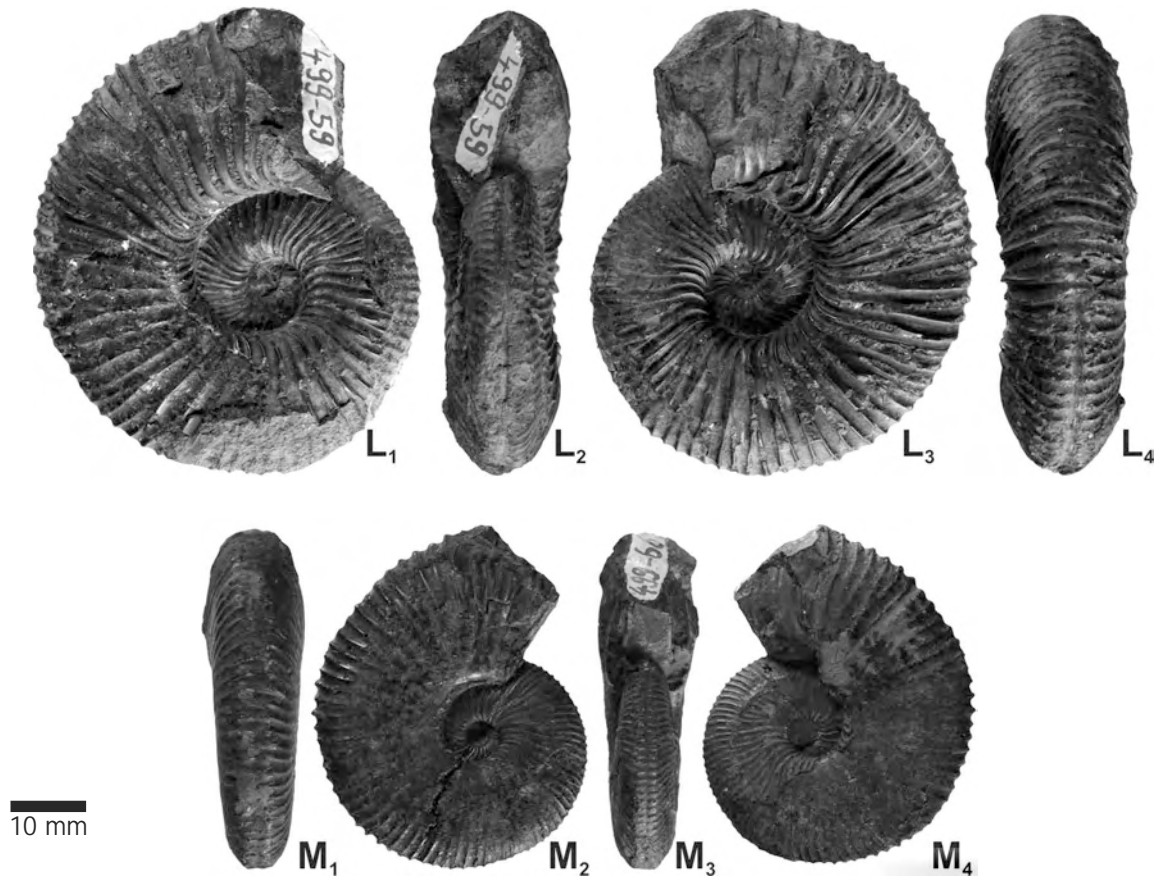
Collection number	Sex	Ph/Bc	D [mm]	U/D	W/D	H _i /D	P	V	Collection number	Sex	Ph/Bc	D [mm]	U/D	W/D	H _i /D	P	V	LBC[*]
<i>Choicosisphinctes n. sp. aff. erinoides</i> (Burckhardt, 1903)									<i>Catutosphinctes inflatus</i> (Leanza, 1945)									
MCNAM 24374 (Fig. 7)	[M] ad	Bc	185.00	0.41	-	-	13	-	Holotype	[M] ad	Ph-Bc	78.00	0.41	0.33	0.31	23	-	-
		Ph-Bc	140.00	-	-	-	-	-			Ph	55.00	0.38	-	-	16	-	-
		Ph	100.00	-	-	-	14	-			Ph	40.00	-	-	-	14	-	-
		Ph	40.00	-	-	-	22	-			Ph	25.00	-	-	-	12	-	-
<i>Choicosisphinctes cf. erinoides</i> (Burckhardt, 1903)									MCNAM 24457/8 (Fig. 21B)									
Fig. 9	[M] ad	Bc	245.00	-	-	-	12	-			Ph	32.00	0.43	0.36	-	16	-	-
		Ph-Bc	180.00	-	-	-	12	-			Ph	23.00	-	-	-	14	-	-
MCNAM 24385 (Fig. 10A)	[M] ad	Ph-Bc	150.00	-	-	-	9	-			Ph	18.00	-	-	-	12	-	-
		Ph	120.00	-	-	-	9	-			Ph	7.50	-	-	-	10	-	-
		Ph	112.00	-	-	0.38	14	-			Ph	5.00	-	-	-	7	-	-
		Ph	88.00	-	-	-	20	-	MCNAM 24457/0 (Fig. 20D)	[M] ad	Bc	100.00	0.45	0.30	0.33	22	-	-
		Ph	60.00	-	-	-	24	-			Ph-Bc	70.00	0.43	-	-	-	-	-
<i>Choicosisphinctes cf. limits</i> (Burckhardt, 1903)									MCNAM 24457/12 (Fig. 20B)									
MCNAM 24383 (Fig. 11A)	[M] ad	Ph	130.00	-	-	-	7	-			Ph	29.00	0.40	-	-	12	-	-
		Ph	92.00	-	-	-	13	-			Ph	20.00	0.39	-	-	12	-	-
		Ph	65.00	-	-	-	26	-			Ph	14.00	-	-	-	11	-	-
MCNAM 24382 (Fig. 11B)	[M] ad	Ph	150.00	-	-	-	7	-			Ph	4.00	-	-	-	8	-	-
		Ph	110.00	-	-	-	8	-			Ph	3.50	-	-	-	6	-	-
		Ph	90.00	-	-	-	11	-			Ph	9.00	-	-	-	11	-	-
		Ph	85.00	-	-	-	13	-			Ph	6.00	-	-	-	9	-	-
MCNAM 24388 (Fig. 13A)	[M] ad	Ph	222.00	-	-	-	10	-			Ph	3.50	-	-	-	8	-	-
		Ph	160.00	-	-	-	11	-	MCNAM 24460/2 (Fig. 21A)	[M] ad	Bc	134.00	-	-	-	-	-	-
		Ph	110.00	-	-	-	15	-			Ph-Bc	105.00	0.41	-	-	-	-	-
<i>Choicosisphinctes erinoides</i> (Burckhardt, 1903)									MCNAM 24457/8 (Fig. 21B)									
Holotype	Ph ad	Ph	170.00	-	-	-	9	-			Ph	55.00	0.44	0.35	0.29	-	-	-
		Ph	120.00	-	-	-	12	-			Ph	39.00	0.42	0.38	0.28	13	-	-
		Ph	87.00	-	-	-	13	-			Ph	12.00	-	-	-	10	-	-
<i>Choicosisphinctes choicensis</i> (Burckhardt, 1903)									MCNAM 24460/3 (Fig. 21D)									
Holotype	[M]	Bc	78.00	-	0.43	0.40	14	-			Ph	27.50	0.45	-	-	13	-	-
		Ph	67.00	-	-	-	18	-			Ph	14.00	-	-	-	12	-	-
<i>Choicosisphinctes australis</i> (Burckhardt, 1903)									MCNAM 24457/8 (Fig. 21E)									
Holotype	[M]	Bc	70.00	-	0.38	-	24	-			Bc	51.00	0.43	0.35	0.33	16	-	-
<i>Catutosphinctes proximus</i> (Steuer, 1897) transient β									MCNAM 24459/2 (Fig. 34E)									
Lectotype		Bc	57.00	0.44	0.26	0.32	18	35			Ph-Bc	47.00	-	-	-	-	-	-
		Ph-Bc	44.00	-	-	-	-	-			Ph	38.00	-	-	-	13	-	-
		Ph	40.00	-	-	-	15	-			Ph	19.00	-	-	-	12	-	-
		Ph	30.00	-	-	-	14	-			Ph	8.00	-	-	-	11	-	-
		Ph	21.00	-	-	-	12	-			Ph	5.00	-	-	-	9	-	-
		Ph	15.00	-	-	-	10	-	MCNAM 24460/3 (Fig. 21D)	[m?] ad	Ph	27.50	0.45	-	-	13	-	-
		Ph	11.00	-	-	-	10	-			Ph	14.00	-	-	-	12	-	-
		Ph	4.50	-	-	-	9	-			Bc	51.00	0.43	0.35	0.33	16	-	-
MCNAM 24466 (Fig. 18A)	[M] ad	Ph-Bc	125.00	0.52	0.27	0.27	16	56	MCNAM 24457/8 (Fig. 21E)	[m?] ad	Ph-Bc	47.00	-	-	-	-	-	-
MCNAM 24439 (Fig. 18E)	[m] ad	Bc	72.00	0.50	0.25	0.28	19	42			Ph	38.00	-	-	-	13	-	-
		Ph-Bc	52.00	0.46	0.29	0.29	18	-			Ph	19.00	-	-	-	12	-	-
		Ph	42.00	0.43	-	-	18	-			Ph	8.00	-	-	-	11	-	-
		Ph	29.00	-	-	-	14	-			Ph	5.00	-	-	-	9	-	-
		Ph	21.00	-	-	-	11	-	<i>Corongoceras mendozanum</i> (Behrendsen, 1891)									
		Ph	14.00	-	-	-	11	-	Holotype	[M] ad	Ph-Bc	70.00	0.37	0.24	0.34	17	21	-
		Ph	10.00	-	-	-	10	-			Ph	53.00	0.34	0.29	-	14	-	-
		Ph	5.00	-	-	-	8	-	MCNAM 24457/1 (Fig. 33B)	[M] ad	Bc	145.00	-	-	-	24	-	> 200
MCNAM 24412 (Fig. 18B)	[M] ad	Bc	70.00	-	-	-	25	-			Ph-Bc	103.00	0.37	0.25	0.38	21	-	-
		Ph-Bc	59.00	-	-	-	-	-			Ph	75.00	-	-	-	16	-	-
		Ph	45.00	-	-	-	18	-			Ph	50.00	-	-	-	15	-	-
MCNAM 24459/25 (Fig. 18C)	[m] ad	Bc	46.00	0.43	0.33	0.33	18	30			Ph	35.00	-	-	-	11	-	-
		Ph-Bc	35.00	0.37	0.34	0.34	16	21			Ph	20.00	-	-	-	15	-	-
		Ph	27.00	-	-	-	13	-			Ph	11.00	-	-	-	15	-	-
		Ph	16.00	-	-	-	13	-	MCNAM 24459/2 (Fig. 34E)	[M] juv	Bc	55.00	0.35	0.29	0.36	11	21	> 270
		Ph	11.00	-	-	-	13	-			Ph-Bc	48.00	-	-	-	11	-	-
MCNAM 24459/26 (Fig. 18D)	[m] ad	Ph-Bc	37.00	0.50	0.30	0.30	-	-			Ph	38.00	0.34	0.32	0.37	11	-	-
		Ph	28.00	0.46	-	-	17	-			Ph	23.00	-	-	-	11	-	-
		Ph	21.00	-	-	-	14	-	MCNAM 24459/4 (Fig. 34F)	[M] ad	Bc	68.00	0.37	-	0.35	16	-	> 180
		Ph	15.00	-	-	-	14	-			Ph-Bc	49.00	0.31	-	-	14	-	-
		Ph	10.00	0.43	0.42	0.32	11	-			Ph	33.00	-	-	-	15	-	-
		Ph	7.00	0.41	0.49	-	10	-	MCNAM 24459/2 (Fig. 34G)	[M]	Ph-Bc	59.00	0.41	0.34	-	16	-	-
		Ph	5.00	0.40	0.60	-	9	-			Ph	33.00	-	-	-	13	-	-
		Ph	4.00	-	0.68	-	-	-	MCNAM 24458/1 (Fig. 34B)	[m] ad	Bc	53.00	0.43	0.32	0.33	13	-	240
MCNMA 24445 (Fig. 18F)	[m] ad	Bc	49.00	0.49	0.33	0.29	17	32			Ph-Bc	37.00	0.39	-	0.29	12	-	-
		Ph-Bc	44.00	-	-	-	-	-			Ph	28.00	-	-	-	13	-	-
		Ph	37.00	-	-	-	14	-			Ph	19.00	-	-	-	14	-	-
		Ph	29.00	-	-	-	13	-			Ph	11.00	-	-	-	17	-	-
		Ph									Ph	7.00	-	-	-	20	-	-
<i>Corongoceras? steinmanni</i> (Krantz, 1926)									MCNAM 24457/1A (Fig. 35A)									
		Ph-Bc	94.00	0.49	0.30	0.29	21	39			Ph-Bc	94.00	0.49	0.30	0.29	21	39	-
		Ph	70.00	0.46	0.27	0.26	19	-			Ph	70.00	0.46	0.27	0.26	19	-	-
		Ph	45.00	-	-	-	16	-			Ph	45.00	-	-	-	16	-	-
		Ph	13.00	-	-	-	13	-			Ph	13.00	-	-	-	13	-	-

Appendix 2. Additional photographic refiguration of specimens figured or described by Steuer (1897, transl. 1921) and Weaver (1931). Figure captions at the end of this appendix.









A: *Krantziceras ellipsostomum* (Steuer, 1897), lectotype (GZG-499-75) of *Odontoceras ellipsostomum* refigured from Steuer (1897: pl. 21: -12, refigured 1921: pl. 21: 1-2), probably complete adult macroconch phragmocone from level Cieneguita-V; the white line drawn on the specimen indicates the portion originally figured, righth. **B-C:** *Substeueroeras koeneni* (Steuer, 1897); **B:** lectotype (plastic cast of GZG-499-57) of *Odontoceras koeneni* refigured from Steuer (1897: pl. 17: 1-2, refigured 1921: pl. 17: 1-2), adult phragmocone from level Cieneguita-IV; **C:** paralectotype (GZG-499-58) refigured from Steuer (1897: pl. 17: 4-5, refigured 1921: pl. 17: 4-5), phragmocone from level Cieneguita-IV (indicated in museum label). **D:** *Blanfordiceras vetustum* (Steuer, 1897), specimen (BM-377-49) refigured from Weaver (1931: pl. 56: 356-357), adult phragmocone with beginning of bodychamber from the upper Tithonian of Arroyo Curacó. **E:** *Blanfordiceras vetustum* (Steuer, 1897), lectotype (GZG-499-133) herein designated of *Hoplites subvetustus* Steuer, 1897, not figured originally, adult ?microconch with bodychamber almost complete from Rodeo Viejo, level Rodeo Viejo-III. **F:** *Corongoceras mendozanum* (Behrendsen, 1891), paralectotype (GZG-499-134) of *Hoplites subvetustus* Steuer, 1897, not figured originally, incomplete macroconch from Rodeo Viejo, level Rodeo Viejo-III. **G:** *Windhausenicerias cf. internispinosum* (Krantz, 1926), adult specimen (GZG-499-46) refigured from Steuer (1897: pl. 14: 11, refigured 1921: pl. 14: 11, under *Reineckeia cf. stephanoides* Oppel) with a quarter whorl of bodychamber from an unspecified Tithonian horizon of Arroyo de la Manga. **H:** *Windhausenicerias internispinosum* (Krantz, 1926), almost complete adult microconch (GZG-499-96), not figured originally (labelled as *Reineckeia stephanoides* Oppel), from Arroyo Cieneguita, level Cieneguita-Ia. **I:** *Physodoceras* sp., specimen (GZG-499-15) figured by Steuer (1897: pl. 14: 11, refigured 1921: pl. 5: 11) as *Aspidoceras* aff. *haynaldi* Herbich, from Arroyo Cieneguita, level Cieneguita-II. **J:** *Parodontoceras calistoides* (Behrendsen, 1891), specimen (GZG-499-64) with part of the bodychamber crushed, refigured from Steuer (1897: pl. 17: 16, refigured 1921: pl. 17: 16), probably juvenil macroconch from level Rodeo Viejo-III. **K:** *Parodontoceras calistoides* (Behrendsen, 1891), holotype by monotypy (GZG-499-48) of *Odontoceras nodulosum* Steuer (1897: pl. 15: 3-4, refigured 1921: pl. 15: 3-4), phragmocone from level Cieneguita-II. **L:** *Parodontoceras calistoides* (Behrendsen, 1891), lectotype (GZG-499-59) designated by Enay et al. (1996: 228) of *Odontoceras beneckeii* Steuer (1897: 17: 6-7, refigured 1921: pl. 17: 6-7), phragmocone with beginning of bodychamber strongly uncoiled, probably adult microconch from level Cieneguita-III. **M:** *Parodontoceras calistoides* (Behrendsen, 1891), paralectotype (GZG-499-60) of *Odontoceras beneckeii* Steuer (1897: pl. 17: 8-9, refigured 1921: pl. 17: 8-9), phragmocone with beginning of bodychamber from level Cieneguita-III. All natural size. The asterisk indicates the last septum.

STUDY OF THE CLAROMECÓ BASIN FROM GRAVITY, MAGNETIC AND GEOID UNDULATION CHARTS

Francisco RUIZ & Antonio INTROCASO



Boletín
del Instituto de
Fisiografía y Geología

Ruiz F. & Introcaso A., 2011. Study of the Claromecó Basin from gravity, magnetic and geoid undulation charts. *Boletín del Instituto de Fisiografía y Geología* 79-81: 95-106. Rosario, 01-07-2011. ISSN 1666-115X.

Abstract. - In this work we analyze crustal characteristics of Claromecó intermontane basin using gravity and magnetic anomalies, and local geoid undulations. They are:

- i) isostatic compensation (based on Airy hypothesis), related to stretching;
- ii) old sediments filling the basin, covering more than 12 km, with a density contrast value of -100 kg m^{-3} , resulting to be well balanced by an antirroot filled with upper mantle materials.

A crustal model is proposed justifying both observed Bouguer anomalies and local geoid undulations. A chart of isobath contours is builded using a quadratic equation involving sediments' thickness and local geoid undulation. Magnetic basement depth Z_T and Curie point depth Z_B are obtained using spectral analysis on a total field magnetic anomaly chart. Results show that Z_T reaches a maximum value of 12 km, whereas Z_B attains a minimum value below the Claromecó basin. The basin puts aside two different depth domains of the Curie isothermal surface: at the southwestern zone of the Ventania ranges Z_B is about 25 km, while northeast of these mountains Z_B is about 30 km.

Key-words: Claromecó sedimentary basin; Potential fields; Isostasy; Crustal model.

Resúmen. - *Estudio de la Cuenca Claromecó a partir de cartas de gravedad, magnetismo y ondulaciones del geoide.* Sobre la base de anomalías de gravedad, anomalías magnéticas y ondulaciones del geoide local determinadas en la cuenca intermontana de Claromecó, se investigaron las siguientes características corticales:

- i) existencia de compensación isostática basada en la hipótesis de Airy, lo cual se relaciona con estiramiento cortical;
- ii) la presencia de más de 12 km de sedimentos antiguos rellenando la cuenca, con un contraste de densidad de -100 kg m^{-3} , bien balanceados por una antirraíz ocupada por materiales del manto superior.

El modelo cortical encontrado puede reproducir tanto las anomalías de Bouguer como las ondulaciones del geoide local observadas. Una ecuación cuadrática que relaciona espesores sedimentarios y ondulaciones locales del geoide, nos permite definir las isobatas de la cuenca. Sobre una carta de anomalías magnéticas de campo total se llevó a cabo análisis espectral para calcular profundidades al basamento magnético Z_T y al punto de Curie Z_B . Z_T llega a un valor máximo de 12 km, mientras que Z_B alcanza valores mínimos bajo la cuenca de Claromecó. Esta cuenca separa dos dominios de profundidad diferente en la superficie de la isoterma de Curie: en la zona sudoeste de las sierras de Ventania las Z_B están en los 25 km de profundidad, mientras que al noreste de estas montañas Z_B son del orden de los 30 km.

Palabras clave: Cuenca sedimentaria Claromecó; Campos potenciales; Isostasia; Modelo cortical.

Adresses of the authors:

F. Ruiz [fruib@unsj-cuim.edu.ar]: *Instituto Geofísico Sismológico "Ing. Fernando Volponi", Universidad Nacional de San Juan, Meglioli 1160 (sur), 5400 Rivadavia, San Juan, Argentina.*

A. Introcaso: *Instituto de Física de Rosario, Universidad Nacional de Rosario and CONICET, Av. Pellegrini 250, 2000 Rosario, Argentina.*

Received: 17/03/2011; accepted: 10/05/2011

INTRODUCTION

It is well known that seismic and gravimetric methods usually produce reliable models to study sedimentary basins. In order to investigate the crustal structure of the Paleozoic Claromecó sedimentary Basin (Fig. 1), we have employed gravity, magnetic and geoid undulation charts, as well as some seismic interpretations (Kostadinoff & Prozzi 1998, Franke et al. 2002, Lesta & Sylwan 2005).

The *P*-wave velocities obtained from refraction tests on dense Paleozoic sedimentary rocks of this basin are very similar to the values determined for the underlying crystalline basement. The small differences make difficult to distinguish both units using seismic speeds exclusively (Zambrano 1974, Introcaso 1982, Ploszkiewicz 1999, Ramos & Kostadinoff 2005). This situation emphasizes the interest in using potential field methods to study the crust in this region.

In this work we build a local chart of geoid undulations for the basin. Turcotte & Schubert (2002) point out that geoid anomalies are not zero on isostatically compensated zones and they provide additional information on density versus depth distribution. These authors also note that isostatic mechanism can be inferred by comparing observed results with predictive ones (*e.g.* Airy-Pratt models). In fact, using traditional gravity methods together with local geoid anomalies, we attempt to define the isostatic compensation system and the

crustal thickness for this area. By analysing magnetic anomalies we calculate depth values for the magnetic basement and Curie point depths for the region.

The intermontane Claromecó Basin has been previously studied using gravity data (Introcaso 1982, Kostadinoff & Font 1982, Ramos & Kostadinoff 2005), or gravity perturbations (Gil et al. 1995). Introcaso (1982) presented three alternative models obtained through the inversion of Bouguer anomalies along a NNE-SSW section near the coast. One of these models showed a maximum sedimentary thickness of about 10 km. Kostadinoff & Font (1982) and Gil et al. (1995) found maximum sedimentary thicknesses of 9 km. Lesta & Sylwan (2005), using 2D seismic studies, oil exploration wells and aeromagnetic data (unpublished information of hydrocarbon exploration) produced a profile in which they assume a crystalline basement depth of more than 10 km.

All previous models have shown very thick sedimentary sequences filling the basin, but they have considered only the sedimentary rocks filling it. In this work we present a more complete model and we also give an interpretation of the whole crustal structure on which the basin could have developed.

Our model shows: (1) the presence of an attenuated crust related to the antiroot thickness and the amount of sediments necessary for isostatic equilibrium, and (2) 12 km of Palaeozoic sediments (Tankard et al. 1996) which could partly be Neoproterozoic (Ramos & Kostadinoff 2005).

GEOLOGICAL SETTING

The Claromecó Basin (Ramos 1984) is located between Tandilia and Ventania ranges in the south of the Buenos Aires Province (Fig. 1). Some authors have considered that it is an intermontane basin (López-Gamundi & Rosello 1992) or a back arc foreland basin (Lesta & Sylwan 2005). Claromecó Basin is asymmetric and has a NW-SE trending axis (Fig. 1). According to Lesta & Sylwan (2005) its onshore sector has a surface of about 50 000 km², although its offshore limits are uncertain. Its location can be approximated by zero gravity anomaly contours (Fig. 2B).

Ramos (1999a) has suggested that Claromecó Basin foundation is due to thrust loading during Devonian-Middle Permian (Chañic-Sanrafaelic tectonic phases). The Late Paleozoic Las Tunas Formation could be the result of synorogenic deposition (López-Gamundi et al. 1995). Sedimentary sequences extensively appear on both sides of the basin. The basin is mainly filled with Neopaleozoic sedimentites (Andreis et al. 1989), which crop out mainly in the Pillahuincó zone and slightly near the Tandilia hills edge (Fig. 1). It was also pointed out (Pucci 1995) that age, deformation and metamorphism of the rock units increase from east to west. Thus, it is possible that gentle deformed structures capable of trapping fluids could be present, east of the Ventania ranges (also known as Sierra de la Ventana), in the basin subsurface. This author also indicated that, west of the Tandilia hills, the basement is block faulted, thus having given rise to anticlinal structures which closures in Post-Precambrian sediments, so in the subsurface there could be traps for hydrocarbons (Lesta & Sylwan 2005).

According to Ramos (1984) the Sanrafaelic (Ventania Ranges) orogeny is a consequence of compressional tectonics that amalgamated Patagonia and Gondwana terranes. The Cape (South Africa) and Ventania Systems share documented common features (du Toit 1927, Tankard et al. 1996, Ramos 1999, 2008, Pankhurst et al. 2006), there is a growing consensus that the Ventania fold-and-thrust belt is the

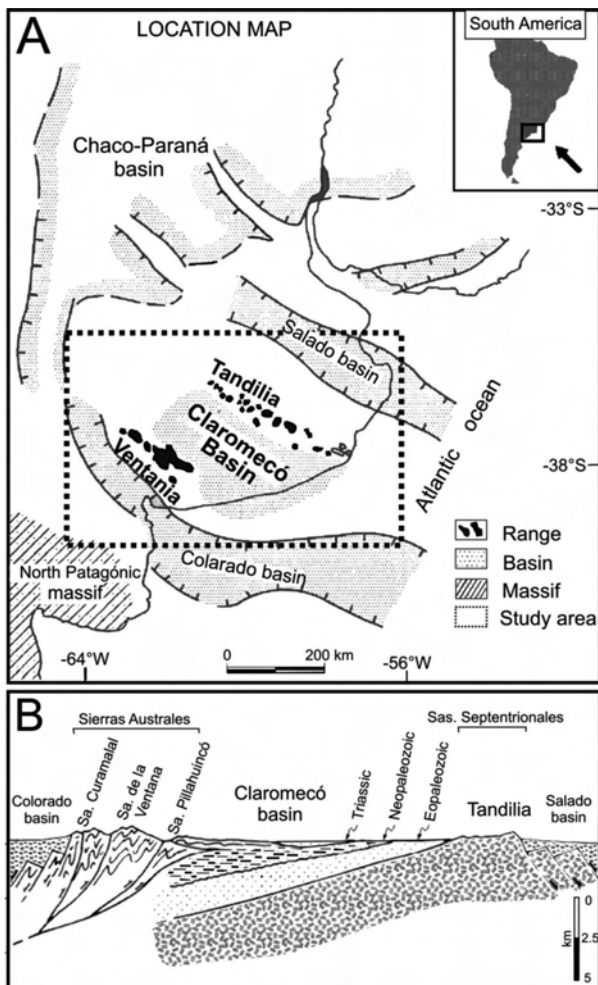


Figure 1. Location map. **A.** Geotectonic sketch map and location of the studied area (modified from Limarino et al. 1999). **B.** Schematic cross section of the Claromecó Basin (after Ramos 1999).

continuation of the Cape fold belt and that the Claromecó foreland Basin is the western end of the Karoo Basin, both of them with a thickness exceeding 10 km.

Most of the present reconstructions of the Gondwana accept that its southwest margin consisted of a continuous clastic passive margin that extended from Ventania ranges to the Cape System (Pankhurst et al. 2006, Ramos 2008). An early stage of rifting affecting the Proterozoic basement was postulated by Rapela et al. (2007), based on geochemical characteristics and the age of some 531–524 Ma granites and rhyolites interpreted as a Cambrian rift and correlated with similar rocks in the conjugate margin of South Africa. Depocenters bounded by northwest-trending normal faults have been observed in the seismic lines of the Claromecó Basin, perpendicular to the margin and correlated with this rifting (Ramos & Kostadinoff 2005). Sequences of platform orthoquartzites (Middle-Late Cambrian and Devonian times) of the Curamalal and Ventana Groups were unconformably deposited on metamorphic basement. Paleocurrent analyses of these mature sequences indicate a provenance from the northeast. A molasse sequence exposed east of the thrust front, the Pillahuincó Group, unconformably overlying the Devonian quartzites and associated with glacial deposits in the lower section has a Late Carboniferous to Early Permian age. These immature sandstones with volcanic clasts have a southwestern provenance. The changes between the stable clastic platform and these immature deposits indicate an important modification in the transport direction from NE to SW in the base, to SW to the NE in the upper section; an increase of instability in the basin, and the existence of a positive relief to the south (López-Gamundi & Rossello 1992).

The Ventania fold-and-thrust belt is characterized by isoclinal folds associated with a high strain in the orthoquartzites (Ramos 2008). The southwestern part of the belt, where the basement is exposed, has evidence of thrusts associated with low grade metamorphism constraining the deformation between Lower and Middle Permian. As a result of the thrust stacking, the Claromecó foreland Basin was formed by flexural loading of the Gondwana margin with a foredeep more than 10 km in thickness. Ramos (2008) proposed a southward subduction of the Gondwana clastic passive margin stopped after the Carboniferous. First contact between Patagonia and Gondwana may have started during the Carboniferous, but collision, deformation and uplift took place in Early Permian times. The compressive stress regime lasted in this sector of South America to the Late Permian, when a generalized extension took place.

CRUSTAL MODEL

In order to design a crustal model we have determined: (1) local geoid undulations (N_i), (2) crustal thicknesses below the Claromecó Basin, (3) Curie point depths, (4) sediments, crust and upper mantle densities, and (5) the isostatic state of the Claromecó Basin. An initial crustal model is thus proposed, and (6) double inversion of gravity anomalies (g) and local geoid undulations (N_i) is applied for improving the model.

Calculation of local geoid undulations

Perdomo & Del Cogliano (1999) have presented a geoid undulations chart of the Buenos Aires Province (Fig. 3). They have calculated geoid undulations (N) from ellipsoidal and orthometric heights ($N \approx h - H$) measured in a regular geodetic network.

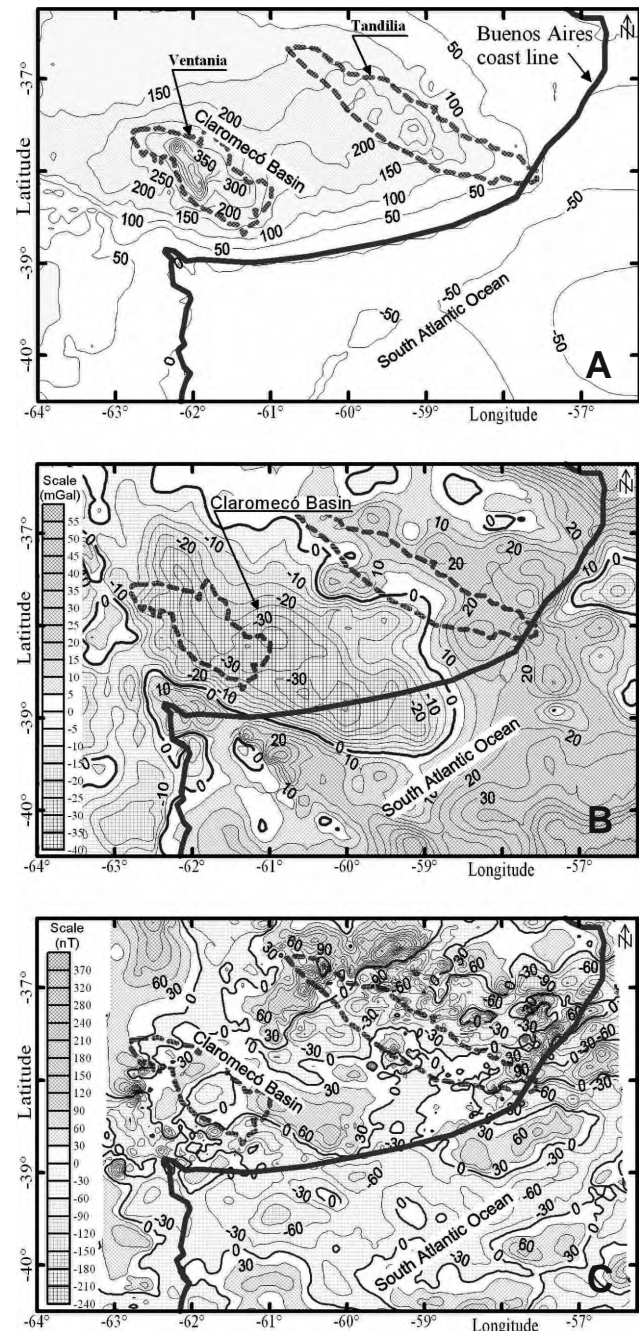


Figure 2. A. Topographic map (contour interval 50 m). B. Bouguer anomaly map (contour interval 10 mGal). C. Total magnetic anomaly map (contour interval 50 nT). Gravity data from Instituto de Física de Rosario, Instituto Geográfico Militar Argentino, Universidad de La Plata, Universidad de Buenos Aires and University of Leeds. Magnetic data from Instituto Antártico Argentino.

The arrows in Fig. 3 indicate the contour deformation tendencies over Salado Basin (S), Tandilia high (T) and Claromecó Basin (C). Undulation contours are interrupted near the coast suggesting an offshore continuation of the basin. Fig. 2B-2A corroborate this possible continuation of the basin on the continental platform. Thus, we have extended the geoid chart into the oceanic zone using the global model EGM2008 (Pavlis et al. 2008) and then we have eliminated Tandilia and Ventania ranges topo-isostatic effects of topographic masses and the corresponding compensation roots (Forsberg 1985).

For the obtention of the local geoid undulations (N_i) on

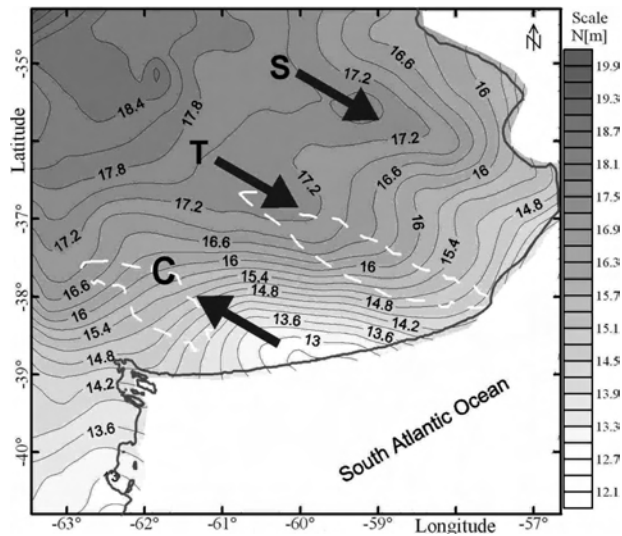


Figure 3. Geoid undulation map 'N' ($N \approx h - H$) based on Perdomo & Del Cogliano (1999), contour interval 0.3 m. Arrows indicate the deformation tendencies of the contours. Salado (S) and Tandilia (T) trends to the SE; Claromecó (C) trend to the NW.

Claromecó Basin, we have removed wavelengths (λ) larger than 500 km (studied geological structure width) applying a band pass filter ($40 \leq \lambda \leq 500$ km). Results are presented in Figure 4B.

Turcotte and Schubert (2002) have pointed out that geoid anomalies are not zero on isostatically compensated zones and they provide additional information on density versus depth distribution. On the Claromecó Basin negative N_i values have been found. In contrast, positive geoid undulations were found on the adjacent Salado and Colorado Cretaceous Basins. Introcaso (2003) has found an excess of isostatic compensation masses in the lower crust for the two latter sedimentary basins, providing arguments for the importance of the study of the Claromecó Basin deep structure.

Crustal thickness

There is no available published information on crustal thickness values for the Claromecó Basin. Franke et al. (2002) have published an integrated interpretation of multichannel reflection seismic data and a wide-angle E-W trending offshore refraction seismic line, at 40°S latitude, along the Colorado Basin axis. Results of seismic reflection measurements (Kostadinoff & Prozzi 1998, Ramos & Kostadinoff 2005) furnish some information on the sedimentary thickness. We have used the seismically derived depths published in those papers to constrain depths to crustal interfaces calculated from potential fields in the Claromecó Basin region.

Gravity anomalies 'g' (terrestrial data from the Instituto de Física de Rosario, 2001, oceanic data from GETECH, Leeds University 1995; Fig. 2B) and total magnetic field anomalies 'T' (Ghidella et al. 2002; fig. 2C) have been used to calculate sedimentary thickness, crustal depths and the geometry of regional geological structures. The following techniques have been used: (1) Fourier analysis of 'g' and 'T'; (2) 3D Euler deconvolutions of 'g' and 'T'; (3) Werner deconvolutions of 'g' and 'T'.

Fourier analysis: Crustal thickness has been calculated from Bouguer gravity anomalies and total magnetic field anomalies.

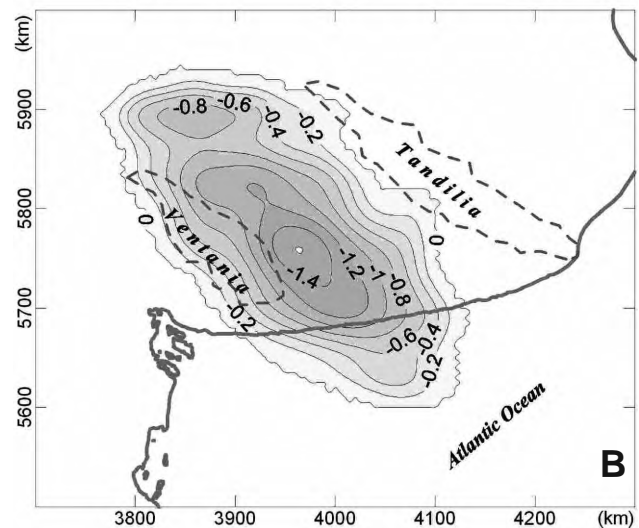
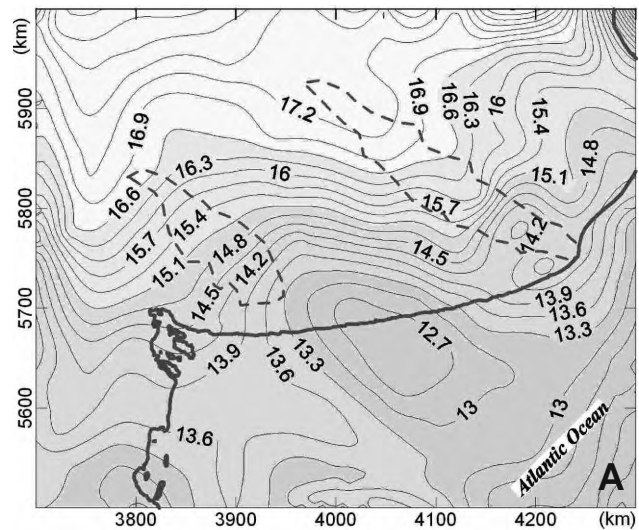


Figure 4. A. N (Perdomo & Del Cogliano 1999) extended into the ocean (EGM2008; Pavlis et al. 2008) and isostatically corrected by elevation above the geoid (mixed continental and oceanic area using equivalent sea/rock root conversion); contour interval 0.3 m; B. Local geoid undulation ' N_i ' in meters, obtained after filtering (band pass filter $40 \leq \lambda \leq 500$ km); contour interval 0.2 m.

The depth of anomalous bodies (N levels of concentration of source material at a depth z_i) has been obtained in the frequency domain from a logarithmic graph of the radially averaged power spectrum $|G(k)|$ versus wave number (k) of the observed potential field (Spector & Grant 1970, Blakely 1995):

$$|G(k)| = \sum_{i=1}^N A_i e^{-z_i|k|} + \overline{WN} \quad (\text{Eq. 1})$$

where A_i depends on the anomalous sources magnitudes and \overline{WN} corresponds to the white noise spectrum.

The long wavelengths of the gravity field have been analyzed in square windows 200 km wide, being displaced by steps of 50 km covering the area which extends from 35° to 42° S latitudes and from 56° to 64° W longitudes. From the lowest wave numbers of the power-density spectra, mean depths (to the base of the crust) have been calculated. The results are shown in Fig. 5A. Near the Claromecó Basin, crustal thicknesses of (36 ± 2) km have been obtained on land, and depths of (32 ± 2) km have been found in the offshore portion of the basin. Lowest depths to the Moho, (30 ± 2) km, have been

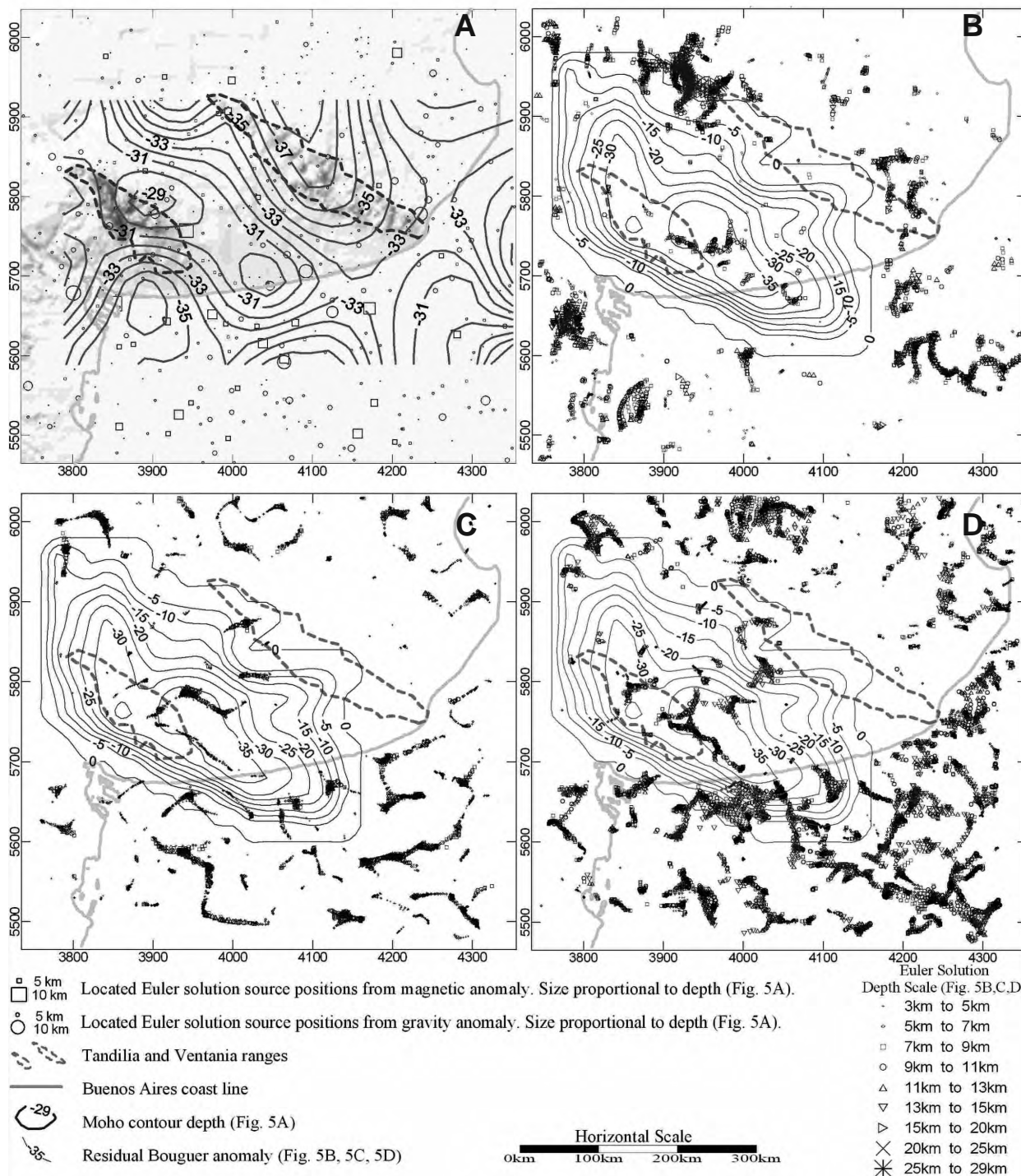


Figure 5. A. Shaded relief map of Buenos Aires Province with superimposed Moho depths obtained from spectral analysis (contour interval 1 km) and located 3D Euler solutions from magnetic data (squares) and from gravity data (circles), size proportional to depth (see references). B. Standard Euler solutions structural index SI = 1 from gravity data. C. Standard Euler solutions SI = 0 from magnetic data. D. Standard Euler solutions SI = 0.5 from magnetic data. In B, C and D residual gravity anomaly, obtained after applying a band pass filter ($20 \leq \lambda \leq 500$ km), contour interval 5 mGal.

obtained below the basin.

In the next section a spectral analysis of magnetic field anomalies has been carried out for determining the Claromec6 Basin magnetic basement thickness (Fig. 7).

3D Euler deconvolutions of 'g' and 'T': 3D Standard Euler deconvolutions (SED) and Located Euler deconvolutions (LED) have been applied to gravity and magnetic data using Oasis Montaj 6.2 software (Geosoft). The apparent depth to the

magnetic (or gravimetric) source has been automatically derived from Euler's homogeneity equation:

$$(x - x_0) \frac{\partial T}{\partial x} + (y - y_0) \frac{\partial T}{\partial y} + (z - z_0) \frac{\partial T}{\partial z} = N(B - T) \quad (\text{Eq. 2})$$

where (x_0, y_0, z_0) is the position of the magnetic (or gravimetric) source whose field (T) is detected at (x, y, z) ; B is the regional field ('g' or 'T'); N is the fall-off rate of the potential field and may be interpreted as the structural index (SI).

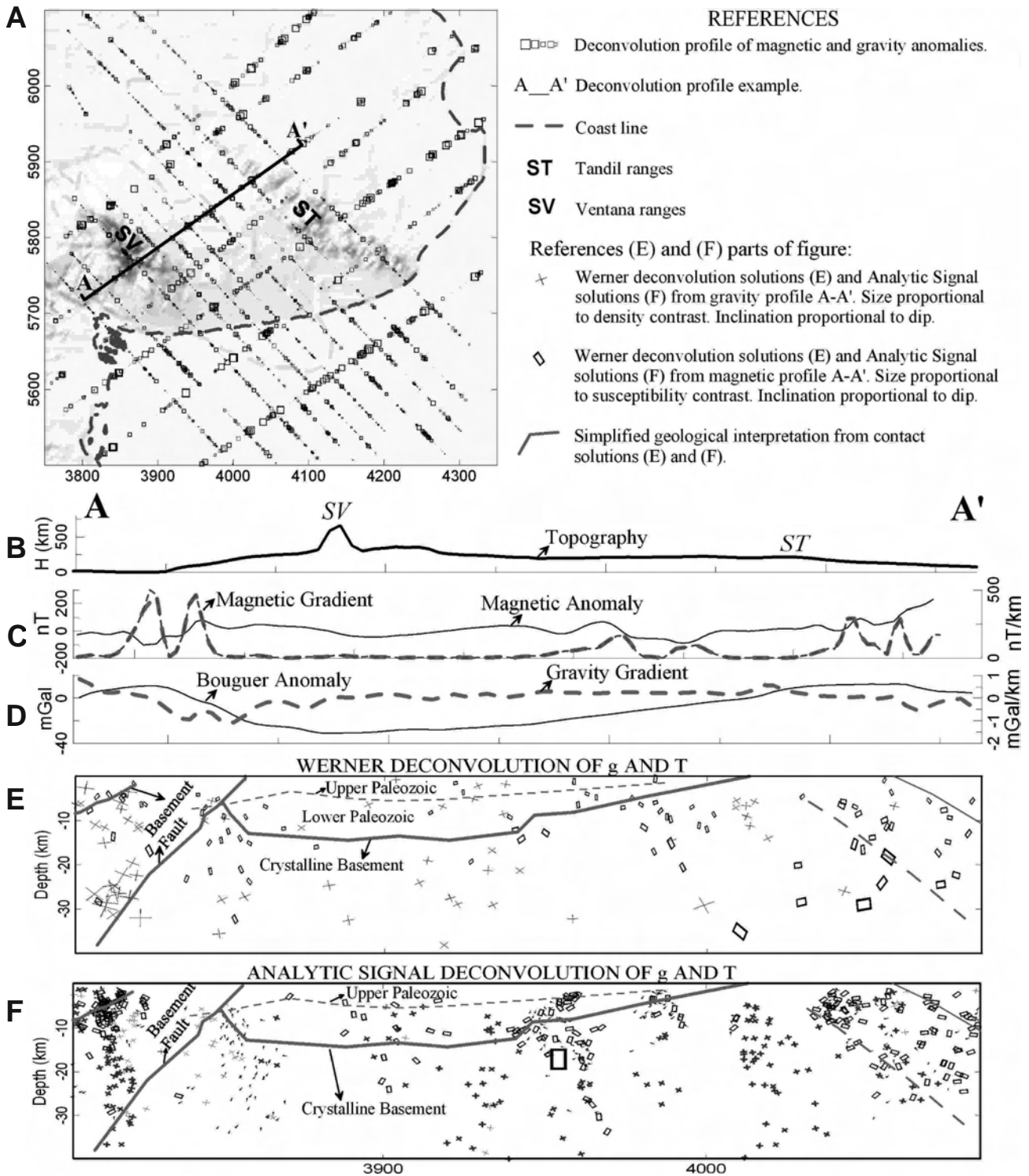


Figure 6. A. Werner and Analytic Signal deconvolutions profiles location (squares: contact solutions size proportional to depth). Deconvolutions cross section example (A-A'): Topographic profile (B); total magnetic anomaly and magnetic gradient (C). D. Bouguer anomaly and gravity gradient. E. Werner deconvolutions from gravity and magnetic data. F. Analytic Signal deconvolutions from gravity and magnetic data. In (E) and (F) interpretations of the principal geological structures.

This process relates the anomaly and its gradient components to the location of the source of an anomaly, with the degree of homogeneity expressed as a structural index (Thompson 1982).

The method consists of setting an appropriate SI value and using a least-squares inversion to solve Eq. 2 for optimum (x_0 , y_0 , z_0) and B (Reid et al. 1990). A square window size must be

specified in the gridded 'T' for to be used in the inversion at each selected solution location and then run over all the anomalies map. In SED the window should be large enough to include each solution anomaly of interest. Using LED the window size is automatically calculated using the Analytic Signal Wavelength (Nabighian 1972). Examples of appropriate models for structural index values are: a) SI = 0 to 0.5; contact

(depth to the border layer with density or susceptibility changes) and step (depth to fault step); b) SI = 1 to 1.5; dipping step, sill, dyke, cylinder and pipe; c) SI = 2 to 3; cylinder and sphere. The method allows to locate or to outline confined sources and provides a series of depth-labeled Euler trends marking edges and faults with high precision (Reid et al. 1990). The correct index for any given feature is chosen as the one giving the tightest solutions cluster.

In the present paper the regional geological structures (top of the basement geometry and deep basement faults) are described by using SED with low structural index in windows sized 30 to 45 km on 'g' and 'T' anomalies. The SED results are plotted in Fig. 5 together with the residual Bouguer anomalies obtained by a band pass filter of $50 \text{ km} \leq \lambda \leq 500 \text{ km}$. The minimum residual anomalies can be associated with the maximum sedimentary thicknesses in the Claromecó Basin.

The northwest-southeast striking basin axis (-35 mGal Bouguer anomaly) is clearly indicated towards the east zone of Ventania from 'T' with SI = 0 (contacts, Fig. 5C) and 0.5 (steps, Fig. 5D) and from 'g' anomalies with SI = 1 (dipping steps, Fig. 5B). This axis indicates maximum depths to basement from 8 km at grid node (3880, 5800), increasing to 11 and 12 km between nodes (3910, 5770) and (3940, 5740); 9 and 10 km at (4040, 5675) and gradually diminishing to 5 km at (4090, 5640) where ends this 400 km long alignment of contacts. This alignment continues offshore in the Colorado Basin domain with index of 0.5 and can be interpreted as a regional basement fault.

North of Ventania the contacts maximum depths reach 7 to 8 km at grid node (3870, 5835) and 15 km northwards the solutions cluster ends. This means that the potential fields do not include significant gradients which could indicate lack of structural complexity.

In accordance with 12 to 14 km maximum depths at (3930, 5780), contact nests 200 km long (SI = 0 and 0.5) align along a west-east strike. Their depth gradually diminishes eastwards to 7 km at (4020, 5770). Maximum depth solutions cluster agrees with the -35 mGal gravity minimum (Fig. 5B-D). At the northeastern of this structure, depth values steeply diminish, thus indicating an elevation of the basement top. These results are also based on Located Euler Deconvolutions carried out on 'g' and 'T' values (Fig. 5A) where maximum sedimentary thicknesses were placed at the axis of the basin.

Werner and Analytic Signal deconvolutions of 'g' and 'T': Werner deconvolutions (WD) and Analytic Signal depth solutions (ASD) were carried out on the magnetic and gravity fields along 18 profiles (Fig. 6A), 11 of them running from NW to SE and the other 7 running from SW to NE, using Pdepth Oasis Montaj 6.2 (Geosoft) module.

The WD (Hartman et al. 1971, Phillips 1997) and ASD (Nabighian 1972, Phillips 1997) methods for magnetic (or gravity) profiles have been widely used as part of an automated interpretation routine system. Assuming hypothetical source geometry, the Werner-based Deconvolution of the recorded field yields to a two-dimensional geologic source distribution and an associated magnetic parameter distribution: Werner's (or SA) depths, horizontal locations, dip angles, and magnetic susceptibility contrasts (Phillips 1997).

The Werner observed field solution is a good indicator of a thin-dike body. The Werner horizontal gradient solution is a good indicator of the edge of a thick interface body (contact). The use of these two extreme types of solutions lead to a close approximation to depth estimation and reveal the geometry of different magnetic (or gravimetric) bodies including those lying somewhere between a thin dike and the edge of a thick

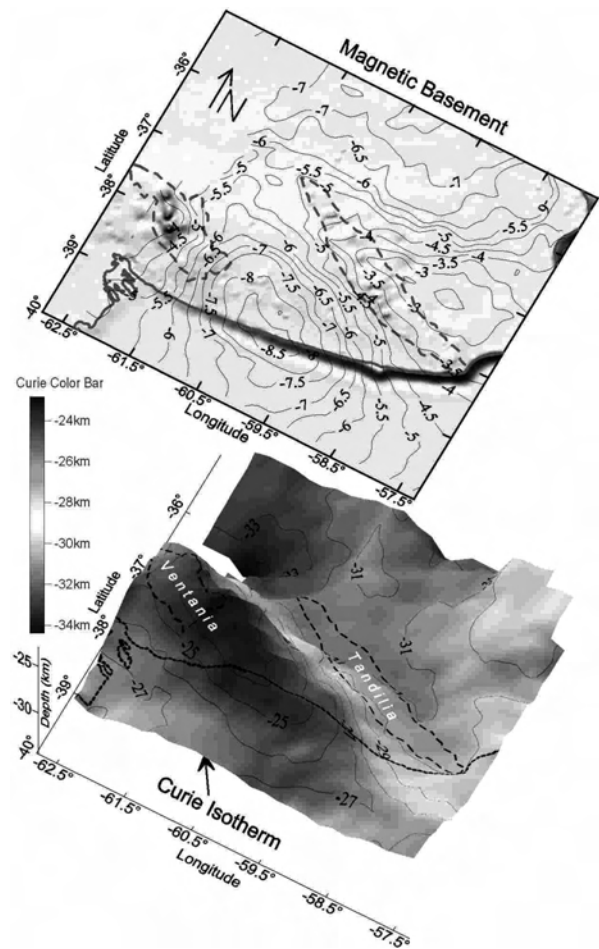


Figure 7. Spectral analysis from magnetic data. Above: magnetic basement mean depth (Z_c); contour interval 0.5 km. Below: Curie isotherm depth (Z_0); contour interval 1 km.

interface (Ku & Sharp 1983). Contact solutions on all the profiles have been analyzed. Claromecó Basin boundaries are clearly identified and regional structures have been enhanced, especially the basement depth (see section A-A' taken as an example in Fig. 6).

Sweeping deconvolution operator along each field profile, different series of solutions can be estimated. Depths are indicated by crosses (from g) and rectangles (from T) respectively with the same dip angles of each solution (dip angle of the body interface), and susceptibility (or density) contrasts proportional to the symbol size (Fig. 6E-F).

Basement outcrops located westwards Ventania ranges make up the western limit of the basin, also defined by the southwest dipping basement fault interpreted in Fig. 6E-F. On the eastern border of the profile we interpret two faults dipping to the east in the Tandilia basement.

Maximum sedimentary depths have been analyzed by separating less than 0.002 emu susceptibilities contact solutions. These solutions are located below and eastwards Ventania ranges and the thickness thereby obtained gradually diminish eastwards and wedge out to the west of the Tandilia Hills. Below Ventania ranges the contact solutions found indicate depths over 12 km.

Subhorizontal top of Analytic Signal solutions are interpreted as Neopaleozoic sediment depths according to Lesta and Sylwan (2005).

A large concentration of contact solutions at progressive 3950 km are interpreted as a structural step in the basement (Fig. 6E-F).

Curie Point Depth

Upper and lower boundaries of the magnetized crust have been obtained from spectral analysis of magnetic anomalies. We have assumed lowest depths obtained for the magnetized crust as corresponding to Curie point depths (Blakely 1995). Frost & Shive (1986) have shown that crustal magnetic sources must lay at a depth in which temperature is high enough for the magnetite to become paramagnetic, *i.e.*, 578°C. Deviation from the Curie point temperature indicates distortion of the thermal structure of the lithosphere (Ruiz & Introcaso 2004).

We have used a method (Ruiz & Introcaso 2004) modified from Tanaka et al. (1999). Upper boundary (Z_1) and the centroid (Z_c) of the magnetic basement (crustal magnetic plate) have been determined from the total-field anomaly power-density spectra. The bottom of the plate (Curie point depth) has been determined as: $Z_b = 2Z_c - Z_1$, where Z_1 can be interpreted as the mean upper boundary of the crystalline basement. It has been determined by using the relationship $\ln[\Phi_{\Delta T}(k)^{1/2}] = \ln A - |k| Z_1$. Besides, the relationship $\ln\{[\Phi_{\Delta T}(k)^{1/2}]/|k|\} = \ln B - |k| Z_c$, has been used to determinate the centroid depth $|\Phi_{\Delta T(k)}|$ is the power-density spectra of magnetic anomalies; k is the wave number; A and B are constants related to magnetic masses. Z_1 and Z_c are estimated by fitting a linear function to the high-wave number and low-wave number parts of the respective logarithms of radially averaged spectrum.

The spectral analysis has been carried out in 300 square windows 175 km side. Steps of displacement are 25 km along the longitude and 50 km along the latitude, covering the whole studied area (which extends from 34°30' S to 40°30' S and from 56°45' W to 63°25' W). Calculated Z_1 and Z_b have been referred to each window centre. Fig. 7 shows mean depths to magnetic basement, reaching 9 km at the south of Ventania.

Results are interesting as they show Curie isothermal significant changes on both sides of the Claromecó Basin axis (Fig. 7). Z_1 depths at the north of the basin are about (31 ± 2) km and below maximum sedimentary thickness Z_b reaches 23 km depth, increasing to 27 km at the basin southwest.

In summary, from the above analysis, we can say that the Claromecó Basin has more than 10 km of sedimentary loading and is set on an attenuated crust with a shallower Curie isotherm below Ventania ranges.

Crust and Upper Mantle densities

In the selection of densities we have taken into account that Zambrano (1974), based on YPF Petroleum Company refraction seismic data, has informed that compression wave velocities V_p of Paleozoic sediments in the basin are very similar to those of the crystalline basement. On the other hand, Zambrano (1974) has concluded that the sedimentary load is very thick. Introcaso (1982) has pointed out that old sediments have suffered strong compression. It seems that these sediments are very compact and dense because of this compression, with an incipient metamorphism. This fact justifies the high velocities V_p found which makes hard to separate sediments from the crystalline basement on the sole basis of seismic velocities. On the other side, the gravimetrical method allows us to justify Bouguer anomalies of -30 mGal from a combination of low negative density contrasts between sediments and crystalline basement, as it was suggested by

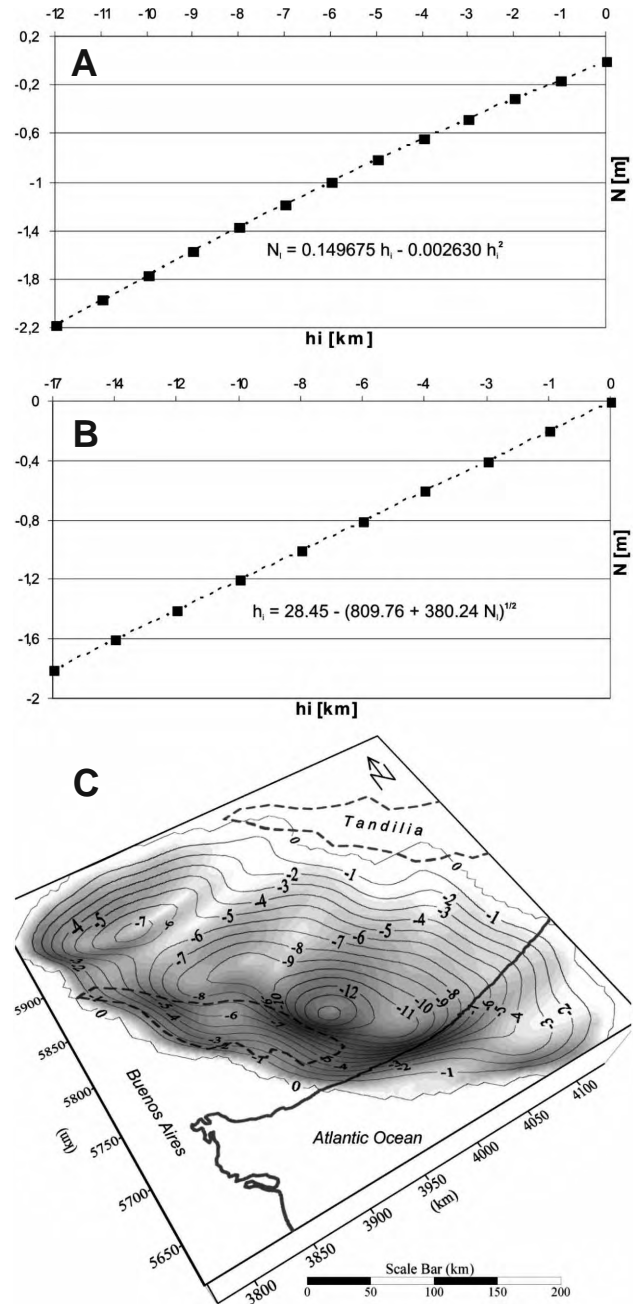


Figure 8. Geoid undulation due to a sedimentary basin isostatically compensated in the Airy system. Density contrasts: $\Delta\sigma_s = -100 \text{ kg m}^{-3}$ and $\Delta\sigma_m = 400 \text{ kg m}^{-3}$, normal crustal thickness 35 km, antiroot $R = 0.25 h_i$, where h_i is the sedimentary thickness of the basin. **A:** Initial crustal model $N_i = 0.149675 h_i - 0.002630 h_i^2$; **B:** Quadratic expression $h_i = -8.45 + (809.76 + 380.24 N_i)^{1/2}$; **C:** Sedimentary thickness of a basin isostatically compensated obtained from **(B)** and Fig. 4B.

seismic results and by the high sedimentary thicknesses.

Using the gravimetric method, considered appropriated to obtain preliminary interpretations, Introcaso (1982) has found a thickness of (10 ± 4) km assuming density contrasts of $\Delta\sigma_s = -(70 \pm 30) \text{ kg m}^{-3}$; Kostadinoff & Font (1982) have found 8 km of sedimentary thickness assuming a density contrast of $\Delta\sigma_s = \sigma_s - \sigma_c = -100 \text{ kg m}^{-3}$ between sediments (σ_s) and crystalline basement (σ_c).

It is well known that there exists a relationship between

compression wave velocities V_p and densities σ (Woollard 1959, Brocher 2005). From recent seismic reflection and airborne gravity surveys and well studies, Lesta & Sylwan (2005) have found more than 10 km sedimentary thickness, indirectly confirming the density contrast previously assumed. These results have been maintained on strict confidentiality by petroleum exploration companies.

It is important to point out that all the models mentioned above are significantly incomplete since they only take into account the highest part of the upper crust. The model we present in this work involves the whole crust, adding another density contrast: lower crust-upper mantle. Lacking deep seismic data (Moho and subMoho) we have assumed $\Delta\sigma_m = \sigma_m - \sigma_{lc} = +400 \text{ kg m}^{-3}$ following studies in nearby regions: (i) Salado Basin (Introcaso & Ramos 1984, Introcaso et al. 2002) and (ii) Colorado Basin (Introcaso 2003). Note that this density contrast is positive because lower crustal attenuation implies materials ascend from lithospheric mantle into the crustal antiroot.

According to the results obtained in the present study we assume: (1) the crust has been attenuated by extensional processes; (2) density contrasts are -100 kg m^{-3} (top of the upper crust-infill sediments) and $+400 \text{ kg m}^{-3}$ (antiroot in lower crust). Using these data we analyze: (i) isostatic state of the basin; (ii) the possibility of quickly obtaining the geometry of the basin (basement isobaths) in view of its isostatic compensation; Haxby and Turcotte (1978) formulas can be employed; (iii) crustal model obtained by double inversion.

Isostatic state of the basin

It has been noted above that the Claromecó Basin is emplaced on an attenuated crust. If there are isostatic equilibrium at crust level, the mass deficit produced by sedimentary load m_s should be balanced by the mass excess of the upper mantle m_m lodged in the antiroot. In this case:

$$|-m_s| = m_m \quad (\text{Eq. 3})$$

The isostatic anomaly AI is obtained by correcting Bouguer anomaly AB by the gravity effect originated by sediments C_s ; then it is necessary to make the correction corresponding to gravity effect of a hydrostatically compensated antiroot model C_m (Introcaso 1993). Then

$$AI = AB + C_s - C_m \quad (\text{Eq. 4})$$

C_s can be computed if density contrast (in this case $+100 \text{ kg m}^{-3}$) and basin geometry are known. In former publications the basin limits were established by Tandilia and Ventania, but the subsurface information was insufficient. Although gravity maps (Fig. 2B) suggest its continuation into the continental platform, NW and SE borders were not well defined (Introcaso 1982, Kostadinoff & Font 1982, Ramos 1984, López-Gamundi & Rosello 1992, Pucci 1995, Lesta & Sylwan 2005, Ramos 2008).

The Local geoid Nl map presented in Fig. 4B can be used to characterize the whole basin. Haxby & Turcotte (1978) pointed out that geoid anomalies could have negative values on isostatically compensated basins (Airy or Pratt models). Thus we have started assuming isostatic balance for the initial model. Simultaneous work with AB and N_l is useful for the analysis of masses balance.

We have used Turcotte & Schubert (2002) models to calculate geoid undulations N_l in Pratt and Airy systems.

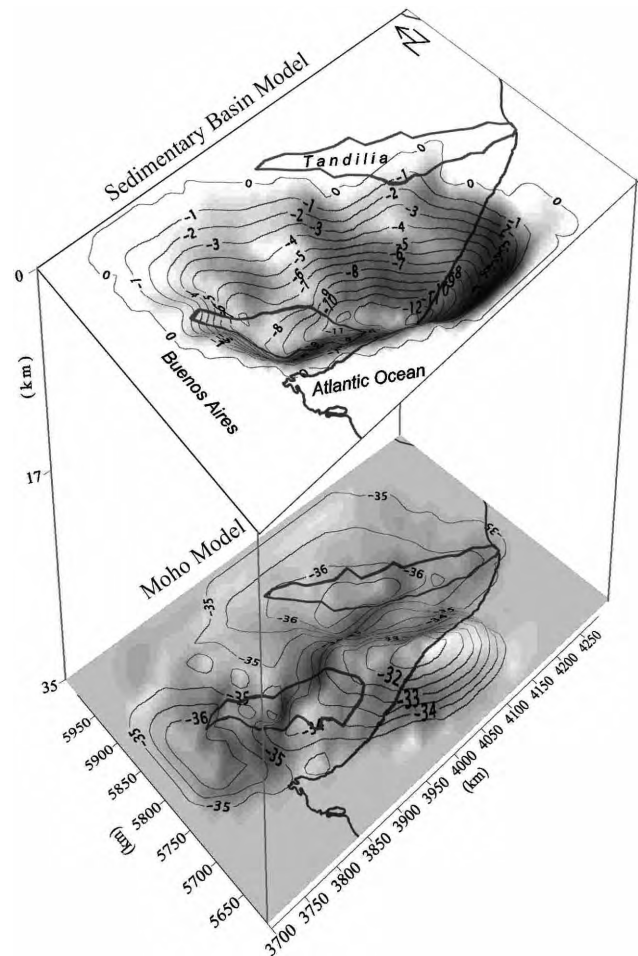


Figure 9. Crustal 3-D gravity-potential model obtained by double inversion. Sedimentary basin model (upper part) in km with root below the ranges and antiroot below the Claromecó Basin (lower part). Inversion model calculated in the Airy system in isostatic equilibrium (see text); density contrasts $\Delta\sigma_s = -100 \text{ kg m}^{-3}$ and $\Delta\sigma_m = 400 \text{ kg m}^{-3}$.

According to crustal attenuation found by stretching, we have adopted the Airy system assuming 35 km crustal thickness (before stretching) and differential densities -100 kg m^{-3} (sediments-basement) and $+400 \text{ kg m}^{-3}$ (upper mantle-lower crust density). Antiroot thickness is $R = (\sigma_c - \sigma_s / \sigma_m - \sigma_{lc}) h_i = 0.25 h_s$, where h_i is the sedimentary thickness of the basin (unknown variable). With these values, Turcotte & Schubert (2002) expressions provide (see Fig. 8A and 8B):

$$Nl = 0.149675 h_i - 0.002630 h_i^2 \quad (\text{Eq. 5})$$

$$h_i = 28.45 - (809.76 + 380.24 Nl)^{1/2} \quad (\text{Eq. 6})$$

Dipolar expressions used have a good performance if the analyzed structure width is much smaller than the Earth radius (Doin et al. 1996).

Geoid undulations shown in Fig. 4B used in Eq. 6 allowed us to obtain the basement isobaths map h_i shown in Fig. 8C. Maximum sedimentary thickness reaches 12 km. These values agree with the depths to basement obtained from spectral analysis, 3D Euler deconvolutions and Werner and Analytic Signal deconvolutions in the present paper.

Double inversion model

In order to validate the isostatic model presented in Fig. 8C, we have carried out a double inversion model from Bouguer anomalies and geoid undulations of the crust in the basin region. The model calculated by direct method from an initial crustal compensated model (Fig. 8C) has been compared with the observed values of gravity anomaly AB and geoid undulations N_i and modeled by trial and error. Computations were made following gravity and geoid expressions of Guspí et al. (1987), Guspí (1999), Introcaso (1999), Guspí et al. (2004) and Introcaso & Crovetto (2005). In the modeling process, depths to the basement values calculated on crustal thickness (see Crustal thickness above) were incorporated to make the model anomalies fit to the observed values of AB and N_i .

Double inversion model (Fig. 9) reveals both the basin geometry and the Moho geometry. Crustal thickness below the basin reaches 32 km to the Southeast, and theoretical root below Tandil ranges reaches 37 km. This model shows reasonable correlation with the Moho depths calculated from spectral analysis.

Fig. 10 exhibits negligible isostatic anomalies over the basin, thus a reasonable masses balance in the basin region could be inferred.

It is worth to note that considering local geoid values and Bouguer anomalies for the obtention of crustal features and isostatic balance state, the consistency of the model is reinforced.

If direct faults are assumed to have existed previous to the sedimentation (Cobbold et al. 1986, Ramos 2008), crustal attenuation (shown in this work) and sedimentary load increment produced by tectonic stacking (Jordan 1981, Ramos 2008), a series of sedimentary and subsidence pulses can be generated (Introcaso 1980, Introcaso & Ramos 1984), converging to:

$$H = h \left(1 - \frac{\sigma_s}{\sigma_m} \right)^{-1} \quad (\text{Eq. 7})$$

using stretching $\beta = 1.7$. In Eq. 7, H is the modern maximum sedimentary thickness (≈ 12 km); σ_s and σ_m are sediment and upper mantle densities (2570 kg m^{-3} and 3300 kg m^{-3} , respectively), and h is the initial graben infill thickness. With these values it is obtained 2.6 km for h and $35 - 2.6 - (35/\beta) = 12$ km for the antiroot R .

Assuming a hypothetical horizontal spinning axis located at the middle of the crust (Fig. 9) and rotating 180° the crustal model, we can roughly obtain: (a) the upper boundary of the basement in the upper crust, and (b) Moho discontinuity in the lower crust. Both discontinuities, (a) and (b), characterize the crustal thickness previous to the sedimentation.

DISCUSSION

Few geophysical interpretations concerning the Claromecó Basin have been published, most of which cover only parts of the basin area. In recent years Oil Industry has carried out some exploration, but the results obtained are kept hidden.

In the present work, the authors have used results of the potential fields observed to tentatively solve some geophysical and geologic problems in this basin.

The geometry of the Claromecó Basin can be analyzed from the residual Bouguer anomaly chart (Fig. 5). Largest sedimentary thicknesses are generally correlated with gravimetric minima. Local geoid undulations calculated (Fig.

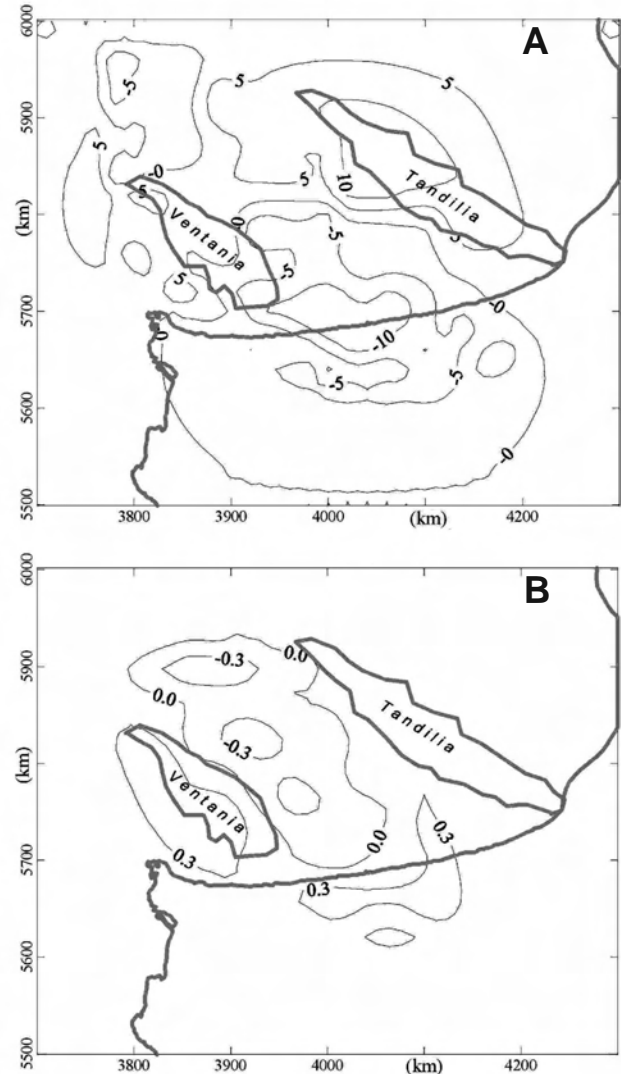


Figure 10. A. Isostatic anomaly from 3D crustal model (expression: $AI = AB + C_s - C_m$). B. The same as in A but with local geoid undulations, N_i (Fig. 4B) minus geoid effects of the crustal model (Fig. 9).

4) have given minimal values agreeing with less dense rocks (Fig. 8C).

The present authors calculations indicate that the maximum depths to the crystalline basement are about 12 km. Moreover, the largest sedimentary thicknesses are located beneath the Ventania ranges, gradually thinning eastwards. Then they wedge out at the western margin of the Tandilia hills (Fig. 6).

A regional fault associated with the Ventania axis has been interpreted. This fault surface dips SW and affects the whole crust (Figs. 5 and 6). The fault zone, 50 km wide, extends along 600 km. In the eastern area of the basin the crustal structures tend to dip NE (Fig. 6E-F).

Euler deconvolutions with low structural indices have given signs of discontinuities, especially in the crystalline basement (Fig. 5), also showing depth of this basement, indicating its main structures: faults and steps (Fig. 5B and 5D) and discontinuities in the basement (Fig. 5C).

The previously analyzed indicators have given information on the middle and upper crust. Nevertheless, the local geoid undulations, analyzed according to Turcotte and Schubert (2002), point out the existence of isostatic compensation in Airy's hypothesis, and a consequent attenuated crust beneath

the basin. This approach does not agree with the foreland model, which is the generally accepted as a geological model to explain the development of the Claromecó Basin (Ramos 1984, 1999a), unless crustal thinning could be a feature that has not been completely erased by the superposition of successive tectonic events during the evolution of the basin.

Respect to the lower crust, long wavelengths of gravimetric and magnetic anomalies have been analyzed. Spectral analysis on the gravimetric data indicates a crustal attenuation beneath the basin (Fig. 5A). The depth to the Curie isotherm is lower also under the highest sedimentary thicknesses of the basin.

A robust cortical model representing the entire crust could be proposed by inverting simultaneously Bouguer anomalies and local geoid undulations. In our model, calculated sedimentary thickness and the antiroot in Airy System (Fig. 9) are isostatically balanced. Sedimentary depths in this model are consistent with those calculated with Euler and Werner deconvolutions.

Moho discontinuity depth obtained by spectral analysis is also consistent with the model (Fig. 5A). Differences were found in the NE sector of Ventania, probably due to the lack of gravimetric data.

Considering a stretching mechanism to explain the development of Claromecó Basin, Eq. 6 can be used to obtain sedimentary load subsidence. This subsidence should have started with a sedimentary thickness of 2.6 km and an antiroot of 12 km. This is the mirror image of the present day crust.

Such a hypothesis can be viewed as excessively simplified. According to what we have just mentioned, the geologic history of the region is very complex and the model presented in this paper might seem to support the rift origin of the Claromecó Basin (Tankard et al. 1996, Pankhurst et al. 2006). Nevertheless results obtained for upper crust are fully consistent with the foreland basin model (Ramos 1984, 2008).

The small crustal attenuation found could be explained also by extensional processes subsequent to the basin foundation, which would have taken place during the Gondwanaland breakup cycle. The modelled Moho geometry is not a clear evidence of the amalgamation of two different thickness crusts in the Tandilia hills as proposed by Ramos (1999b).

CONCLUSIONS

We have prepared a complete local geoid undulations map for the Claromecó intermontane Basin, in order to study its crustal features and isostatic balance. Studying it, together with the Bouguer and magnetic anomalies, we have found that:

- (1) The basin is set on a crust with a smooth antiroot, and it is about 12 km thick. Sediments are mainly Paleozoic in age.
- (2) Curie isotherm below the Claromecó Basin is lower than below the basin rims, confirming the crustal attenuation beneath the basin.
- (3) The basin is isostatically balanced in the Airy system, with a relation 4 to 1 between sedimentary thickness and antiroot height.
- (4) From the current model and assuming additional sedimentary load for tectonic stacking as the principal subsidence mechanism, it can be concluded that the sedimentation of the basin could have began with the formation of a graben about 2.6 km thick, and with an antiroot whose thickness could have been about the same as the actual

sedimentary thickness.

(5) The top of the basement geometry and deep basement faults were described by using Euler and Werner deconvolutions obtained from gravity and magnetic data.

(6) A simple relationship between local geoid undulations and basement isobaths depths was obtained. This relationship can be used to establish the basin boundaries and sedimentary thickness.

(7) By using a Bouguer anomaly chart together with a local geoid undulations chart the probabilities of obtaining a consistent model are increased. In our model, the calculated sedimentary thickness and Moho depths are consistent with those obtained from the spectral analysis, Euler and Werner deconvolutions.

Acknowledgements

This work was partially supported by grants from the Agencia Nacional de Promoción Científica y Tecnológica and CONICET: "Estudio del margen continental argentino y áreas adyacentes con métodos geopotenciales" (PICT2002-00166), "Estudio de la evolución futura de cuencas sedimentarias (continuación)" (PIP 03056) and "Tectónica en la Argentina con datos satelitales GOCE" (PICT2007-01903) respectively. CICITCA of Universidad Nacional de San Juan collaborated in this research. Thanks are given to Dr. Pedro Lesta because of his important suggestions and Dr. Marta Ghidella for magnetic data and her suggestions. Dr. Mario E. Gimenez (Universidad Nacional de San Juan) and a further anonymous referee, as reviewers of the journal, helped us in improving the manuscript.

REFERENCES

- Andreis R., Iñiguez A., Lluch S. & Rodríguez S., 1989. Cuenca paleozoica de Ventania, Sierras Australes, Provincia de Buenos Aires. In: G. Chebli & L.A. Spalletti. (eds.): *Cuencas Sedimentarias Argentinas. Serie Correlación Geológica* 6: 265-298.
- Blakely R.J., 1995. *Potential theory in gravity and magnetic applications*. Cambridge University Press, New York, p. 441.
- Brocher T.M., 2005. Empirical Relations between Elastic Wavespeeds and Density in the Earth's Crust. *Bulletin of the Seismological Society of America* 95(6): 2081-2092.
- Cobbold P., Massabie A. & Rossello E., 1986. Hercynian wrenching and thrusting in the Sierras Australes foldbelt, Argentina. *Hercynica* 112: 135-148.
- Doint M., Fleiteau L. & McKenzie D., 1996. Geoid anomalies and the structure of continental and oceanic lithospheres. *Journal Geophysical Research* 101: 16119-16135.
- Du Toit A., 1927. A geological comparison of South America with South Africa. With a paleontological contribution by F. Cowper Reed. *Carnegie Institute of Washington* 381: 1-158.
- Franke D., Neben S., Hinz K., Meyer H. & Schreckenberger B., 2002. Deep crustal structure of the Argentine continental margin from seismic wide-angle and multichannel reflection seismic data. *AAPG Hedberg Conference. Hydrocarbon Habitat of Volcanic Rifted Passive Margins*, p. 4. http://www.searchanddiscovery.net/abstracts/pdf/2002/hedberg_norway/extended/ndx_franke.pdf
- Forsberg R., 1985. Gravity Field Terrain Effect Computations by FFT. *Bulletin Geodesique* 59: 342-360.
- Frost B. and Shive P., 1986. Magnetic mineralogy of the lower continental crust. *Journal Geophysical Research* 91: 6513-6521.
- Ghidella M.E., Köhn C. & Gianibelli J.C., 2002. Low Altitude Magnetic Anomaly Compilation in Argentina: its Comparison with Satellite Data. *American Geophysical Union, 2002 Spring Meeting*.
- Gil M., Font G. & Usandivaras J.C., 1995. Modelado de estructuras profundas a partir de datos satelitales. *Actas de las IV Jornadas Geológicas y Geofísicas Bonaerenses* (Buenos Aires) 2: 117-124.

- Guspi F., 1999. Fórmulas compactas para el cálculo del potencial gravitatorio de prismas rectangulares. *In: Contribuciones a la geodesia en la Argentina de fines del siglo XX. Homenaje a O. Parachú*. UNR Editora (Rosario): 129-133.
- Guspi F., Introcaso A. & Introcaso B., 2004. Gravity-enhanced representation of measured geoid undulations using equivalent sources. *Geophysical Journal International* **158**: 1-8.
- Guspi F., Introcaso A. & Huerta E., 1987. Calculation of gravity effects of three-dimensional structures by analytical integration of a polyhedral approximation and application to the inverse problem. *Geofísica Internacional* **26**: 407-428.
- Hartman R.R., Teskey D. J. & Friedberg J.L., 1971. A system for rapid digital aeromagnetic interpretation. *Geophysics* **36**: 891-918.
- Haxby W. F. & Turcotte D.L., 1978. On isostatic geoid anomalies. *Journal Geophysical Research* **83**: 5473-5478.
- Introcaso A., 2003. Significativa descompensación isostática en la Cuenca del Colorado (República Argentina). *Revista de la Asociación Geológica Argentina* **58(3)**: 474-478.
- Introcaso A., 1999. Introducción a la inversión desde las ondulaciones del geode. *In: Contribuciones a la geodesia en la Argentina de fines del siglo XX. Homenaje a O. Parachú*. U.N.R. Editora (Rosario): 135-164.
- Introcaso A., 1993. Predicción del movimiento vertical de una cuenca sedimentaria utilizando el método gravimétrico. *Actas del XII Congreso Geológico Argentino* **1**: 1-4.
- Introcaso A., 1982. Resultados gravimétricos sobre las cuencas de la Provincia de Buenos Aires y zonas vecinas. Instituto de Física de Rosario (Rosario): 1-36.
- Introcaso A. 1980. A gravimetric interpretation on the Salado Basin (Argentina). *Bolletino di Geofisica Teorica ed Applicata (Trieste)*: **87**: 187-200.
- Introcaso A. & Crovetto C., 2005. Introducción a la construcción del geode. *Temas de Geociencias* **12**: 1-56.
- Introcaso A., Guspi F. & Introcaso, B., 2002. Interpretación del estado isostático de la cuenca del Salado (Provincia de Buenos Aires) utilizando un geode local obtenido mediante fuentes equivalentes a partir de anomalías de Aire Libre. *Actas del XV Congreso Geológico Argentino (El Calafate, Argentina)*. CD-ROM: 1-4.
- Introcaso A. & Ramos V., 1984. La cuenca del Salado: un modelo de evolución aulacogénico. *Actas del IX Congreso Geológico Argentino. Tectonofísica en áreas cratónicas móviles* **3**: 27-46.
- Jordan T., 1981. Thrust loads and foreland basin evolution, Cretaceous, western United States. *American Association of Petroleum Geologists Bulletin* **65**: 2506-2520.
- Kostadinoff J. & Prozzi C., 1998. Cuenca de Claromecó. *Revista de la Asociación Geológica Argentina* **53**: 461-468.
- Kostadinoff J. & Font G., 1982. Cuenca Interserrana Bonaerense, Argentina. *Actas del V Congreso Latinoamericano de Geología, Buenos Aires* **IV**: 105-121.
- Ku C.C. & Sharp J.A., 1983, Werner deconvolution for automated magnetic interpretation and its refinement using Marquart's inverse modeling. *Geophysics* **48(6)**: 754-774.
- Lesta P. & Sylwan C., 2005. Cuenca de Claromecó. *Actas del VI Congreso de Exploración y Desarrollo de Hidrocarburos, IAPG (Mar del Plata)*: 217-231.
- Limarino C., Massavie A., Rossello E., Lopez-Gamundi O., Page R. & Jalfin G., 1999. El Paleozoico de Ventania, Patagonia e Islas Malvinas. *In: R. Caminos (Ed): Geología Argentina. Anales del Servicio Geológico Minero Argentino* **29**: 319-348.
- López-Gamundi O., Conaghan P., Rossello E. & Cobbold P., 1995. The Tunas Formation (Permian) in the Sierras Australes foldbelt, East-Central Argentina: evidence of syntectonic sedimentation in a Variscan foreland Basin. *Journal of South American Earth Sciences* **8(2)**: 129-142.
- López-Gamundi O. & Rosello E., 1992. La cuenca Interserrana de Claromecó, Argentina: un ejemplo de cuenca de antepaís hercínica. *Actas del 8° Congreso Geológico Latinoamericano* **I**: 55-59.
- Nabighian M., 1972. The analytic signal of two-dimensional magnetic bodies with polygonal cross-sections: Its properties and use for automated anomaly interpretation. *Geophysics* **37**: 507-517.
- Pankhurst R.J., Rapela C.W., Fanning C.M. & Márquez M., 2006. Gondwanide continental collision and the origin of Patagonia. *Earth-Science Reviews* **76**: 235-257.
- Pavlis N., Holmes S., Kenyon S. & Factor J., 2008. An Earth Gravitational Model to Degree 2160: EGM2008. *EGU General Assembly 2008 Presentation, European Geosciences Union General Assembly, Vienna, April 13-18, 2008*. <http://earth-info.nga.mil/GandG/wgs84/gravitymod/egm2008/index.html>
- Perdomo R. & Del Cogliano D., 1999. The geoid in Buenos Aires region. *International Geoid Service Bulletin (Special Issue for South America)* **9**: 109-116.
- Phillips J. D., 1997. Potential-field geophysical software for PC, version 2.2: *U.S.G.S. Open-File Report* **97-725**.
- Ploszkiewicz J.V., 1999. ¿Será Buenos Aires una nueva provincia petrolera? Antecedentes, hipótesis y certezas. *Boletín de Informaciones Petroleras, June 1999 (Buenos Aires)*: 36-45.
- Pucci J.C., 1995. Argentina's Claromecó Basin needs further exploration. *Oil-Gas Journal, September 1995 (Buenos Aires)*: 93-96.
- Ramos V., 2008. Patagonia: A paleozoic continent adrift? *Journal of South American Earth Sciences* **26**: 235-251.
- Ramos V., 1999a. Las provincias geológicas del territorio argentino. *In: R. Caminos (Ed): Geología Argentina. Servicio Geológico Minero Argentino, Anales* **29**: 41-96.
- Ramos V., 1999b. Rasgos estructurales del territorio argentino. Evolución tectónica de la Argentina. *In: R. Caminos (Ed): Geología Argentina. Servicio Geológico Minero Argentino, Anales* **29**: 715-784.
- Ramos V., 1984. Patagonia: un continente a la deriva?. *Actas del IX Congreso Geológico Argentino* **2**: 311-328.
- Ramos V.A. & Kostadinoff J., 2005. La cuenca de Claromecó. *In: R. E. de Barrio, R. O. Etcheverry, M. F. Caballé, E. Llambías (eds.), Geología y recursos minerales de la Provincia de Buenos Aires. Relatorio del 16° Congreso Geológico Argentino*: 473-480.
- Rapela C.W., Pankhurst R.J., Casquet C., Fanning C.M., Baldo E.G., González-Casado J.M., Galindo C. & Dahlquist J., 2007. The Río de la Plata craton and the assembly of SW Gondwana. *Earth-Science Reviews* **83**: 49-82.
- Rapela C.W., Pankhurst R.J., Fanning C.M. & Grecco L.E., 2003. Basement evolution of the Sierra de la Ventana Fold Belt: new evidence for Cambrian continental rifting along the southern margin of Gondwana. *Journal of the Geological Society (London)* **160**: 613-628.
- Reid A., Allsop J., Granser H., Millett A. & Somerton I., 1990. Magnetic interpretation in three dimensions using Euler Deconvolution. *Geophysics* **55**: 80-91.
- Ruiz F. & Introcaso A., 2004. Curie point depths beneath Precordillera Cuyana and Sierras Pampeanas obtained from spectral analysis of magnetic anomalies. *Journal Gondwana Research* **8(4)**: 1133-1142.
- Spector A. & Grant F., 1970. Statistical models for interpreting aeromagnetic data. *Geophysics* **35**: 293-302.
- Tanaka A., Okubo Y. & Matsubayashi O., 1999. Curie point depth based on spectrum analysis of the magnetic anomaly data in East and Southeast Asia. *Tectonophysics* **306**: 461-470.
- Tankard A., Uliana M., Welsink O., Ramos V., Turic M., Franca A., Milani M., De Brito Neves B., Eiles N., Skarmeta J. & Santa-Ana H., 1996. Tectonic controls of basin evolution in southwestern Gondwana. *Petroleum Geologists Memoir* **62**: 5-52.
- Thompson D.T., 1982. EULDPH: A new technique for making computer-assisted depth estimates from magnetic data. *Geophysics* **47**: 31-37.
- Turcotte D.L. & Schubert G., 2002. *Geodynamics (Second Edition)*. Cambridge University Press, New York, p. 472.
- Woollard G.P., 1959. Crustal structure from gravity and seismic measurements. *Journal Geophysical Research* **64**: 1521-1544.
- Zambrano J.J., 1974. Cuencas sedimentarias en el subsuelo de la provincia de Buenos Aires y zonas adyacentes. *Revista Asociación Geológica Argentina* **29(4)**: 443-469.

COPPER IN DECCAN BASALTS (INDIA): REVIEW OF THE ABUNDANCE AND PATTERNS OF DISTRIBUTION

Pramod O. ALEXANDER.& Harel THOMAS



**Boletín
del Instituto de
Fisiografía y Geología**

Alexander P.O. & Thomas H., 2011. Copper in Deccan Basalts (India): review of the abundance and patterns of distribution. *Boletín del Instituto de Fisiografía y Geología* 79-81: 107-112. Rosario, 01-07-2011. ISSN 1666-115X.

Abstract.- In comparison to world larger flood basalts, the Deccan Trap exhibits more than double the amount of copper abundance. This is true for most basalt types but quartz tholeiites are particularly rich in copper, the absolute abundance reaching up to 0.05% Cu in certain areas. In such areas it can be established that apart from entry into silicates and oxides, the major portion of copper was removed as sulphides.

While studying the variation of copper abundance and variation within the Deccan Trap and comparing it with other basaltic rocks around the world, the occurrence of native copper and other cupriferous minerals copper is discussed here. Review of earlier work is done in the light of some new findings. Prospects of finding native copper mineralization and copper rich flows are discussed. It is concluded on the importance of studying the copper mineralization in the Deccan Trap.

Key-words: Deccan Basalts, India, Copper, quartz tholeiites.

Resúmen.- *Cobre en los Basaltos de Deccan (India): revisión de la abundancia y patrones de distribución.* En comparación con los mayores mantos volcánicos del mundo, el llamado Deccan Trap muestra una abundancia de Cobre mayor que el doble del promedio. Esto es comprobable para la mayoría de los tipos de basaltos, pero las toleítas cuarcíticas son particularmente ricas en Cobre, alcanzando hasta un 0.05% en determinadas áreas. En dichas áreas pudo establecerse que además del ingreso en silicatos y óxidos, la mayor parte del Cobre fué removido como sulfuros.

Sobre la base del estudio de la variación de abundancia de Cobre en el Deccan Trap, incluyendo una comparación con otras rocas basálticas de distintas partes de la Tierra, se discute la ocurrencia de Cobre nativo y otros minerales cupríferos. Una revisión de trabajos anteriores se lleva a cabo a la luz de nuevos hallazgos. Estrategias y métodos para el hallazgo de Cobre nativo y coladas ricas en Cobre son discutidas. Se concluye sobre la importancia de estudiar las mineralizaciones de Cobre en el Deccan Trap.

Palabras clave: Basaltos de Deccan, India, Cobre, Toleítas cuarcíferas.

Adresses of the authors:

P.O. Alexander: *Department of Applied Geology - School of Engineering and Technology, Dr. H. S. G. Central University, Sagar, India.*

H. Thomas [harelthomas@yahoo.com]: *Department of Applied Geology - School of Engineering and Technology, Dr. H. S. G. Central University, Sagar, India.*

Received: 21/02/2011; accepted: 10/06/2011

INTRODUCTION

Copper is one of the ubiquitous trace elements in basaltic magma. During magmatic crystallization its complex geochemical behaviour can make it appear either in silicates and oxides, sulphides or in native state. About 60-70% of the world copper production comes from sulphides of the late magmatic, hydrothermal stage. However, the Upper Michigan basalt flows hosting an outstanding deposit of native copper is a reminder that where massive basaltic lavas occur, chances of finding deposits of native copper cannot be ruled out.

In spite of being one of the largest basaltic provinces in the world, the minor and trace element distribution in the the extensive basaltic plateau of the Deccan Trap (Fig. 1) has received attention only in the last years. The present paper presents a review of the occurrence of native copper and sulphides in the Deccan Trap considering our new observations and, then, a brief discussion on the abundance and distribution patterns of Cu in Deccan basaltic rocks. Cu concentration in the north-east corner of the Deccan province showing the highest value (up to 0.05% Cu), is considered in some detail.

COPPER IN DECCAN BASALT

The interest of one of the authors (POA) in the subject began in the decade 1970 when studying a large part of the Deccan Trap and carried out an intensive geochemical research of the northeastern corner of the Deccan province (Alexander 1977, Alexander & Paul 1977). Exceptionally high values for copper (around 500 ppm by XRF and confirmed by Emission Spectrograph) in these parts together with stray occurrences of native copper, sulphides and malachite prompted a more detailed regional study on the subject.

Only recently high quality data for Cu abundance in the western side of Deccan Trap are available. Main data are compiled in Table 1, pending a statistical analysis.

NATIVE AND COPPER MINERALS IN DECCAN TRAP

Deccan Trap covers extensive areas in the states of

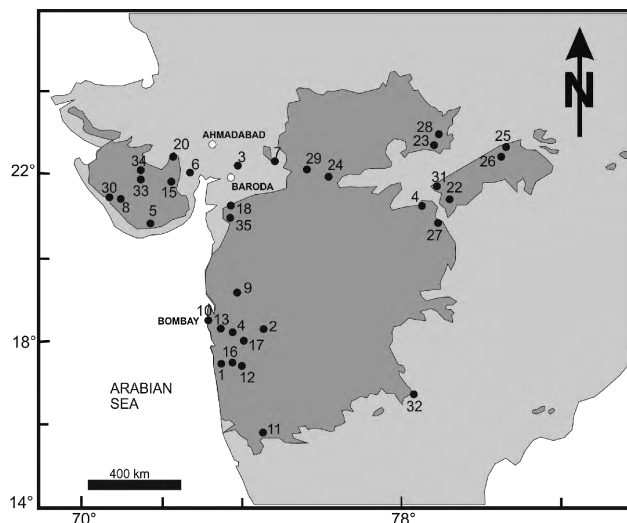


Figure 1. The Deccan Outcrop showing localities for the occurrences of native copper and other copper minerals. See Table 1 for locality names.

Table 1. Compilation of mean contents of Cu (in ppm) in the Deccan volcanics. Main localities located in Figure 1.

Locality	Cu	Reference
Western parts		
01. Ambenali	210	Cox & Hawksworth (1985)
02. Bhimashankar	212	Cox & Hawksworth (1985)
03. Botad	102	Krishnamurthy (1974)
04. Bushe	103	Beane et al. (1986)
05. Dedan	069	Krishnamurthy (1974)
05. Dhandhuka	105	Krishnamurthy (1974)
07. Dohad	259	Alexander (1977)
08. Girnar	139	Murali (1974)
09. Igatpuri	137	Alexander (1977)
10. Khandala	169	Beane et al. (1986)
11. Koyna	309	Alexander (1977)
12. Mahabaleshwar	217	Beane et al. (1986); Nefaji et al. (1981)
13. Neral	104	Cox & Hawksw. (1985), Beane et al. (1986)
14. Nipani	238	Ghose & Trofimov (1972)
15. Pavagrah	100	Alexander (1977)
16. Poladpur	094	Beane et al. (1986), Cox & Hawksw. (1985)
17. Pune	183	Alexander (1977)
18. Rajpipla	296	Krishnamurthy (1974)
19. Thakurvadi	130	Beane et al. (1986)
20. Wadhwan	131	Krishnamurthy (1974)
21. Bhoiwada	102	Vallance (1974)
Central and Eastern Part		
22. Chhindwara	230	Alexander (1977)
23. Dewalchori	517	Alexander (1977)
24. Indore	100	Ghose & Trofimov (1974)
25. Jabalpur	215	Alexander (1977), Ghose & Trofimov (1972)
26. Katangi	163	Alexander (1977)
27. Nagpur	205	Ghose & Trofimov (1972)
28. Sagar	155	Alexander (1977)
29. Malwa Traps, Dhar	321	Khadari et al. (1999)
Poladpur Formation	175	Khadari et al. (1999)
Bhimashankar Formation	248	Khadari et al. (1999)
Deccan Trap Dykes		
28. Sardhar dyke, Saurashtra	132	Alexander (1977)
29. Pachmari dyke, Central India	289	Alexander (1977)
30. Hyderabad	158	Alexander (1977)
31. Jetpur, Gujrat	100	Alexander (1977)
32. Rajkot, Gujrat	122	Alexander (1977)
33. Nandurbar, Maharashtra	225	Melluso et al. (1999)

Maharashtra, Gujarat and Madhya Pradesh. Engineering constructions and excavations have been helpful in presenting better rock exposures and their structures, and thereby exposing copper mineralization in the past. More than twenty localities in these three states are known to have provided records of occurrences of native copper and sulphides/oxides of copper. One of the better known locality is the Mojdam site in the Saurashtra region, about 3 km southeast Bhayavadar (21°51'N, 70°15'E) described by Roy (1969). Other localities in Gujarat include Beh (22°17'N, 69° 30'E), Sherdi (21°35'N, 70°08'E), Buri (21°33'N, 70°07'E) and Athmanbara in Jamnagar district; Jetpur (21°43'N, 70°07'E), Virpur (21°51'N, 70°42'E) in Rajkot district and Gir Forest (21°03'N, 70°54'E) in Junagarh district. From Maharashtra, where the Deccan Trap has maximum coverage, native copper has been recorded from

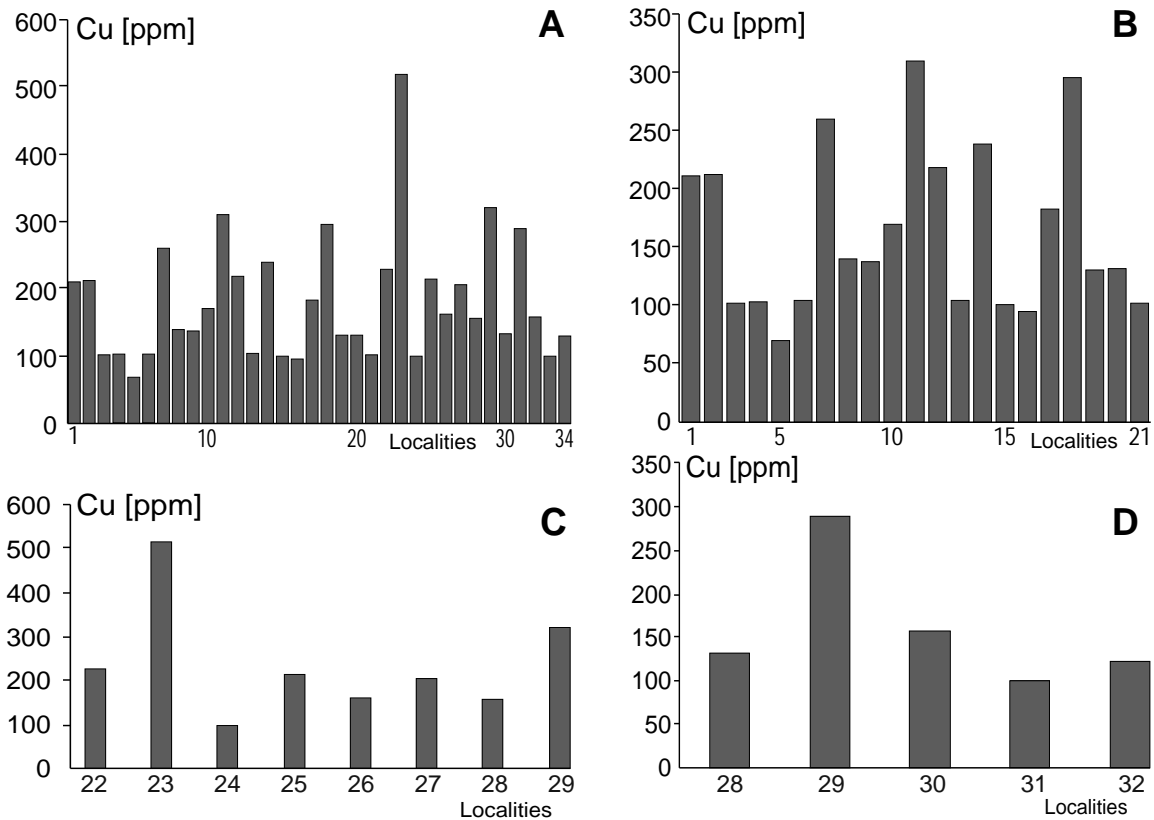


Figure 2. Distribution of Cu abundance in the Deccan Traps. Numbering of localities as in Table 1 and partially in Fig. 1. **A.** Distribution in the Deccan volcanics in the whole area. **B.** Distribution in localities of the western part. **C.** Distribution in localities of central and eastern parts. **D.** Distribution in the Deccan trap dykes.

Kohlapur (16°42'N, 74°55'E), Sirsondi (20°26'N, 74°25'E) and at Jalakundi (17°24'N, 73°45'E) in a quarry excavated for the Koyna Project. Native copper has also been reported from Handigund (16°25'N, 75°05'E) in the Belgaum district of Karnataka near the Maharashtra border. Most of these occurrences among others appear to be too small and limited and have been described briefly by Raghunandan et al. (1981) and also earlier by Dunn & Jhingran (1965) and Radhakrishna & Pandit (1973). In the north-eastern part of the Deccan, specks of native copper and chalcopyrite have been observed in Sagar district (23°56'N, 78°38'E) by one of the authors (POA). Malachite stains have also been noted generally in the topmost flows of the Sagar, Narsinghpur, Jabalpur and Chhindwara districts of Central India. Figure 1 gives an overall picture of occurrence of native copper and other copper minerals in the Deccan Basalts.

DISCUSSION

Copper concentration in “basalts” has an arithmetic mean value of 116 ppm and a median of 100 ppm (Prinz, 1967). Earlier reported values are even lower: Vinogradov (1962) indicates 100 ppm, Wedepohl (1962) 88 ppm, Turekian & Wedepohl (1961) 87 ppm. Deccan Trap basalts, which on the average have quartz tholeiitic composition exhibit more than normal abundance of copper. In this study, around 200 high quality determinations are considered with an attempt to study its geographical and petrological variations within the Deccan Trap and comparing it with other flood basalts.

The abundance of Cu for different localities in western and central regions of the Deccan Basalts is compiled in Table 1. From the large number of data which are not included in Table 1, it is observed that the lowest value is 45 ppm for basalt from

Table 2. Arithmetic mean (*m*) and median (*M*) of Cu abundance in different basalt types. Values in ppm.

		Quartz normative tholeiite	Olivine normative tholeiite	Olivine normative alkali basalt	Nepheline normative basalt
Deccan Trap	<i>m</i>	299	97	120	122
	<i>M</i>	307	106	101	120
World Average (Prinz 1967)	<i>m</i>	135	75	126	47
	<i>M</i>	125	75	105	35

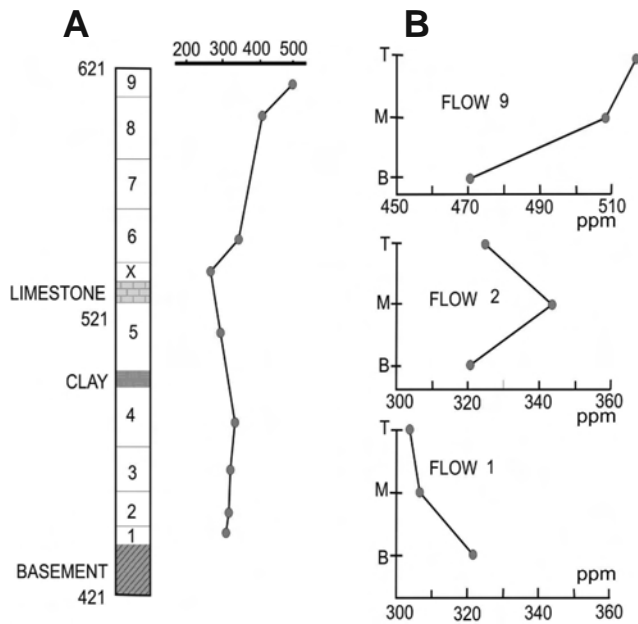


Figure 3. A. Variation of Cu contents (in ppm) in the ten-flow sequence at Sagar, showing a consistent trend of maximum values towards the top of the sequence. B. Intra-flow variation of Cu contents (in ppm) in the flows 1, 2 and 9 showing different trends through the basal (B), middle (M) and upper (T) portions of each flow.

Girnar, Western India (Murali 1974) while the highest, 540 ppm, is for basalt from Dewalchori ($23^{\circ}45'N$, $78^{\circ}34'E$) in the Sagar district (Alexander 1977) and both being quartz tholeiites in character. Fig. 2 shows copper abundance in the Deccan Trap as a whole, irrespective of rock type showing a consistent pattern: within the wide variation in absolute values, ranging from 45 to 540 ppm of Cu, values higher than 200 ppm are generally restricted to quartz normative tholeiites.

Out of the available data for the Deccan Trap, the normative character for 129 basalts is known. In Table 2 it is used to characterize the variation in copper abundance in term of different basalts types, and, at the same time, compared with the world average for the same type. Considering the arithmetic mean among the Deccan Trap, the highest Cu concentration is found in the quartz normative tholeiites (299 ppm) like in the case of basalts around the world. But the difference is larger than twice, the Deccan quartz tholeiites being richer in copper. In the world average, next in the order of decreasing abundance are olivine normative tholeiites (126 ppm) and the nepheline normative basalt poorest, with 47 ppm Cu only. However, surprisingly, in case of the Deccan Trap, nepheline normative basalt is next to quartz tholeiite in their copper abundance (122 ppm) which is nearly three times the world average for the same type (47 ppm).

After comparing other flood basalts of the world, and some of the well known basaltic units, the Deccan Trap shows invariably greater abundance of copper. Indeed, the value of 299 ppm of the Deccan Trap is much higher than those of 148 ppm of Columbia river basalt (Prinz 1967), 125 ppm of Koweonuan lavas of Michigan (Prinz 1967), 197 ppm of the Shaergaard intrusion, 126 ppm of Aleutian volcanism, Alaska (Prinz 1967), 125 ppm Karroo basalt (Alexander 1977), 110 ppm of Siberian Trap (Nesterenko et al. 1967). The Kilauea basalts of Hawaii (207 ppm Cu, Prinz 1967) having more than normal copper abundance than in average basalts, fall poorer to Deccan basalt from this point of view.

Table 3. Ratios Cu/Na and Cu/Fe of the five flows of the higher part of the sequence.

Flow	Cu / Na	Cu / Fe
9	0.027	0.0059
8	0.021	0.0052
7 (weathered)	0.016	0.0041
6	0.020	0.0051
5	0.017	0.0040

There are some smaller volcanic piles which apparently have greater copper abundance than the Deccan. Seachondong basalt flow in Yongyang basin Korea contains on the average 1020 ppm Cu (Lee and Kim, 1970). Similarly, Triassic volcanics of North Mountain, Nova Scotia, Eastern North America have recorded Cu abundance which is higher than for the Deccan Trap. Sinha (1970) has established that the average value in the North Mountain basalt is 496 ppm Cu, which is comparable to the higher copper values of the Deccan Trap around Sagar (see Alexander 1977) but portions of Nova Scotia have even 683 ppm Cu which is quite remarkable.

Within the Deccan Trap itself, there seems to be considerable variation in Cu abundance from different localities (Table 1) in the north eastern corner around the Sagar District, exhibiting the highest abundance with an average of 321 ppm. The highest flow around Dewalchori ($23^{\circ}45'N$, $78^{\circ}34'E$) having the highest value of 540 ppm copper. In other parts of Deccan, especially the western Ghats, values of over 200 ppm Cu are fairly common in individual flows like at Khandala (366 ppm), Koyana (309 ppm), Ambenali (299 ppm), Pune (296 ppm), Mahabaleshwar (290 ppm), Poladpur (268 ppm). Dohad, an isolated outcrop near Pawagarh, has also a fairly high Cu content of 259 ppm (Alexander 1977, Cox & Hawkesworth 1985, Beane et al. 1986). Even within a small area within the same petrographic type, however, there can be considerable variation in copper concentration of basalt. Two quartz tholeiites from Girnar show values of 45 and 279 ppm respectively (Murali 1974). Similarly, there is a considerable variation in flows of the Neral Formation. Commonly, Mg-rich flows have an average content of Cu of 104 ppm, while giant phenocryst basalt in the same locality in Western Ghats have on the average, 238 ppm Cu (Beane et al. 1986). This would suggest that the large phenocrysts of plagioclase are the main host for Cu in these flows.

In restricted areas of the Deccan where acid differentiates accompany basalts, as around Bombay, the Cu values drop down to 12 ppm in trachytes and rhyolites (Lightfoot et al. 1984) while Deccan trap dykes of different ages are comparable to average Deccan Trap in their Cu contents, ranging from 100 ppm to 289 ppm (Table 1).

Copper in Sagar Flows

Abundance of Cu in the 190 m thickness basaltic plateau at Sagar ($23^{\circ}56'N$, $78^{\circ}38'E$) has been studied in greater detail (Alexander, 1976). General concentration of copper in this singular quartz tholeiite province is far richer with an average of 341 ppm as against 100 ppm for the average basaltic rocks. Among the ten-flow sequence, the flow 5 is the oldest (Alexander & Paul, 1977) and the mean content is 293 ppm Cu. Inter-flow variation for the entire sequence is represented in Fig. 3A. Five flows of the higher sequence exhibit a normal differentiation trend (Alexander 1988), increasing from lower to higher flows with a maximum of 500 ppm in the topmost flow.

Taylor (1965) has pointed out that Cu^{++} is closer in ionic size to Fe^{++} among the major elements and Cu is geochemically similar to Na^+ . The Cu-O bond is more covalent than either the Na-O or Fe-O bonds, as is clearly shown by both electro negativity and ionization potential values ($I \text{Cu}^+/I \text{Na}^+ = 1.53$ and $I \text{Cu}^{++}/I \text{Fe}^{++} = 1.25$). Thus Cu/Fe and Cu/Na ratios should increase during fractionation. The four non weathered flows of the higher part of the sequence which have a normal differentiation trend have the ratios indicated in Table 3. This table does not show the entry of part of Cu into silicate lattices substituting for Na^+ and Fe^{++} and possibly Ca in plagioclases and pyroxenes. Since titanomagnetite is a significant phase in these high titania basalts (average TiO_2 , 2.55%) a portion of copper is bound to be with that phase as has also been demonstrated by Vincent in this study of copper contents of Skaergaard minerals (Vincent 1974). In view of considerable high copper concentration of these basalts it is however, reasonable to assume that the bulk of Cu must have separated originally as immiscible sulphides. This is supported by the presence of native copper and copper sulphides in these basalts as also by the presence of secondary copper minerals like malachite stains in particular.

Intra-flow variation in copper is also considerable and pattern varied. In Fig. 3B three different patterns are shown. In flow 9, the trend is what is generally known to be true with maximum Cu concentration towards the top of the flow (517 ppm) with 407 ppm at the bottom and 508 ppm in the middle portions. Flow 2 exhibits another trend where maximum Cu concentration is observed in the middle portion of the flow. Flow 1 shows a pattern which is exactly reverse of flow 9 with maximum Cu concentration in the bottom layers (321 ppm) while Cu concentration decreasing progressively upwards. This however, is not surprising as the entire geochemical trends in the flows of the lower sequence in this area are demonstrated to exhibit a reserved trend (Alexander 1988)

CONCLUSION

There are over 30 areas of basaltic lavas around the world that are known to contain Cu, some of which with potential commercial value (Cornwall 1956). The present paper aims to bring together two different, yet related aspects of the Deccan Trap (one of the world largest continental volcanic piles). Occurrence of native copper in them, and their absolute abundance. It is worth to ask if the latter could serve as a guide to the former. Obviously, with the enormous size of the Deccan outcrop, the present field and analytical data are not enough to make categorical statement but certain observations and suggestions for further studies in the field arise.

1. The Deccan Trap exhibit significantly higher copper values than the average basaltic rocks including the major flood basalt provinces of the world. This fact indicates an anomalous source region with respect to this metal. Even from the Proterozoic to Mesozoic Zaskar sequence of Kashmir it has been reported the occurrence of native copper that is apparently related to trap rocks of the Phe volcanics (Lydekker 1823, Raghu-Nandan et al. 1981). "Zaskar" in Ladakhi language means "Copper Fort". Some of the Cu nodules recovered from this area in ancient times are up to 10 kg weight (Lydekker 1823, Wadia 1978). Therefore, it should not be surprising to find within the massive Deccan volcanic pile the existence of other areas of native Cu and sulphides mineralization together with Cu rich flows (like that of Seachondong basalt in Korea, see Lee & Kim 1970) which could consist of smaller deposits.

2. Most of the discoveries of native copper and sulphides occurrences from the Deccan Trap came to light during engineering excavations for railways, roads and at dam sites. In our opinion Cu occurrence in other localities is very probable. Exploration might be focussed on vesicular, scoracious, pipes, fractured and brecciated portions of the trap, as also ash beds. Malachite stains (which can be confused with the common secondary mineraloid "green earth"), which can be easily tested in the field with rubeanic acid paper, has been helpful in the authors experience to locate sulphide minerals and high copper proportions within a basaltic plateau. Basalt with exceptionally high Cu concentration are significant as such but may or may not indicate native copper mineralization within a flow or nearby. In Lake Superior region, the Keweenaw lavas which host the richest deposit in the world of native copper have almost normal abundance (125 ppm, Prinz 1967).

3. Subvolcanic intrusions within the Deccan Trap also need to be examined specifically with this purpose. It can be recalled here that copper occurs in sulphides ores associated with the subvolcanic intrusions of the Siberian Trap (Nalvikin 1960).

4. Even though there is potential for finding many new localities for copper mineralization in the Deccan Trap, it is unlikely that these have a scale as that of the Lake Superior Copper deposit. Obviously, there are differences in the tectonic environment, the latter constituting a volcanogenic-sedimentary sequence in a geosynclinal setup while the Deccan is a typical continental flood eruptions. However, several small occurrences of native copper and sulphides and flows that are abnormally rich in copper brought together can be a substantial future potential for this strategic metal once the enormous area and volume of volcanic pile is considered. It is significant to note that in Sagar flows which have the highest recorded Cu abundance in the Deccan Trap, over 300 ppm of Copper of flow 9 (which contains on the average 500 ppm of Cu) is removed easily by treatment with cold, weak acids. Sodium Acetate-Acetic acid mixture is also capable of extracting the bulk of copper from powdered basalts. This form of Copper, readily extractable from an ordinary rock material, should be attractive for when regular supply of this important base metal reaches exhaustion. Moreover, it could be tried bacterial leaching on high copper basalts. Bacterially extracted copper from low grade ores and mine wastes is a practice that is increasingly becoming adopted in USA, Canada and Australia.

Acknowledgements.- We are thankful to Prof. Arun K. Shandilaya, Department of Applied Geology (University of Sagar, India) for its support. Two anonymous referees have greatly contributed for enhancing the manuscript.

REFERENCES

- Alexander P.O., 1977. Geochemistry and geochronology of Deccan Trap lava flows around Sagar, M.P. India. Unpublished Ph.D. thesis, 305 p., *University of Saugar*, India.
- Alexander P.O. & Paul D.K., 1977. Geochemistry and Strontium isotopic composition of Basalts from the eastern Deccan volcanic province, India. *Mineral Magazine* **41**: 165-172.
- Alexander P.O., 1984. Petrochemical reversal's in the lava sequence at Sagar, M.P. *Geological Survey of India Special Publication* **12**: 145-149.
- Alexander P.O., 1995. In: R.K. Srivastava & R. Chandra (eds.): Magmatism in relation to Diverse Tectonic settings. Oxford & IBH Publishing Com Pvt. Ltd.

- Beane J.E., Turner C.A., Hooper P.R., Subbarao K.V. & Walsh, J.N., 1986. Stratigraphy, composition and forms of the Deccan Basalts, Western Ghats. *India Bulletin Volcanology* **48**: 61-83.
- Cornwall H.R., 1956. A summary of ideas on the origin of native copper deposits. *Economic Geology* **51**: 615-627.
- Cox K.G. & Hawksworth C.J., 1985. Geochemical stratigraphy of the Deccan Traps at Mahabaleshwar area Western Ghats, India with implications for open system magmatic processes. *Journal of Petrology* **26**: 355-377.
- Dunn J.A. & Jhingran A.G., 1965. "Copper". *Bulletin of the Geological Survey of India, Economic Geology* **23**: 1-204.
- Engel A.E.G., Engel C.G. & Havens R.G., 1965. Chemical characteristics of oceanic basalts and the upper mantle. *Geological Society of America Bulletin* **76**: 719-734.
- Ghose N.C. & Trofimov N.N., 1972. Abundance of copper, lead, zinc and gallium in the basaltic rocks of India and their genetic significance. *Proceedings of the 24th Indian Geological Congress* **10**: 193-198.
- Khadri S.F.R., Walsh, J.N. & Subbarao K.V., 1999. Chemical and magnetostratigraphy of Malva Traps around Mograba region, Dhar District (M.P.). *Memories of the Geological Society of India* **43**: 203-218.
- Krishnamurthy P., 1974. Petrological and chemical studies of Deccan Trap lava flows from Western India. Unpublished Ph.D. thesis, 267 p., *University of Edinburgh*, England.
- Lee J. H. & Kim S.V., 1970. Mineralization and ore deposits of native copper in Seachondong basalt flows in Yongyang basin. *Journal of the Geological Survey of Korea* **6**: 233-248.
- Lydekker R., 1883. The geology of the Kashmir and Chamba territories. *Memories of the Geological Survey of India* **22**: 1-334.
- Melluso L., Sethna S.F., Morra V., Khateeb A. & Javeri P., 1999. Petrology of the mafic dyke swarm of the Tapti river in the Nandurbar area (Deccan Volcanic Province). *Memories of the Geological Society of India* **43**: 735-755.
- Murali A.V., 1974. Some aspects of the geochemistry of the Girnar Igneous Complex, Western India. Unpublished Ph.D. thesis, 295 p., *University of Saugar*.
- Nalivkin D.V., 1960. The Geology of the USSR: a short outline, Oxford, Pergamon press. 170 p.
- Najafi S.J., Cox K.G. & Sukeshwala R.N., 1981. Geology and geochemistry of the basalt flows (Deccan Trap) of the Mahad-Mahabaleshwar section. *Memories of the Geological Society of India* **3**: 300-315.
- Nesterenko G.V., Avilova, N.S & Smirnova N.P., 1964. Rare elements in the Traps of the Siberian Platform. *Geokhimiya* **10**: 1015-1021.
- Prinz, M., 1967. Geochemistry of the basaltic rocks: Trace elements. In: H.H. Hess & A. Poldervaart (eds.): Basalts. New York. *Interscience Publication*: 271-323.
- Raghunandan K.R., Dhruva-Rao B.K. & Singhal M. L., 1981. Exploration for copper, lead and zinc ores in India. *Geological Survey of India Report* **47**: 1-186.
- Radhakrishnan B.P. & Pandit S.A., 1973. On the occurrences of native copper in Deccan Traps. *Department of Mines and Geology, Government of Karnataka Report* **73**: 283-286.
- Sinha R.P., 1970. Petrology of volcanic rocks of North Mountain, Nova Scotia. Unpublished Ph.D. thesis, 256 p., *Dalhousie University*, Canada.
- Taylor S.R., 1965. The application of trace element data to problems in petrology. *Physical Chemistry of the Earth* **6**: 133-214.
- Turekian K.K. & Wedepohl K.H., 1961. Distribution of the elements in some major units of the Earth's crust. *Geological Society of America Bulletin* **72**: 175-192.
- Vallance T.G., 1974. Spilitic Degradation of tholeiitic basalts. *Journal of Petrology* **15**: 79-96.
- Vincent E.A., 1974. Trace elements in minerals from the Skaergarr gabbroic intrusion, east Greenland: a general summary. *Revue de la Haute Auvergne* **1**: 470-471
- Vinogradov A.P., 1972. Average contents of chemical elements in the principal types of igneous rocks of the Earth's Crust. *Geochemistry* **9**: 801-812.
- Wadia D.N., 1978. Geology of India. New Delhi, Tata McGraw Hill Publ. Co.: 508p.
- Wedepohl K.H., 1962. Beitrage zur Geochemie des Kupfers. *Geologische Rundschau* **52(1)**: 492-504.

INSTRUCCIONES PARA LOS AUTORES

Texto: Los artículos deben estar escritos en Español o Inglés. Tres copias completas del manuscrito (incluyendo todas las ilustraciones) serán remitidas a los editores. El texto debe ser tipeado en una cara de hojas A4 (210 x 297 mm), doble interlineado y con un margen derecho amplio. Una vez que el artículo sea aceptado, y luego de las últimas correcciones, el texto debe enviarse, junto a todas las ilustraciones por correo-e, ó bien en CD-ROM o DVD-ROM. Formatos para texto: rich text format (.rtf), ó Word (.doc). El título del artículo y la traducción al segundo idioma, el (los) nombre(s) del (los) autor(es) y las direcciones postal y electrónica deben colocarse en la primera página. El texto debe paginarse a partir de la página con el título. El título debe ser tan corto como sea posible, con indicación acerca del área geográfica tratada en el texto; en los artículos de estratigrafía y/o paleontología debe incluirse, si correspondiera, además la edad. Un resumen conciso que condense todos los resultados obtenidos debe colocarse al comienzo del artículo, en castellano/español y su traducción al inglés o francés. La totalidad del texto debe escribirse en letras minúsculas, utilizando las mayúsculas sólo al principio de oraciones y para los títulos de capítulos. En el texto, las referencias serán como sigue: Aguirre (1984); Dommergues & Meister (1995); Naruto et al. (1989). Notas al pie no serán admitidas. Solamente se admitirá el uso de unidades del Sistema Internacional. Los autores de artículos paleontológicos deben seguir las reglas de los Códigos Internacionales de Botánica y Zoología. Los tipos y los fósiles ilustrados deben ser registrados y depositados en una institución apropiada permanente, debiendo citarse los números de colección y el nombre de dicha institución. Las abreviaturas para nuevos taxa deben ser n. gen., n. sp., etc. Los números de láminas y figuras que fueron originalmente expresados en números no arábigos deben ser transformados a arábigos. Ejemplos:

1873 *Aspidoceras Beckeri* n. sp. - Neumayr: 202, pl. 18: 3.
1925 *Garantiana conjugata* Quenstedt. - Bentz: 162, pl. 6: 5-6.

Referencias bibliográficas: Debe ser exhaustiva y exclusiva de las citas en el texto. Los artículos citados se ordenarán alfabéticamente por el apellido del autor principal, y cronológicamente cuando se citen más que un trabajo de un mismo autor. Las referencias a artículos de un mismo autor en el mismo año se distinguirán en el texto y en el listado de referencias por las letras a, b, etc.: Pasotti (1977a, 1977b). Ejemplos:

Teichert C., 1987. An early German supporter of continental drift. *Earth Sciences Review* 5(1): 134-136.
Arkell W.J., 1957. Jurassic ammonites. In: Arkell W.J., Kummel B. and Wright C.W.: *Treatise on Invertebrate Paleontology*, (L) Mollusca 4, R.C. Moore (ed.). University of Kansas Press and Geological Society of America, Kansas and New York, 22+490p.
Brillouin L., 1962. *Science and information theory*, 2nd ed., 347 p., Academic Press, New York.

Figuras: Todas las ilustraciones (dibujos, diagramas, fotografías) deben ser numeradas como figuras y citadas en el texto, ser independientes y estar identificadas por numeración correlativa, con una explicación concisa y precisa. Su emplazamiento en el cuerpo del texto debe ser sugerido en el margen izquierdo del manuscrito. Todas las ilustraciones, incluyendo las fotos, deben ser de excelente calidad y estar preparadas para eventual copia directa por barrido digital (escaneado). Tamaño máximo, en el caso de página completa, 170 x 247 mm. No se aceptarán figuras o láminas que excedan el tamaño máximo ni láminas que requieran plegarse (véanse posibilidades adicionales en Material Suplementario Digital). Cuando sea necesario indicar escala se hará en forma tan precisa como sea posible en la explicación de la figura y con una barra en la figura. Cuando una figura incluya varias partes o ilustraciones, éstas deben ser designadas con letras mayúsculas

subordinadas al número de figura. Los originales de las ilustraciones serán remitidas solamente una vez que el manuscrito haya sido aceptado. Las fotografías deben montarse en cartulina flexible blanca, y deben ser claras, contrastadas y en el mismo tono dentro de una misma figura. La numeración de las fotos dentro de cada figura se indicará solamente en una cubierta de papel transparente (la numeración definitiva será preparada por los editores). Es preferible bajo cualquier circunstancia enviar todas las figuras en formato digital. Los editores prestarán todo el asesoramiento necesario para que los autores puedan enviar sus figuras de esta forma. Las figuras una vez preparadas y en su versión final pueden enviarse en formato TIFF o BMP con una calidad no inferior a 600 dpi, en grises de hasta 16 bits o 1200dpi para blanco y negro. No se aceptarán figuras en color.

Pruebas de imprenta: El autor recibirá un juego de pruebas. En el caso de artículos con más de un autor, deberá indicarse a cual enviar las pruebas para corrección tipográfica. En general no se aceptarán cambios ni agregados una vez confeccionadas las pruebas. Las pruebas de imprenta deben ser devueltas dentro de los 15 días posteriores a la recepción para asegurar la continuidad del proceso de edición. En caso de no devolución o devolución atrasada, los editores procederán con la revisión y eventuales correcciones.

Separatas: Se entregarán 50 separatas sin cargo al autor.

Envío de manuscritos:

Preferentemente por correo-e: ifg@fceia.unr.edu.ar (información completa en www.fceia.unr.edu.ar/fisiografia).

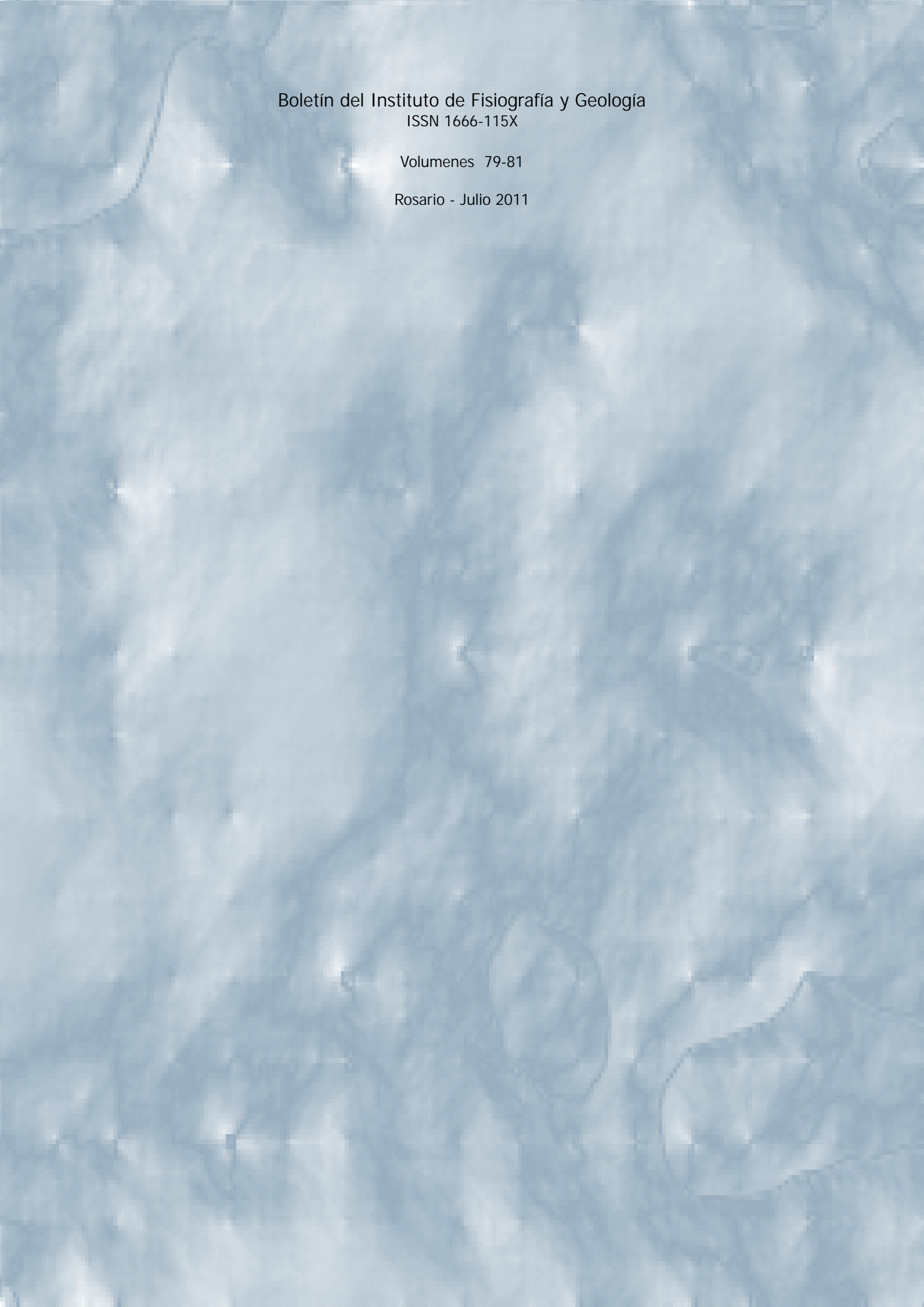
Por correo postal a la dirección:
Instituto de Fisiografía y Geología, Boletín IFG, FCEIA-Universidad Nacional de Rosario, Pellegrini 250, 2000 Rosario, Argentina.

Material suplementario digital (MSD): Los autores pueden incluir suplementariamente, en forma digital, información y datos adicionales pertinentes al contenido de cada artículo publicado. Este material suplementario digital estará disponible en la página web del Boletín IFG: www.fceia.unr.edu.ar/fisiografia, asociado con el artículo correspondiente. Podrán incluirse como MSD:

- 1) Figuras en color y/o tamaños que superen el de la revista impresa 210 x 297 mm (formatos sugeridos: mapas de bits *.tif, *.bmp, *.eps, *.pdf).
- 2) Tablas numéricas muy extensas o listados (formatos sugeridos: *.xls, *.doc, *.pdf).
- 3) Programas informáticos (enviar comprimidos: *.zip ó *.rar).
- 4) Listados de literatura publicada y/o inédita, no referida en el texto del artículo publicado (formato sugerido: *.pdf, *.doc, *.txt).

El MSD debe enviarse en CD-ROM o DVD-ROM, junto con el manuscrito según las instrucciones para autores; los editores evaluarán la posibilidad de su publicación y decidirán el formato definitivo de cada uno de los archivos.

El MSD no puede estar referido en el texto, el cual debe ser completamente autónomo del material suplementario.

The background of the page is a topographic map with contour lines and some shaded areas, rendered in a light blue and grey color scheme. The map shows a complex terrain with various elevations and features.

Boletín del Instituto de Fisiografía y Geología
ISSN 1666-115X

Volumenes 79-81

Rosario - Julio 2011